UTS UNIVERSITY OF TECHNOLOGY SYDNEY

A Suite of Analytical Solutions for Free Strain Consolidation of Soft Soil Reinforced by Stone Columns

by Sam Huu Doan

Thesis submitted in fulfilment of the requirements for the degree of

Doctor of Philosophy

under the supervision of A/Prof Behzad Fatahi and

A/Prof Hadi Khabbaz

University of Technology Sydney
Faculty of Engineering and Information Technology

September 2020

CERTIFICATE OF ORIGINAL AUTHORSHIP

I, Sam Huu Doan declare that this thesis, is submitted in fulfilment of the requirements for the award of the degree Doctor of Philosophy, in the School of Civil and Environmental Engineering, Faculty of Engineering and Information Technology at the University of Technology Sydney.

This thesis is wholly my own work unless otherwise referenced or acknowledged. In addition, I certify that all information sources and literature used are indicated in the thesis.

This document has not been submitted for qualifications at any other academic institution.

This research is supported by the Australian Government Research Training Program and the Ministry of Education and Training (MoET) – Vietnam.

Signature: Production Note:
Signature removed prior to publication.

Date: 30 September 2020

ABSTRACT

Most existing analytical studies on the consolidation of stone column stabilised soft soils adopt equal strain hypothesis for the column and soil settlements, which cannot capture the response of the composite ground (i.e. unequal column and soil settlements) under a typical flexible embankment – platform system accurately. Thus, the differential settlement and column – soil interaction along the interface during the consolidation process were ignored in the available analytical studies. In contrast, several researchers proposed analytical models to investigate the final deformation of the composite stone column – soft ground considering free strain settlement of stone column and soft soil (i.e. differential settlement). Indeed, these studies were for time-independent deformation analysis of the composite ground or considered the effect of consolidation in an uncoupled fashion. To address the above mentioned shortcomings of analytical studies in the literature, this thesis presents a suite of analytical models to the consolidation of soft soils reinforced by stone columns, adopting unit cell concept and one-dimensional free strain condition (i.e. vertical deformation) for stone column and encircling soft soil. The thesis first examines the consolidation behaviour of the composite ground subjected to constant loadings under plane strain and axisymmetric conditions. Then, the mathematical model for the axisymmetric consolidation is developed to account for the effect of time-dependent loadings on consolidation response of the composite ground. Lastly, an analytical model for the coupled consolidation – deformation analysis of stone column reinforced soft soils is formulated. In this thesis, the mathematical formulations are integrated with the associated horizontal and vertical flows of pore water in stone column and soft soil regions with orthotropic permeability for each region. Various total vertical

stress distributions in the composite ground induced by external loadings are adopted including uniform and spatial variation patterns.

In an attempt to develop novel analytical solutions for the free strain consolidation with the incorporation of deformation analysis of the composite ground, the method of separation of variables in conjunction with eigenfunction expansion technique, Green's formula and Green's function method are employed for the analytical derivations. The obtained analytical solutions can capture the excess pore water pressure variations with time at any point in the composite ground. Thus, the column and soil settlements and accompanying differential settlements can be achieved along with other performance objectives such as average degrees of consolidation and normalised average surface settlements of stone column and soft soil. Furthermore, for the combined consolidation – deformation analysis, the transferring of total vertical stress from soft soil to stone column via their interface, as a result of differential settlement and the shear stress distribution in soft soil during the consolidation process, are also captured. Several worked examples and parametric analyses using the achieved analytical solutions are conducted thoroughly. The verifications of the obtained analytical solutions in this thesis against finite element simulations and field measurements show reasonable agreements, which validate the capability of the proposed analytical models and the attained analytical solutions. It can be noted that the proposed analytical solutions may be applicable to the consolidation and deformation analysis of soft soils supported by other pervious columns such as compacted sand columns and soil-cement mixing columns, taking consideration of corresponding physical and mechanical properties.

To my wife, *Sinh Thi Minh Nguyen*, and my daughter, *Linh Vu Nhat Doan*, who shared love, trust and strength with me throughout this glorious journey.

ACKNOWLEDGEMENT

The PhD program at the University of Technology Sydney (UTS), which I have pursued up to date has afforded me academic experience and ability intensely. Throughout my PhD course, I have built up a variety of research skills and academic passion that promote mindset in addressing research questions conscientiously and creatively. Nevertheless, this wonderful achievement would be impossible without enormous supports from my supervisors, my family and fellow members.

First and foremost, I would like to express the deepest gratitude to my principal supervisor, A/Prof Behzad Fatahi, and my co-supervisor, A/Prof Hadi Khabbaz, for their professional supervision, enthusiasm and encouragement. They have been always willing to support and give me exhaustive advice to surmount challenging academic matters effectively. Particularly, my research project might not have been attainable without the valuable comments and recommendations, the patience and unmeasurable favour from A/Prof Behzad Fatahi.

Second of all, I would like to thank all geotechnical research fellows who shared with me academic experience, skill and support. I would also like to thank Dr Liem Huu Ho for his useful recommendations on my research topic at the beginning of my PhD study. I would like to sincerely acknowledge the scholarships and funding awarded by UTS and Ministry of Education and Training (MOET) – Vietnam, which allow me to accomplish my PhD course. Additionally, I would like to extend my appreciation to Van Le and Responsible Academic Officers at UTS Faculty of Engineering and Information Technology for their timely assistance.

Finally, I am extremely grateful to my wife, daughter, parents, relatives and friends for their love, trust, favour and encouragement dedicating to me. They all and my wife and daughter, in particular, have been the strong spiritual supports, which motivates me to work hard, overcome difficult time and achieve my goals successfully.

LIST OF PUBLICATIONS

❖ Journal Articles

Doan S, Fatahi B. Analytical solution for free strain consolidation of stone column-reinforced soft ground considering spatial variation of total stress and drain resistance. Computers and Geotechnics. 2020; 118:103291.

Doan S, Fatahi B. Green's function analytical solution for free strain consolidation of soft soil improved by stone columns subjected to time-dependent loading. Computers and Geotechnics. 2021; 136:103941.

❖ Conference Papers

Doan S, Fatahi B, Khabbaz H. Exact series solution for plane strain consolidation of stone column improved soft soil accounting for space-dependent total stresses. Proceedings of the 16th International Conference of the International Association for Computer Methods and Advances in Geomechanics (IACMAG). Turin, Italy: Springer International Publishing. 2021; 794-802.

Doan S, Fatahi B, Khabbaz H, Rasekh H. Analytical solution for plane strain consolidation of soft soil stabilised by stone columns. Proceedings of the 4th International Conference on Transportation Geotechnics (ICTG). Chicago, USA: Springer International Publishing. 2021. (in press)

TABLE OF CONTENTS

ABSTRACT i

ACKNOWLEDGEMENT iv

LIST OF PUBLICATIONS vi

TABLE OF CONTENTS vii

LIST OF TABLES xiii

LIST OF FIGURES xiv

LIST OF NOTATIONS xxi

CHAPTER 1 INTRODUCTION 1

1.1 General 1

1.2 Stone columns to stabilise soft soil foundations 2

1.3 Statement of problem 6

1.4 Objectives and scope of research 9

1.5 Organisation of thesis 11

CHAPTER 2 LITERATURE REVIEW 14

2.1 General 14

2.2 Terzaghi's theory of consolidation 17

2.3 Biot's theory of consolidation 20

2.4 Consolidation of soft soils assisted by pervious elements 25

2.5 Equal strain and free strain consolidations of soft soil stabilised by stone columns 32

2.6 Effects of drain resistance, clogging, smear and partially drained boundaries 34

2.7 Impacts of total stress variations against space and time on consolidation 37

2.8 Effects of layered soils and partially penetrated columns 39

2.9 Effects of nonlinearity, rheology and unsaturation of soil on consolidation 40

2.10 Deformation of the composite stone column stabilised soft ground supporting embankments 42

2.11 Analytical methods for consolidation of soft soils supported by pervious columns 45

2.12 Summary 49

CHAPTER 3 ANALYTICAL SOLUTION FOR PLANE STRAIN CONSOLIDATION OF SOFT SOIL STABILISED BY STONE COLUMNS 53

3.1 Introduction 53

3.2 Problem description 54

3.3 Analytical solution 57

3.4 Validation of the proposed analytical solution 63

3.5 Summary 72

CHAPTER 4 ANALYTICAL SOLUTION FOR FREE STRAIN CONSOLIDATION OF STONE COLUMN-REINFORCED SOFT GROUND

CONSIDERING SPATIAL VARIATION OF TOTAL STRESS AND DRAIN RESISTANCE 74

4.1 Introduction 74

4.2 Basic assumptions and mathematical model 75

4.3 Analytical solution 80

4.4 Worked example and verification 86

4.4.1 Worked example 87

4.4.2 Verification against finite element simulation 96

4.4.3 Verification against field measurements and existing analytical studies 102

4.5 Parametric study 110

4.6 Summary 121

CHAPTER 5 GREEN'S FUNCTION ANALYTICAL SOLUTION FOR FREE STRAIN CONSOLIDATION OF SOFT SOIL IMPROVED BY STONE COLUMNS SUBJECTED TO TIME-DEPENDENT LOADING 123

5.1 Introduction 123

5.2 Description of the problem 124

5.3 Analytical solution for excess pore water pressure dissipation and consolidation settlement 127

5.4 Worked examples 129

5.4.1 Step loading 134

5.4.2 Ramp loading 140

5.4.3 Sinusoidal loading 146
5.5 Verification against field measurements 153
5.6 Summary 160
CHAPTER 6 SIMPLIFIED ANALYTICAL SOLUTION FOR COUPLED ANALYSIS OF CONSOLIDATION AND DEFORMATION OF STONE COLUMN IMPROVED SOFT SOIL 162
6.1 Introduction 162
6.2 Governing equations, boundary and initial conditions of the consolidation 164
6.3 Deformation of the stone column reinforced ground at the end of consolidation 167
6.4 Coupled analysis for the consolidation and deformation of soft ground reinforced by stone columns 174
6.5 Worked example 180
6.5.1 Total vertical stresses in stone column and soft soil 181
6.5.2 Excess pore water pressure dissipations in stone column and soft soil .. 185
6.5.3 Consolidation settlements in stone column and soft soil 189
6.5.4 Distribution of shear stresses in soft soil 192
6.6 Verification against finite element modelling 197
6.7 Verification against full-scale test 206
6.8 Summary 210
CHAPTER 7 CONCLUSIONS AND RECOMMENDATIONS 212

7.1 Summary 212

7.2 Key concluding remarks 216

7.2.1 General 216

7.2.2 Analytical investigation of the two-dimensional plane strain and axisymmetric consolidations under constant loadings 218

7.2.3 Analytical examination of the axisymmetric consolidation under time-dependent loadings 221

7.2.4 Analytical evaluation of the associated consolidation – deformation response under constant loading condition 223

7.3 Recommendations for further studies 225

REFERENCES 228

APPENDICES 250

Appendix A. Derivation of the solutions for excess pore water pressure $(u_c^{(i)}, u_s^{(i)})$ and $(u_c^{(ii)}, u_s^{(ii)})$ corresponding to the eigenfunctions $(R_{cmn}^{(i)}, R_{smn}^{(i)})$ and $(R_{cmn}^{(ii)}, R_{smn}^{(ii)})$ 250

Appendix B. Derivation of the eigenvalues pairs $(\nu_{cmn}^{(i)}, \nu_{smn}^{(i)})$ and $(\nu_{cmn}^{(ii)}, \nu_{smn}^{(ii)})$ and their corresponding eigenfunctions $(R_{cmn}^{(i)}, R_{smn}^{(i)})$ and $(R_{cmn}^{(ii)}, R_{smn}^{(ii)})$ 254

Appendix C. Derivation of Green's function for the non-homogeneous consolidation problem 261

Appendix D. Derivation of the excess pore water pressure $u_i^{(*)}$ in Equation (5.6) corresponding to the investigation loadings in the example 265

Appendix E. Derivation of the average excess pore water pressure in soft soil $\bar{\bar{\Theta}}_2$ corresponding to the homogeneous consolidation formulation 268

Appendix F. Derivation of the excess pore water pressure solutions for the non-homogeneous consolidation formulation 270

LIST OF TABLES

Table 5.1. Selected loading parameters for the worked example 133

Table 5.2. Geometric and material parameters for the verification 155

Table 6.1. Parameters for the verification against case study 209

LIST OF FIGURES

Figure 1.1. Stone column installation methods: (a) wet top feed and (b) dry bottom feed (modified after Taube and Herridge [3])....4

Figure 1.2. Arrangements of stone columns on soft soils and the corresponding influence zone of each stone column (after Balaam and Booker [4])....5

Figure 2.1. Saturated soil stratum endures (a) one-way drainage and (b) two-way drainage of excess pore water pressure induced by uniform surcharge....17

Figure 2.2. Arrangement pattern of drain wells on plan and unit cell model for the consolidation of soil (after Barron [64]) 28

Figure 2.3. Conversion of (a) axisymmetric unit cell into (b) plane strain unit cell (after Indraratna and Redana [103])....29

Figure 2.4. Consolidation settlement of the composite stone column – soft ground under equal strain and free strain conditions....34

Figure 2.5. Deformation of a typical embankment fill – soft soil foundation system stabilised by stone columns (after Deb [184] and Basack et al. [185])....45

Figure 3.1. The model of the problem 55

Figure 3.2. Excess pore water pressure isochrones against width at depth $z = 0.5H$ for the stone column and soft soil regions 65

Figure 3.3. Dissipation of excess pore water pressure against time at different points in the stone column and soft soil regions 66

Figure 3.4. Plane strain finite element model of the example....67

Figure 3.5. Comparison in average degree of consolidation obtained from proposed analytical solution and finite element result....68

Figure 3.6. Effect of permeability ratio k_{1h}/k_{2h} on (a) average degree of consolidation of stone column and of soft soil, and (b) average differential settlement between stone column and soft soil 70

Figure 3.7. Effect of modulus ratio E_1/E_2 on (a) average degree of consolidation of stone column and of soft soil, and (b) average differential settlement between stone column and soft soil 71

Figure 4.1. The unit cell model of the problem 76

Figure 4.2. The variation of total vertical stresses against depth for the stone column and soft soil regions 88

Figure 4.3. Excess pore water pressure isochrones against radius at depth $z = 0.5H$ for the stone column and soft soil regions 91

Figure 4.4a. Excess pore water pressure isochrones against depth at radius $r = 0.5a$ within the stone column region 92

Figure 4.4b. Excess pore water pressure isochrones against depth at radius $r = 0.5(a+b)$ within the soft soil region 92

Figure 4.5. Dissipation of excess pore water pressure against time at various points in the stone column and soft soil regions 94

Figure 4.6a. Surface settlement isochrones against radius for the stone column and soft soil regions 95

Figure 4.6b. Settlement isochrones against radius at time $t = 5\times10^6 s$ for the stone column and soft soil regions with different investigating depths 96

Figure 4.7. Finite element model used for the verification exercise 98

Figure 4.8. Comparison in dissipation of excess pore water pressure between proposed analytical solution and finite element result at points in the stone column and soft soil regions with depth (a) $z = 0.25H$, (b) $z = 0.5H$, and (c) $z = 0.75H$ 101

Figure 4.9. Comparison in average degree of consolidation between proposed analytical solution and finite element result for the stone column and soft soil regions..... 101

Figure 4.10. Comparison of excess pore water pressure dissipation against time between proposed analytical solution in this study and field measurement at the investigation point ($r = 0.7$ m, $z = 1.5$ m) in soft soil..... 106

Figure 4.11. Comparison of average surface settlement of soft soil against time between proposed analytical solution in this study and field measurement..... 107

Figure 4.12. Comparison of average degree of consolidation between proposed analytical solution and Barron's solution 109

Figure 4.13. Influence of permeability ratio k_{ch}/k_{sh} on (a) average degree of consolidation of stone column and of soft soil, and (b) average differential settlement between stone column and soft soil 113

Figure 4.14. Influence of radius ratio n_e on (a) average degree of consolidation of stone column and of soft soil, and (b) average differential settlement between stone column and soft soil..... 114

Figure 4.15. Influence of modulus ratio E_c/E_s on (a) average degree of consolidation of stone column and of soft soil, and (b) average differential settlement between stone column and soft soil 116

Figure 4.16. Influence of α value on (a) average degree of consolidation of stone column and of soft soil, and (b) average differential settlement between stone column and soft soil..... 118

Figure 4.17. Influence of H/a ratio on (a) average degree of consolidation of stone column and of soft soil, and (b) average differential settlement between stone column and soft soil 120

Figure 5.1. The axisymmetric model of the problem 125

Figure 5.2. Three investigation loading types in the example: (a) Step, (b) Ramp, and (c) Sinusoid 131

Figure 5.3. Dissipation rates of excess pore water pressure at investigation points in (a) stone column and (b) soft soil varying with time duration t_1 of the step loading 136

Figure 5.4. Influence of time duration t_1 of the step loading on normalised average surface settlements of (a) stone column and (b) soft soil 138

Figure 5.5. Influence of time duration t_1 of the step loading on the differential average surface settlement between stone column and soft soil 140

Figure 5.6. Dissipation rates of excess pore water pressure at investigation points in (a) stone column and (b) soft soil varying with construction time t_1 of the ramp loading 142

Figure 5.7. Influence of construction time t_1 of the ramp loading on normalised average surface settlements of (a) stone column and (b) soft soil 144

Figure 5.8. Influence of construction time t_1 of the ramp loading on the differential average surface settlement between stone column and soft soil 145

Figure 5.9. Variation of excess pore water pressure at investigation points in (a) stone column and (b) soft soil with time considering different angular frequencies φ_B of the sinusoidal loading 149

Figure 5.10. Influence of angular frequency φ_B of the sinusoidal loading on normalised average surface settlements of (a) stone column and (b) soft soil 152

Figure 5.11. Influence of angular frequency φ_B of the sinusoidal loading on the differential average surface settlement between stone column and soft soil 153
Figure 5.12. Verification of excess pore water pressure dissipation rate obtained from the proposed analytical solution and field measurement at an investigation point in soft soil 158
Figure 5.13. Verification of average surface settlement rate of soft soil obtained from the proposed analytical solution and field measurement 159
Figure 6.1. The axisymmetric unit cell model for the consolidation analysis 166
Figure 6.2. Assumed deformation pattern of the composite stone column – soft ground and induced stress components on the column and soil elements at the end of consolidation process 169
Figure 6.3. Distribution of total vertical stresses in (a) stone column and (b) soft soil against depth varying with time 183
Figure 6.4. Variation of total vertical stresses in stone column and soft soil against time at different depths 184
Figure 6.5. Excess pore water pressure isochrones against depth at radii (a) $r = 0.5a$ in stone column and (b) $r = 0.5(a + b)$ in soft soil 187
Figure 6.6. Dissipation rates of excess pore water pressure at various investigation points in stone column and soft soil 188
Figure 6.7. Surface settlement isochrones for stone column and soft soil against radius 190
Figure 6.8. Settlements of stone column and soft soil against radius at time $t = 10^6 s$ for different investigation depths 192

Figure 6.9. Isochrones of the shear stress in soft soil against radius at depth $z = 0.1H$ 193

Figure 6.10. Variation of the shear stress in soft soil against radius at time $t = 10^6 s$ for different investigation depths 194

Figure 6.11. Isochrones of the shear stress in soft soil against depth at radius $r = 0.5(a+b)$ 195

Figure 6.12. Variation of the shear stress in soft soil against depth at time $t = 2\times10^6 s$ for different investigation radii 196

Figure 6.13. Finite element model for the verification exercise 198

Figure 6.14. Verification on the distribution of final total vertical stresses in stone column and soft soil against depth between proposed analytical solution and finite element result 199

Figure 6.15. Verification on the change of total vertical stresses in stone column and soft soil against time at depth $z = 0.5H$ between proposed analytical solution and finite element result 200

Figure 6.16. Verification on the dissipation rate of excess pore water pressures at various points in stone column and soft soil with depths (a) $z = 0.25H$, (b) $z = 0.5H$, and (c) $z = 0.75H$ between proposed analytical solution and finite element result 202

Figure 6.17. Verification on the average degree of consolidation of stone column and of soft soil between proposed analytical solution and finite element result 204

Figure 6.18. Verification on the surface settlement of stone column and soft soil at various time t between proposed analytical solution and finite element result 205

Figure 6.19. Verification on the distribution of final shear stress in soft soil against depth at two different radii between proposed analytical solution and finite element result .. 206

Figure 6.20. Verification on surface settlements of soil-cement deep mixing column and surrounding soft soil between proposed analytical solution and field measurement....208

LIST OF NOTATIONS

Latin Notations

a	Radius or half width of stone column
b	Radius or half width of unit cell
A	Rate of the ramp loading
B	Parameter controlling the amplitude of the sinusoidal loading
$A_{2mn}^{(i)}$, $B_{2mn}^{(i)}$	Constants for eigenfunctions $\Psi_{2mn}^{(i)}$
$A_{2mn}^{(ii)}$, $B_{2mn}^{(ii)}$	Constants for eigenfunctions $\Psi_{2mn}^{(ii)}$
$A_{cmn}^{(i)}$, $B_{cmn}^{(i)}$	Constants to be determined for eigenfunctions $R_{cmn}^{(i)}$
$A_{smn}^{(i)}$, $B_{smn}^{(i)}$	Constants to be determined for eigenfunctions $R_{smn}^{(i)}$
$A_{cmn}^{(ii)}$, $B_{cmn}^{(ii)}$	Constants to be determined for eigenfunctions $R_{cmn}^{(ii)}$
$A_{smn}^{(ii)}$, $B_{smn}^{(ii)}$	Constants to be determined for eigenfunctions $R_{smn}^{(ii)}$
c	Transferring rate of total vertical stress from soft soil to stone column
c_{1h}, c_{1v}	Horizontal and vertical consolidation coefficients of stone column, respectively
c_{2h}, c_{2v}	Horizontal and vertical consolidation coefficients of soft soil, respectively
c_{ch}, c_{cv}	Horizontal and vertical consolidation coefficients of stone column, respectively
c_{sh}, c_{sv}	Horizontal and vertical consolidation coefficients of soft soil, respectively

$C_{mn}^{(i)},\ C_{mn}^{(ii)}$	Fourier-Bessel coefficients
$C_{mn}^{T(*)}$	Fourier-Bessel coefficients
$C_{mn}^{(*)}$	Alternative notation of the coefficients $C_{mn}^{(i)}$ and $C_{mn}^{(ii)}$
d	Parameter regulating the change of $\sigma_{1f}(z)$ with depth, $d = 25/(H\ n_e)$
$E_1,\ E_2$	Young's moduli of stone column and soft soil, respectively
$E_c,\ E_s$	Young's modulus of stone column and soft soil, respectively
$f_{cz},\ f_{sz}$	Variation of total vertical stress against depth for stone column and soft soil, respectively
G_2	Shear modulus of soft soil
$G_{ij}^{(*)}$	Green's function
H	Thickness of soft soil stratum
$i,\ j$	Subscripts denote regions of the unit cell; $i, j = 1$ for stone column region; $i, j = 2$ for soft soil region
$(i),\ (ii)$	Superscripts denote different real eigenvalues pairs to be considered
$I_0,\ I_1$	Modified Bessel functions of the first kind of order zero and one, respectively
$J_0,\ J_1$	Bessel functions of the first kind of order zero and one, respectively
$k_{1h},\ k_{1v}$	Horizontal and vertical permeability coefficients of stone column, respectively
$k_{2h},\ k_{2v}$	Horizontal and vertical permeability coefficients of soft soil, respectively

k_{ch}, k_{cv}	Horizontal and vertical permeability coefficients of stone column, respectively
k_{sh}, k_{sv}	Horizontal and vertical permeability coefficients of soft soil, respectively
m	Integer index corresponding to z-domain
M_1, M_2	Constrained moduli of stone column and soft soil, respectively
n	Integer index corresponding to r-domain
n_e	Radius ratio of unit cell to stone column, $n_e = b/a$
n_{scr}	Stress concentration ratio
N_k	Horizontal permeability ratio of stone column to soft soil, $N_k = k_{1h}/k_{2h}$ or $N_k = k_{ch}/k_{sh}$
$N_{mn}^{(i)}$, $N_{mn}^{(ii)}$	Norms to determine $C_{mn}^{(i)}$ and $C_{mn}^{(ii)}$, respectively
$N_{mn}^{(*)}$	Constant to determine the coefficient $C_{mn}^{(*)}$, $C_{mn}^{T(*)}$
q	External loading
q_0	Uniform external loading or initial surcharge
$q_{\max}$	Maximum of step and ramp loadings on the composite ground surface
r, z	Cylindrical coordinates
r', z'	Integration variables corresponding to the cylindrical coordinates
$R_{cmn}^{(i)}$, $R_{smn}^{(i)}$	Eigenfunctions of eigenvalues $\nu_{cmn}^{(i)}$ and $\nu_{smn}^{(i)}$, respectively
$R_{cmn}^{(ii)}$, $R_{smn}^{(ii)}$	Eigenfunctions of eigenvalues $\nu_{cmn}^{(ii)}$ and $\nu_{smn}^{(ii)}$, respectively
$\overline{S}_1$, $\overline{S}_2$	Average surface settlements of stone column and soft soil, respectively (Chapter 5)

$\overline{S}_{1ref}$, $\overline{S}_{2ref}$	Referenced average surface settlements of stone column and soft soil, respectively (Chapter 5)
$\overline{S}_1^*$, $\overline{S}_2^*$	Normalised average surface settlements of stone column and soft soil, respectively (Chapter 5)
$\overline{S}_{\sigma 01}$, $\overline{S}_{\sigma 02}$	Average surface settlements of stone column and soft soil due to the total vertical stress values σ_{01} and σ_{02}, respectively (Chapter 5)
S_1, S_2	Settlements of stone column and soft soil, respectively (Chapter 6)
$\overline{S}_2$	Average settlement of soft soil against radius (Chapter 6)
S_{1f}, S_{2f}	Final settlements of stone column and soft soil, respectively (Chapter 6)
S_c, S_s	Settlement at points with depth $z = z_0$ in stone column and soft soil, respectively
$\overline{S}_c$, $\overline{S}_s$	Average surface settlement of stone column and soft soil, respectively
t	Elapsed time
t'	Integration variable corresponding to time
t_1	Duration for the first step loading or construction time for the ramp loading
t_f	Ending time of the consolidation in soft soil, corresponding to the homogeneous consolidation formulation
$T_{mn}^{(i)}$, $T_{mn}^{(ii)}$	Time-dependent functions of eigenvalues $\beta_{mn}^{(i)}$ and $\beta_{mn}^{(ii)}$, respectively
u_1, u_2	Excess pore water pressures at any point in stone column and soft soil, respectively

$u_i^{(i)}$	Excess pore water pressure at any point in the foundation corresponding to the contribution of eigenvalues pair $(\nu_{1mn}^{(i)}, \nu_{2mn}^{(i)})$
$u_i^{(ii)}$	Excess pore water pressure at any point in the foundation corresponding to the contribution of eigenvalues pair $(\nu_{1mn}^{(ii)}, \nu_{2mn}^{(ii)})$
$u_i^{(*)}$	Alternative notation of $u_i^{(i)}$ and $u_i^{(ii)}$
$\overline{u}_1$, $\overline{u}_2$	Average excess pore water pressures within stone column and soft soil, respectively (Chapter 5)
$\overline{u}_1$, $\overline{u}_2$	Average excess pore water pressures against radius of stone column and soft soil, respectively (Chapter 6)
u_c, u_s	Excess pore water pressure at any point in stone column and soft soil, respectively
$u_c^{(i)}$, $u_s^{(i)}$	Excess pore water pressure at any point in stone column and soft soil due to the contribution of eigenvalues pair $(\nu_{cmn}^{(i)}, \nu_{smn}^{(i)})$, respectively
$u_c^{(ii)}$, $u_s^{(ii)}$	Excess pore water pressure at any point in stone column and soft soil due to the contribution of eigenvalues pair $(\nu_{cmn}^{(ii)}, \nu_{smn}^{(ii)})$, respectively
$\overline{u}_c$, $\overline{u}_s$	Average excess pore water pressure within stone column and soft soil, respectively
$\overline{U}_1$, $\overline{U}_2$	Average degree of consolidation for stone column and for soft soil, respectively
$\overline{U}_c$, $\overline{U}_s$	Average degree of consolidation of stone column and of soft soil, respectively
Y_0, Y_1	Bessel functions of the second kind of order zero and one, respectively
z_0	Depth of equal strain plane (i.e. no differential settlement)

Z_m	Eigenfunctions of eigenvalues λ_m

Greek Notations

α	Ratio of bottom to top vertical stress of stone column and soft soil
α_1	Settlement parameter against *z*-domain at time t
α_{1f}	Final settlement parameter against *z*-domain
β_f	Settlement parameter against *r*-domain
$\beta_{mn}^{(i)},\ \beta_{mn}^{(ii)}$	Eigenvalues corresponding to pairs $(\nu_{1mn}^{(i)},\nu_{2mn}^{(i)})$ and $(\nu_{1mn}^{(ii)},\nu_{2mn}^{(ii)})$, respectively
γ	Shear strain in soft soil
γ_f	Final shear strain in soft soil
γ_w	Unit weight of water
$\overline{\varepsilon}_{vc},\ \overline{\varepsilon}_{vs}$	Average volumetric strain of stone column and soft soil, respectively
$\kappa_c,\ \kappa_s$	Square root of vertical to horizontal permeability ratio of stone column and soft soil, respectively
$\Delta_{mn}^{(i)},\ \Delta_{mn}^{(ii)}$	Temporary variables
$\Delta\overline{S}$	Average differential settlement between soft soil and stone column
$\Theta_i^{(i)}$	Excess pore water pressure at any point in the foundation corresponding to the contribution of eigenvalues pair $(\nu_{1mn}^{(i)},\nu_{2mn}^{(i)})$ for the homogeneous consolidation formulation

$\Theta_i^{(ii)}$	Excess pore water pressure at any point in the foundation corresponding to the contribution of eigenvalues pair $(\nu_{1mn}^{(ii)}, \nu_{2mn}^{(ii)})$ for the homogeneous consolidation formulation
$\Theta_i^{(*)}$	Alternative notation of $\Theta_i^{(i)}$ and $\Theta_i^{(ii)}$
$\bar{\bar{\Theta}}_1$, $\bar{\bar{\Theta}}_2$	Average excess pore water pressures within stone column and soft soil corresponding to the homogeneous consolidation formulation, respectively
λ_m	Eigenvalues in *z*-domain
$\mu_{cmn}^{(i)}$, $\mu_{smn}^{(i)}$	Alternative forms of the eigenvalues $\beta_{mn}^{(i)}$ for stone column and soft soil, respectively
$\mu_{cmn}^{(ii)}$, $\mu_{smn}^{(ii)}$	Alternative forms of the eigenvalues $\beta_{mn}^{(ii)}$ for stone column and soft soil, respectively
$\nu_{1mn}^{(i)}$, $\nu_{2mn}^{(i)}$	Eigenvalues in *r*-domain corresponding to eigenfunctions $\Psi_{1mn}^{(i)}$ and $\Psi_{2mn}^{(i)}$, respectively
$\nu_{1mn}^{(ii)}$, $\nu_{2mn}^{(ii)}$	Eigenvalues in *r*-domain corresponding to eigenfunctions $\Psi_{1mn}^{(ii)}$ and $\Psi_{2mn}^{(ii)}$, respectively
$\nu_{cmn}^{(i)}$, $\nu_{smn}^{(i)}$	Eigenvalues corresponding to $R_{cmn}^{(i)}$ and $R_{smn}^{(i)}$, respectively
$\nu_{cmn}^{(ii)}$, $\nu_{smn}^{(ii)}$	Eigenvalues corresponding to $R_{cmn}^{(ii)}$ and $R_{smn}^{(ii)}$, respectively
ν_{P1}, ν_{P2}	Poisson's ratios for stone column and soft soil, respectively
σ_{01}, σ_{02}	Initial total vertical stresses within stone column and soft soil, respectively

$\sigma_1,\ \sigma_2$	Total vertical stresses within stone column and soft soil, respectively
$\bar{\sigma}_1,\ \bar{\sigma}_2$	Average total vertical stresses within stone column and soft soil, respectively
$\bar{\sigma}_2$	Average total vertical stress in soft soil against radius (Chapter 6)
$\sigma_{1f}(z)$	Final total vertical stress in stone column at any depth z
$\sigma_{2f}(r,z)$	Final total vertical stress at any coordinate (r,z) in soft soil
$\bar{\sigma}_{2f}$	Average of final total vertical stress in soft soil against radius
$\sigma_c',\ \sigma_c$	Effective and total vertical stress in stone column, respectively
$\sigma_s',\ \sigma_s$	Effective and total vertical stress in soft soil, respectively
$\sigma_{cr},\ \sigma_{sr}$	Total vertical stress distribution on the top of stone column and soft soil under the applied external loading, respectively
$\bar{\sigma}_c,\ \bar{\sigma}_s$	Average total vertical stress within stone column and soft soil, respectively
$\bar{\sigma}_{cr},\ \bar{\sigma}_{sr}$	Average total vertical stress on top of stone column and soft soil, respectively
τ	Shear stress in soft soil
τ_f	Final shear stress in soft soil
φ_B	Angular frequency of the sinusoidal loading
ω_m	Temporary variable
$\Psi_{1mn}^{(i)},\ \Psi_{2mn}^{(i)}$	Eigenfunctions corresponding to eigenvalues $\nu_{1mn}^{(i)}$ and $\nu_{2mn}^{(i)}$, respectively

$\Psi_{1mn}^{(ii)}$, $\Psi_{2mn}^{(ii)}$	Eigenfunctions corresponding to eigenvalues $\nu_{1mn}^{(ii)}$ and $\nu_{2mn}^{(ii)}$, respectively
$\Psi_{imn}^{(*)}$	Alternative notation of $\Psi_{imn}^{(i)}$ and $\Psi_{imn}^{(ii)}$
$(*)$	Alternative superscript of (i) and (ii)

CHAPTER 1

INTRODUCTION

1.1 General

The increase of population accompanied by the rapid urbanisation have led to the expansion of construction projects over marginal soil areas worldwide since the last several decades. It is well recognised that these areas are commonly the lowlands located in coastal regions whose soil deposits are resulted from the sedimentation process. Several coastal areas experienced very soft soils (e.g. marine, estuarine and alluvium) that cannot be used as foundations for construction facilities due to the high compressibility, low bearing capacity and shear strength of the soils. Soft soils subjected to surcharge loadings can result in extremely large total settlement and differential settlement in long-term after construction, as well as soil collapse under the undrained condition during the construction process. Therefore, it is crucial to employ ground improvement techniques to these soil types prior to any further construction activities to avoid the potential failure of the natural soil foundation and excessive post-construction settlements.

Numerous construction methods of infrastructure and embankments on soft soil deposits have been studied and applied in real practice. These methods can be listed as soft soil replacement, temporary surcharge on soil foundations, multi-stage construction on soils, equilibrium berms and reinforced embankments, lightweight fills, vertical drain assisted preloading (e.g. with prefabricated vertical drains (PVDs) and sand drains), vacuum preloading, granular column reinforced soft soils (e.g. stone columns and compacted sand columns), and embankments on piles or deep mixing or jet grouting soil

columns [1]. The suitable method for a particular construction project would be chosen considering various decisive factors such as geotechnical properties of soil deposits, expected loading conditions, impacts to existing infrastructures in their proximity, construction schedule restrictions and cost-effectiveness analysis. In this thesis, the construction method utilising the inclusion of stone columns in soft soil foundations is of interest. Therefore, this chapter presents briefly the usage of stone columns in improving soft soils and states the research objectives, while further considerations are provided in the remaining chapters of the thesis.

1.2 Stone columns to stabilise soft soil foundations

To reinforce soft soils with stone columns, the stone materials in form of aggregates are installed into the soil foundations as compacted vertical columns of aggregates using vibroflotation (vibroflot) equipment. Two common methods for stone column installation are known as vibro-replacement and vibro-displacement [2].

For the vibro-replacement method, a vibroflot is used to create a vertical hole along soil depth with the assistance of high pressure water jet. This method is generally suitable for the sites underlain by very soft soil with high groundwater level, where the stability of the unsupported hole is uncertain. During the construction process, the water jets at the tip and along the side of probe unit assist the penetration of vibroflot and the washing-out of loose soil volume from the hole. The flushing water also supports the stabilisation of the uncased hole. Once the vibroflot has reached the desired depth, the excavated hole is backfilled with aggregate (size 40-75 mm) from the ground surface via the space between the vibroflot and the side of hole. In each filling cycle, the aggregates are added in 0.3-

1.2 m increments while the vibrating probe is usually kept inside the hole to compact the stone backfill. The filling and compaction processes are repeated until a stone column has been established up to the native soil surface. Due to the usage of jetting water during the construction process and the filling of stone from the top ground surface, the vibro-replacement method is frequently referred to as *wet top feed* method.

For the vibro-displacement method, the vibroflot is also utilised to open the hole for stone backfill. However, air jetting is employed for the penetration and extraction of the vibroflot. This method is appropriate for partially saturated and firmer soils compared to the previous mentioned method, where the groundwater table is relatively low and the created hole can stand open during the extraction of the probe. The hole is supplied with the aggregate (size 15-45 mm) from the vibroflot tip through an attached tube alongside the vibroflot. Similar to the vibro-replacement technique, the stone backfill is also densified by repeated penetrations of the vibroflot during each backfill increment till forming a complete stone column. From the installation method of stone column, the vibro-displacement technique is usually named *dry bottom feed* method.

Figure 1.1 presents typical stages of stone column inclusion applying the *wet top feed* and *dry bottom feed* methods. It should also be noted that stone columns can be penetrated fully or partially into soil strata depending on the expected loading conditions. Moreover, the arrangement of stone columns on soft soils is commonly conducted as three types of patterns including triangular, square and hexagonal patterns as shown in Figure 1.2. The influence zone of each column is denoted by the diameter d_e of a circle obtained from the grid shape surrounding each column on the basis of equivalent area. Thus, the diameter d_e can be determined as a constant multiple of the column spacing s.

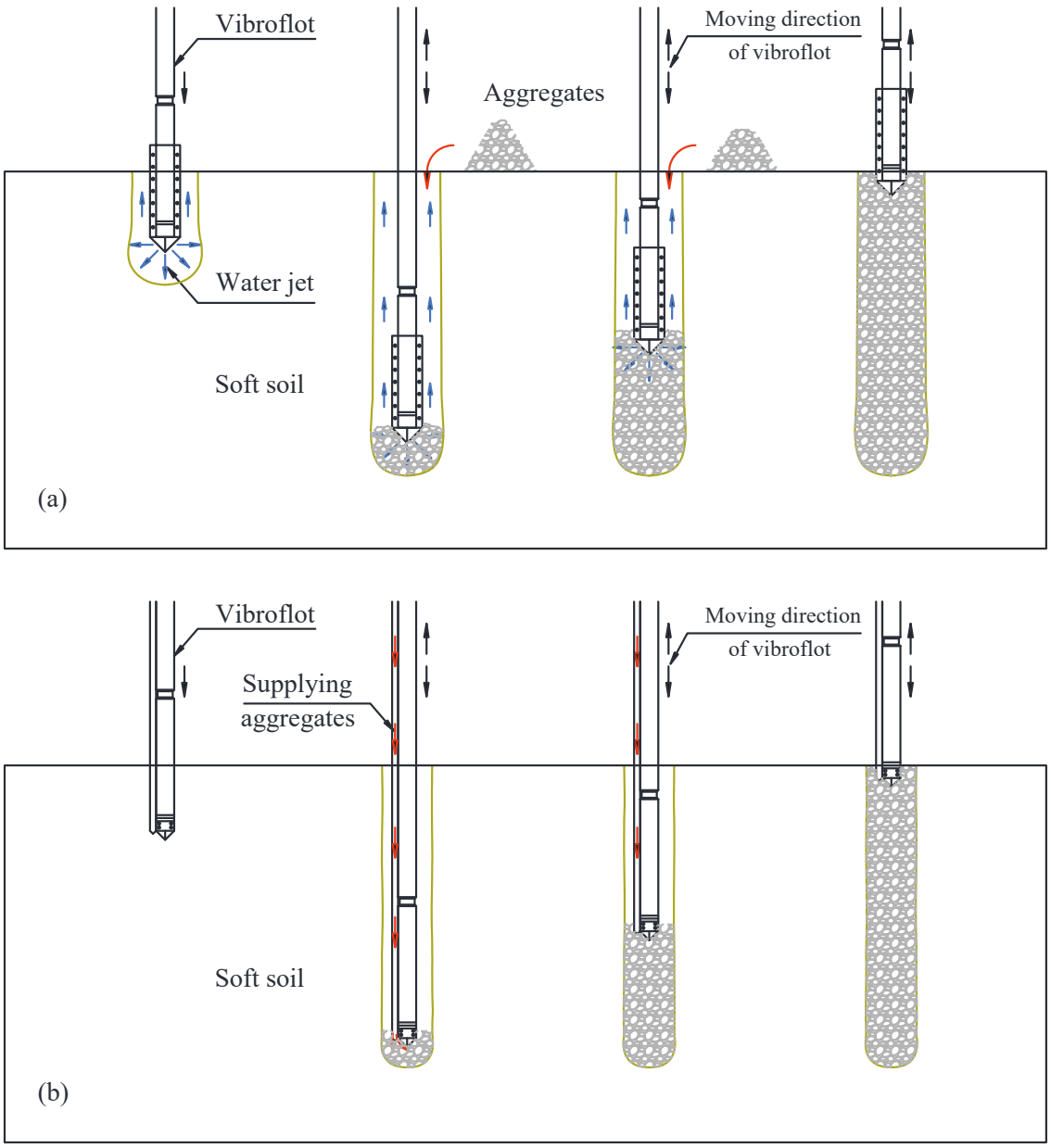

Figure 1.1. Stone column installation methods: (a) wet top feed and (b) dry bottom feed (modified after Taube and Herridge [3])

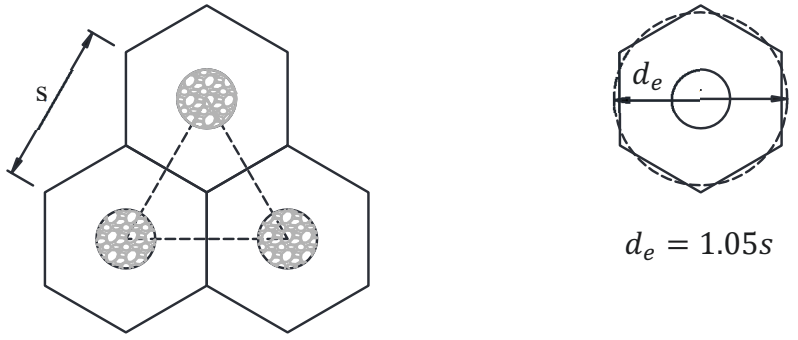

(a) Triangular arrangement pattern of stone columns

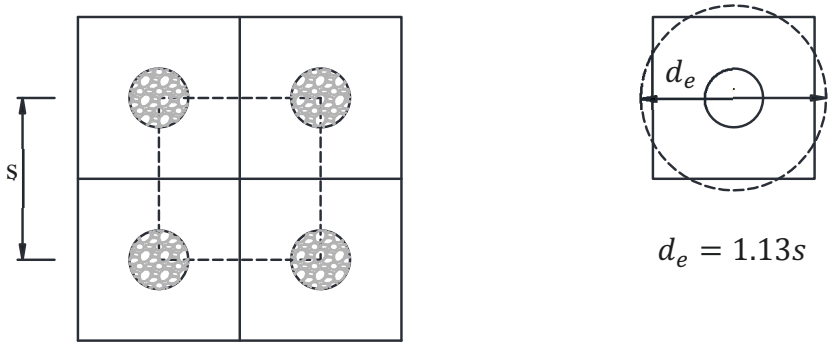

(b) Square arrangement pattern of stone columns

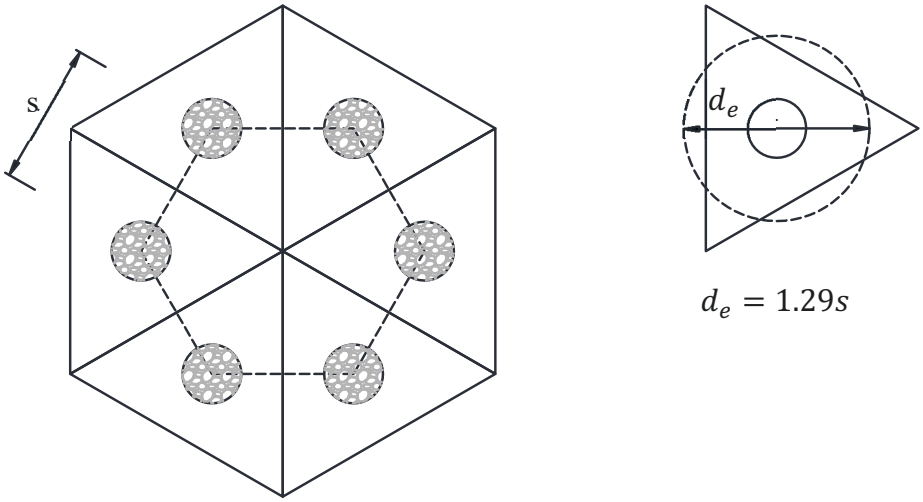

(c) Hexagonal arrangement pattern of stone columns

Figure 1.2. Arrangements of stone columns on soft soils and the corresponding influence zone of each stone column (after Balaam and Booker [4])

1.3 Statement of problem

Application of stone columns to reinforce soft soil foundation underneath structures such as embankments, airport runways, seaports, buildings, warehouses, tanks and other construction facilities is a prevalent ground improvement technique, which has been studied and applied for many decades [5-17]. Owing to the large diameter and high hydraulic conductivity (permeability), stone column has a great discharge capacity and supplies a short horizontal drainage path towards the column for pore water in surrounding soft soil during the consolidation process. Moreover, under the lateral confinement of encircling soil, stone columns can carry a large portion of surcharge, reduce much of that on the soil surface, which leads to low excess pore water pressure to be dissipated from the soil itself. As a result, the excess pore water pressure in the soft soil generated by external loadings dissipates more quickly via the radial flows to stone columns, and thus the consolidation of the composite stone column – soft soil foundation is accelerated significantly. Besides, the inclusion of stone columns into soft soil deposit can enhance the stiffness and shear strength of the composite foundation, which diminishes the compressibility or settlement, increases the bearing capacity and stability, and decreases the liquefaction potential [2, 18-23].

The above-mentioned effects of stone columns in improving soft soil are commonly considered as performance objectives which have been investigated in numerous studies. A number of research studies were conducted to examine the load-bearing enhancement and settlement performance of soil foundations reinforced by conventional, encapsulated single stone column, and group of stone columns such as those reported by Black et al. [14], Malarvizhi and Ilamparuthi [24], Ghazavi and Afshar [25], Malarvizhi [26],

Murugesan and Rajagopal [27, 28]. Several examinations on the stabilisation of granular column supported soft ground were also carried out employing the theory of critical slip surface [29-31], whereas many other studies considered the failure mechanism of composite granular column – soil foundation comprehensively [32-38]. It is worth mentioning that most studies concerning settlement, bearing capacity and stability take account of static external loadings. In contrast, the assessment of liquefaction resistance is related to dynamic excitation conditions in which dynamic responses such as excess pore water pressure and liquefaction induced deformation and displacement are examined [39-43]. Among various studies on behaviours of soft soils strengthened with stone columns, the prediction of consolidation response plays a prominent role in design and construction where the variation of excess pore water pressure and consolidation settlement with time are of interests. Furthermore, during the consolidation process, the dissipation of excess pore water pressure leads to a diminution of volumetric strain of composite ground, which increases stiffness and strength of the foundation. Many studies addressed the consolidation of reinforced soft ground, accounting for various influencing factors to simulate the practical conditions more accurately. These factors comprise of time and depth dependent loadings, smear and drain resistance effects, coupled horizontal – vertical flow of pore water [44, 45], partially drained boundaries [46, 47], multilayer soft soils and floating columns [48-51], clogging, lateral deformation and yielding of pervious columns [52-59], nonlinearity and rheology of composite grounds [60-63]. However, most studies, particularly analytical ones adopted the equal strain assumption for the consolidation of composite granular column – soft ground. In other words, the settlements due to the excess pore water pressure dissipation at points with the same depth in the composite foundation are assumed to be the same when adopting equal strain

condition. It should be noted that, for a specific external loading acting on the foundation surface via a flexible platform, the settlements at a given depth along the radial direction of stone column and surrounding soft soil are unequal at a particular time. Since the soft soil has much lower stiffness than the stone column, the soil settlement is larger than the column settlement in most of the consolidation time; also, the settlement increases for the soil bodies further away from the column. These differential settlements can only be captured by assuming a free strain condition for the consolidation of composite ground, which has been barely considered in existing studies, particularly for analytical examinations.

Among various methods to study the consolidation problem, analytical methods play an important role in preliminary designs since the analysis using analytical solutions requires much less time and computational effort than that by applying complex numerical solutions. Furthermore, analytical solutions can provide insight into the problem by conducting sensitivity analysis and parametric study, which can be more inconvenient via numerical modelling. Generally, analytical solutions can be useful for the purpose of practical designs and cross checking the complex numerical simulations by supplying correlations between influencing factors and performance objectives such as degree of consolidation. Having realised the shortcomings of the existing analytical studies on consolidation of soft soil reinforced by stone column inclusions, it is vital to conduct further analytical examinations to evaluate the consolidation behaviour of the composite stone column – soft soil foundations considering the free strain condition while considering various loading conditions.

1.4 Objectives and scope of research

The primary objective of this study is to derive analytical solutions for consolidation of the composite stone column – soft ground under two-dimensional (2D) plane strain and axisymmetric configurations accounting for the free strain condition. The mathematical models are formulated incorporating the orthotropic flows of excess pore water pressure in stone column and soft soil rigorously, so the drain resistance effect in stone column can be captured. The effects of space and time dependent total vertical stresses in the composite ground induced by external loadings are also considered. Moreover, the coupled analysis of consolidation and deformation of the composite stone column – soft soil foundation, which is one of the significant shortcomings in the available analytical studies will be addressed in the present analytical study. The specific objectives of this study are described as follows:

- Deriving analytical solutions to predict the free strain consolidation behaviour of soft soils improved by stone columns, considering the coupled vertical – radial flows of excess pore water pressure in stone column and soft soil stringently.
- Developing analytical solutions to investigate the effects of total vertical stress variations against space and time on free strain consolidation of the composite stone column – soft ground subjected to instantaneous and time-dependent loadings.
- Formulating a simplified analytical solution for the combined consolidation – deformation analysis of the composite ground under flexible uniform loading and free strain conditions.

- Validating the proposed analytical solutions in this study and verifying the accuracy of the obtained analytical solutions against finite element simulations and field measurements.
- Conducting worked examples and parametric studies employing the attained analytical solutions in the present study to examine the influence of various factors (e.g. stiffness and permeability of soft soil, stone column spacing, soil thickness, depth and time dependent total vertical stresses) on consolidation and deformation responses of the composite stone column – soft soil composite foundation.

In this study, the consolidation formulations are developed on the basis of the vertical drain consolidation theory, which was originally proposed by Barron [64]. To derive the simplified analytical solution for the coupled consolidation – deformation analysis of the composite ground, the deformation pattern suggested by Alamgir et al. [65] is adopted. Therefore, the research scope is restrained in accordance with the following adopted assumptions:

- The column and soil materials are homogeneous and fully saturated, in which the soil particles and pore water are incompressible. Additionally, the flows due to excess pore water pressure dissipation in the composite ground are orthotropic and obey Darcy's law.
- The stone column and soft soil are assumed to deform solely in vertical direction (one-dimensional settlement theory is adopted). In other words, the horizontal deformation of the composite ground is ignored.
- The permeability and volume change coefficients of stone column and soft soil are assumed unchanged during the consolidation process under an expected increment of the external loading.

1.5 Organisation of thesis

The thesis is organised in seven chapters as follows:

- Chapter 1 provides an overview on ground improvement techniques in geotechnical engineering, focusing on the reinforcement of soft soils by stone column inclusions and the significance of analytical studies on free strain consolidation of stone column stabilised soft soil foundations. The research objectives and research scope are also discussed clearly in this chapter.
- Chapter 2 presents a thorough review of existing studies on soft soil consolidation assisted by various pervious columns (e.g. vertical drains, granular columns, soil-cement mixing columns), particularly for the analytical examinations of saturated soils in line with the research scope. Furthermore, a review of studies on behaviour of embankment fill – soft soil foundation systems reinforced by stone columns are conducted to highlight the necessity for analytical derivations of coupled consolidation – deformation analysis allowing time-dependent differential settlement predictions.
- Chapter 3 introduces an analytical solution for free strain consolidation of a stone column stabilised soft soil under instantly applied loading and two-dimensional plane strain conditions. Both horizontal and vertical flows of excess pore water pressure are integrated into the mathematical model of the problem, while the total vertical stresses induced by the external loads are assumed to distribute uniformly within each column and soil region. A worked example investigating the dissipation of excess pore water pressure is conducted to exhibit the capabilities of the obtained analytical solution, whereas the reliability of the solution is

verified against a finite element modelling. Besides, a parametric study to inspect the influence of consolidation parameters of soil on performance objectives (e.g. average degree of consolidation and average differential settlement) is also reported in this chapter.

- Chapter 4 proposes an analytical solution for axisymmetric consolidation problem of a stone column-improved soft soil deposit subjected to an instantly applied loading under free strain condition. The radial and vertical consolidation equations are solved in a coupled fashion for both the stone column and its surrounding soil. The capabilities of the proposed solution are exhibited through a comprehensive worked example, while the accuracy of the solution is verified against a finite element simulation and field measurements of a case history. To examine the effect of various factors on consolidation behaviour of the composite ground, a parametric study involving column spacing, modulus and permeability of soft soil along with distribution pattern of total stresses and thickness of soil deposit is also conducted in this chapter.
- Chapter 5 develops an analytical solution in terms of Green's function formulations for axisymmetric consolidation of a stone column improved soft soil deposit subjected to time-dependent loading under free strain condition. The mathematical derivations incorporate the pore water flows in radial and vertical directions in stone column and soft soil synchronously. The capabilities of the proposed analytical solution are evaluated via worked examples investigating the influences of three common time-dependent external surcharges (namely step, ramp and sinusoidal loadings) on consolidation response of the composite ground. Finally, the proposed analytical solution is employed to evaluate the excess pore

water pressure dissipation rate at an investigation point in soft clay of a case history foundation.

- Chapter 6 derives a simplified analytical solution to analyse the coupled excess pore water pressure dissipation and deformation response of a composite stone column – soft soil foundation. The mathematical formulations are derived by integrating the orthotropic flows due to induced excess pore water pressures in stone column and soft soil, and adopting the settlement pattern for the composite ground suggested by an existing study in the literature. The proposed analytical solution is validated via a worked example in conjunction with a verification exercise against finite element simulation. The analytical predictions are presented in terms of the total vertical stress variations and excess pore water pressure dissipation against depth and time, the settlement and average degree of consolidation for stone column and the surrounding soft soil, and the shear stress distribution in the soil region.
- Eventually, Chapter 7 summarises the thesis briefly, provides concluding remarks from the present study and recommendations for further research. After this chapter, references and appendices of the thesis are presented.

CHAPTER 2

LITERATURE REVIEW

2.1 General

Soil body in geotechnical engineering is usually simplified into three phases which are solid (soil particles), water and air occupying the voids of soil mass. Similar to any other materials, the volume of a soil body reduces when it is compressed by external forces. The soil property capturing volume change subjected to compressive stresses is recognised as the compressibility of soil. Generally, the reduction of soil volume subjected to a compressive pressure can take place owing to the compression of soil particles, the compression of water and air in voids, the expulsion of water and air out of the soil body, and the elastic compression and the readjustment of soil skeleton [66, 67]. However, under the range of pressures encountered in geotechnical engineering, the compression of water and soil particles are negligible and they are frequently considered to be incompressible. In contrast, the air phase in the voids is highly compressible and the compression of the air in soil body occurs rapidly.

For a saturated soil where the voids are regarded to contain solely water, the reduction of soil volume (i.e. volumetric strain in the soil body) under compressive pressures is primarily due to the expulsion of water from the void spaces of soil body. This phenomenon is known as the consolidation of saturated soils. Indeed compression process of soils can be divided into two stages:

- Primary consolidation: According to Terzaghi [68], when saturated soil is subjected to a compressive pressure, the applied pressure is initially carried by

water in void spaces due to the incompressibility of water and soil particles compared to the soil skeleton in the saturated soil mass. Water in voids takes up the applied pressure in terms of induced excess pore water pressure accompanied by a hydraulic gradient towards the drainage boundaries, which expel the pore water from the void spaces and result in the decrease of soil volume. This diminution in the volume of soil is called primary consolidation. The rate of primary consolidation depends on the permeability and stiffness of soil. The primary consolidation progresses slowly in fine-grained soils owing to their low permeability, and vice versa for coarse-grained soils. Moreover, the stiffer the soil, the faster the transfer of applied pressure from the pore water onto soil skeleton in accordance with the transfer of excess pore water pressure into the effective stress in soil body when water escapes from the soil. As a result, the effective stress in soil increases progressively during the primary consolidation period.

- Secondary compression: When the excess pore water pressure in soil mass induced by the applied pressure has dissipated entirely and the primary consolidation process has completed, the soil volume still decreases at a very slow rate. This additional diminution of soil volume is described as secondary compression, which is attributable to the plastic readjustment of soil skeleton under the constant effective stress achieved at the end of primary consolidation. The contribution of the secondary compression to the settlement of soft soil is frequently examined employing two different approaches. Several researchers assumed the secondary compression takes place after the completion of primary consolidation [69-71], whereas other researchers reported that the secondary

compression also progresses during the primary consolidation [72-74]. The volumetric strains due to secondary compression may be noticeable in soft saturated cohesive soils and particularly organic soils, whereas those are generally small in most inorganic stiff soils.

The consolidation (i.e. primary consolidation) is a time-dependent response of saturated soft soils, where the soils undergo the process of volume change from the undrained compression condition immediately after applying loading till the drained compression state of soils corresponding to the full dissipation of excess pore water pressure. During the consolidation process, the soil volume decreases and soil mass becomes denser progressively that enhances the shear strength and bearing capacity of the soil. The understanding of consolidation behaviour of soft soils plays a vital role in the design and construction of infrastructures built on soft soils since unreasonable predictions in the dissipation of excess pore water pressure, the gained shear strength and load bearing of soils during the consolidation under various loading conditions (e.g. step loadings, progressive loadings) may lead to fails in ensuring the technical and economic characteristics. Therefore, the consolidation of soft soils is one of the subject matters, which has attracted the interest of researchers and engineers in geotechnical engineering. This chapter presents the development history of classical theory of consolidation for saturated soft soils, followed by a detailed literature review on consolidation of pervious column stabilised soft grounds. Several influencing factors regarding construction methods, construction processes and nature of geotechnical materials on consolidation of the composite grounds will be sufficiently discussed, particularly for analytical studies. A summary on potential analytical methods for the derivation of analytical solutions to consolidation of pervious column improved soft soils will also be provided in this chapter.

2.2 Terzaghi's theory of consolidation

The consolidation theory was originally established by Terzaghi [68, 75] for saturated soft soils. This theory has built a framework for numerous advanced research studies and practical applications in engineering. In the original work developed by Terzaghi [68, 75], a saturated soft soil stratum subjected to an instantly applied uniform surcharge q was investigated, in which the soil is underlain by either impermeable or permeable rigid layer; additionally, the top soil surface is considered as a fully drained boundary (see Figure 2.1). Under the application of external surcharge, the generated excess pore water pressure in the soil stratum dissipates towards the drainage boundaries along the vertical direction (i.e. one-dimensional consolidation). The soil would undergo one-way drainage of excess pore water pressure from the bottom to top of the soil layer in the case of the impermeable base (refer to Figure 2.1a) or two-way drainage from the middle soil depth to the top and bottom of the soil stratum in the case of the permeable base (refer to Figure 2.1b).

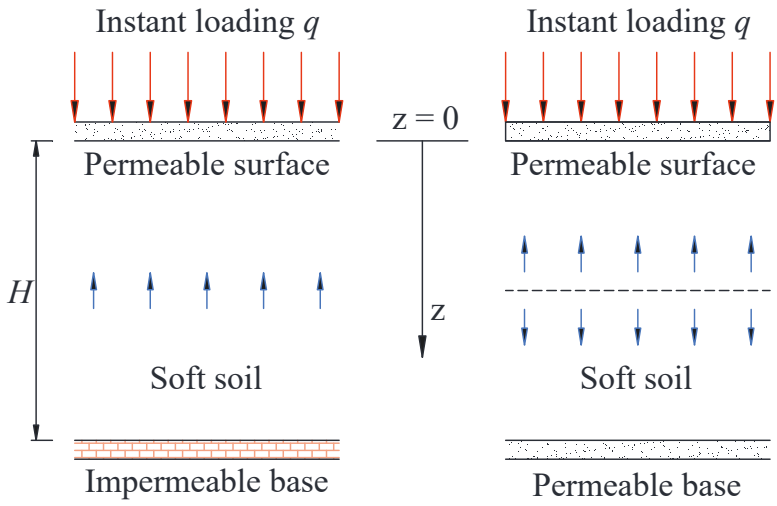

Figure 2.1. Saturated soil stratum endures (a) one-way drainage and (b) two-way drainage of excess pore water pressure induced by uniform surcharge

According to Terzaghi [68, 75], the mathematical formulations for the one-dimensional consolidation of saturated soils can be derived adopting the following basic assumptions:

- The soil stratum is homogeneous and completely saturated.
- The compressibilities of soil particles and water are negligible. In other words, soil particles and water in void spaces are supposed to be incompressible.
- The excess pore water flows are in the vertical direction only, which correspond to the one-dimensional compression of soil stratum, and Darcy's law is valid for the pore water flow.
- The relationship of void ratio and effective pressure under the surcharge is linear, time-independent and the same at any soil depth. In other words, the compressibility coefficient and thus the volume change coefficient are assumed to be constant.
- The soil stratum holds a homogeneous coefficient of permeability which also remains unchanged during the consolidation period (i.e. time-independent coefficient of permeability is assumed).

Referring to Terzaghi [68, 75], by investigating the vertical flow of pore water through a prismatic soil element in the soil stratum in which the rate of squeezing water out of the soil element is equal to the rate of volume change of that soil element, the following governing equation for the dissipation of excess pore water pressure in the soil can be obtained:

$$c_v \frac{\partial^2 u(z,t)}{\partial z^2} = \frac{\partial u(z,t)}{\partial t} \tag{2.1}$$

where u is the excess pore water pressure at depth z and time t; $c_v = k/(\gamma_w m_v)$ is the coefficient of consolidation; k is the permeability cofficient; m_v is the volume change coefficient; γ_w is the unit weight of water.

In connection to the drainage boundaries adopted in the mathematical model, the boundary conditions for excess pore water pressure would be expressed as:

$$u(0,t) = 0 \tag{2.2}$$

$$\frac{\partial u(H,t)}{\partial z} = 0 \quad \text{for one-way drainage condition} \tag{2.3a}$$

$$u(H,t) = 0 \quad \text{for two-way drainage condition} \tag{2.3b}$$

where H is the thickness of soft soil stratum.

It should be noted that the permeable surfaces are described by Dirichlet boundary conditions as in Equations (2.2) and (2.3b). On the other hand, the impermeable surface (refer to Figure 2.1a) is expressed by a Neumann boundary condition as in Equation (2.3a), which indicates a zero flow condition of excess pore water pressure at the impermeable base.

Finally, the mathematical derivations for the consolidation of the saturated soil are finalised by binding the excess pore water pressure in the soil with an initial condition. It is worth mentioning that the soil stratum is assumed to deform only in vertical direction under the instantaneously applied uniform loading q. This assumption corresponds to the condition that the surcharge loading distributes uniformly and boundlessly on the soil surface, which results in a uniform distribution of total stress in the soil stratum. Furthermore, the total stress caused by the external loading is deemed to be carried entirely by the excess pore water pressure immediately after applying loading, due to the

assumption of incompressibility of water in voids. Therefore, the initial condition of excess pore water pressure would be described by:

$$u(z,0) = q \tag{2.4}$$

The solution for excess pore water pressure at any depth z and time t of the one-dimensional consolidation problem can be achieved by employing the method of separation of variables as presented in several engineering books [66-68].

$$u(z,t) = \sum_{m=1}^{\infty}\left[\frac{2q}{M}\sin\left(\frac{Mz}{H}\right)\right]e^{-c_v\frac{M^2}{H^2}t} \qquad \left(m = 1,2,3,...\right) \tag{2.5}$$

$$M = (2m-1)\pi/2 \qquad \text{for one-way drainage condition} \tag{2.6a}$$

$$M = m\pi \qquad \text{for two-way drainage condition} \tag{2.6b}$$

2.3 Biot's theory of consolidation

Biot's consolidation theory is regarded as the earliest and most rational theory capturing the multiphase and multidimensional nature of saturated soils, which is related to porous medium and poroelasticity theory. Biot [76, 77] originated successfully the poroelasticity theory to saturated soils assuming Hookean response for the porous soil skeleton and Darcy's law for the water flow in void spaces of soil mass. As a result, partial differential equations (PDEs) for the displacement of soil skeleton and the excess pore water pressure were formulated, which form a coupled system of PDEs representing the conservation of mass and momentum in the soil mass. According to Biot [77], the transient process of soil consolidation can be simulated by adopting the following assumptions:

- The soil mass is isotropic.
- The stress-strain relations are reversible and linear.

– The strains in soil are small.

– The pore water is incompressible and the flow of pore water obeys Darcy's law.

The consolidation of soil is a time-dependent process in which the stress distribution, pore water pressure and soil settlement are functions of time under given applied loadings. Considering a cubic saturated soil element in Cartesian coordinates, where the sides of soil element are parallel to the coordinate axes. Referring to Biot [77], the system of PDEs governing the consolidation behaviour of soil is given by:

$$G\nabla^2 u + \frac{G}{1-2\nu}\frac{\partial \epsilon}{\partial x} - \alpha\frac{\partial \sigma}{\partial x} = 0 \tag{2.7a}$$

$$G\nabla^2 \upsilon + \frac{G}{1-2\nu}\frac{\partial \epsilon}{\partial y} - \alpha\frac{\partial \sigma}{\partial y} = 0 \tag{2.7b}$$

$$G\nabla^2 \omega + \frac{G}{1-2\nu}\frac{\partial \epsilon}{\partial z} - \alpha\frac{\partial \sigma}{\partial z} = 0 \tag{2.7c}$$

$$\nabla^2 = \partial^2/\partial x^2 + \partial^2/\partial y^2 + \partial^2/\partial z^2 \tag{2.7d}$$

$$\alpha = \frac{2(1+\nu)G}{3(1-2\nu)H} \tag{2.7e}$$

where u, υ, ω denote the displacement components of soil corresponding to the Cartesian coordinate axes x, y, z; σ denotes the pore water pressure; ϵ denotes the volume change of soil; G, ν denote the shear modulus and Poisson's ratio of soil skeleton; H is a physical constant.

According to Darcy's law, the components of the flow rate of water in the porous soil can be expressed by:

$$V_x = -k\frac{\partial \sigma}{\partial x} \tag{2.8a}$$

$$V_y = -k\frac{\partial \sigma}{\partial y} \tag{2.8b}$$

$$V_z = -k\frac{\partial \sigma}{\partial z} \tag{2.8c}$$

where V_x, V_y, V_z are the flow rate components corresponding to the Cartesian coordinate axes x, y, z; k is the permeability coefficient of soil.

Due to the assumption of incompressibility of pore water, the rate of water content should be equal to the rate of volume change, i.e.

$$\frac{\partial \theta}{\partial t} = -\frac{\partial V_x}{\partial x} - \frac{\partial V_y}{\partial y} - \frac{\partial V_z}{\partial z} \tag{2.9}$$

Substituting Equations (2.8) into Equation (2.9) would lead to:

$$k\nabla^2 \sigma = \alpha\frac{\partial \epsilon}{\partial t} + \frac{1}{Q}\frac{\partial \sigma}{\partial t} \tag{2.10}$$

where

$$\frac{1}{Q} = \frac{1}{R} - \frac{\alpha}{H} \tag{2.11}$$

According to Biot [77], the coefficients $1/H$ and $1/R$ denote the soil compressibility and the water content change corresponding to a particular change in pore water pressure. The system of PDEs presented in Equations (2.7) and (2.10) are the consolidation governing equations, which are satisfied by the displacement components u, v, ω and the pore water pressure σ in the soil.

As summarised by Selvadurai [78], even though Biot's theory was originally developed for investigating the behaviour of saturated porous soils, his pioneering work

has been applied to various disciplines for a variety of other materials considering several aspects of poroelastic medium such as basic concepts, analytical derivations of solutions, computational programming, nonlinearity of porous skeleton.

The analytical solutions for three-dimensional consolidation of soil subjected to a rectangular load were first derived by Biot [79] and Biot and Clingan [80]. After that, Biot and Clingan [81] studied the plane strain consolidation settlement of a slab under line load and halfspace conditions. De Jong [82] examined the consolidation response encircling pore pressure meters employing Biot's theory. Biot [83] derived successfully the general solutions for the elasticity and consolidation equations of a porous elastic material under isotropic conditions. The displacement and stress fields analogous to the solution of Boussinesq-Papkovitch and the stress function of the elasticity theory were achieved in his study. De Jong [84] applied the stress function to Biot consolidation subjected to a rigid sphere load implanted in a poroelastic halfspace. Gibson and McNamee [85] developed the solution for consolidation of a poroelastic halfspace under a uniform load distributing on a rectangular area. Mandel [86] explained mathematically the influence of pore pressure increase in a poroelastic media due to loadings under plane strain conditions, and Cryer [87] examined the consolidation of a poroelastic sphere due to exterior radial stresses with the existence of drainage boundary. Gibson [88] conducted critical experiments to investigate the three-dimensional consolidation theory. These studies [86-88] confirmed the Mandel–Cryer effect which demonstrates the phenomenological differences in consolidation theories developed by Terzaghi [75] and Biot [77]. Booker [89] derived a solution for consolidation of a clay stratum underlain by a rough stiff base, considering various values of Poisson's ratio and different uniform loadings (strip, circle and square). Booker and Small [90, 91] developed solutions for

two- and three-dimensional consolidations of layered soil by utilising Fourier transform technique in combination with finite layer and finite difference approaches. Smith and Booker [92] and Jiang and Rajapakse [93] investigated mathematically the combined heat-moisture transfer (thermal consolidation) in porous medium. Recently, several remarkable theoretical studies have been also carried out to examine the response of saturated porous medium accounting for various aspects such as thermal consolidation of multilayered soils with anisotropic permeability and thermal diffusivity, dynamic behaviour of layered saturated soil under impulsive, harmonic and moving loads, multi-dimensional consolidation of viscoelastic saturated soils [94-97].

Although the consolidation analysis based on Biot's theory is supposed to be rigorous in nature of loaded saturated porous medium, this approach might cause major challenge to the derivation of analytical solutions for consolidation of soft soils supported by pervious columns. Indeed, Biot [77] developed consolidation theory considering three-dimensional configuration, where the consolidation and deformation of soil body are incorporated concurrently in the mathematical model assuming some physical constants for the property of soils (e.g. $G, \nu, H \; and \; R$ as mentioned above). In contrast, the theory of consolidation initiated by Terzaghi [68, 75] ignored the deformation aspect and thus the mathematical formulation is simplified with less parameters characterising the property of soils than Biot's theory. As a result, the multi-dimensional consolidation of soft soils can be examined in a simpler way, such as the consolidation analysis of drain well assisted fine-grained soils conducted by Barron [64] and Yoshikuni and Nakanodo [98] in which the soil was assumed to deform vertically (i.e. one-dimensional deformation) and the effect of shear strains was neglected (i.e. ignoring the deformation aspect). Even though the consolidation investigations based on Terzaghi's theory are not

stringent compared to Biot's theory, these approaches may be applicable to the consolidation of soft soils subjected to loading conditions such that the soil deformation is likely to be one-dimensional (e.g. soft soils under large area of uniform loadings or vicinity of embankment centre).

2.4 Consolidation of soft soils assisted by pervious elements

Saturated soft soils subjected to external surcharges exhibit a very slow dissipation of excess pore water pressure towards their natural drainage boundaries. Therefore, to accelerate the dissipation rate of excess pore water pressure and hence the consolidation process of the soils, vertical drains are usually installed into the saturated soil stratum to provide additional drainage paths in horizontal directions for the excess pore water pressure. The concept of fine-grained soil consolidation supported by vertical drains was introduced in 1930s by several researchers [64, 99-101]. Barron [64] developed successfully the consolidation theory for drain well assisted fine-grained soils, analysing the dissipation of excess pore water pressure in a unit cell model. A unit cell is a cylindrical drain well – soil system including a vertical drain well of radius r_w and the adjoining soil expanding to the influence radius r_e of that drain well (refer to Figure 2.2). This concept has been also applied widely to study the consolidation of soft soils reinforced by other types of pervious columns, such as compacted sand columns, stone columns and soil-cement mixing column. As indicated by Balaam and Booker [4], the behaviour of this unit cell sufficiently describes the behaviour of a pervious column supported ground, particularly for the composite ground region near the centre of the embankments.

Analogous to the study conducted by Terzaghi [75], on the basis of the equilibrium principle between the rate of squeezing water and the rate of volume change in a soil element, Barron [64] derived the following partial differential governing equation for the axisymmetric consolidation of soft soil under the application of instant loading:

$$c_h\left(\frac{\partial^2 u(r,z,t)}{\partial r^2}+\frac{1}{r}\frac{\partial u(r,z,t)}{\partial r}\right)+c_v\frac{\partial^2 u(r,z,t)}{\partial z^2}=\frac{\partial u(r,z,t)}{\partial t}\quad\left(r_w\le r\le r_e\right) \tag{2.12}$$

where u is the excess pore water pressure at any coordinate (r,z) and time t; $c_h=k_h/(\gamma_w m_v)$ and $c_v=k_v/(\gamma_w m_v)$ are the consolidation coefficients of soil in the radial and vertical directions, respectively; k_h and k_v are the radial and vertical permeability coefficients of soil, respectively.

Although the obtained governing equation includes the orthotropic flows of excess pore water pressure in radial and vertical directions, Barron [64] derived the solutions by separating roughly the governing equation into two one-dimensional consolidation equations in accordance with the vertical and radial flows as follows:

$$c_v\frac{\partial^2 u_z(z,t)}{\partial z^2}=\frac{\partial u_z(z,t)}{\partial t} \tag{2.13}$$

$$c_h\left(\frac{\partial^2 u_r(r,t)}{\partial r^2}+\frac{1}{r}\frac{\partial u_r(r,t)}{\partial r}\right)=\frac{\partial u_r(r,t)}{\partial t}\quad\left(r_w\le r\le r_e\right) \tag{2.14}$$

where $u_z=u_z(z,t)$ and $u_r=u_r(r,t)$ denote the excess pore water pressures corresponding to z- and r-domain.

The excess pore water pressure solution for the vertical consolidation is derived resembling completely the formulations proposed by Terzaghi [75], whereas the solution for the radial consolidation adopts the following boundary conditions:

$$u_r(r_w, t) = 0 \tag{2.15a}$$

$$\frac{\partial u_r(r_e, t)}{\partial r} = 0 \tag{2.15b}$$

The boundary condition in Equation (2.15a) simulates the fully drained surface of the drain well, while Equation (2.15b) implies no radial flow across the exterior vertical surface of the unit cell.

Likewise the consolidation in the vertical direction, the excess pore water pressure corresponding to the radial consolidation of soil is supposed to carry entirely the total stress induced by the instantly applied loading q, which distributes uniformly over the soil area. Thus, the initial condition of excess pore water pressure for the radial consolidation would be expressed by:

$$u_r(r, 0) = q \tag{2.16}$$

The radial consolidation formulation presented in Equations (2.14) − (2.16) is a free strain consolidation problem, which can be solved to achieve the excess pore water pressure solution utilising the method of separation of variables. Barron also developed the solution for the case of equal strain consolidation in the same study. Further discussion on the concepts of equal strain and free strain consolidations will be provided in the next section.

For the combined effect of vertical and radial flows, Barron [64] suggested an approximate solution as the product of the excess pore water pressure solutions obtained from the vertical and radial consolidation analyses.

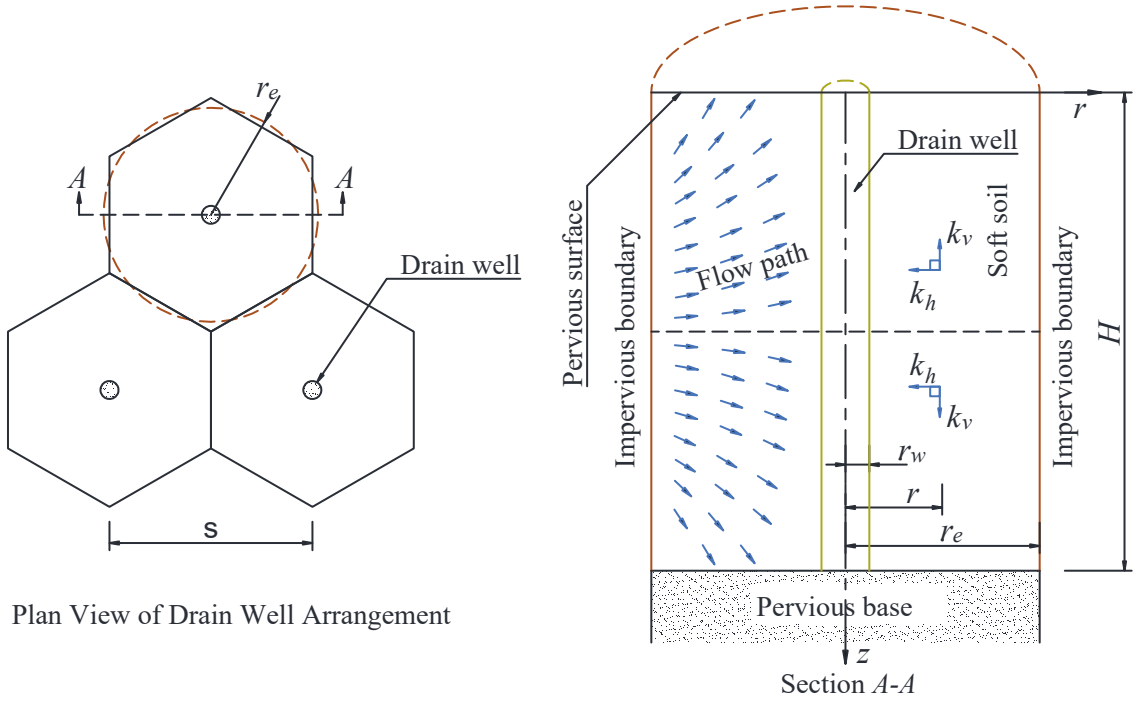

Figure 2.2. Arrangement pattern of drain wells on plan and unit cell model for the consolidation of soil (after Barron [64])

It is noteworthy mentioned that the axisymmetric unit cell model shown in Figure 2.2 can be converted into a two-dimensional plane strain model for the sake of simplification in calculations. To establish an equivalent plane strain model, a number of studies have been carried out matching the analytical solution of the plane strain model to that of the axisymmetric model, such as those by Hird et al. [102], Indraratna and Redana [103], Tan et al. [104], Parsa-Pajouh et al. [105], Indraratna and Redana [106]. By means of that, the equivalent geometries or material properties (e.g. stiffness and permeability) of the drain well and encircling soil can be attained for the consolidation analysis. Figure 2.3 presents the schematic conversion reported by Indraratna and Redana [103], which includes a smear zone (disturbed soil) around the drain due to the effect of drain installation process.

The same conversion method is applicable to the consolidation analysis of soft soil reinforced by various permeable columns.

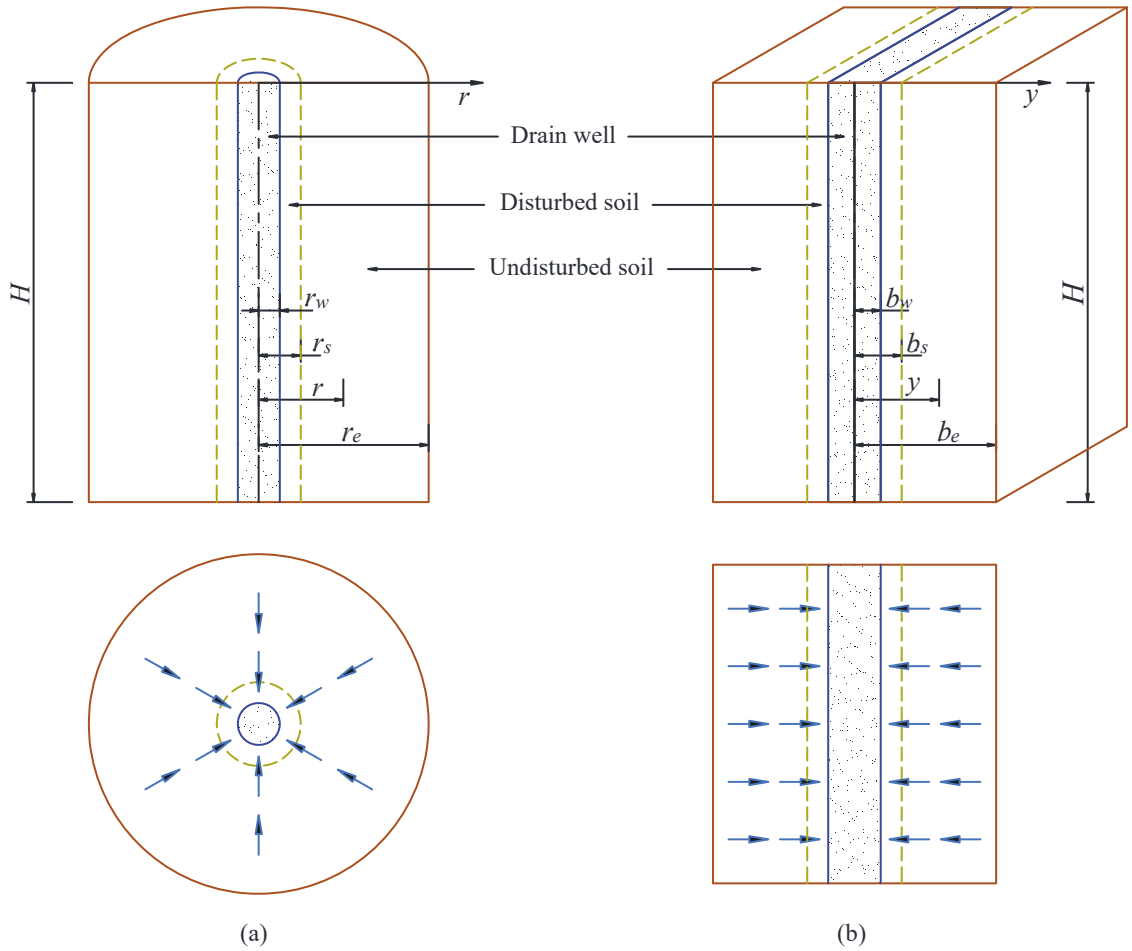

Figure 2.3. Conversion of (a) axisymmetric unit cell into (b) plane strain unit cell (after Indraratna and Redana [103])

Drain wells and stone columns in combination with surcharge preloading are extensively utilised to speed up the consolidation of soft soil. Since the well-known study of Barron [64], there have been a large number of theoretical investigations on vertical drain considering the effect of many influencing factors to reflect more precisely on the realistic consolidation behaviour of composite ground. These factors include well

resistance with a finite hydraulic conductivity assigned to the vertical drain, smearing effect for the soil surrounding the drain due to the installation of drain system, the variation of total stress in soil under surcharge loading with respect to time and depth, the simultaneous consideration of vertical and radial flows in the governing equations of consolidation, the nonlinear and viscoelastic properties of soil, and so on. Several remarkable analytical solutions were presented by various researchers addressing the above issues [98, 107-117]. Apart from the aforementioned studies for saturated soils, recent years have also experienced vibrant progress in theoretical analyses for the consolidation of unsaturated soils [118-126].

On the basis of consolidation theories developed for soft ground with vertical drains, further studies were conducted for stone column-improved foundations in which granular columns not only accelerate the consolidation rate and reduce the total and differential settlements, but also intensify the bearing capacity, enhance the embankment and natural slope stability, and diminish the liquefaction potential [55]. As reported by several researchers [16, 58, 127], in addition to accelerating the consolidation process, since stone columns are generally stiffer than the surrounding soft soil, they also decrease the compressibility of the composite ground leading to a reduction in settlement of the ground subjected to applied loads.

In the last few decades, numerous studies with significant contributions on the consolidation response of soft ground improved with granular columns have been carried out by researchers, particularly with ground improvement interests. Balaam and Booker [4, 128] presented an elastic solution considering both vertical and radial deformations of a single granular column and its surrounding soil underneath rigid foundations, which

was then extended by the assumption of elastic - perfectly plastic material for the column. Han and Ye [129] proposed a simplified closed-form solution for the radial consolidation of soft soil with granular columns taking into account smear and well resistance effects by using a modified consolidation coefficient which contains the volumetric compressibility of stone column. Zhang et al. [130] considered the variation of horizontal permeability coefficient of the soil around a stone column with the simultaneous investigation of radial and vertical flows in governing equation, while Wang [131] obtained an analytical solution under different types of time-dependent loading accounting for the radial flow only. Lu et al. [132] derived the governing equations for consolidation of a stone column and its surrounding soil considering the variation of horizontal permeability coefficient of the disturbed soil and the linear variations of total stresses with depth. By introducing an initial condition based on the equilibrium condition of the vertical stresses and the equal vertical strain assumption, they achieved a theoretical solution for the radial and vertical consolidations in a coupled manner. Castro and Sagaseta [55] developed a closed-form analytical solution for radial consolidation accounting for the longitudinal and lateral deformation of a stone column in both elastic and elastoplastic states. Additionally, Castro and Sagaseta [56] conducted a numerical analysis to investigate the deformation and consolidation around stone columns in a coupled fashion and examined the reliability of various analytical solutions. The laboratory study of the same problem was also performed by Cimentada et al. [57]. A series of numerical models analyzing the behaviour of granular column-improved soft ground was also employed by other researchers [16, 105, 133, 134].

It is important to note that there are two significant differences in consolidation of soft soils using drain wells and high modulus granular columns (e.g. stone columns). Firstly,

the stiffness of stone column is dominantly higher than that of surrounding soft soil. According to Barksdale and Bachus [2] and Balaam and Booker [4], the ratio of elastic drained modulus between stone column and enclosing soil for a typical stone column stabilised soft soil foundation could range from 10 to 40. This dramatic difference in stiffness would lead to a redistribution of total stresses caused by external loadings between the column and soil regions in the composite foundation, which has a substantial impact on the consolidation as well as the general response of the reinforced foundation. Secondly, stone columns have a smaller radius ratio (i.e. the ratio between the influence radius of a column and the radius of that column) compared to drain wells. Han and Ye [127, 129] reported the typical range of radius ratio for stone columns about 1.5 – 5, whereas Barron [64] suggested this ratio varying between 5 and 100 for drain wells. The influence zone of each granular column and drain well, which is related to the lateral pressure of encircling soil is impacted by construction methods considerably. For example, the compaction of aggregates using the vibroflot during the installation of stone columns would cause significant cavity expansion and accompanying lateral pressure from stone columns towards the surrounding soil. In contrast, the lateral pressure due to the penetration of vertical drains (e.g. prefabricated vertical drains) would be smaller than that of stone columns. The effects of various factors on the consolidation of soft soils reinforced by drain wells and stone columns will be mentioned more in the next sections.

2.5 Equal strain and free strain consolidations of soft soil stabilised by stone columns

Most of the available analytical models for consolidation of soft soil reinforced by stone columns in the literature are based on the assumption of equal vertical strain and thus

incapable of predicting varying ground surface settlement with the radial distance from the stone column. As explained by Indraratna et al. [133], the equal strain condition is applicable only when the surcharge load is applied on the soil surface through a rigid platform inducing an unequal stress distribution on the ground surface. For example, referring to Barron [64], a typical low embankment applies a uniform surcharge on a flexible platform, resulting in a rather uniform distribution of stress on the ground surface, which induces a differential surface settlement (i.e. free strain condition). Owing to the certain flexibility of platform and embankment, the free strain approach can represent more realistic results than the equal strain hypothesis. Furthermore, under free strain condition, the encircling soil undergoes larger settlements than the stone column and the soil settlement is prone to increase with radius away from the column as the consolidation time elapses, owing to the significant lower stiffness of the soil compared to the stone column. The difference between equal strain and free strain consolidations of the composite stone column – soft ground is illustrated schematically in Figure 2.4.

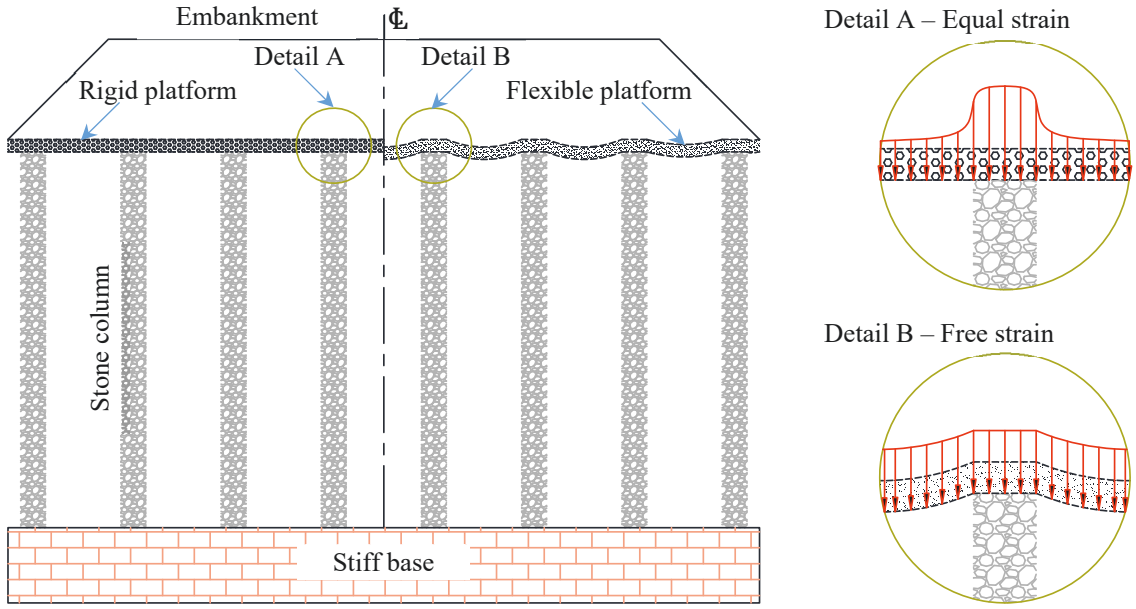

Figure 2.4. Consolidation settlement of the composite stone column – soft ground under equal strain and free strain conditions

2.6 Effects of drain resistance, clogging, smear and partially drained boundaries

During the consolidation of soft soils improved with vertical drains, the excess pore water pressure dissipates towards the vertical drain where the pore water enters the drain and is expelled along the length of drain to drainage soil boundaries. The dissipation rate of excess pore water pressure depends upon not only the consolidation parameter of the soil body (i.e. permeability and volume change coefficients) but also the discharge capacity of the drain. The discharge capacity of a drain well is characterised by cross-sectional area and permeability of the drain. In real practice, the discharge capacity of the drain is governed by various additional factors, which comprises of the lateral pressure from surrounding soil, the possible bending, crimping, folding, buckling and kinking of drains (in case of using prefabricated vertical drains), the intrusion of fine soil particles into drains obstructing the flow of pore water [135, 136]. The finiteness or reduction in

discharge capacity of drains is known as the drain resistance phenomenon. Similar to drain wells, stone columns also endure the drain resistance due to the finite permeability of stone material (in terms of aggregate), which decelerates the consolidation process of the composite stone column – soft soil foundation.

Even though stone columns possess high permeability, the voids among solid aggregate particles are extremely large, which are easily infiltrated by the fine soil particles from the encircling soft soil during the construction and consolidation periods. As a consequence, the void spaces and accompanying permeability of stone columns are decreased, that leads to the deceleration of excess pore water pressure dissipation and consolidation process. The effect in which the dissipation of excess pore water pressure in the granular column supported soft soil is decelerated due to the contamination of aggregates in the column with fine-grained soil particles is called clogging.

In addition to the drain resistance and clogging phenomena, another effect which is unavoidable during the installation of vertical drains and granular columns is the smearing of soil surrounding the drains and columns. The influence of smearing on the consolidation is commonly taken into account by capturing the size of smear zone and the variation of consolidation parameters in smeared (disturbed) soil. Numerous laboratory experiments show that the permeability of disturbed soil around the installed drain decreases gradually towards the drain surface [137-139], whereas the radius of smear zone is assumed in range of 1.6 – 4 times the mandrel (or the equivalent drain) radius [107, 140].

Another issue regarding drainage efficiency is the drained capacity of drainage boundaries. Analogous to drain wells, the top drainage surface of soil stratum (in case of

one-way drainage in the vertical direction) or both top and bottom drainage soil surfaces (in case of two-way drainage in the vertical direction) are not fully drained boundaries because of the finiteness of hydraulic conductivity (permeability) of the drainage materials at these locations. Such boundaries for the dissipation of excess pore water pressure are referred to as impeded drainage boundaries which were investigated by several researchers [141-144].

Several studies have been performed to consider the independent or combined effects of well resistance, smearing, clogging and impeded drainage boundaries on the consolidation of soft soils stabilised with vertical drains or granular columns. Indraratna and Redana [103, 106] developed two-dimensional plane strain numerical models accounting for the smear and well resistance effects in combination with the modified Cam-clay theory for single- and multi-drain cases. Han and Ye [129] proposed a simplified solution for the radial consolidation of stone column improved soft soil considering the impacts of smear and drain resistance, in which the effect of the difference in stiffness between the column and soil areas is included by introducing modified coefficients of consolidation. Walker and Indraratna [145] conducted a simplified analytical examination on the overlapping smear zones of vertical drain consolidation assuming a linear diminution in the permeability of disturbed soil towards a drain. The investigation on the overlapping smear zones can provide an interpretation for a minimum drain spacing, below which the consolidation rate does not increase any more. Deb and Behera [146] developed an analytical model for the consolidation of soil stabilised by stone columns adopting the variation of horizontal permeability and volume change coefficients for the disturbed soil zone. Three change patterns of consolidation parameters against radius of smear zone were taken into consideration including constant, linear and

parabolic distributions. Deb and Shiyamalaa [52] provided a mathematical model to examine the effect of clogging on consolidation rate of stone column improved soft soil, taking account of the migration of fine-grained soil particles into the void spaces of aggregates around the vertical surface of stone column. Tai et al. [53] investigated experimentally the time-dependent clogging in a unit cell model, applying the computed tomography to determine clogging and accompanying void space in the column sample. Then, they proposed a mathematical model to evaluate the variation of clogging with consolidation time. Many researchers developed analytical solutions for consolidation of permeable column supported soft soils incorporating the associated effects of partially drained boundaries, smear and drain resistance, such as those by Lei et al. [46], Zhou et al. [47].

2.7 Impacts of total stress variations against space and time on consolidation

One of the important factors that highly affects the consolidation of permeable column improved soft ground is the rate of loading on the ground surface. The change of external loading against time is commonly encountered in real construction projects, where any construction process takes time to be finalised and thus results in the increase or decrease of loading with construction time. It is recognised that the loading rate during the construction stages of infrastructures built on soft soils should be controlled properly. A rapid increase of external surcharge on soft soils corresponding to the undrained condition of the soils may cause the collapse of soil foundation and superstructures. On the other side, an extremely slow increase of load on the ground surface to avoid completely the failure of soil foundation may prolong the construction time and affect the general construction schedule, which is usually related to the economic efficiency. Therefore, a

reasonable loading rate such that the saturated soft soil foundation has sufficient time to dissipate parts of the excess pore water pressure induced by external loading and gain sufficient increase in shear strength and bearing capacity for the next surcharge loading would guarantee the technical and economic efficiency. The loading and unloading processes may also occur repeatedly during the service stages of some construction facilities, for instance, storage tanks, silos, warehouses, seaports and stockpiles.

The consolidation analysis of the composite ground subjected to a time-varying loading is carried out via the presence of time-varying total stresses caused by the loading in the mathematical model. It should be noted that the total stresses in the composite ground may also vary against radius and depth. Considering a composite ground subjected to a uniform loading on the surface, the induced total stresses in the ground are deemed to decrease with depth rather than being distributed uniformly, particularly when the thickness of soft soil stratum is much larger than the distribution area of loading on the ground surface. Additionally, under the free strain condition, the distribution of total stresses in the soil stratum would become more complicated, in which the total stresses experience the redistribution process against both radius and depth due to the development of shear strains and shear stresses induced by the progressive differential settlements during the consolidation. By adopting the equal strain assumption for the settlement of granular column supported soft soils (i.e. the differential settlements and the mentioned effects of shear strains cannot be captured), numerous analytical studies have been taken to examine the effects of depth- and time-varying total stresses induced by external surcharges on consolidation response [44, 45, 131, 132].

2.8 Effects of layered soils and partially penetrated columns

The in-situ soils are often non-homogeneous where the soil stratigraphy consists of multilayers. Thus, it is unrealistic to model the soil in field with a simplified soil layer in many cases, for example, consolidation of multi-layered soils. While the analytical solutions for one-dimensional consolidation of layered soils may be developed readily, the computational efforts would be required significantly when the number of soil layers increases. This is due to the increase in the number of interface boundary conditions which simulate the continuity of excess pore water pressure and flow rate at interfaces. For instance, a double-layered soil would require four boundary conditions and a triple-layered soil would need six boundary conditions [147, 148]. Consequently, the size of matrix equation which is established from the boundary conditions of excess pore water pressure dissipation becomes larger along with the increase in the number of unknown coefficients to be determined from the matrix equation. The problem would be significantly complicated for coupled radial (or horizontal) – vertical consolidation of multi-layered soils, particularly when there are also more than two layers in radial (or horizontal) direction to be included to model the clogging and smear zones around pervious columns.

Even though there have been numerous analytical studies for consolidation of soils with pervious columns [149-151], the complexity of the mathematical derivations would limit the application of the obtained solutions. Another issue which has a similar nature to multi-layered soils in deriving the consolidation solutions is the partially penetrated columns in soil stratigraphy. For example, the partial penetration of columns in a single-layered soil might be considered as a consolidation problem of a two-layered soil, which

includes a homogeneous soil layer below the column tip and a column reinforced layer. To derive the consolidation solutions for layered soils and soils stabilised by partially penetrated columns or floating columns avoiding the complexity of analytical solutions, the spectral method [152, 153] or matrix method [154] can be employed. For the sake of simplification, numerous studies also developed consolidation solutions for soft soils supported by floating columns or partially installed columns by converting the column supported layer to an equivalent soil layer characterised by composite consolidation parameters [49, 155-158]. Thus, the simplified analytical solutions can be achieved corresponding to the equivalent one-dimensional consolidation of multi-layered soils.

2.9 Effects of nonlinearity, rheology and unsaturation of soil on consolidation

The conventional consolidation theories commonly adopt several assumptions to simplify the mathematical models and obtain the analytical solutions, in which the soil properties are considered as unchanged with depth and time and fully saturated. In many cases, the adoption of these assumptions may cause significant disparities in estimating the consolidation response of soft soils in field. Indeed, the consolidation of soft soils is regulated by various factors regarding the nonlinear, rheological and unsaturated characteristics of the soils, such as the nonlinearity in relationships among permeability, compressibility, void ratio and effective stress in the soil. As the consolidation progresses, the void ratio reduces with the increase of effective stress owing to the dissipation of excess pore water pressure, which leads to the reduction in permeability and compressibility of soils. Considering the major effects of the nonlinear properties of soft soils on their consolidation behaviour, Davis and Raymond [159] developed a one-dimensional analytical solution for consolidation of soft soil subjected to a constant

loading, assuming that the permeability reduction is proportional to the compressibility diminution during the consolidation and the initial effective stress distributes uniformly over the soil depth. Gibson et al. [160], Gibson et al. [161] proposed nonlinear finite strain theories to predict the one-dimensional consolidation of thin and thick saturated homogeneous soil layers, respectively. Based on the study conducted by Davis and Raymond [159], the analytical solutions for nonlinear consolidation of single- and double-layered soils under time-dependent loading were derived by Xie et al. [147], Xie et al. [162]. The nonlinearity effects of soil properties on the soil consolidation stabilised by drains and stone columns were also investigated analytically by various researchers [60, 163-165].

The theory for consolidation of soft soils incorporating the secondary compression of the soils was developed early by Taylor and Merchant [166]. After that, several efforts were made to capture the influence of rheological property of soils on the long-term one-dimensional consolidation [167-171]. However, there have been limited analytical studies on two-dimensional or axisymmetric consolidation of soils, particularly with the inclusion of vertical drains or granular columns integrating the effect of rheological characteristics of soil stratum [96, 172]. This may be due to the complex nature of the mathematical derivations for the problem under consideration.

In the last few decades, an emerging consolidation problem that has attracted the great interest of researchers is related to the unsaturated soils. In engineering practice, it is common to encounter the construction projects which are built on unsaturated soils. While the traditional consolidation theories can provide acceptable predictions in excess pore water pressure dissipation and consolidation settlement of the saturated soils, these

classical theories are obviously inappropriate for unsaturated soils. Therefore, several researchers have developed new theoretical models for unsaturated soil consolidation in the early 1960s [173-176]. On the basis of these pioneering works, recent years experienced vibrant progress in developing analytical consolidation solutions for unsaturated soils [123, 124, 177-182]. Nevertheless, there have been very limited analytical consolidation studies for unsaturated soils reinforced by compacted granular columns, particularly under free strain condition for the composite ground owing to the complexity of the mathematical formulations.

2.10 Deformation of the composite stone column stabilised soft ground supporting embankments

Unlike the vertical drain consolidation where the stiffness of drains is ignored, the consolidation behaviour of stone column reinforced soft ground depends upon the stone column stiffness predominantly. During the consolidation process, the deformations of the stone column and surrounding soft soil regions are governed by the dissipation of excess pore water pressure, the difference in stiffness between the stone column and soft soil, and the flexibility of the platform – embankment system.

Since the stiffness of stone columns is substantially higher than that of encircling soft soil, the dominant portion of the embankment loading would be carried by stone columns. In case of the embankment supported by the composite ground through a rigid platform, the column and soil settlements are equal at any time during the consolidation. The embankment loading would be shared between the stone column and surrounding soft soil as a proportional relationship to the stiffness (modulus) ratio of the column to the soft

soil [127]. In contrast, when the platform – embankment system is rather flexible, the differential settlement between the soft soil and stone column would happen. Considering an instant construction of the embankment on the saturated composite stone column – soft soil, the column settlement progresses rapidly due to the extremely quick dissipation of excess pore water pressure in the stone column, while the soil settlement is negligible under the undrained condition of soft soil right after loading. Thus, the surrounding soil tends to carry more loads than the stone column as a result of soil arching over the top of stone column. After that, the soft soil consolidates as the excess pore water pressure in the soil dissipates, which leads to the increase of soil settlement and the decrease in the differential settlement between the stone column and soft soil during the very beginning stage of soil consolidation. The applied loading tends to be shared equally between stone column and surrounding soft soil when the soil settlement is equal to the column settlement. Thereafter, the soft soil continues to consolidate and settle more than the stone column, which results in the soil arching in the embankment between consecutive stone columns (i.e. the inversion of the previous soil arching). Due to the inverse soil arching, the stone column would carry more loads than the soft soil. The larger settlement of soft soil compared to stone column would also lead to the transfer of loads from soft soil onto stone column along the column – soil interface, which causes the increase of stone column settlement to counteract the increase in the differential settlement between soft soil and stone column. The redistribution of loading and accompanying total stresses between the stone column and surrounding soft soil progresses until the end of the consolidation process.

It should be noted that, under the applied loading on the ground surface, the stone columns tend to deform laterally towards the encircling soft soil, particularly at the upper

part of the stone column where exists the extremely high concentration of total stresses. The stress concentration might cause the bulging of stone columns and failure in terms of shearing when the confinement pressure provided by encircling soft soil is low. Therefore, the usage of stone columns would be effective when they are penetrated in soft soils having appropriate shear strength, specifically with a minimum undrained shear strength of about 20 kPa [183]. Figure 2.5 illustrates the deformation mechanism of a typical embankment fill – soft soil foundation system improved by stone columns, in which the platform is reinforced with geosynthetics. The differential settlement ΔS between soft soil and stone column cause the mobilised shear stress in the embankment, which forms the soil arching. Moreover, the concentration of total stress on the column top due to the soil arching induces the lateral yield (bulging) at the upper part of the stone column.

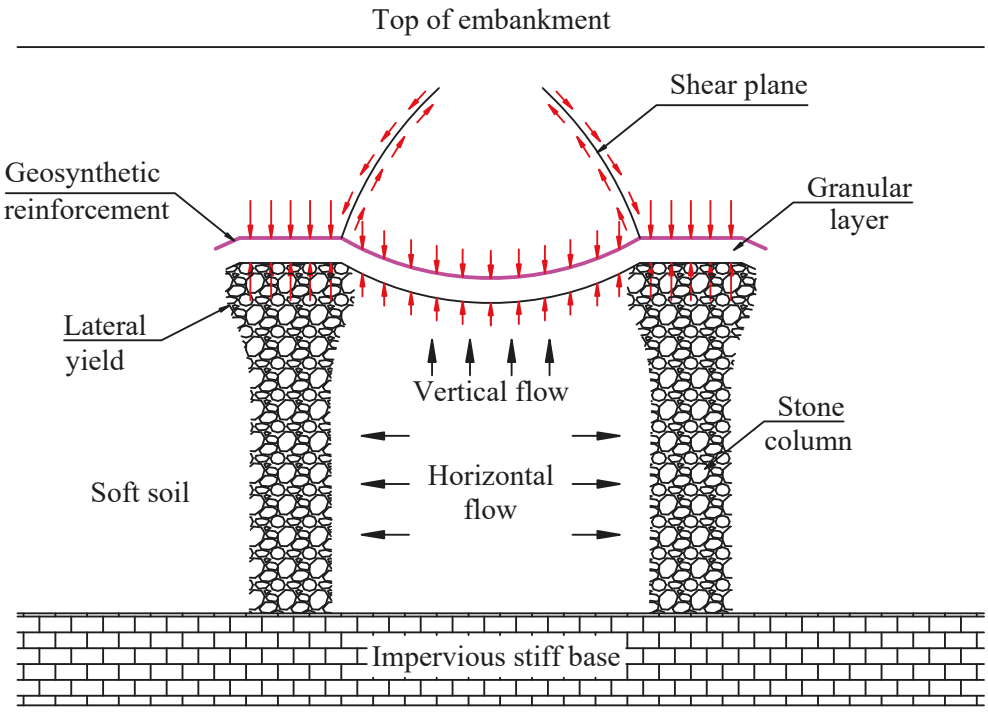

Figure 2.5. Deformation of a typical embankment fill – soft soil foundation system stabilised by stone columns (after Deb [184] and Basack et al. [185])

2.11 Analytical methods for consolidation of soft soils supported by pervious columns

The consolidation problem of soft soils reinforced by permeable columns is a kind of diffusion problem encountered in several fields of study, which is related to porous medium. The mathematical model for the consolidation is formulated via governing equations, boundary and initial conditions [186, 187]. The governing equations are partial differential equations (PDEs) which can be independent or dependent of each other, homogeneous or non-homogeneous and linear or nonlinear. These PDEs are usually in form of second-order parabolic equations. The boundary and initial conditions can also be homogeneous or non-homogeneous. In case of independent PDEs, the governing equations are bound via boundary conditions, which are related to the boundary value

problems (Sturm–Liouville problem) [186, 188]. In contrast, when the PDEs are dependent and form a system of PDEs, the problem under consideration becomes more complex and is frequently known as the diffusive Lotka-Volterra problem [189, 190]. While the derivations for the analytical solutions of boundary value problems are possible in many cases, those of Lotka-Volterra problems are very challenging. Therefore, the solutions for the latter are frequently derived in form of semi-analytical or numerical outputs [191-194]. To derive the analytical solutions for the consolidation of soft soils improved with pervious columns, the following common approaches might be employed [188, 195-197]:

- Method of separation of variables.
- Duhamel's theorem.
- Laplace transform technique.
- Integral transform technique.
- Green's function method.

The separation of variables is a conventional approach which is the basis of several other methods. The method of separation of variables is commonly used to solve homogeneous problems (i.e. homogeneous PDEs) under one- or multi-dimensional configurations. The solution of homogeneous problems can be readily derived using this approach when there is only one non-homogeneous term regarding initial or boundary conditions and the PDEs and boundary conditions are linear. For the problem with more than one non-homogeneous term (non-homogeneity in either PDEs or initial and boundary conditions), this method can also be applied to obtain analytical solutions by splitting up the original problem into more simple problems and using the superposition principle. However, the non-homogeneity in PDEs (the non-homogeneous terms in PDEs

are usually called generation terms or source terms) and boundary conditions, which are time-dependent ones, may not be handled using the method of separation of variables. By taking separation of variables, the PDEs would be separated into ordinary differential equations (ODEs) and accompanying boundary conditions, which form boundary value problems. The process of solving boundary value problems results in eigenfunctions (i.e. corresponding to dependent variables) and eigenvalues (i.e. corresponding to independent variables), where the eigenfunctions are orthogonal functions [198]. Indeed, an important technique utilised while solving boundary value problems is the orthogonal expansion (eigenfunction expansion) technique.

To overcome the above-mentioned disadvantages of the method of separation of variables, several other methods can be employed such as Duhamel's theorem, Laplace transform, integral transform and Green's function method.

On the basis of superposition principle, Duhamel's theorem is applicable to non-homogeneous linear consolidation problems, where the non-homogeneous terms in PDEs and boundary conditions can be time-dependent terms. The method is conducted by taking advantage of the solution of the same consolidation problem yet with time-independent source terms and boundary conditions.

The application of Laplace transform technique is related to the elimination of partial derivatives with regard to time variable. Therefore, this method is applicable to the problem with non-homogeneous time-dependent source terms and boundary conditions in which the time-dependent functions are transformed into the corresponding functions in Laplace domain. This method allows to address the transient problem in a small-time domain with a rapid convergence of the obtained analytical solution, due to the

availability of small-time approximations. The transient problems with small values of time are commonly seen in the study of heat conduction. In contrast, the consolidation is a time-dependent problem corresponding to the long-term behaviour of soft soils, where the soil permeability is low and the dissipation of excess pore water pressure progresses slowly. In the method of Laplace transformation, the original problem is first transformed into Laplace domain to derive the corresponding solution. Then, the final solution in physical domain (i.e. corresponding to the original problem) would be derived by taking inverse Laplace transform. However, the inversion of Laplace transform is not always available and the numerical approximations would be applied for this purpose in many cases.

While the use of Laplace transform approach would remove the time variable in consolidation problems, the employment of integral transform technique would eliminate the space variables in the problems. By imposing integral transforms on the mathematical model of consolidation problem in physical domain, PDEs would be transformed into first-order ODEs of the transformed dependent variable (i.e. transformed excess pore water pressure in the consolidation problem) with respect to time variable (i.e. independent variable). The ODEs would be solved considering the transformation of initial conditions, then the outputs are inverted to achieve the final solutions in physical domain (i.e. excess pore water pressure). The integral transform technique is derived on the basis of the separation of variables approach, where an integral transform pair (i.e. inversion formula and integral transform) required for the solution of a particular problem is formulated by taking advantage of eigenfunction expansion technique. Thus, the establishment of the integral transform pair is the mandatory demand prior to any derivation to obtain the final solutions.

Finally, this section mentions about Green's function method which might be considered as the powerful and general method to solve the consolidation problem with a generalised non-homogeneity in source terms and boundary conditions. Compared to the Laplace transform and integral transform techniques, the Green's function approach without using the intermediate steps of transformation and inversion in the mathematical model is more straightforward to derive the final solution. The utilisation of Green's function approach uses Green's formula and the derivation of Green's function which is the major implementation to obtain the final solutions of the consolidation problem. Once the Green's function has been established for the problem, the final solution can be achieved by substituting the Green's function into Green's formula of the excess pore water pressures. To derive the Green's function, several methods can be employed including some of the previous mentioned methods such as separation of variables, Laplace transform, images, product solution, and eigenfunction expansion [196, 197].

2.12 Summary

Most existing analytical consolidation studies adopt the equal strain condition for the settlement, which is supposed to be suitable for the consolidation of soft soils assisted by prefabricated vertical drains (PVDs) or sand drains where the stiffness of drains is ignored in the mathematical formulation. The equal strain hypothesis is also applicable to the composite ground supporting surcharge loadings via a rigid platform which ensures no differential settlement occurs on the ground surface and at any depth of the ground. In contrast, for a flexible platform, a uniform surcharge loading would cause significant differential settlement between the column (e.g. stone columns and soil-cement mixing columns) and the surrounding soft soil. Indeed, the extreme higher stiffness of the column

in comparison to the soft soil would lead to unequal settlements at a given depth. In reality, the settlement increases gradually from the column – soil interface towards the mid-point between two columns within the soil region. The differential settlement also increases with time as a consequence of excess pore water pressure dissipation in the soft soil during the consolidation process. In contrast, by ignoring the time-dependent consolidation analysis, several researchers investigated the free strain deformation of the composite stone column – soft soil foundations. Alamgir et al. [65] proposed a theoretical method to predict the elastic vertical deformation of the mentioned composite ground subjected to a uniform load through a flexible platform, by assuming a settlement pattern for the ground. Taking advantage of this study, Deb and Mohapatra [199] developed a model to study the two-dimensional (2D) plane strain behaviour of a stone column improved soft soil under a geosynthetic-reinforced embankment. On the same basis, Zhao et al. [22] and Zhao et al. [23] provided the axisymmetric deformation models for the systems of soft soil foundations overlain by geosynthetic-unreinforced and -reinforced embankments, respectively. Another series of theoretical studies [184, 200-202] has also been done to examine the 2D plane strain response of the embankment fill – soft soil foundation systems assisted by stone columns, considering various influencing factors capturing the consolidation of soft soil. However, these studies analysed the deformation and consolidation of the composite stone column – soft soil foundations in an uncoupled manner. Indeed, to account for the consolidation effect in the proposed models, they adopted the simplified consolidation solution developed by Han and Ye [127] in combination with a modification to convert the axisymmetric unit cell model into a plane strain unit cell configuration as suggested by Hird et al. [102]. While ignoring the drain resistance and smear effects, Han and Ye [127] employed Carrillo's method [203] to

combine the radial and vertical consolidations in the analysis, which is only valid for the homogeneous governing equations of consolidation [204]. It should be noted that the distribution of total vertical stresses on the composite ground would vary with time due to the interaction between the stone column and surrounding soft soil. In other words, there is a progressive stress transfer mechanism from the soft soil onto the column along the column – soil interface when incorporating the deformation analysis into the process of consolidation. The stress transfer mechanism progresses in reaction to the development of differential settlement between soft soil and stone column as the excess pore water pressure dissipates during the consolidation process. As a consequence, the governing consolidation equations for stone column and soft soil regions in the unit cell model would be non-homogeneous due to the existence of the non-homogeneous terms (i.e. time-dependent total vertical stresses), and thus the application of the Carrillo's method [203] is not applicable or accurate. It is worthwhile to mention that the combined deformation – consolidation analysis should be considered for a saturated soft soil deposit stabilised by stone columns in which the deformation of ground is recognised as the accompanying output of the free strain consolidation process. In fact, the composite ground deforms progressively from the undrained condition right after applying the instant loading until the fully drained condition at the end of consolidation when the excess pore water pressure in the soil foundation would dissipate completely. Eventually, all of the existing theoretical studies on the composite ground deformation in the literature [22, 23, 65, 184, 199-202] employed the numerical finite difference approach for the unit cell in which the stone column and soft soil regions were divided into a mesh of finite number of column and soil elements. This theoretical approach might cause inconvenience for the practical application due to the challenge of computational efforts.

Therefore, the following chapters of this thesis will present innovative analytical approaches to address the shortcomings of the available analytical studies on the consolidation of the composite stone column – soft ground discussed in the literature review. It is emphasised that the analytical derivations in this thesis are conducted adopting the assumption of one-dimensional settlement and neglecting the horizontal deformation of the composite ground analogous to the studies by Barron [64] and Terzaghi [75], as mentioned in the scope of research. Therefore, the Mandel–Cryer effect demonstrating the increase of excess pore water pressure in the composite ground subjected to the lateral compression under an instant loading cannot be captured during the early stage of consolidation. Such effect can only be investigated by adopting Biot's theory of consolidation as reported by Helm [205] and McKinley [206].

CHAPTER 3

ANALYTICAL SOLUTION FOR PLANE STRAIN CONSOLIDATION OF SOFT SOIL STABILISED BY STONE COLUMNS

3.1 Introduction

From the existing literature, there is a lack of the analytical solution for plane strain consolidation of the composite stone column – soft ground considering the differential settlement condition (i.e. free strain assumption). Obviously, the behaviour of a permeable column improved soft soil can be more accurately analysed under three-dimensional (3D) or axisymmetric conditions resembling the actual column – soil foundation in real practice than under the two-dimensional (2D) equivalent plane strain consideration. As reported in various studies [15, 207, 208], however, the equivalent plane strain model of the composite pervious column – soil foundation can provide acceptable predictions for the foundation settlement and excess pore water pressure dissipation, particularly at the regions close to the centre of embankment.

The aim of this chapter is to provide an analytical solution to investigate the free strain consolidation of a stone column reinforced soft soil subjected to an instantly applied uniform loading under plane strain condition. A general solution to predict the excess pore water pressure dissipation and thus the consolidation settlement at any point in the model was achieved applying the method of separation of variables. To validate the capabilities of the obtained analytical solution, a worked example was conducted to examine the excess pore water pressure dissipation in the stone column and soft soil. The accuracy of the proposed solution was also verified against a finite element simulation.

Besides, a parametric analysis was performed to investigate the effect of permeability and stiffness of soft soil on the average degree of consolidation for each region of the model and the differential settlement between the two regions.

3.2 Problem description

Similar to the consolidation of soil with the inclusion of vertical drains, stone columns are commonly installed into soft ground in a square or triangular pattern in real practice [209, 210]. To develop an equivalent plane strain model, several models from available studies [102-105] can be applied in which the equivalent geometries or material properties (e.g. permeability and stiffness) of stone column and surrounding soil are obtainable by matching the analytical solution for consolidation between plane strain and axisymmetric models. It should be emphasised that the main objective of this study is to derive the analytical solution for plane strain consolidation model while the equivalent conversion factors relating to the geometry or material property of the model are assumed to be obtained using the available studies.

Figure 3.1 illustrates a typical plane strain consolidation model with a stone column region of width $2a$ enclosed by the soft soil region extended to width $2b$. The soil stratum has a thickness H underlain by a stiff layer and the column is entirely penetrated along the soil depth. The exterior boundaries and bottom base are impervious, while the upper surface of the model is considered to be freely draining. To derive the solution in this study, the following assumptions have been made:

- The column and soil regions are homogeneous.
- The foundation is completely saturated in which soil solid and water are incompressible

with the assumption of Darcy's law for the water flow.

– The free strain assumption is adopted; the column and soil solely deform vertically.

– The permeability and compressibility of the column and soil are assumed to be constant under surcharge loading.

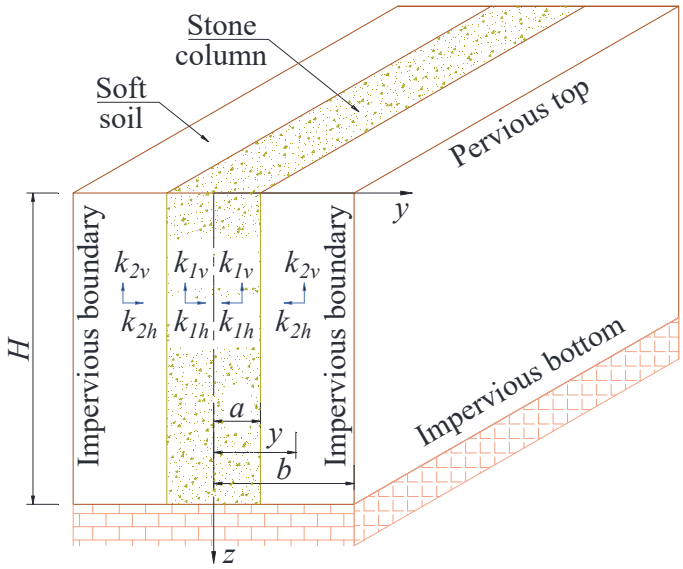

Figure 3.1. The model of the problem

It is also assumed that the external load is applied instantaneously and remained unchanged during the consolidation period, which induces time-independent total stress applied in each region of the model. Then, referring to the studies by other researchers [64, 98] and considering the symmetry of the problem, the equations for consolidation of the plane strain model can be expressed by:

$$c_{1h}\frac{\partial^2 u_1(y,z,t)}{\partial y^2}+c_{1v}\frac{\partial^2 u_1(y,z,t)}{\partial z^2}=\frac{\partial u_1(y,z,t)}{\partial t} \qquad (0\le y\le a) \tag{3.1a}$$

$$c_{2h}\frac{\partial^2 u_2(y,z,t)}{\partial y^2}+c_{2v}\frac{\partial^2 u_2(y,z,t)}{\partial z^2}=\frac{\partial u_2(y,z,t)}{\partial t} \qquad (a\le y\le b) \tag{3.1b}$$

where u_1 and u_2 are the excess pore water pressures at any points in the stone column and soft soil, respectively; y and z are Cartesian coordinates as displayed in Figure 3.1; t is the time; $c_{1h} = (k_{1h} M_1) / \gamma_w$ and $c_{1v} = (k_{1v} M_1) / \gamma_w$ are the horizontal and vertical consolidation coefficients of the stone column, respectively; $c_{2h} = (k_{2h} M_2) / \gamma_w$ and $c_{2v} = (k_{2v} M_2) / \gamma_w$ are the horizontal and vertical consolidation coefficients of the soft soil, respectively; k_{1h}, k_{1v}, and M_1 are the horizontal and vertical permeability coefficients and constrained modulus of the stone column, respectively; similarly, k_{2h}, k_{2v}, and M_2 are the horizontal and vertical permeability coefficients and constrained modulus of the soft soil, respectively; and γ_w is the unit weight of water $(10\,kN/m^3)$.

Pertaining to Figure 3.1, the conditions of no horizontal flows at the centerline and outside boundary of the model can be represented by Equations (3.2a) and (3.2d), respectively; whereas the continuities of excess pore water pressure and flow rate at the column-soil interface can be described by Equations (3.2b) and (3.2c), respectively.

$$\partial u_1 / \partial y = 0 \quad at\ y = 0 \tag{3.2a}$$

$$u_1 = u_2 \quad at\ y = a \tag{3.2b}$$

$$k_{1h}\, \partial u_1 / \partial y = k_{2h}\, \partial u_2 / \partial y \quad at\ y = a \tag{3.2c}$$

$$\partial u_2 / \partial y = 0 \quad at\ y = b \tag{3.2d}$$

The top surface of the composite ground is considered as fully permeable, while the bottom one rests on an impermeable rigid stratum (see Figure 3.1). Then, the following conditions can be included in these two boundaries as:

$$u_1 = u_2 = 0 \quad at\ z = 0 \tag{3.3a}$$

$$\partial u_1 / \partial z = \partial u_2 / \partial z = 0 \quad at\ z = H \tag{3.3b}$$

It is worth noting that the total stresses in the composite foundation are supposed to be carried completely by the excess pore water pressures immediately after loading due to the second assumption. Assuming the total stresses in the stone column and soft soil regions caused by the external load distribute uniformly in each region, the initial conditions for excess pore water pressure can be expressed by:

$$u_1(t=0) = \sigma_1 \qquad (0 \le y \le a) \tag{3.4a}$$

$$u_2(t=0) = \sigma_2 \qquad (a \le y \le b) \tag{3.4b}$$

where σ_1 and σ_2 are the total vertical stresses in the column and soil, respectively.

3.3 Analytical solution

The set of Equations (3.1) − (3.4) describe the plane strain consolidation problem in which the governing equations and boundary conditions are homogeneous, while the initial conditions are non-homogeneous.

According to the studies by Aviles-Ramos et al. [211], the method of separation of variables can be applied and the solution for the excess pore water pressure at any point in the model is defined as:

$$u_i(y,z,t) = u_i^{(i)}(y,z,t) + u_i^{(ii)}(y,z,t) \qquad \left(y_i \le y \le y_{i+1}\right) \qquad (i = 1,2) \tag{3.5}$$

In which the subscript $i = 1, 2$ denotes the stone column and soft soil regions, respectively; $y_1 = 0$, $y_2 = a$, $y_3 = b$; $u_i^{(i)}$ and $u_i^{(ii)}$ are determined as follows:

$$u_i^{(i)}(y,z,t) = \sum_{m=1}^{\infty}\sum_{n=1}^{\infty} C_{mn}^{(i)}\, Z_m(z)\; Y_{imn}^{(i)}(y)\; e^{-\beta_{mn}^{(i)\,2} t} \qquad \left(y_i \le y \le y_{i+1}\right) \tag{3.6a}$$

$$u_i^{(ii)}(y,z,t) = \sum_{m=1}^{\infty}\sum_{n=1}^{F(m)} C_{mn}^{(ii)}\, Z_m(z)\; Y_{imn}^{(ii)}(y)\; e^{-\beta_{mn}^{(ii)\,2} t} \qquad \left(y_i \le y \le y_{i+1}\right) \tag{3.6b}$$

where m and n are integer index corresponding to *z*- and *y*-directions, respectively; $Z_m(z)$ are the eigenfunctions with respect to *z*-direction and defined by:

$$Z_m(z) = \sin \lambda_m z \tag{3.7}$$

The term λ_m are the eigenvalues corresponding to $Z_m(z)$ and determined as:

$$\lambda_m = (2m-1)\pi / (2H) \qquad for\ m = 1,2,3,... \tag{3.8}$$

Considering Equation (3.6a), the terms $Y_{imn}^{(i)}(y)$ are the eigenfunctions with respect to *y*-direction, which are defined respectively for the stone column and soft soil regions by substituting the subscript $i = 1,2$ as:

$$Y_{1mn}^{(i)}(y) = A_{1mn}^{(i)} \cos\left(\nu_{1mn}^{(i)} y\right) + B_{1mn}^{(i)} \sin\left(\nu_{1mn}^{(i)} y\right) \tag{3.9a}$$

$$Y_{2mn}^{(i)}(y) = A_{2mn}^{(i)} \cos\left(\nu_{2mn}^{(i)} y\right) + B_{2mn}^{(i)} \sin\left(\nu_{2mn}^{(i)} y\right) \tag{3.9b}$$

where $A_{1mn}^{(i)}$, $B_{1mn}^{(i)}$, $A_{2mn}^{(i)}$ and $B_{2mn}^{(i)}$ are the constants to be determined; $\nu_{1mn}^{(i)}$ and $\nu_{2mn}^{(i)}$ are the eigenvalues corresponding to $Y_{1mn}^{(i)}(y)$ and $Y_{2mn}^{(i)}(y)$, respectively. The relationships between the eigenvalues pair $(\nu_{1mn}^{(i)}, \nu_{2mn}^{(i)})$ and the term $\beta_{mn}^{(i)}$ in Equation (3.6a) are given by the following equations:

$$\nu_{1mn}^{(i)} = \sqrt{\beta_{mn}^{(i)\,2} / c_{1h} - \kappa_1^2\, \lambda_m^2} \quad \text{where} \quad \beta_{mn}^{(i)\,2} / c_{1h} - \kappa_1^2\, \lambda_m^2 \ge 0 \tag{3.10a}$$

$$\nu_{2mn}^{(i)} = \sqrt{\beta_{mn}^{(i)\,2} / c_{2h} - \kappa_2^2\, \lambda_m^2} \quad \text{where} \quad \beta_{mn}^{(i)\,2} / c_{2h} - \kappa_2^2\, \lambda_m^2 \ge 0 \tag{3.10b}$$

$$\kappa_1 = \sqrt{c_{1v} / c_{1h}} = \sqrt{k_{1v} / k_{1h}} \quad \text{and} \quad \kappa_2 = \sqrt{c_{2v} / c_{2h}} = \sqrt{k_{2v} / k_{2h}} \tag{3.11}$$

It is worth mentioning that the conditions $c_{1h} > c_{2h}$ and $c_{1v} > c_{2v}$ hold true because the stone column possesses larger permeability and constrained modulus than the soft soil. Then, the following condition for $\beta_{mn}^{(i)}$ values can be derived on the basis of the concurrent satisfactory of the inequalities provided in Equations (3.10a) and (3.10b):

$$\beta_{mn}^{(i)} \geq \max\left\{\kappa_1 \lambda_m \sqrt{c_{1h}},\, \kappa_2 \lambda_m \sqrt{c_{2h}}\right\} = \kappa_1 \lambda_m \sqrt{c_{1h}} = \lambda_m \sqrt{c_{1v}} \tag{3.12}$$

For a specified value of m, the subscript n implies an infinite number of different eigenvalues $\beta_{mn}^{(i)}$ and consequent pairs $(\nu_{1mn}^{(i)}, \nu_{2mn}^{(i)})$. The eigenfunctions $Y_{1mn}^{(i)}(y)$ and $Y_{2mn}^{(i)}(y)$ are completely disclosed only when the corresponding constants and the eigenvalues pair $(\nu_{1mn}^{(i)}, \nu_{2mn}^{(i)})$ are achieved by taking advantage of the boundary conditions in *y*-direction.

Imposing the boundary condition presented in Equation (3.2a) on the solution reported in Equation (3.6a) and noting that the subscript $i = 1$ for the stone column region, yields $B_{1mn}^{(i)} = 0$. It should also be noted that the incorporation of the boundary conditions described by Equations (3.2b), (3.2c) and (3.2d) into the solution in Equation (3.6a) with the subscript $i = 1, 2$ would lead to a matrix equation in which the constants $A_{1mn}^{(i)}$, $A_{2mn}^{(i)}$ and $B_{2mn}^{(i)}$ can be determined in terms of any non-vanishing one [188]. By assigning $A_{1mn}^{(i)} = 1$ for simplicity, therefore, the following matrix equation for the determination of $A_{2mn}^{(i)}$ and $B_{2mn}^{(i)}$ is obtained:

$$\mathbf{\Omega}^{(i)}\, \mathbf{K}^{(i)} = \mathbf{0} \tag{3.13}$$

where

$$\mathbf{\Omega}^{(i)} = \begin{bmatrix} \cos\left(\nu_{1mn}^{(i)} a\right) & -\cos\left(\nu_{2mn}^{(i)} a\right) & -\sin\left(\nu_{2mn}^{(i)} a\right) \\ -N_k\, \nu_{1mn}^{(i)} \sin\left(\nu_{1mn}^{(i)} a\right) & \nu_{2mn}^{(i)} \sin\left(\nu_{2mn}^{(i)} a\right) & -\nu_{2mn}^{(i)} \cos\left(\nu_{2mn}^{(i)} a\right) \\ 0 & -\nu_{2mn}^{(i)} \sin\left(\nu_{2mn}^{(i)} b\right) & \nu_{2mn}^{(i)} \cos\left(\nu_{2mn}^{(i)} b\right) \end{bmatrix} \tag{3.14a}$$

$$\mathbf{K}^{(i)} = \left\{1,\ A_{2mn}^{(i)},\ B_{2mn}^{(i)}\right\} \tag{3.14b}$$

where $N_k = k_{1h} / k_{2h}$ is the horizontal permeability ratio between stone column and soft soil. Substituting $\nu_{1mn}^{(i)}$ and $\nu_{2mn}^{(i)}$ from Equations (3.10a) and (3.10b) into Equation (3.14a), the matrix $\mathbf{\Omega}^{(i)}$ with respect to $\beta_{mn}^{(i)}$ is attained. Then, the transcendental equation to determine the eigenvalues $\beta_{mn}^{(i)}$ can be derived by the demand that Equation (3.13) has a nontrivial solution (i.e. $\det \mathbf{\Omega}^{(i)} = 0$). Once $\beta_{mn}^{(i)}$ have been achieved, $\nu_{1mn}^{(i)}$ and $\nu_{2mn}^{(i)}$ can be calculated by Equations (3.10a) and (3.10b), respectively.

Pertaining to Equation (3.6b), similar to the eigenfunctions $Y_{imn}^{(i)}(y)$, the eigenfunctions $Y_{imn}^{(ii)}(y)$ corresponding to the stone column and soft soil regions are defined as:

$$Y_{1mn}^{(ii)}(y) = A_{1mn}^{(ii)} \cosh\left(\nu_{1mn}^{(ii)} y\right) + B_{1mn}^{(ii)} \sinh\left(\nu_{1mn}^{(ii)} y\right) \tag{3.15a}$$

$$Y_{2mn}^{(ii)}(y) = A_{2mn}^{(ii)} \cos\left(\nu_{2mn}^{(ii)} y\right) + B_{2mn}^{(ii)} \sin\left(\nu_{2mn}^{(ii)} y\right) \tag{3.15b}$$

where $A_{1mn}^{(ii)}$, $B_{1mn}^{(ii)}$, $A_{2mn}^{(ii)}$ and $B_{2mn}^{(ii)}$ are the constants to be determined; $\nu_{1mn}^{(ii)}$ and $\nu_{2mn}^{(ii)}$ are the eigenvalues corresponding to $Y_{1mn}^{(ii)}(y)$ and $Y_{2mn}^{(ii)}(y)$, respectively. The relationships between the eigenvalues pair $(\nu_{1mn}^{(ii)}, \nu_{2mn}^{(ii)})$ and the term $\beta_{mn}^{(ii)}$ in Equation (3.6b) are given by the following equations:

$$\nu_{1mn}^{(ii)} = \sqrt{\kappa_1^2\, \lambda_m^2 - \beta_{mn}^{(ii)\,2} / c_{1h}} \quad \text{where} \quad \kappa_1^2\, \lambda_m^2 - \beta_{mn}^{(ii)\,2} / c_{1h} > 0 \tag{3.16a}$$

$$\nu_{2mn}^{(ii)} = \sqrt{\beta_{mn}^{(ii)\,2} / c_{2h} - \kappa_2^2 \lambda_m^2} \quad \text{where} \quad \beta_{mn}^{(ii)\,2} / c_{2h} - \kappa_2^2 \lambda_m^2 \geq 0 \tag{3.16b}$$

To fulfil the two inequalities provided in Equations (3.16a) and (3.16b) simultaneously, the $\beta_{mn}^{(ii)}$ values must satisfy the following:

$$\lambda_m \sqrt{c_{2v}} \leq \beta_{mn}^{(ii)} < \lambda_m \sqrt{c_{1v}} \tag{3.17}$$

where the condition $c_{1v} > c_{2v}$ and Equation (3.11) have been utilised to derive the condition for the $\beta_{mn}^{(ii)}$ values. For a given value of m in this case, there is a finite number of eigenvalues $\beta_{mn}^{(ii)}$, which is denoted by $F(m)$ as a function of m. Thus, the index n of the second summation in Equation (3.6b) adopts a finite value of the upper limit $F(m)$.

Conducting the derivation analogous to the case of the eigenvalues pair $(\nu_{1mn}^{(i)}, \nu_{2mn}^{(i)})$, while $B_{1mn}^{(ii)} = 0$ due to the boundary condition given by Equation (3.2a) and $A_{1mn}^{(ii)} = 1$ for the sake of simplicity, the matrix equation to determine the constants $A_{2mn}^{(ii)}$ and $B_{2mn}^{(ii)}$ can be derived as follows:

$$\mathbf{\Omega}^{(ii)} \mathbf{K}^{(ii)} = \mathbf{0} \tag{3.18}$$

where

$$\mathbf{\Omega}^{(ii)} = \begin{bmatrix} \cosh\left(\nu_{1mn}^{(ii)} a\right) & -\cos\left(\nu_{2mn}^{(ii)} a\right) & -\sin\left(\nu_{2mn}^{(ii)} a\right) \\ N_k \nu_{1mn}^{(ii)} \sinh\left(\nu_{1mn}^{(ii)} a\right) & \nu_{2mn}^{(ii)} \sin\left(\nu_{2mn}^{(ii)} a\right) & -\nu_{2mn}^{(ii)} \cos\left(\nu_{2mn}^{(ii)} a\right) \\ 0 & -\nu_{2mn}^{(ii)} \sin\left(\nu_{2mn}^{(ii)} b\right) & \nu_{2mn}^{(ii)} \cos\left(\nu_{2mn}^{(ii)} b\right) \end{bmatrix} \tag{3.19a}$$

$$\mathbf{K}^{(ii)} = \left\{1,\ A_{2mn}^{(ii)},\ B_{2mn}^{(ii)}\right\} \tag{3.19b}$$

The matrix $\mathbf{\Omega}^{(ii)}$ with respect to $\beta_{mn}^{(ii)}$ can be obtained by substituting $\nu_{1mn}^{(ii)}$ and $\nu_{2mn}^{(ii)}$ provided in Equations (3.16a) and (3.16b) into Equation (3.19a). Then, the eigenvalues

$\beta_{mn}^{(ii)}$ are determined by the requirement $\det \mathbf{\Omega}^{(ii)} = 0$, and $\nu_{1mn}^{(ii)}$ and $\nu_{2mn}^{(ii)}$ are calculated by Equations (3.16a) and (3.16b), respectively.

To finalise the solutions in Equations (3.6a) and (3.6b), the initial conditions in Equations (3.4a) and (3.4b) are applied for which the coefficients $C_{mn}^{(i)}$ and $C_{mn}^{(ii)}$ are obtainable by taking the orthogonal expansion technique as presented in the study by Aviles-Ramos et al. [211]:

$$C_{mn}^{(*)} = \frac{1}{N_{mn}^{(*)}} \sum_{i=1}^{2} \frac{k_{ih}}{c_{ih}} \int_{z=0}^{H} \int_{y=y_i}^{y_{i+1}} Z_m(z)\, Y_{imn}^{(*)}(y)\, \sigma_i \, dy\, dz \tag{3.20}$$

and

$$N_{mn}^{(*)} = \sum_{i=1}^{2} \frac{k_{ih}}{c_{ih}} \int_{z=0}^{H} \int_{y=y_i}^{y_{i+1}} \left[Z_m(z)\, Y_{imn}^{(*)}(y) \right]^2 dy\, dz \tag{3.21}$$

where the new superscript $(*)$ has been used to denote the superscript (i) or (ii) in order to avoid repeating expressions which have the same formulation.

Once the solutions in Equations (3.6a) and (3.6b) have been disclosed, the excess pore water pressure at any point in the model is captured using Equation (3.5).

By taking average in *y*- and *z*-directions, the average excess pore water pressure for stone column $\overline{u}_1$ and for soft soil $\overline{u}_2$ are achieved as:

$$\overline{u}_1(t) = \left[\int_{z=0}^{H} \int_{y=0}^{a} u_1 \, dy\, dz \right] / \left[a\, H \right] \quad \text{and} \quad \overline{u}_2(t) = \left[\int_{z=0}^{H} \int_{y=a}^{b} u_2 \, dy\, dz \right] / \left[(b-a) H \right] \tag{3.22}$$

The average surface settlement of stone column $\overline{S}_1(t)$ and of soft soil $\overline{S}_2(t)$ at time t due to the dissipation of excess pore water pressure are obtainable via the following equation:

$$\bar{S}_1(t) = \left[\sigma_1 - \bar{u}_1(t)\right] H / M_1 \quad \text{and} \quad \bar{S}_2(t) = \left[\sigma_2 - \bar{u}_2(t)\right] H / M_2 \tag{3.23}$$

The average degree of consolidation of the stone column $\bar{U}_1$ and of the soft soil $\bar{U}_2$ based on the average surface settlement can be derived as:

$$\bar{U}_1(t) = \frac{\bar{S}_1(t)}{\bar{S}_1(\infty)} = \frac{\sigma_1 - \bar{u}_1(t)}{\sigma_1} \quad \text{and} \quad \bar{U}_2(t) = \frac{\bar{S}_2(t)}{\bar{S}_2(\infty)} = \frac{\sigma_2 - \bar{u}_2(t)}{\sigma_2} \tag{3.24}$$

where $\bar{S}_1(\infty)$ and $\bar{S}_2(\infty)$ are the final average surface settlements of stone column and of soft soil when time t approaches infinity, respectively.

It is obvious that once the average excess pore water pressures $\bar{u}_1$ and $\bar{u}_2$ and the total vertical stresses σ_1 and σ_2 have been determined, the average surface settlement and the average degree of consolidation are completely captured by Equations (3.23) and (3.24), respectively.

3.4 Validation of the proposed analytical solution

To validate the capabilities of the proposed analytical solution, this section provides a numerical example in conjunction with a parametric study to investigate the effect of consolidation parameters (e.g. permeability and modulus) on the consolidation behaviour of the composite ground subjected to an instantly applied loading $q = 100\,kPa$.

Referring to [104], for simplicity, the geometric parameters and material properties of the equivalent plane strain consolidation model in this example after converting from the axisymmetric configuration were adopted in a typical range as follows:

$H = 5\,m$, $a = 0.4\,m$, $b = 1.2\,m$,

$$k_{1h} = 4\times10^{-5}\ m/s,\ k_{1v} = k_{1h},\ E_1 = 30\times10^3\ kPa,\ \nu_{P1} = 0.33,$$

$$k_{2h} = 4\times10^{-10}\ m/s,\ k_{2v} = 0.5k_{2h},\ E_2 = 1.5\times10^3\ kPa,\ \nu_{P2} = 0.33.$$

where E_1 and E_2 are Young's modulus of the stone column and soft soil, respectively; ν_{P1} and ν_{P2} are Poisson's ratio of the stone column and soft soil, respectively. Then, the constrained modulus for the stone column and soft soil can be calculated as $M_1 = E_1(1-\nu_{P1})/\left[(1+\nu_{P1})(1-2\nu_{P1})\right]$ and $M_2 = E_2(1-\nu_{P2})/\left[(1+\nu_{P2})(1-2\nu_{P2})\right]$, respectively.

The validation was conducted by inspecting the excess pore water pressure dissipation in the model. Besides, the performance objectives were evaluated via the average degree of consolidation for the stone column $\bar{U}_1$ and for the soft soil $\bar{U}_2$ along with the average differential settlement $\Delta\bar{S}$ between the two regions. The average differential settlement $\Delta\bar{S}$ was calculated as the difference in average surface settlement between the column and soil regions determined by Equation (3.23).

In connection to Equation (3.5), the change of excess pore water pressure against each variable y, z, or t can be captured by keeping the remaining variables unchanged.

Figure 3.2 illustrates the isochrones of excess pore water pressure at various time t along the *y*-direction of the model. It is observed that the isochrones complied with the zero flow conditions as in Equations (3.2a) and (3.2d) and column-soil interface conditions expressed by Equations (3.2b) and (3.2c) where excess pore water pressures distributed almost uniform along the column width and attained the maximum values at the exterior boundary $y = b$. The nonzero values of excess pore water pressure in the

stone column region illustrate the drain resistance presence for a specified hydraulic conductivity (permeability) of the column. The excess pore water pressure within the stone column dissipated extremely quickly and reduced to almost $7\,kPa$ at time $t = 2\times10^{2}\,s$ meanwhile that within most of the soft soil stayed almost same as the initial value.

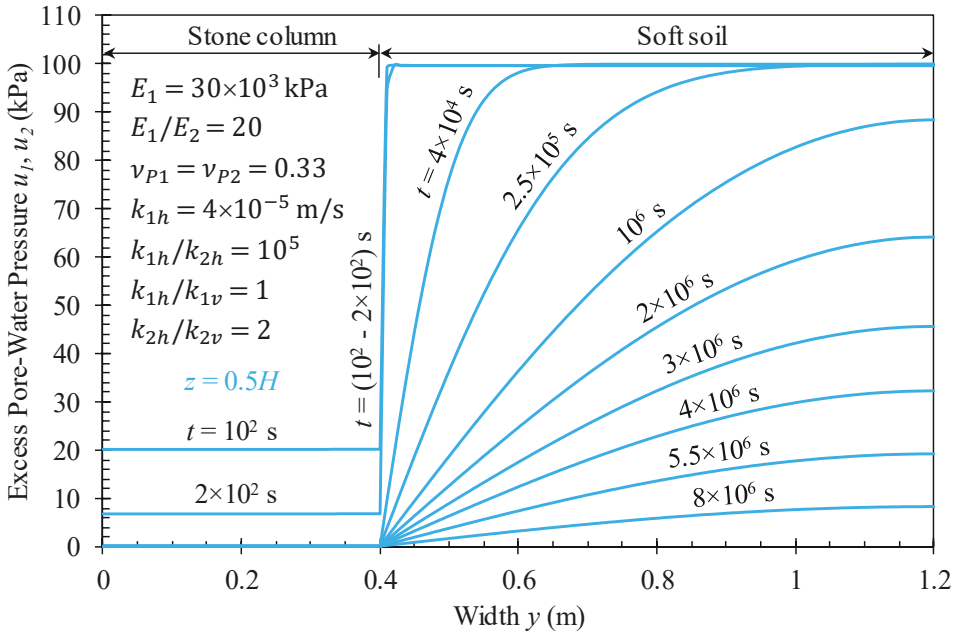

Figure 3.2. Excess pore water pressure isochrones against width at depth $z = 0.5H$ for the stone column and soft soil regions

Figure 3.3 depicts the excess pore water pressure dissipation at points with depth $z = 0.25H$, $z = 0.5H$ and $z = 0.75H$ and $y = 0.5a$ (in stone column region) and $y = 0.5(a+b)$ (in soft soil region). As expected, the dissipation of excess pore water pressure for the deeper point of investigation was slower due to the longer upward drainage path to the surface drainage boundary, particularly in the column. Regardless of

the difference in depth of the investigation points in the soil, there was almost no discrepancy in the rate of excess pore pressure dissipation among these points. The reason is attributable to the dominance of horizontal flow in the soil together with the extremely faster dissipation rate of excess pore pressure in the column than in soft soil.

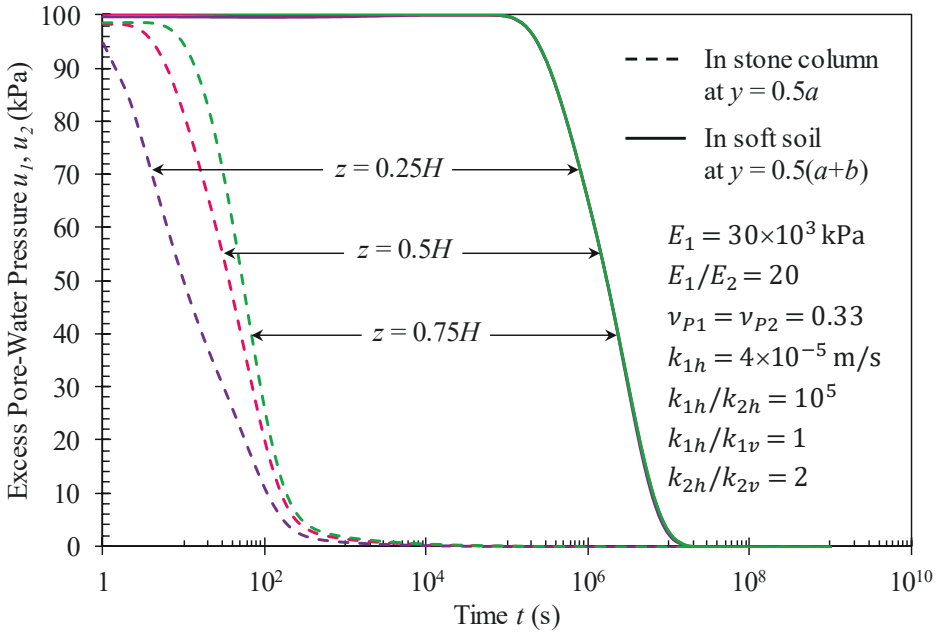

Figure 3.3. Dissipation of excess pore water pressure against time at different points in the stone column and soft soil regions

Figure 3.5 presents the verification on average degree of consolidation achieved from the proposed analytical solution and the finite element simulation employing the software PLAXIS 2D [212]. Due to the symmetry of external loading, geometry, boundary and initial conditions of excess pore water pressures against z-axis, the numerical model was simulated as a half of the problem model shown in Figure 3.1 utilising the plane strain configuration feature and 15-node triangular elements (see Figure 3.4). The stiffness and permeability of stone column and soft soil in the numerical model were identical to those

in the analytical model. As observed from Figure 3.5, the analytical predictions agree well with the results obtained from the finite element simulation.

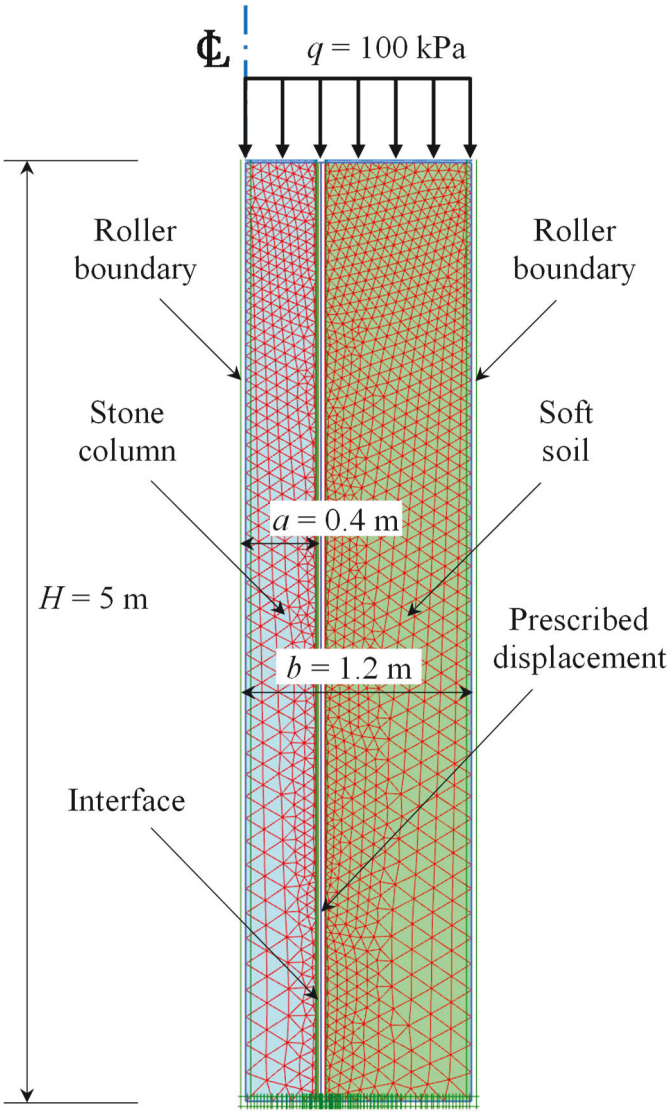

Figure 3.4. Plane strain finite element model of the example

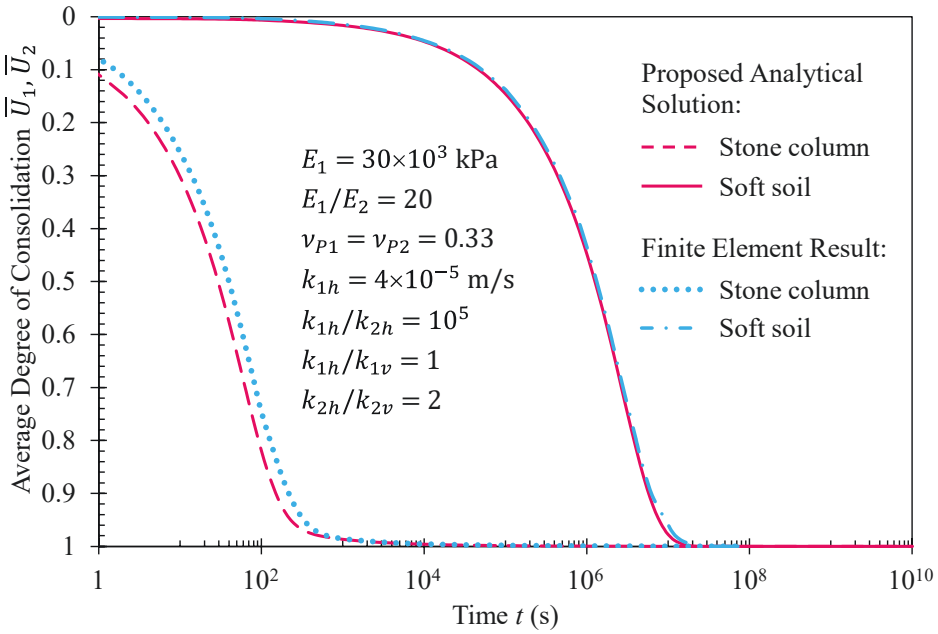

Figure 3.5. Comparison in average degree of consolidation obtained from proposed analytical solution and finite element result

The investigation parameters in this study including the horizontal permeability coefficient and modulus of soft soil were varied independently in a typical range, while the remaining parameters of the model remained unchanged and the same as the initial values in the defined example. Also for the sake of cross-reference and generality, the investigation factors were examined using normalised parameters k_{1h}/k_{2h} and E_1/E_2.

Figure 3.6a exhibits a significant change of consolidation rate with the permeability ratio k_{1h}/k_{2h}, particularly in the soft soil region. The process of consolidation completed earlier when the ratio k_{1h}/k_{2h} became smaller. It should be noted that the consolidation of the model was primarily controlled by the horizontal flow from soft soil to stone column and the upward flow to the top drainage boundary in the stone column. A decline in k_{1h}/k_{2h} ratio (i.e. an increase in the horizontal permeability of soft soil) sped up the

horizontal flow in soft soil, which accelerated the consolidation of soil considerably but decelerated the consolidation of column. Figure 3.6b shows the average differential settlement variation with time for different permeability ratio. As observed, the $\Delta\overline{S}$ change patterns were analogous to $\overline{U}_2$ change patterns in the soil region (see Figure 3.6a), where the average differential settlement was accelerated to attain the highest value earlier, corresponding to the decrease of k_{1h} / k_{2h} ratio. The analogy may be elucidated in connection to Equations (3.23) and (3.24) in which $\overline{S}_2(\infty)$ is much greater than $\overline{S}_1(\infty)$ due to the significantly smaller stiffness of the soft soil compared to the stone column. As a result, the $\Delta\overline{S}$ calculations are mainly governed by $\overline{U}_2$ regardless of the changes of $\overline{U}_1$ and $\overline{U}_2$ during the process of consolidation.

Figure 3.7a indicates that a decline of the modulus ratio E_1 / E_2 (i.e. an increase in the modulus of soft soil) sped up the consolidation significantly. Furthermore, the acceleration became more remarkable gradually when the smaller modulus ratio E_1 / E_2 was adopted. Indeed, the greater the soil stiffness, the faster the transfer process of excess pore pressure onto the effective stress in the soil, which accelerated the consolidation of the composite ground. It is worth noting that the decrease in E_1 / E_2 ratio not only increased the consolidation rate but also reduced the average differential settlement dramatically (Figure 3.7b), particularly during the later stages of consolidation. The changes in $\Delta\overline{S}$ predictions against consolidation time were principally regulated by the product of $\overline{U}_2$ and $\overline{S}_2(\infty)$ in which an increase in the soil stiffness diminished $\overline{S}_2(\infty)$ and accompanying $\Delta\overline{S}$ substantially.

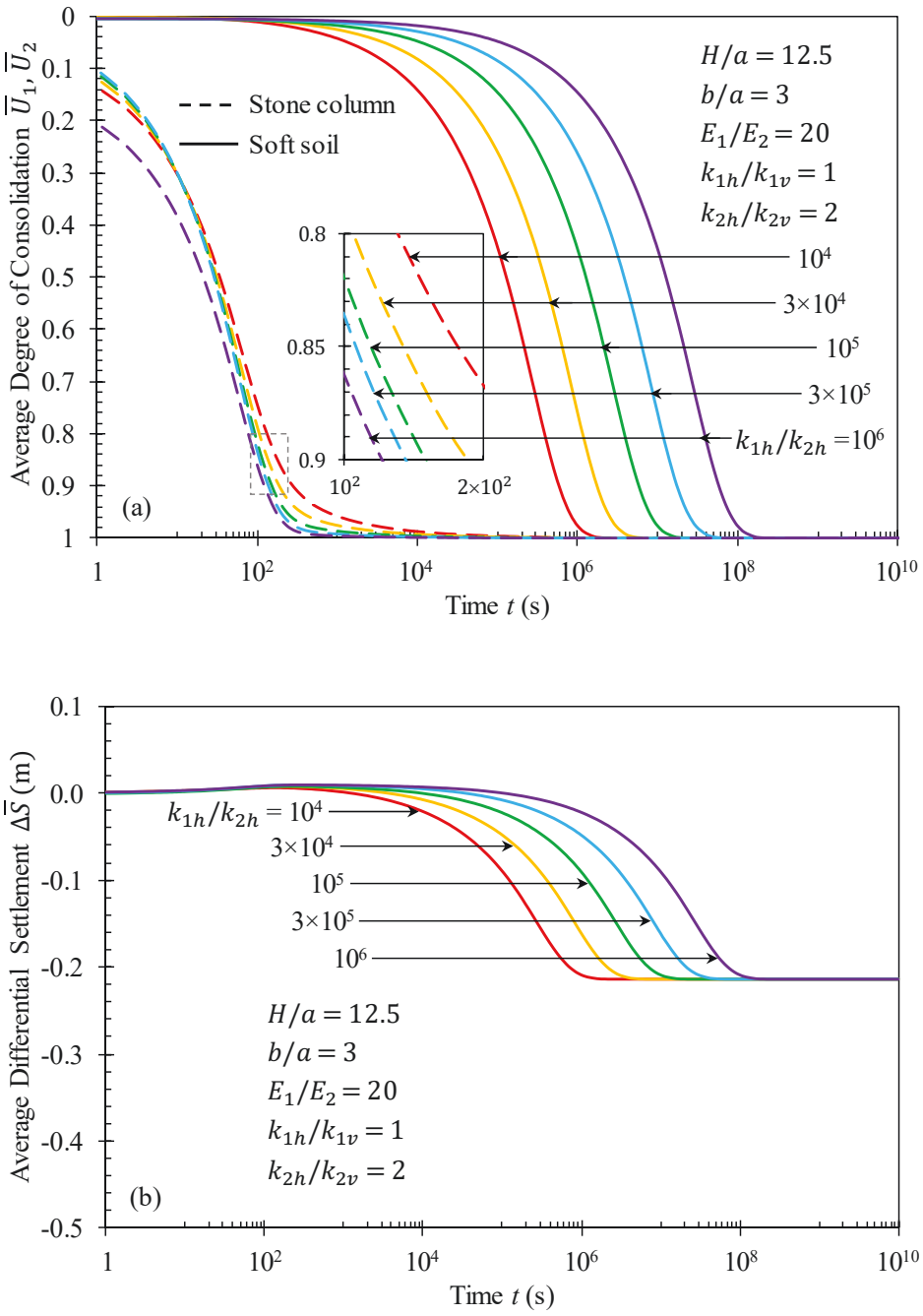

Figure 3.6. Effect of permeability ratio k_{1h}/k_{2h} on (a) average degree of consolidation of stone column and of soft soil, and (b) average differential settlement between stone column and soft soil

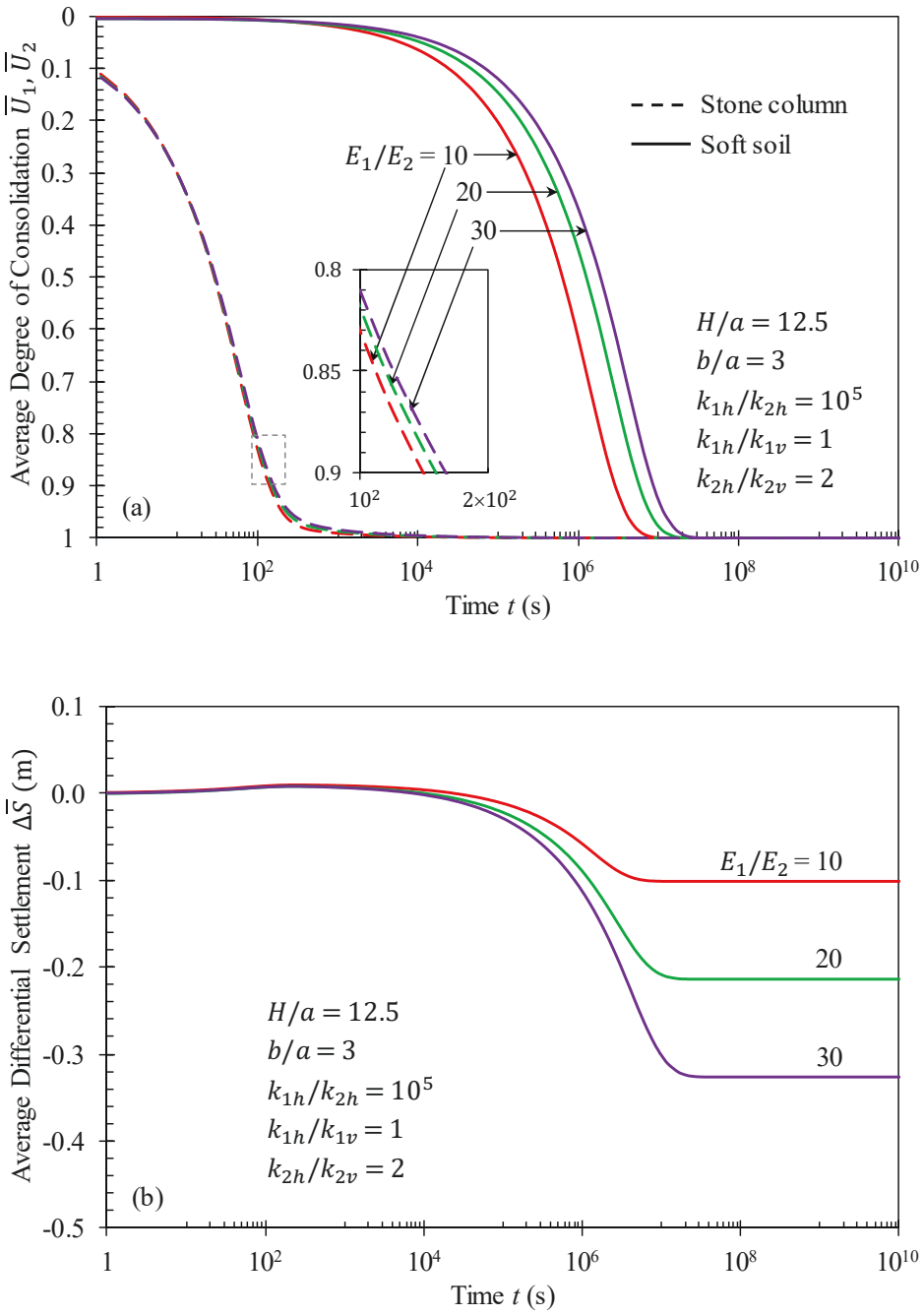

Figure 3.7. Effect of modulus ratio E_1/E_2 on (a) average degree of consolidation of stone column and of soft soil, and (b) average differential settlement between stone column and soft soil

3.5 Summary

This chapter introduces an analytical solution to the consolidation of a stone column reinforced soft soil adopting free strain condition for the column and soil under plane strain configuration and instantaneous loading. A mathematical model was developed incorporating simultaneous horizontal and vertical flows in the stone column and soft soil with an orthotropic permeability for each region. Then, an analytical solution in terms of exact double series was derived employing the method of separation of variables and orthogonal expansion technique. The obtained analytical solution is capable of predicting the change of excess pore water pressure and thus settlement against time at any point in the model. Consequently, the differential settlement between stone column and soft soil regions is readily captured during the consolidation process. The capabilities of the proposed solution were validated via an example investigating the excess pore water pressure dissipation in the model, incorporated with the parametric study examining the influence of consolidation parameters of soft soil on performance objectives. The accuracy of the proposed solution was verified against a finite element modelling, which shows good agreements. The achieved analytical solution is also applicable to the consolidation of soft ground improved by prefabricated vertical drains (PVDs) or permeable columns (e.g. sand column and soil-cement mixing column) in which the consolidation parameters of PVDs and columns may be assigned appropriately. Additionally, a corresponding stress concentration ratio defined as $n_{scr} = \sigma_1/\sigma_2$ should also be adopted along with the equilibrium condition of total vertical stresses over the composite ground area to determine σ_1 and σ_2. For example, $n_{scr}=1$ should be adopted for PVDs or sand column assisted ground to simulate a uniform distribution of vertical stresses on the ground surface due to the slight difference in stiffness between PVDs or

sand column and surrounding soil, while n_{scr}=2-6 could be assigned to the stone column improved soft ground supporting a specific flexible embankment [213]. The consolidation behaviour of pervious column supported soft soil can be analysed via the equivalent plane strain model with acceptable predictions; particularly for the vicinity of embankment centre and when the column spacing in a given direction is small (e.g. continuous column row or column wall), which highly satisfies the symmetry and plane strain conditions of the mathematical model. Therefore, the proposed analytical solution in this study can be utilised as a simple tool to predict the consolidation of the composite ground as well as verify the complex numerical modelling. For further research, the unsaturation and creep effects of soil [122, 214] can be included.

CHAPTER 4

ANALYTICAL SOLUTION FOR FREE STRAIN CONSOLIDATION OF STONE COLUMN-REINFORCED SOFT GROUND CONSIDERING SPATIAL VARIATION OF TOTAL STRESS AND DRAIN RESISTANCE

4.1 Introduction

So far, there have been very limited analytical solutions for consolidation of composite ground supported by stone columns considering the free strain condition. Even though Alamgir et al. [65] obtained a new solution accounting for the differential settlement, their study had addressed the time-independent deformation problem rather than a time-dependent consolidation analysis of soft soil reinforced with columnar inclusions. In their theoretical model, a deformation mode of the column-soil system was assumed in advance through the acceptance of a governing equation with unknown parameters. After that, the solutions for the parameters were obtained by applying the equilibrium condition of vertical stresses, the elastic deformation characteristics of column and soil, and the displacement compatibility between column and soil elements. Consequently, the displacement and stress fields together with the settlement of the composite ground were obtained; however it is well recognised that the deformation pattern should be the output of free strain consolidation analysis.

Therefore, the main objective of this chapter is to develop an analytical solution for investigating the consolidation response of stone column-reinforced soft ground under free strain axisymmetric conditions considering drain resistance effect and the spatial variation of total vertical stress. The radial and vertical consolidation equations are solved

in a coupled fashion for both the stone column and its surrounding soil assuming different vertical and horizontal permeability coefficients. A general solution for excess pore water pressure at any point in the unit cell was obtained using the method of separation of variables. From the achieved solution, the settlement at an arbitrary point, as well as the average degree of consolidation for the stone column and for the surrounding soil, are readily determined. A worked example applying the proposed solution is conducted along with verification exercises comparing the analytical results with finite element predictions, field measurements and existing analytical studies. Furthermore, a parametric study is also conducted to examine the extent to which the model parameters can impact the consolidation response of the composite ground.

4.2 Basic assumptions and mathematical model

The unit cell model in this study is shown in Figure 4.1 with a cylindrical stone column of radius a surrounded by the soft soil extended to radius b. The soft soil layer has a thickness H overlying a rigid stratum and the stone column is fully penetrated. The top surface is assumed to be freely draining while the bottom base is impervious. Referring to Biot [77] and Barron [64], the following basic assumptions are made during the derivations of analytical solution in the present study.

(i) The stone column and soil deposit are homogeneous.

(ii) The composite ground is fully saturated while the soil particles and water are assumed to be incompressible with the flow of water obeying Darcy's law.

(iii) The free strain assumption is adopted while the stone column and its surrounding soil can only deform vertically. In other words, the effect of shear strains developed in the column and soil body is neglected similar to Barron [64].

(iv) The coefficients of permeability and volume change of the stone column and soil remain constant during the loading process.

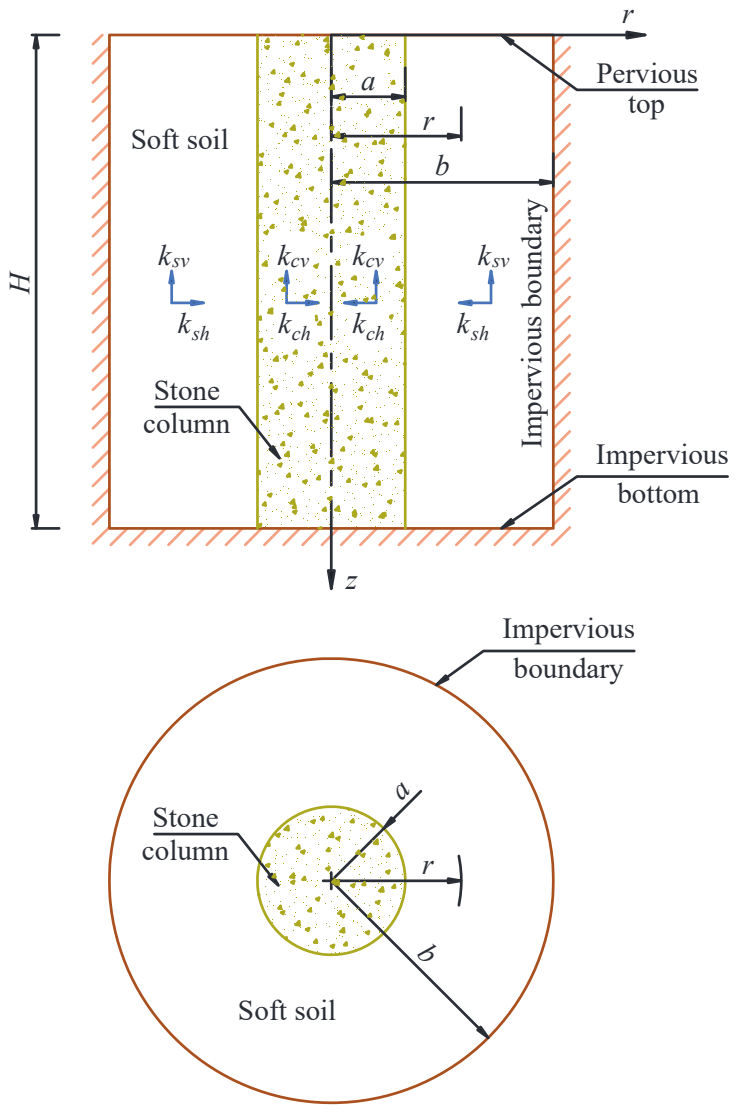

Figure 4.1. The unit cell model of the problem

It should be noted that the permeabilities of materials in the unit cell vary with void ratio and consolidation pressure during the consolidation period of composite ground. Likewise, the volume change coefficients are not constant due to the nonlinear relationship between void ratio and effective pressure under surcharge loading. However, these consolidation parameters can be accepted as constant properties for an expected pressure increment induced by external loading. Following the equation governing the three-dimensional consolidation originally established by Biot [77], Castro and Sagaseta [55] reported the general equation for axisymmetric consolidation of soil around a stone column in the unit cell model in the case of anisotropic permeability as follows:

$$\frac{k_{sh}}{\gamma_w}\left(\frac{\partial^2 u_s(r,z,t)}{\partial r^2}+\frac{1}{r}\frac{\partial u_s(r,z,t)}{\partial r}\right)+\frac{k_{sv}}{\gamma_w}\frac{\partial^2 u_s(r,z,t)}{\partial z^2}=-\frac{\partial \varepsilon_{vs}(r,z,t)}{\partial t} \tag{4.1}$$

The right-hand side of Equation (4.1) is the volumetric strain rate of the soil which can be expressed in terms of the excess pore water pressure. It is worth noting that by assuming one-dimensional deformation theory, the volumetric strain ε_v is identical with the vertical strain ε_z because of the assumption (iii) about the vertical deformation of composite ground. Then, considering the soil compressibility, the following equation for the volumetric strain of soil can be written:

$$\varepsilon_{vs}=\varepsilon_{zs}=\frac{\sigma_s(r,z,t)-u_s(r,z,t)}{M_s} \tag{4.2}$$

and the rate of volumetric strain would be expressed as:

$$\frac{\partial \varepsilon_{vs}}{\partial t}=\frac{\partial \varepsilon_{zs}}{\partial t}=\frac{1}{M_s}\left[\frac{\partial \sigma_s(r,z,t)}{\partial t}-\frac{\partial u_s(r,z,t)}{\partial t}\right] \tag{4.3}$$

where σ_s is the total vertical stress within the surrounding soil under applied external loading.

The derivation for the consolidation of stone column can be developed in a similar manner. In the present study, it is assumed that the external loading is applied instantly and maintained constant during the consolidation process; in other words, the total stresses caused by the loading are independent of time. Therefore, the general equations for consolidation of the unit cell under axisymmetric configuration can be written as:

$$c_{ch}\left(\frac{\partial^2 u_c(r,z,t)}{\partial r^2}+\frac{1}{r}\frac{\partial u_c(r,z,t)}{\partial r}\right)+c_{cv}\frac{\partial^2 u_c(r,z,t)}{\partial z^2}=\frac{\partial u_c(r,z,t)}{\partial t} \quad \left(0\le r\le a\right) \tag{4.4a}$$

$$c_{sh}\left(\frac{\partial^2 u_s(r,z,t)}{\partial r^2}+\frac{1}{r}\frac{\partial u_s(r,z,t)}{\partial r}\right)+c_{sv}\frac{\partial^2 u_s(r,z,t)}{\partial z^2}=\frac{\partial u_s(r,z,t)}{\partial t} \quad \left(a\le r\le b\right) \tag{4.4b}$$

where u_c and u_s are the excess pore water pressures at any point in the stone column and the surrounding soil, respectively; r and z are the cylindrical coordinates as displayed in Figure 4.1; t is the time; $c_{ch}=(k_{ch}M_c)/\gamma_w$ and $c_{cv}=(k_{cv}M_c)/\gamma_w$ are the horizontal and vertical consolidation coefficients of the stone column, respectively; $c_{sh}=(k_{sh}M_s)/\gamma_w$ and $c_{sv}=(k_{sv}M_s)/\gamma_w$ are the horizontal and vertical consolidation coefficients of the surrounding soil, respectively; k_{ch}, k_{cv}, and M_c are the horizontal and vertical permeability coefficients and constrained modulus of the stone column, respectively; similarly, k_{sh}, k_{sv}, and M_s are the horizontal and vertical permeability coefficients and constrained modulus of the surrounding soil, respectively; and γ_w is the unit weight of water.

Referring to Figure 4.1, the continuity of the excess pore water pressure and the flow velocity at the column-soil interface can be expressed by:

$$u_c(r=a)=u_s(r=a) \tag{4.5a}$$

$$k_{ch}\left.\frac{\partial u_c}{\partial r}\right|_{r=a} = k_{sh}\left.\frac{\partial u_s}{\partial r}\right|_{r=a} \tag{4.5b}$$

Considering the axisymmetric unit cell condition adopted in this study, the exterior radial boundary of the cell should satisfy the zero flow condition (see Figure 4.1), i.e.

$$\left.\frac{\partial u_s}{\partial r}\right|_{r=b} = 0 \tag{4.5c}$$

The top surface of the cell is assumed completely permeable (or fully drained), while the base is assumed impermeable resembling the impermeable stiff layer as shown in Figure 4.1. Therefore, the following boundary conditions can be applied to the top and bottom of the model:

$$u_c(z=0) = u_s(z=0) = 0 \tag{4.6a}$$

$$\left.\frac{\partial u_c}{\partial z}\right|_{z=H} = \left.\frac{\partial u_s}{\partial z}\right|_{z=H} = 0 \tag{4.6b}$$

As a result of the constant loading assumption, the total vertical stresses in the composite foundation are functions of spatial variables. Under the assumption (ii), the total stresses within the stone column and its surrounding soil are supposed to be entirely carried by the excess pore water pressure in each region immediately after the loading ($t = 0$), respectively. Therefore, the initial conditions for the excess pore pressure taking the separation of variables can be written by:

$$u_c(t=0) = \sigma_c(r,z) = \sigma_{cr}(r)\, f_{cz}(z) \qquad (0 \le r \le a) \tag{4.7a}$$

$$u_s(t=0) = \sigma_s(r,z) = \sigma_{sr}(r)\, f_{sz}(z) \qquad (a \le r \le b) \tag{4.7b}$$

where $\sigma_c(r,z)$ and $\sigma_s(r,z)$ denote the total vertical stress within the column and soft soil, respectively; $\sigma_{cr}(r)$ and $\sigma_{sr}(r)$ denote the total vertical stress distribution on the

top of column and soft soil under the applied external loading, respectively; $f_{cz}(z)$ and $f_{sz}(z)$ denote the variation of total vertical stress against depth for column and soft soil, respectively.

4.3 Analytical solution

The set of Equations (4.4)-(4.7) address the axisymmetric consolidation problem where the governing equations and boundary conditions are homogeneous, while the initial conditions are non-homogeneous. The analytical solution in this chapter is derived following the studies by Aviles-Ramos et al. [211] and Aviles-Ramos and Rudy [215] for the heat conduction problem of 2-region media in which one of the two regions was thermally isotropic. Their solutions were obtained employing a coordinate transformation for the orthotropic region, whereas the analytical solution in the present study is solved directly for the consolidation problem with the orthotropic permeability for both stone column and soft soil regions.

According to the studies by Aviles-Ramos et al. [211] and Aviles-Ramos and Rudy [215], the method of separation of variables is applied and the solutions for the excess pore water pressure in the two regions would follow the following forms:

$$u_c(r,z,t) = R_c(r)\ Z_c(z)\ T_c(t) \qquad \left(0 \le r \le a\right) \tag{4.8a}$$

$$u_s(r,z,t) = R_s(r)\ Z_s(z)\ T_s(t) \qquad \left(a \le r \le b\right) \tag{4.8b}$$

satisfying the following conditions:

$$\frac{Z_c''(z)}{Z_c(z)} = \frac{Z_s''(z)}{Z_s(z)} = -\lambda^2 \tag{4.9}$$

$$\frac{T_c'(t)}{T_c(t)} = \frac{T_s'(t)}{T_s(t)} = -\beta^2 \tag{4.10}$$

where λ and β are the real and non-negative separation constants; $R(r)$, $Z(z)$, and $T(t)$ (with subscripts c and s) are the separated functions with respect to the variables r, z, and t, respectively.

Substituting u_c and u_s from Equations (4.8a) and (4.8b) into Equations (4.4a) and (4.4b) leads to:

$$c_{ch}\left(\frac{R_c''(r)}{R_c(r)} + \frac{1}{r}\frac{R_c'(r)}{R_c(r)}\right) - c_{cv}\,\lambda^2 = -\beta^2 \qquad \left(0 \le r \le a\right) \tag{4.11a}$$

$$c_{sh}\left(\frac{R_s''(r)}{R_s(r)} + \frac{1}{r}\frac{R_s'(r)}{R_s(r)}\right) - c_{sv}\,\lambda^2 = -\beta^2 \qquad \left(a \le r \le b\right) \tag{4.11b}$$

Rearranging the above yields:

$$R_c''(r) + \frac{1}{r}R_c'(r) + \nu_c^2\,R_c(r) = 0 \qquad \left(0 \le r \le a\right) \tag{4.12a}$$

$$R_s''(r) + \frac{1}{r}R_s'(r) + \nu_s^2\,R_s(r) = 0 \qquad \left(a \le r \le b\right) \tag{4.12b}$$

where

$$\nu_c^2 = \frac{\beta^2}{c_{ch}} - \frac{c_{cv}}{c_{ch}}\lambda^2 = \frac{\beta^2}{c_{ch}} - \kappa_c^2\,\lambda^2 \tag{4.13a}$$

$$\nu_s^2 = \frac{\beta^2}{c_{sh}} - \frac{c_{sv}}{c_{sh}}\lambda^2 = \frac{\beta^2}{c_{sh}} - \kappa_s^2\,\lambda^2 \tag{4.13b}$$

$$\kappa_c = \sqrt{\frac{c_{cv}}{c_{ch}}} = \sqrt{\frac{k_{cv}}{k_{ch}}} \qquad \text{and} \qquad \kappa_s = \sqrt{\frac{c_{sv}}{c_{sh}}} = \sqrt{\frac{k_{sv}}{k_{sh}}} \tag{4.14}$$

Equation (4.9) is commonly known as a homogeneous linear second-order differential equation in which the general solution can be easily obtained. By imposing the boundary conditions provided in Equations (4.6a) and (4.6b) on the general solution, the following equation is derived:

$$Z_{cm}(z) = Z_{sm}(z) = Z_m(z) = \sin \lambda_m z = \sin \frac{\omega_m}{H} z \tag{4.15}$$

where $Z_m(z)$ are the eigenfunctions of the corresponding eigenvalues λ_m in z-direction. The term λ_m is defined as:

$$\lambda_m = \frac{(2m-1)\pi}{2H} = \frac{\omega_m}{H} \quad for\ m = 1, 2, 3, ... \tag{4.16}$$

and $$\omega_m = (2m-1)\pi / 2 \tag{4.17}$$

The solutions for Equation (4.10) are readily achieved as:

$$T_{cmn}(t) = T_{smn}(t) = T_{mn}(t) = e^{-\beta_{mn}^2 t} \tag{4.18}$$

where $T_{mn}(t)$ are the time-dependent functions of the eigenvalues β_{mn}. The subscript n denotes that there is an infinite number of distinct eigenvalues for a given value of m.

Introducing the subscripts m and n into Equations (4.13a) and (4.13b) yields:

$$\nu_{cmn} = \sqrt{\frac{\beta_{mn}^2}{c_{ch}} - \kappa_c^2 \lambda_m^2} \tag{4.19a}$$

$$\nu_{smn} = \sqrt{\frac{\beta_{mn}^2}{c_{sh}} - \kappa_s^2 \lambda_m^2} \tag{4.19b}$$

It should also be noted that the values of ν_{cmn} and ν_{smn} for which the boundary value problem (i.e. Equations (4.12a) and (4.12b) along with their appropriate radial boundary conditions) possesses nontrivial solutions are called eigenvalues, and the corresponding

solutions (i.e. R_{cmn} and R_{smn}) are called eigenfunctions. Obviously, the aim of solving the problem is to achieve only nontrivial solutions; therefore, the notations ν_{cmn} and ν_{smn} denote the eigenvalues and R_{cmn} and R_{smn} denote the corresponding eigenfunctions in *r*-direction as a convention from now on.

For the given values of c_{ch}, c_{sh}, κ_c, and κ_s, it is important to note that the values of ν_{cmn} and ν_{smn} can be real or complex relying on the values of λ_m and β_{mn}. Hence, there are four possible combinations of ν_{cmn} and ν_{smn} values that can be attained from Equations (4.19a) and (4.19b). These combinations are (real, real), (complex, real), (real, complex), and (complex, complex) which are in turn denoted by $(\nu^r_{cmn}, \nu^r_{smn})$, $(\nu^c_{cmn}, \nu^r_{smn})$, $(\nu^r_{cmn}, \nu^c_{smn})$, and $(\nu^c_{cmn}, \nu^c_{smn})$.

Owing to the fact that the constrained modulus and permeability coefficients of the stone column are much higher than those of the surrounding soft soil, the stone column always possesses larger consolidation coefficients than the surrounding soil for both horizontal and vertical directions (i.e. $c_{ch} > c_{sh}$ and $c_{cv} > c_{sv}$). Therefore, the following inequality holds true:

$$\frac{\beta_{mn}^2}{c_{ch}} - \kappa_c^2 \lambda_m^2 < \frac{\beta_{mn}^2}{c_{sh}} - \kappa_s^2 \lambda_m^2 \qquad \left(i.e., \ \frac{\beta_{mn}^2 - c_{cv} \lambda_m^2}{c_{ch}} < \frac{\beta_{mn}^2 - c_{sv} \lambda_m^2}{c_{sh}} \right) \tag{4.20}$$

Equation (4.20) must be satisfied for all possible pairs of ν_{cmn} and ν_{smn} values. In order to construct the final complete solution of the problem, all the four combinations of ν_{cmn} and ν_{smn} will be in turn taken into consideration. Referring to Zill et al. [216], if any combination includes at least one complex value, then all complex values will be

transformed into real values by taking advantage of the imaginary unit $i=\sqrt{-1}$ in complex number theory. Consequently, the original pairs become new pairs which only have real values. This procedure enables the convenience to achieve the general solutions for Equations (4.12a) and (4.12b).

Actually, the only pairs $(\nu_{cmn}^{r},\nu_{smn}^{r})$ and $(\nu_{cmn}^{c},\nu_{smn}^{r})$ will contribute to the final solution while the remaining two do not exist corresponding to the conditions $c_{ch}>c_{sh}$ and $c_{cv}>c_{sv}$ in the problem. The combination $(\nu_{cmn}^{r},\nu_{smn}^{r})$ is a real value pair which is denoted as $(\nu_{cmn}^{(i)},\nu_{smn}^{(i)})$, while the term ν_{cmn}^{c} in the combination $(\nu_{cmn}^{c},\nu_{smn}^{r})$ will be transformed into real value to obtain a new pair including only real numbers denoted as $(\nu_{cmn}^{(ii)},\nu_{smn}^{(ii)})$. The derivation of $(\nu_{cmn}^{(i)},\nu_{smn}^{(i)})$ and $(\nu_{cmn}^{(ii)},\nu_{smn}^{(ii)})$ together with their corresponding eigenfunctions (i.e. $(R_{cmn}^{(i)},R_{smn}^{(i)})$ and $(R_{cmn}^{(ii)},R_{smn}^{(ii)})$) is provided in Appendix B.

Eventually, the final solutions for excess pore water pressure at points in the stone column and soft soil regions are defined as:

$$u_c(r,z,t)=u_c^{(i)}(r,z,t)+u_c^{(ii)}(r,z,t) \tag{4.21a}$$

$$u_s(r,z,t)=u_s^{(i)}(r,z,t)+u_s^{(ii)}(r,z,t) \tag{4.21b}$$

where $u_c^{(i)}$ and $u_c^{(ii)}$ are determined by Equations (A.3a) and (A.9a), respectively; $u_s^{(i)}$ and $u_s^{(ii)}$ are determined by Equations (A.3b) and (A.9b), respectively (see Appendix A).

The settlements at points with depth $z=z_0$ in the stone column and soft soil regions resulting from the dissipation of excess pore water pressure can be determined by:

$$S_c(r,z_0,t)=\frac{1}{M_c}\int_{z=z_0}^{H}\sigma_c'(r,z,t)\,dz=\frac{1}{M_c}\int_{z=z_0}^{H}\left[\sigma_c-u_c(r,z,t)\right]dz \tag{4.22a}$$

$$S_s(r,z_0,t)=\frac{1}{M_s}\int_{z=z_0}^{H}\sigma_s'(r,z,t)\,dz=\frac{1}{M_s}\int_{z=z_0}^{H}\left[\sigma_s-u_s(r,z,t)\right]dz \tag{4.22b}$$

where σ_c' and σ_c are the effective and total vertical stress in the stone column region, respectively; σ_s' and σ_s are the effective and total vertical stress in the soft soil region, respectively.

The average excess pore water pressure within the stone column and surrounding soil can be achieved by averaging the excess pore pressure in both *r*- and *z*-directions as follows:

$$\overline{u}_c(t)=\frac{1}{\pi a^2 H}\left[\int_{z=0}^{H}\int_{r=0}^{a}2\pi\,u_c(r,z,t)\,r\,dr\,dz\right] \tag{4.23a}$$

$$\overline{u}_s(t)=\frac{1}{\pi(b^2-a^2)H}\left[\int_{z=0}^{H}\int_{r=a}^{b}2\pi\,u_s(r,z,t)\,r\,dr\,dz\right] \tag{4.23b}$$

The average surface settlement (i.e. the average settlement at $z_0=0$) of the stone column and surrounding soil can also be obtained via the following equations:

$$\overline{S}_c(z_0=0,t)=\overline{\varepsilon}_{vc}(t)\,H=\frac{\overline{\sigma}_c-\overline{u}_c(t)}{M_c}H \tag{4.24a}$$

$$\overline{S}_s(z_0=0,t)=\overline{\varepsilon}_{vs}(t)\,H=\frac{\overline{\sigma}_s-\overline{u}_s(t)}{M_s}H \tag{4.24b}$$

where $\overline{\varepsilon}_{vc}(t)$ and $\overline{\varepsilon}_{vs}(t)$ are the average volumetric strain of the column and soil at time t, respectively; $\overline{\sigma}_c$ and $\overline{\sigma}_s$ are the average total vertical stresses within the column and soil induced by external loading, respectively.

The average degree of consolidation for the stone column and for the surrounding soil based on the settlement (or volumetric strain) can be derived as follows:

$$\bar{U}_c(t) = \frac{\bar{S}_c(z_0 = 0, t)}{\bar{S}_c(z_0 = 0, \infty)} = \frac{\bar{\varepsilon}_{vc}(t)}{\bar{\varepsilon}_{vc}(\infty)} = \frac{\bar{\sigma}_c - \bar{u}_c(t)}{\bar{\sigma}_c} = 1 - \frac{\bar{u}_c(t)}{\bar{\sigma}_c} \tag{4.25a}$$

$$\bar{U}_s(t) = \frac{\bar{S}_s(z_0 = 0, t)}{\bar{S}_s(z_0 = 0, \infty)} = \frac{\bar{\varepsilon}_{vs}(t)}{\bar{\varepsilon}_{vs}(\infty)} = \frac{\bar{\sigma}_s - \bar{u}_s(t)}{\bar{\sigma}_s} = 1 - \frac{\bar{u}_s(t)}{\bar{\sigma}_s} \tag{4.25b}$$

where $\bar{S}_c(z_0 = 0, \infty)$ and $\bar{S}_s(z_0 = 0, \infty)$ are the final average surface settlement, and $\bar{\varepsilon}_{vc}(\infty)$ and $\bar{\varepsilon}_{vs}(\infty)$ are the final average volumetric strain when time t approaches infinity. The subscripts c and s indicate the stone column and surrounding soil region, respectively.

It is observed that the average surface settlement and average degree of consolidation described in Equations (4.24) and (4.25) can be captured when the average total vertical stress (i.e. $\bar{\sigma}_c$ and $\bar{\sigma}_s$) and the average excess pore water pressure (i.e. $\bar{u}_c(t)$ and $\bar{u}_s(t)$) have been achieved.

4.4 Worked example and verification

In this section, a numerical example is conducted to validate the proposed analytical solution while the accuracy of the solution is verified by a finite element simulation and field measurements of a case history. Moreover, the proposed analytical solution in this chapter is also verified against available analytical studies in the literature.

4.4.1 Worked example

In many available studies on the consolidation of soil with vertical drains or stone columns, the stress induced by external load was assumed to be uniform with soil depth. However, this assumption may be only applicable when the external loading distributes uniformly and infinitely on the ground surface. In reality, the stress in the composite ground may reduce with depth when the thickness of soft soil layer is large in comparison with the loading area on the soil surface. Referring to the studies by other researchers [115, 132, 217], the same linear distribution of total stress with depth for both column and soil was adopted in this study. The equations of total stresses caused by the external loading were assumed to have the following forms:

$$\sigma_c(r,z) = \sigma_{cr}(r)\, f_{cz}(z) = \sigma_{cr}(r)\left[1+(\alpha-1)\frac{z}{H}\right] \tag{4.26a}$$

$$\sigma_s(r,z) = \sigma_{sr}(r)\, f_{sz}(z) = \sigma_{sr}(r)\left[1+(\alpha-1)\frac{z}{H}\right] \tag{4.26b}$$

where $\sigma_{cr}(r)$ and $\sigma_{sr}(r)$ denote the total vertical stress distribution on the top of column and soft soil under the applied external loading, respectively; $f_{cz}(z)$ and $f_{sz}(z)$ denote the variation of total vertical stress against depth for column and soft soil, respectively (Figure 4.2), and defined as:

$$f_{cz}(z) = f_{sz}(z) = 1+(\alpha-1)\frac{z}{H} \tag{4.27}$$

where α is the ratio of the bottom to top vertical stress of the column and soil. This ratio would range from 0 to 1, representing different patterns of vertical stress distribution along *z*-direction. When $\alpha = 0$, the triangular distribution of vertical stress is produced;

when α value is between 0 and 1, the distribution is a trapezoidal pattern (Figure 4.2); and when $\alpha = 1$, the vertical stress distributes uniformly with depth.

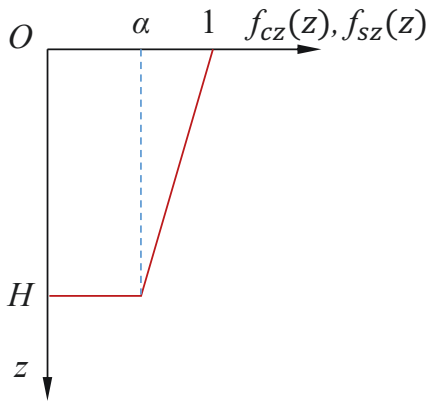

Figure 4.2. The variation of total vertical stresses against depth for the stone column and soft soil regions

The input data of the problem under consideration were selected in accordance with the benchmark values that are likely to encounter in practice as shown below.

- Geometric dimensions:

  $H = 10\,m$, $a = 0.5\,m$, $b = 1.25\,m$;

- Material properties:

  $k_{ch} = 5\times10^{-5}\,m/s$, $k_{cv} = k_{ch}$, $E_c = 60\times10^{3}\,kPa$, $\nu_{Pc} = 0$,

  $k_{sh} = 5\times10^{-10}\,m/s$, $k_{sv} = 0.5\,k_{sh}$, $E_s = 2\times10^{3}\,kPa$, $\nu_{Ps} = 0$;

where E_c and E_s are Young's modulus of the stone column and soft soil, respectively; ν_{Pc} and ν_{Ps} are Poisson's ratio of the stone column and soft soil, respectively.

- Other properties:

  $q = 100\,kPa$, $\alpha = 0.75$, $\gamma_w = 10\,kN/m^3$;

where q is the external load which is applied instantaneously on the top of unit cell and kept constant during the consolidation process.

To investigate the variation of excess pore water pressure, the particular points at depth $z = 0.25H$, $z = 0.5H$ and $z = 0.75H$ with radius $r = 0.5a$ and $r = 0.5(a+b)$ corresponding to the region of column and soil in the unit cell were selected.

Applying Equations (4.21), the variation of the excess pore water pressure with respect to each single variable r, z, or t can be captured when the remaining variables are kept constant.

Figures 4.3 and 4.4 depict the excess pore water pressure isochrones at different time t along the *r*- and *z*-directions, respectively. As observed, the isochrones in Figure 4.3

satisfied the finiteness condition at the column centre, as well as the interface and radial boundary conditions corresponding to Equations (4.5a), (4.5b) and (4.5c) in which excess pore pressures were almost unchanged along the radius of stone column at a particular time and reached the highest values at the boundary $r = b$. The finite values of excess pore pressure within the column demonstrate the presence of drain resistance effect for a given permeability of the column. The excess pore pressure in the column dissipated rapidly and decreased to approximately $2\,kPa$ at time $t = 10^4\,s$ meanwhile the corresponding excess pore water pressure in most of soft soil region (i.e. $r \geq 0.6\,m$) remained the same as the initial excess pore pressure. Figures 4.4a and 4.4b illustrate the excess pore pressure isochrones in response to the linear distribution of total vertical stress with depth in the column and soft soil, respectively. The excess pore pressures endured the dissipation and redistribution process to achieve the equilibrium state where the pressures immediately reduced to zero at the top drainage boundary of the unit cell after applying external loading. The distribution pattern of excess pore water pressure in the column changed dramatically with depth in which the location of maximum pressure value moved downward and reached the stone column base right after loading roughly 20 s (see Figure 4.4a). It should be noted that the excess pore water pressure would dissipate from the location of high pressure value towards the location of lower pressure value. Therefore, during about the first 20-second period of loading, the dominant portion of excess pore water pressure in stone column dissipated towards the top and bottom of the column. When dissipating downward, the excess pore water pressure encountered the impervious column base which resisted the dissipation process and thus the excess pore pressure at the lower part of the column (i.e. $z \geq 0.8H$) became increasing slightly. After that, the dissipation process in stone column only occured upward the column top

drainage boundary and the excess pore pressure along the entire length of column decreased with time. Figure 4.4b displays a gradual variation in the pattern of excess pore pressure distribution over the thickness of soft soil region against time. The location of the peak excess pore pressure also moved towards the bottom of the soil deposit; however, this downward movement was extremely slower than that in the column.

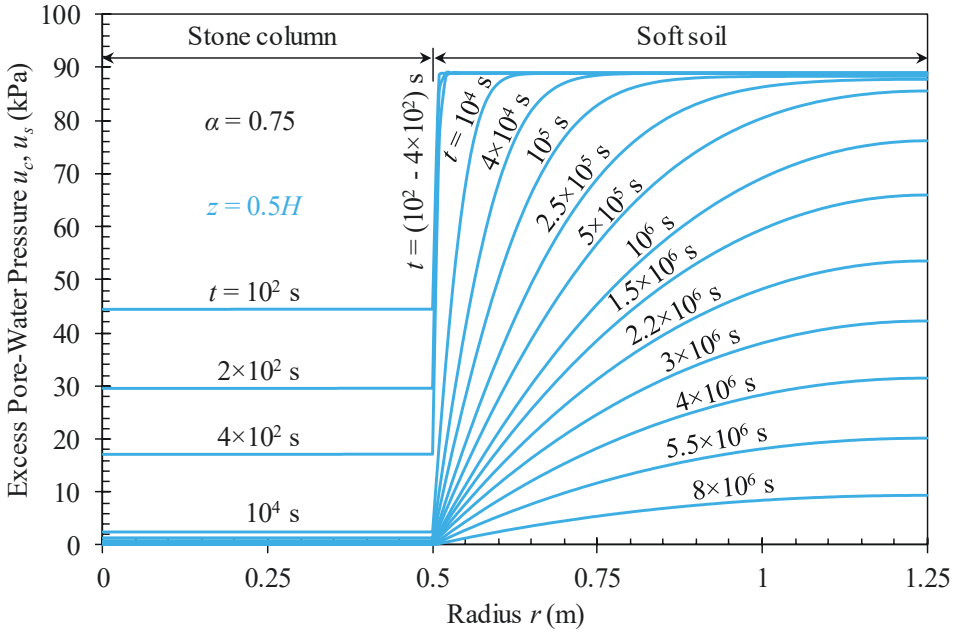

Figure 4.3. Excess pore water pressure isochrones against radius at depth $z = 0.5H$ for the stone column and soft soil regions

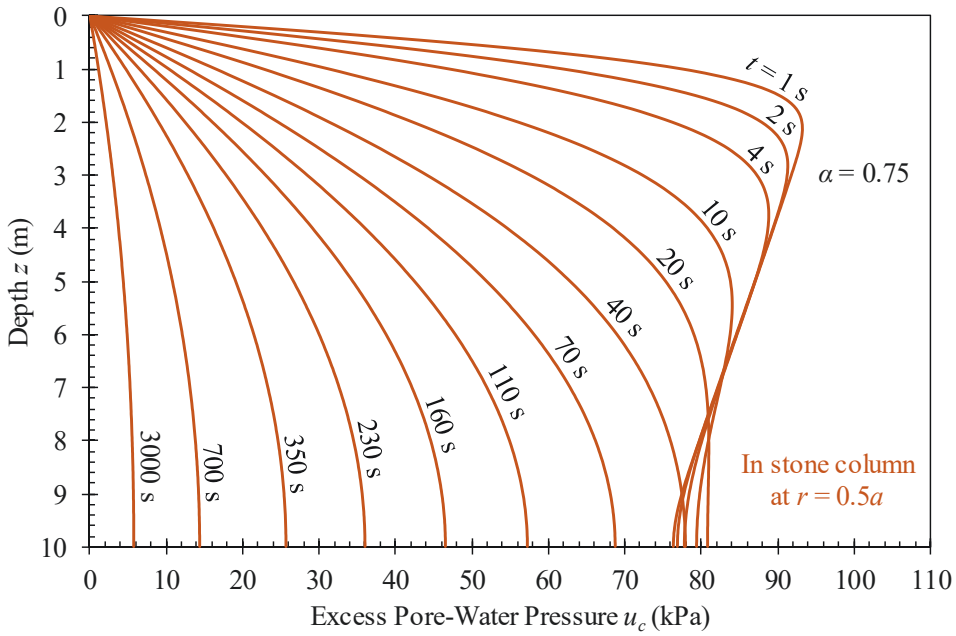

Figure 4.4a. Excess pore water pressure isochrones against depth at radius $r = 0.5a$ within the stone column region

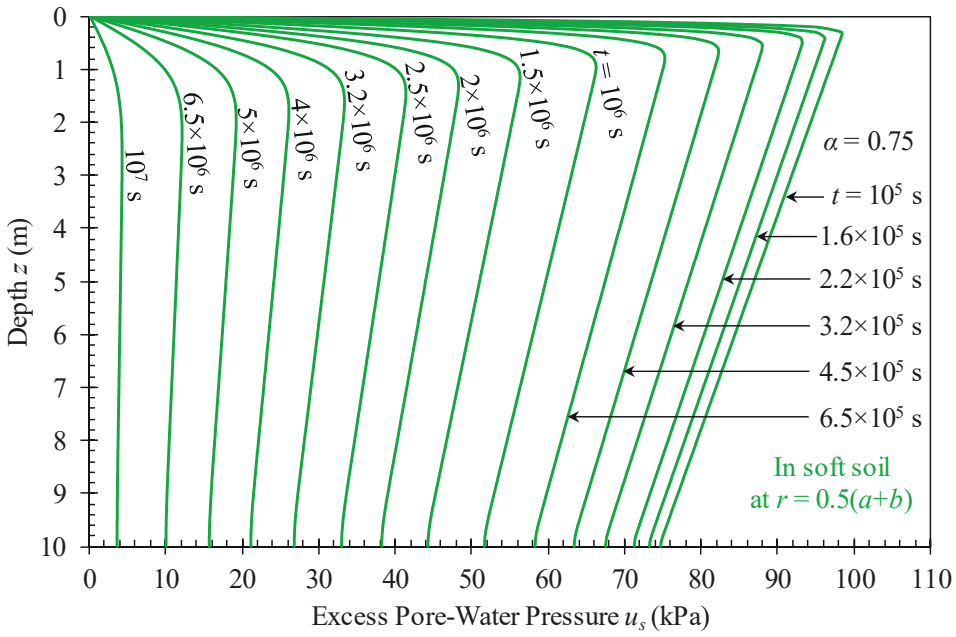

Figure 4.4b. Excess pore water pressure isochrones against depth at radius $r = 0.5(a+b)$ within the soft soil region

Figure 4.5 shows the dissipation of excess pore water pressure at various points in the unit cell. As expected, the initial excess pore pressures at different depths were compatible with the linear distribution against depth of the total vertical stress ($\alpha = 0.75$) generated by the constant applied loading on the ground surface. It should be noted that the dissipation rates of excess pore pressure in both column and soft soil regions are slower when the point of interest is deeper. The observed results for the soil region can be seen clearer particularly when $\alpha = 1$ and the horizontal permeability ratio of column to soil (k_{ch} / k_{sh}) becomes smaller; a decline of k_{ch} / k_{sh} reduces the difference in excess pore pressure between column and soft soil regions during the consolidation process. However, for $\alpha = 0.75$ and $k_{ch} / k_{sh} = 10^5$ adopted in this example, the deeper point of interest in the soil had a smaller initial excess pore pressure and a faster rate of excess pore pressure dissipation. The reason can be attributed to the control of radial flow in the soil towards the column along with the extremely faster dissipation of excess pore pressure in the column than that in the soil. Further discussion on the effect of k_{ch} / k_{sh} and α values is provided in the parametric study in the following section.

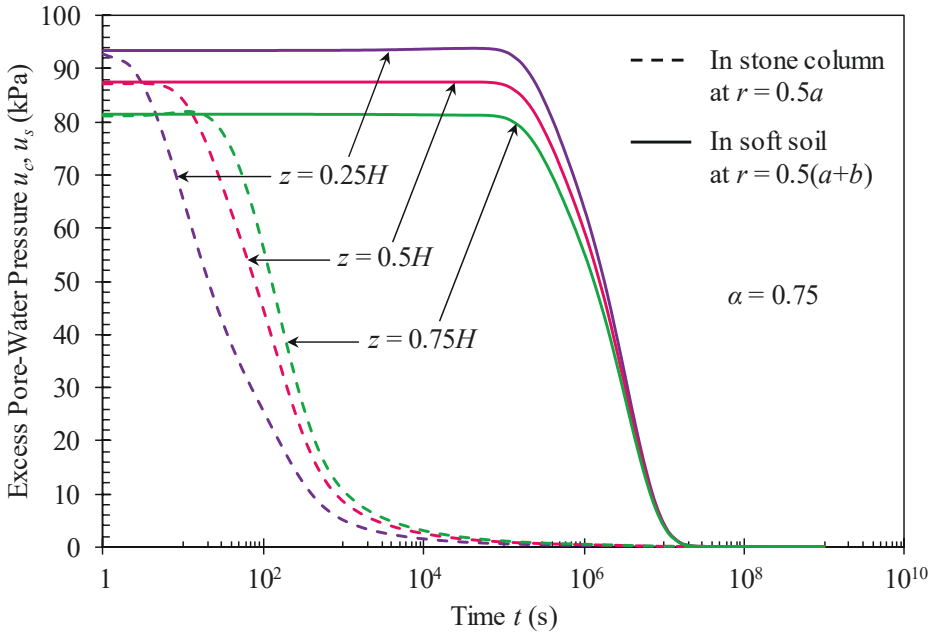

Figure 4.5. Dissipation of excess pore water pressure against time at various points in the stone column and soft soil regions

Referring to Equations (4.22) and assigning $z_0 = 0$ (i.e. ground surface), the surface settlement of the unit cell due to the dissipation of excess pore water pressure was captured as a set of isochrones varying with time (Figure 4.6a). The top surface settlement of the column was nearly uniform over the radial direction, which promptly reached the maximum of $0.015\,m$. There was a significant differential settlement along the radial direction within the soil at the early consolidation stages; nevertheless, this difference diminished with consolidation time and a more uniform surface settlement for the soft soil was achieved at the later stages of consolidation. This phenomenon results from the fact that the excess pore water pressure in the vicinity of the stone column dissipated much faster than that in the rest of soft soil domain. Immediately after loading while the undrained condition can be assumed, the settlement in most domains of soft soil was insignificant. Figure 4.6b presents the differential settlements at a specified time for

distinctive depths of the unit cell. The larger the examined depth, the smaller differential settlement between column and soil as well as the soil itself.

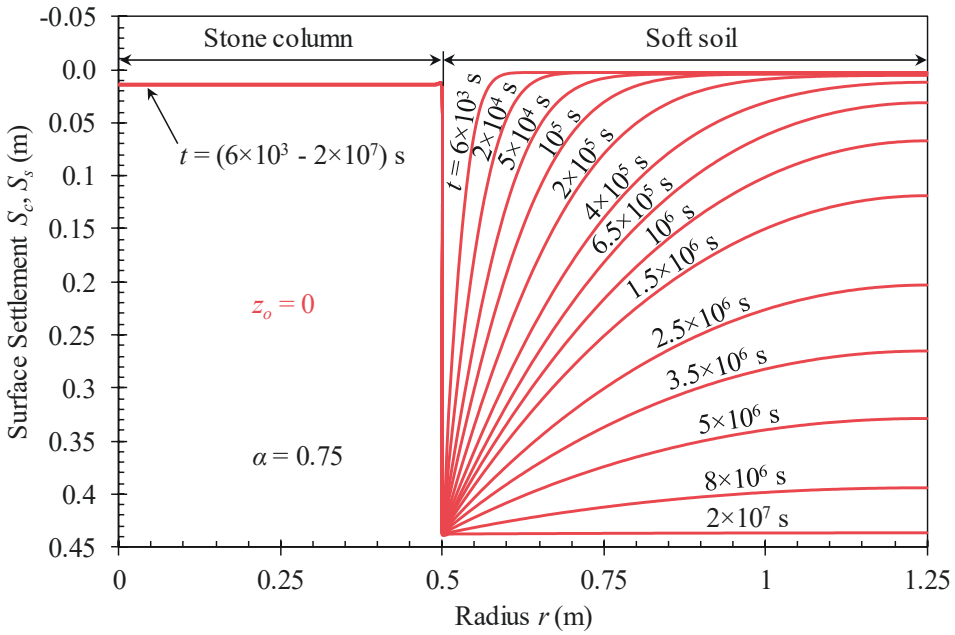

Figure 4.6a. Surface settlement isochrones against radius for the stone column and soft soil regions

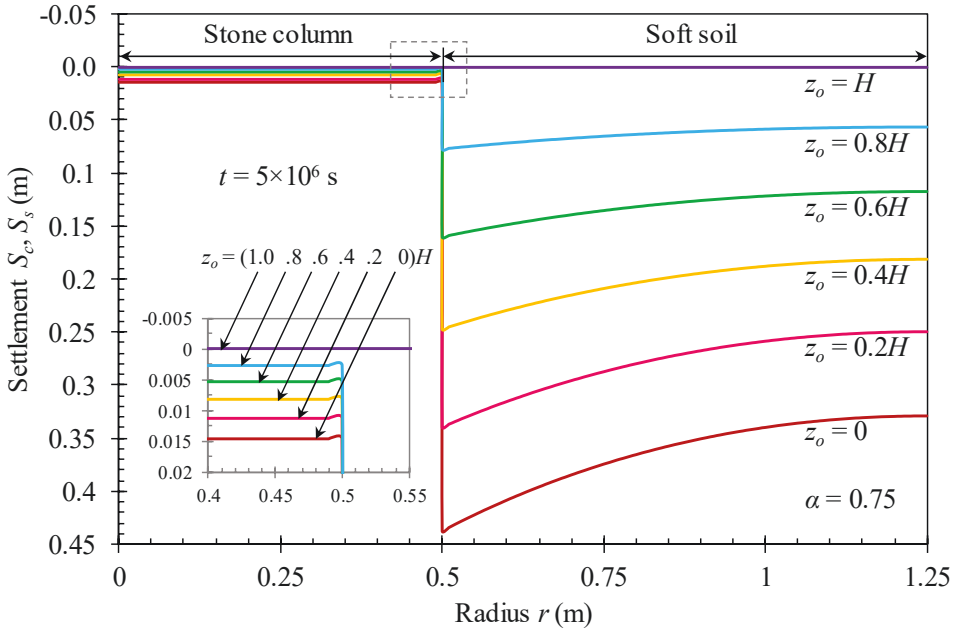

Figure 4.6b. Settlement isochrones against radius at time $t = 5\times10^6 s$ for the stone column and soft soil regions with different investigating depths

4.4.2 Verification against finite element simulation

A finite element analysis using the PLAXIS 2D [212] software was conducted to verify the proposed analytical solution. Considering the axisymmetric condition, the numerical model with 15-node triangular elements was generated as displayed in Figure 4.7 in which 2717 elements and 23221 nodes had been created. The normal displacements on vertical and bottom boundaries of the numerical model were not allowed, while the top surface was simulated as a free boundary. On the other hand, to consider one-dimensional deformations as in the analytical formulations, only vertical deformation in the interface of soil-column was allowed while radial displacements were set to be zero. The interface was assigned as a drained element with negligible stiffness (Young's modulus equal 10^{-3} kPa and Poisson's ratio equal zero) to simulate free strain condition of the proposed

analytical model ignoring shear strain effect at the column-soil interface. In addition, to set the flow boundary conditions to enable consolidation of the composite ground, no flow was permitted across the centerline, the exterior radial boundary of the unit cell, and the cell base; while the upper surface of the model was a fully permeable boundary. The soil and column properties including stiffness and hydraulic permeability in both analytical and numerical models were identical. It should be noted that for this verification exercise $\alpha = 1$ was selected in the proposed analytical solution simulating the uniform distribution of the initial excess pore water pressure as a result of the applied uniform load on the ground surface.

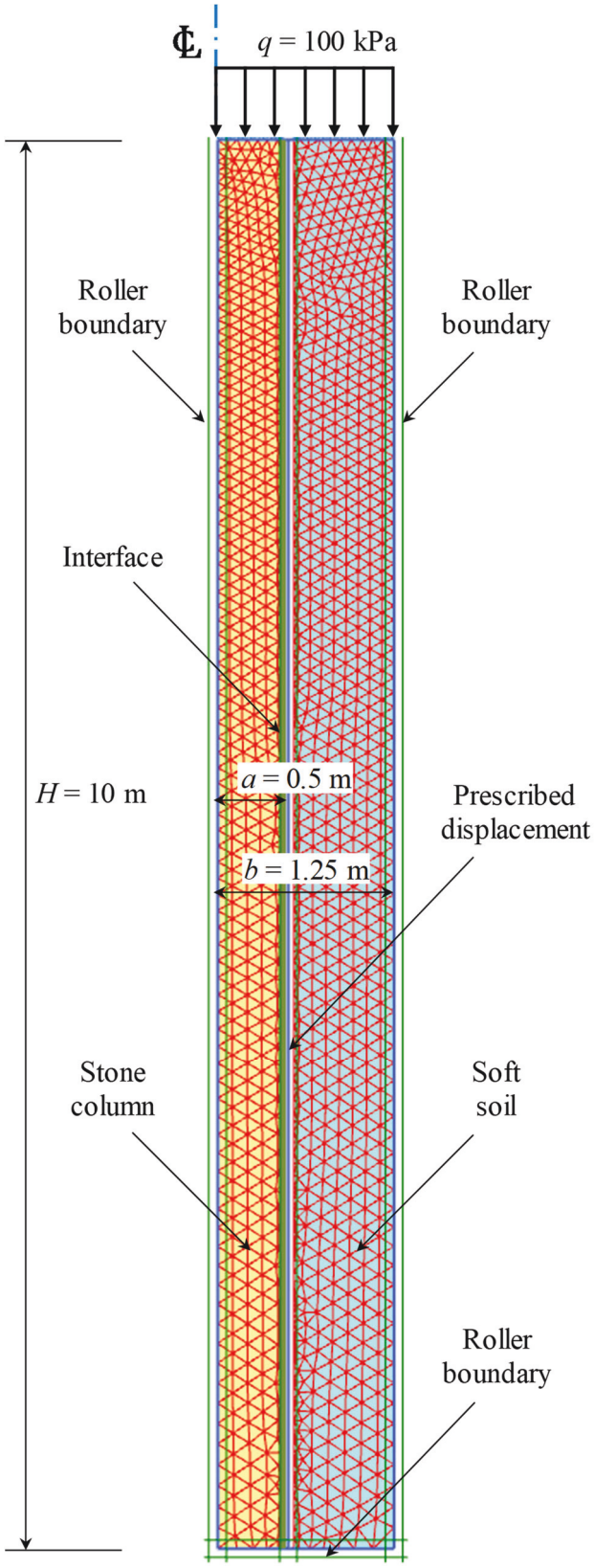

Figure 4.7. Finite element model used for the verification exercise

The verification was performed by investigating and comparing the dissipation of excess pore water pressure at various points obtained from the proposed analytical solution and numerical simulation. Besides, the average degree of consolidation for each region of the unit cell (i.e. stone column and soft soil) was also compared between the two cases.

Figure 4.8 compares the predicted excess pore pressure variations with time at selected points obtained from the proposed analytical solution and the finite element simulation. As can be seen, the analytical and numerical predictions are in good agreement verifying the reliability of analytical solution. The slight discrepancies between predictions may be due to the redistribution of the total vertical stress in the soil region in the numerical model induced by the shear strain developed under the differential settlement condition, which was ignored in the proposed analytical solution. It should be noted that due to the rapid excess pore water pressure dissipation in the stone column, the settlement of stone column remains rather uniform and so the shear strain effect and accompanying total stress redistribution are negligible within the column region.

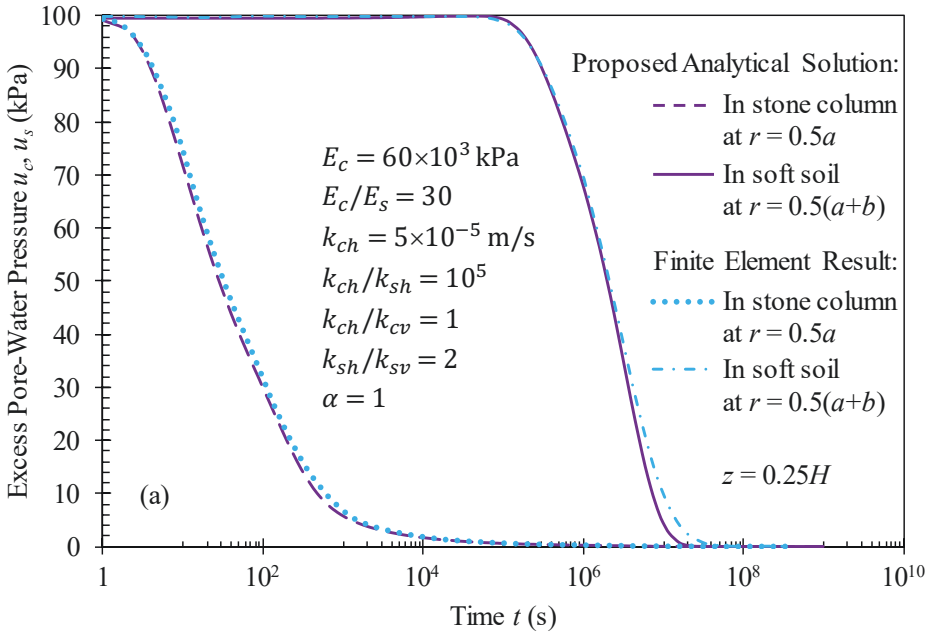
Excess Pore-Water Pressure u_c, u_s (kPa)
Time t (s)
$E_c = 60\times10^3$ kPa
$E_c/E_s = 30$
$k_{ch} = 5\times10^{-5}$ m/s
$k_{ch}/k_{sh} = 10^5$
$k_{ch}/k_{cv} = 1$
$k_{sh}/k_{sv} = 2$
$\alpha = 1$
(a)
Proposed Analytical Solution:
In stone column at $r = 0.5a$
In soft soil at $r = 0.5(a+b)$
Finite Element Result:
In stone column at $r = 0.5a$
In soft soil at $r = 0.5(a+b)$
$z = 0.25H$

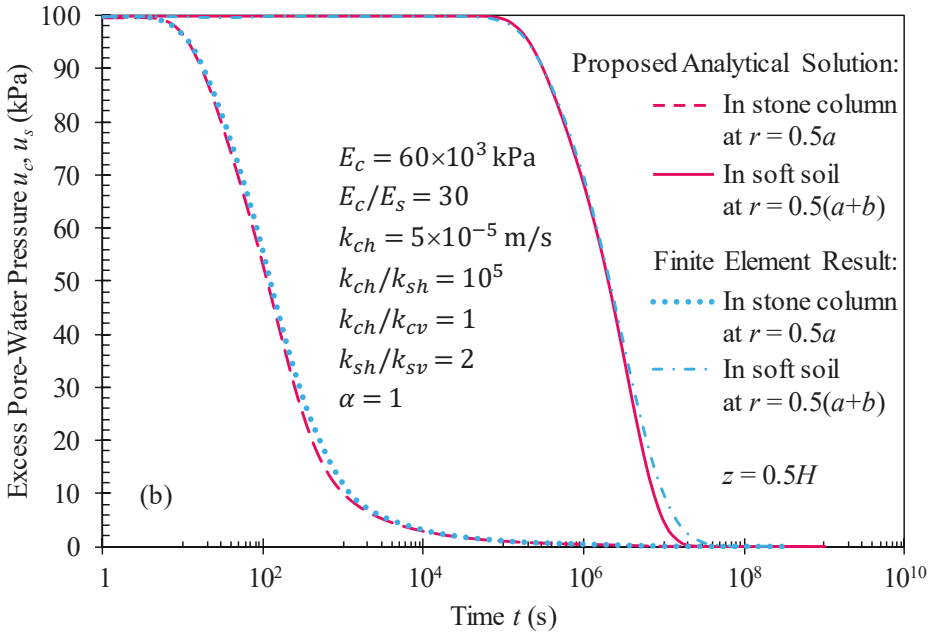
Excess Pore-Water Pressure u_c, u_s (kPa)
Time t (s)
$E_c = 60\times10^3$ kPa
$E_c/E_s = 30$
$k_{ch} = 5\times10^{-5}$ m/s
$k_{ch}/k_{sh} = 10^5$
$k_{ch}/k_{cv} = 1$
$k_{sh}/k_{sv} = 2$
$\alpha = 1$
(b)
Proposed Analytical Solution:
In stone column at $r = 0.5a$
In soft soil at $r = 0.5(a+b)$
Finite Element Result:
In stone column at $r = 0.5a$
In soft soil at $r = 0.5(a+b)$
$z = 0.5H$

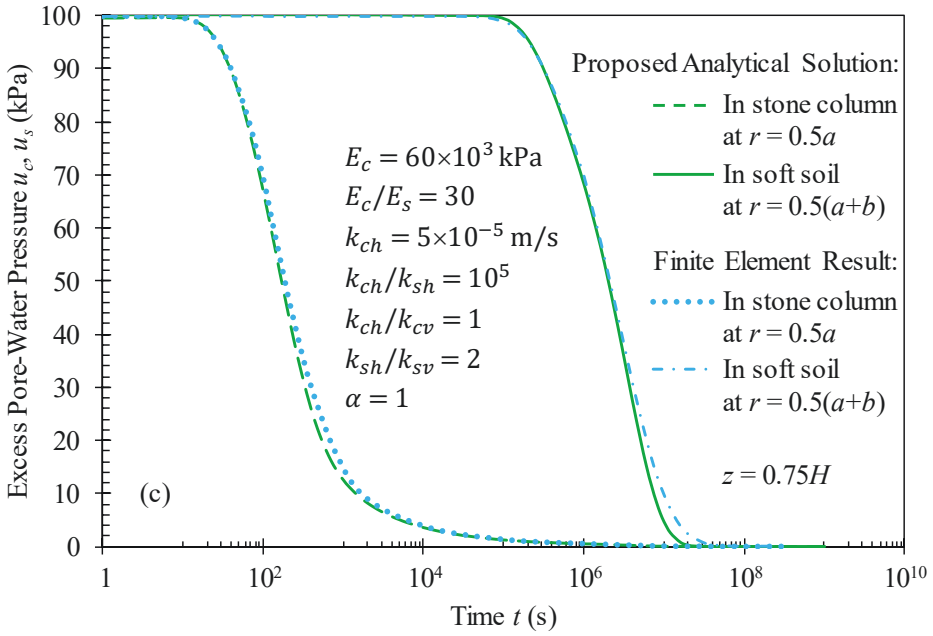

Figure 4.8. Comparison in dissipation of excess pore water pressure between proposed analytical solution and finite element result at points in the stone column and soft soil regions with depth (a) $z = 0.25H$, (b) $z = 0.5H$, and (c) $z = 0.75H$

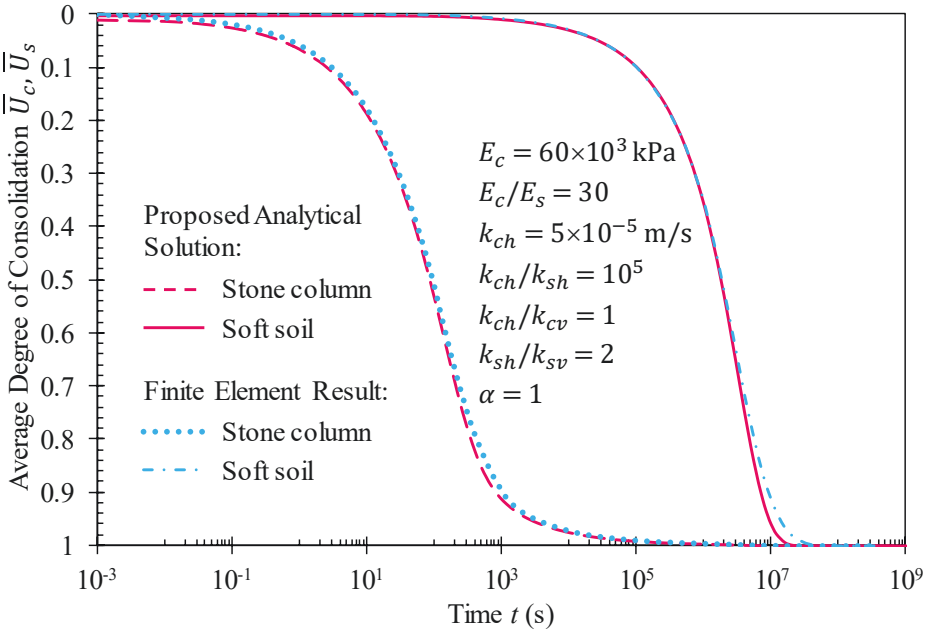

Figure 4.9. Comparison in average degree of consolidation between proposed analytical solution and finite element result for the stone column and soft soil regions

Then, the average degree of consolidation for each region of the unit cell based on Equations (4.25a) and (4.25b) was verified against the results from the finite element model. Referring to Figure 4.9 and analogous to the verification on the dissipation of excess pore pressure, the predictions of average degree of consolidation from the proposed analytical solution and finite element simulation were almost identical during the consolidation process.

It is worth mentioning that Poisson's ratio equal zero was adopted in the above example and numerical modelling to simulate the one-dimensional consolidation in vertical direction as assumed in the mathematical model. In case $\nu_{Pc} = \nu_{Ps} = 0$, the assignment of zero radial displacements for the column-soil interface in the finite element model can be released without influencing the numerical results. In contrast, the radial displacements of the interface element would be set equal zero to enable the one-dimensional deformations of the stone column and soft soil bodies when Poisson's ratio is non-zero, similar to the example in Chapter 3.

4.4.3 Verification against field measurements and existing analytical studies

An additional verification of the proposed analytical solution with field measurements of a case history was also carried out in terms of excess pore water pressure dissipation and settlement rates in the composite stone column - clay foundation. The selected case study here is the foundation system of the Nelson Point iron ore stockyard in Western Australia. Referring to information available in the literature about this project [218-220], the strata of the relevant stockyard was composed of a very soft clay layer of up to 3 m thickness

overlain by about 3 m of sandy dredged fill and underlain by 1-3 m limestone; while a 10-15 m dense clayey sand layer with high strength and low permeability was recognised beneath the limestone stratum. The water level was 1.5-2.5 m below the ground surface, within the sandy fill. As reported by Dunbavan and Carter [219], to improve the soft clay, stone columns which were 1.1 m diameter (i.e. radius $a = 0.55\,m$) were fully penetrated on a triangular pattern with an approximate spacing of 2.25 m (corresponding to the radius of unit cell model $b = 1.125\,m$). Dunbavan and Carter [219] also reported in-situ permeabilities $k_{sh} = k_{sv} = 1.5\times10^{-5}\,m/day$ (i.e. $\approx 1.74\times10^{-10}\,m/s$) and coefficients of consolidation $c_{sh} = c_{sv} = 0.2-1 m^2/year$ (i.e. $c_{sh} = c_{sv} = 0.63\times10^{-8} - 3.17\times10^{-8}\,m^2/s$) for the soft clay surrounding stone columns. Moreover, Stewart and Fahey [218] suggested a range of modulus ratio $E_c / E_s = 20-40$ in their study on the above mentioned composite foundation. The reinforced ground was subjected to a surface loading induced by the filling operation of the ore stockpile in which the average unit weight of ore was estimated to be $28\,kN/m^3$. The stockpile filling was conducted in two stages where the first filling to the height 17 m had occurred within about 25 hours and the second filling from the height 17 to 19 m started at about 900 hours after the beginning of first filling.

It should be noted that the equilibrium of total vertical stresses at any time for a given average external load q can be written as below:

$$\bar{\sigma}_{cr}\,\pi a^2 + \bar{\sigma}_{sr}\,\pi(b^2 - a^2) = q\,\pi b^2 \tag{4.28}$$

where $\bar{\sigma}_{cr}$ and $\bar{\sigma}_{sr}$ are the average vertical stresses on top of stone column and surrounding soil in the unit cell model, respectively.

On the other hand, to consider the soil arching effect in a given embankment loading which induces a greater vertical stress on stone column compared to encircling soft soil, a stress concentration ratio n_{scr} would be utilised in the analytical derivation. The stress concentration ratio n_{scr} is defined as the ratio of the average vertical stress on top of the stone column to that on surface of the surrounding soft soil:

$$n_{scr} = \frac{\bar{\sigma}_{cr}}{\bar{\sigma}_{sr}} \tag{4.29}$$

Therefore, $\bar{\sigma}_{cr}$ and $\bar{\sigma}_{sr}$ can be determined for a particular value of n_{scr} by combining Equations (4.28) and (4.29). For the adopted verification exercise against the field measurements, it is assumed that the vertical stresses on the top of stone column and soft soil regions caused by the stockpile loading distribute uniformly in each region. Hence, the functions $\sigma_{cr}(r)$ and $\sigma_{sr}(r)$ can be replaced respectively by $\bar{\sigma}_{cr}$ and $\bar{\sigma}_{sr}$ in the mathematical model and the proposed analytical solution.

According to Dunbavan and Carter [219], the average vertical stress on the stone column was approximate twice the average surface pressure of the ore stockpile immediately after the first filling (i.e. $n_{scr} \approx 2.5$). At the later stages of consolidation, the former increased to approximately four times the latter (i.e. $n_{scr} \approx 5$).

Figure 4.10 compares the dissipation rate of excess pore water pressure obtained by the proposed analytical solution with field measurement at the investigation point in soft soil ($r = 0.7$ m, $z = 1.5$ m), which was very close to stone column [220]. The proposed analytical solution adopted consolidation parameters as reported in the existing literature [218, 219], whereas permeabilities of stone column were assumed to be

$k_{ch} = k_{cv} = 5 \times 10^{-5}\ m/s$ within the range of benchmark values in practice due to the lack of measurement on site. Besides, the average external load in the analytical solution is equivalent to the first filling to 17 m height of the stockpile (i.e. $q = 476$ kPa). Under the extremely rapid filling of the ore stockpile in each loading stage (almost step loading), the excess pore water pressure increased quickly to maximum corresponding to the increase in average vertical stress on soft clay surface as shown by field data. In order to verify the proposed analytical solution which adopts the instant loading, the field measurement of excess pore water pressure dissipation under the 17 m height of filling is of interest. It can be observed that the proposed analytical solution agreed well with the field observations particularly during the first 60% of consolidation, where excess pore water pressure dissipated to a value of approximately 150 kPa while $n_{scr} = 2.5$ had been applied. After that, the proposed analytical solution underestimated the dissipation rate compared with the field measurement. The reason is attributable to the increase of stress concentration ratio during consolidation process, due to which the total vertical stress on soft clay and excess pore water pressures reduced more quickly, while the stress concentration ratio remained unchanged in the analytical solution. However, it can also be observed that the trend of field data due to the first filling tends to approach the results from proposed analytical solution at the later period of consolidation adopting $n_{scr} = 5$.

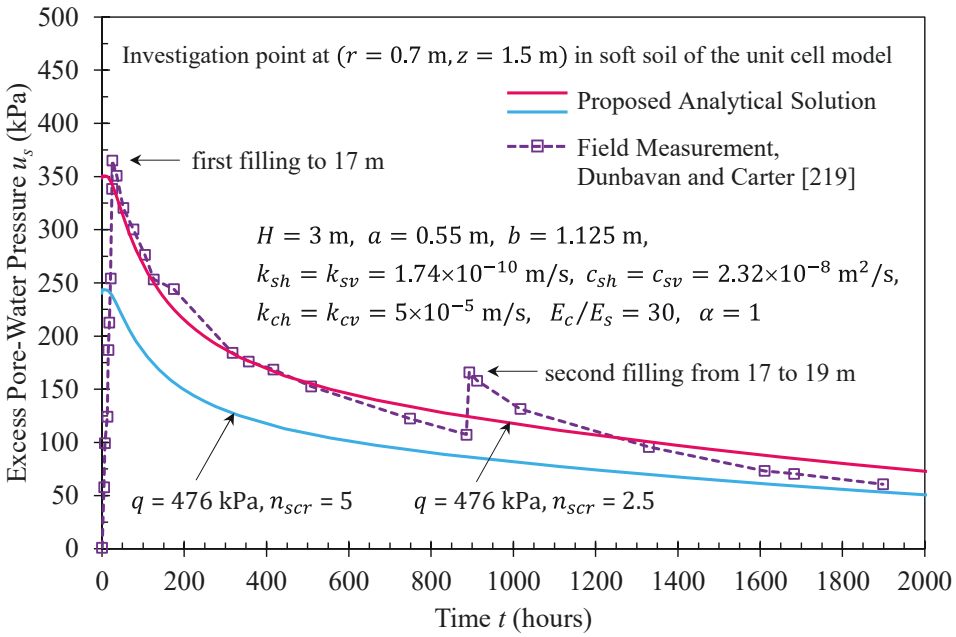

Figure 4.10. Comparison of excess pore water pressure dissipation against time between proposed analytical solution in this study and field measurement at the investigation point ($r = 0.7$ m, $z = 1.5$ m) in soft soil

Figure 4.11 compares the settlement rate of soft soil obtained from the proposed analytical solution and field observation. As reported by Dunbavan and Carter [219], the measured settlement of soft soil right after the first filling was approximate 290 mm. At this point of time, the analytical solution in this chapter resulted in a consolidation settlement of soft soil around 60 mm, adopting stress concentration ratio $n_{scr} = 2.5$. Therefore, it is supposed that the immediate settlement of soft soil after the first filling of stockpile was approximate 230 mm, as a difference between the measured settlement at field and the calculated consolidation settlement. By combining this immediate settlement with consolidation settlement of soft soil calculated using the proposed analytical solution for time $t \geq 25$ hours, the variation of predicted soil settlement with time can be achieved as shown in Figure 4.11. Due to the assumption of instant loading in this chapter,

the settlement prediction under the first loading of stockpile is of concern. As observed, the proposed analytical solution adopting $n_{scr} = 2.5$ predicted the field measurement during the early stages of consolidation reasonably. The field settlement owing to the first surcharge was prone to approach the soil settlement predicted by the proposed analytical solution employing larger stress concentration ratio as the consolidation progressed. The underestimate of the analytical solution obtained in this chapter is attributed to the lateral displacement and inelastic deformation of soft soil during the consolidation in practice, which was not integrated into the proposed analytical solution.

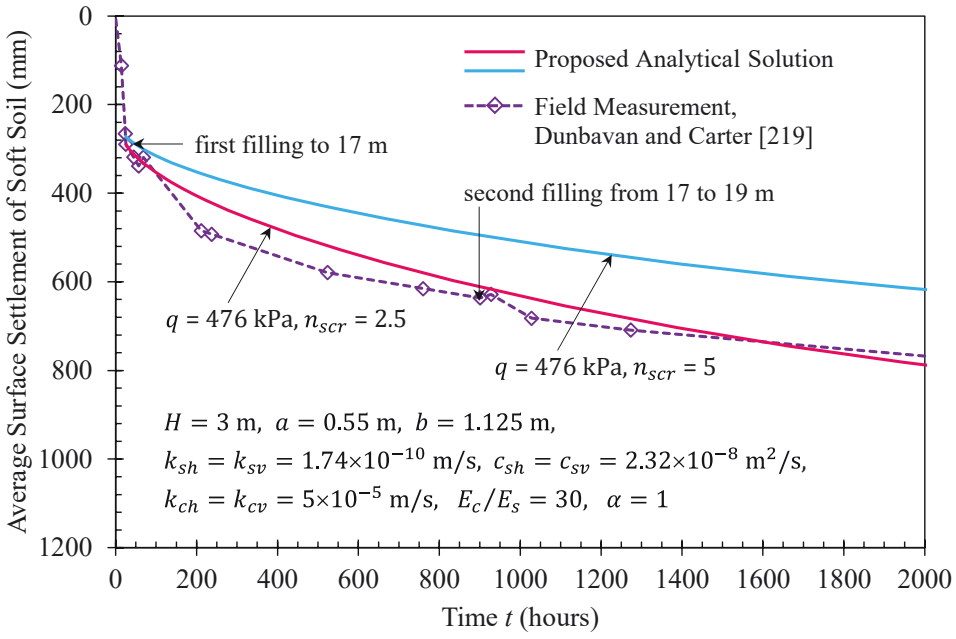

Figure 4.11. Comparison of average surface settlement of soft soil against time between proposed analytical solution in this study and field measurement

Therefore, the proposed analytical solution is capable of predicting the variation of excess pore water pressure and consolidation settlement in soft soil surrounding stone columns with time assuming a lower bound of stress concentration ratio for the early

stages of consolidation and an upper bound of that for the later stages. For the practical usage, the lower and upper bounds of stress concentration ratio could be assumed $n_{scr} = 2 - 6$ for a typical flexible embankment following the observations by various researchers [213, 221].

Finally, this section presents a verification of the proposed analytical solution against the analytical study conducted by Barron [64], examining average degree of consolidation of the composite stone column – soft ground. It is worth noting that the analytical solution in this chapter is derived employing Barron's theory of consolidation for coupled radial – vertical flows of excess pore water pressure in stone column and soft soil, where consolidation parameters for both stone column and soft soil are integrated into the mathematical formulation. Furthermore, the unequal distribution of applied vertical stresses on stone column and encircling soft soil regions due to the significant difference in stiffness between regions can be considered by introducing a stress concentration ratio n_{scr} into the proposed analytical model and solution. Therefore, Barron's solution is a particular case of the proposed analytical solution. In Barron's solution, the vertical flow of excess pore water pressure in soft soil was not included rigorously, while the radial flow was ignored (i.e. assuming an infinite radial permeability) in vertical drain. The stiffness of drain was also neglected in the analytical study by Barron [64] and thus soft soil is deemed to carry external loading entirely.

Figure 4.12 illustrates the average degree of consolidation of composite stone column – soft soil foundation resulted from the proposed analytical solution and Barron's solution. The average degree of consolidation of the composite foundation $\overline{U} = \overline{S}(t)/\overline{S}(\infty)$ is calculated as a ratio between average surface settlement at any point of consolidation time and final average surface settlement. The stress concentration ratio

$n_{scr} > 1$ is adopted in the proposed analytical solution to simulate the larger concentration of applied vertical stress on stone column compared to surrounding soil. The calculation results obtained from proposed analytical solution would approach those obtained from Barron's solution by adopting $n_{scr} = 1$, k_{sv} approaching zero and k_{ch} approaching infinity. In addition, the values of $\overline{S}$ and $\overline{U}$ would be calculated corresponding to soft soil region only simulating soft soil carrying entire applied load. Figure 4.12 shows that Barron's solution underestimated the consolidation rate of composite ground compared to the proposed analytical solution adopting $n_{scr} > 1$. Also, an increase in stress concentration ratio led to the accelerated consolidation of composite stone column – soft ground.

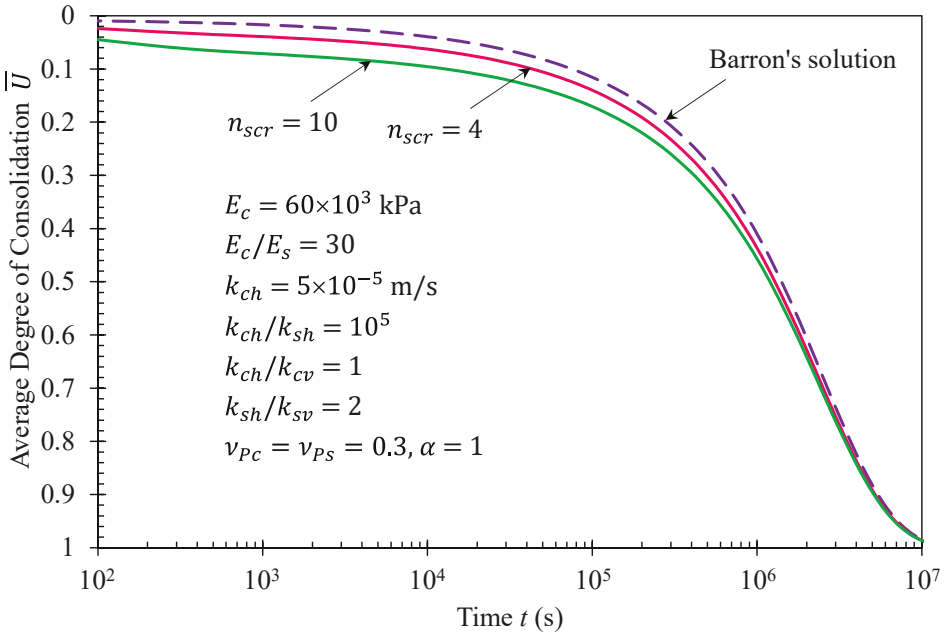

Figure 4.12. Comparison of average degree of consolidation between proposed analytical solution and Barron's solution

4.5 Parametric study

This section presents results of a parametric analysis to investigate the influence of several factors on the consolidation behaviour of the soft ground reinforced by stone column adopting the proposed analytical solution. The investigating parameters consisted of column spacing, stiffness and radial permeability of soft soil, variation pattern of total stress with depth, and thickness of the soil deposit to be improved. On the other hand, the consolidation response of the composite ground was assessed in terms of the average degree of consolidation for stone column and for surrounding soil together with the average differential settlement between them. The average degree of consolidation for each region of the unit cell can be calculated using Equations (4.25a) and (4.25b); thus the average differential settlement ($\Delta\overline{S}$) is determined as a difference in the average surface settlement between the column and surrounding soil calculated by Equations (4.24a) and (4.24b), respectively. During the analysis, the parameters of stone column including radius, modulus and permeability coefficient remained unchanged, while the investigating factors were changed independently in a typical range encountered in real practice and field. Additionally, the horizontal and vertical permeability coefficients of the column were adopted to be the same (i.e. $k_{ch} = k_{cv}$), while the ratio of horizontal to vertical permeability coefficients of surrounding soil remained at 2 (i.e. $k_{sh} = 2k_{sv}$). In all cases, the platform was considered as flexible satisfying free strain condition and thus the external loading distributes uniformly on the ground surface with a value of $100\,kPa$. For the purpose of generality and cross-reference, the aforementioned influencing factors were investigated in terms of normalised parameters as n_e, E_c / E_s, k_{ch} / k_{sh}, α and H / a

.

Figure 4.13a depicts a substantial variation in consolidation rate with the permeability ratio (k_{ch} / k_{sh}). As can be seen, the end of consolidation process was reached earlier when smaller permeability ratio k_{ch} / k_{sh} was adopted. It is important to note that the consolidation of the unit cell primarily depends on the radial flow from the soft soil into the stone column and the upward flow out from the column. Immediately after applying external loading, the difference in excess pore pressure between the soil and column regions and the accompanying pore pressure gradient in radial direction was insignificant. As a result, the flow rate from surrounding soil to stone column was minor and the consolidation at the early stage of stone column was principally controlled by the quantity of water flowing out from the column region. At the later stage of consolidation of the column, the radial pore pressure gradient increased together with the dissipation of excess pore pressure in the column dramatically that led to an increase in the radial flow rate from surrounding soil into stone column. During this period, the radial flow decelerated the consolidation of stone column and accelerated the consolidation of surrounding soil. An increase in the horizontal permeability of surrounding soil (i.e. a decrease in k_{ch} / k_{sh} ratio) might result in a radial flow rate increase considerably although the radial pore pressure gradient was reduced; and thus speeded up the consolidation of soft soil intensely, but decelerated the consolidation of column particularly at the later stage of consolidation. Figure 4.13b plots the changes of average differential settlement against time for varying permeability ratio. The $\Delta\overline{S}$ variation patterns were similar to $\overline{U}_s$ variation patterns for soft soil (see Figure 4.13a) in which the average differential settlement occurred and reached the maximum value earlier in accordance with the adopted smaller permeability ratio. This similarity may be explained by referring to Equations (4.24) and (4.25), where due to the extremely higher stiffness of stone column

compared to the soft soil, the value of $\overline{S}_s(z_0 = 0, \infty)$ is much larger than $\overline{S}_c(z_0 = 0, \infty)$. Consequently, the $\Delta\overline{S}$ predictions are mostly influenced by $\overline{U}_s$ regardless of the variation of $\overline{U}_c$ and $\overline{U}_s$ values during the consolidation process.

Figure 4.14a exhibits a significant effect of the radius ratio ($n_e = b / a$) on the average degree of consolidation of soft soil. The consolidation rate declined and the time to reach the end of consolidation prolonged when the radius ratio increased (i.e. the spacing of columns increased). Indeed, an increase in the column spacing led to a longer radial drainage path in soft soil which decelerated the dissipation process of excess pore pressure and thus reduced the consolidation rate of the soft soil. However, the variations became less pronounced progressively corresponding to a larger n_e value, particularly when $n_e > 3$. In contrast and as expected, the column spacing nearly did not affect the consolidation rate of column itself. Figure 4.14b presents the average differential settlement against consolidation time for different values of radius ratio (n_e). Similar to the above explanation for Figure 4.13b, the $\Delta\overline{S}$ predictions were mainly regulated by $\overline{U}_s$ because of the extreme difference in stiffness between stone column and soft soil ($E_c / E_s = 30$). Therefore, the variation patterns of $\Delta\overline{S}$ in Figure 4.14b were identical to $\overline{U}_s$ reported in Figure 4.14a, particularly when the predicted $\overline{U}_c$ was almost unchanged for varying radius ratio.

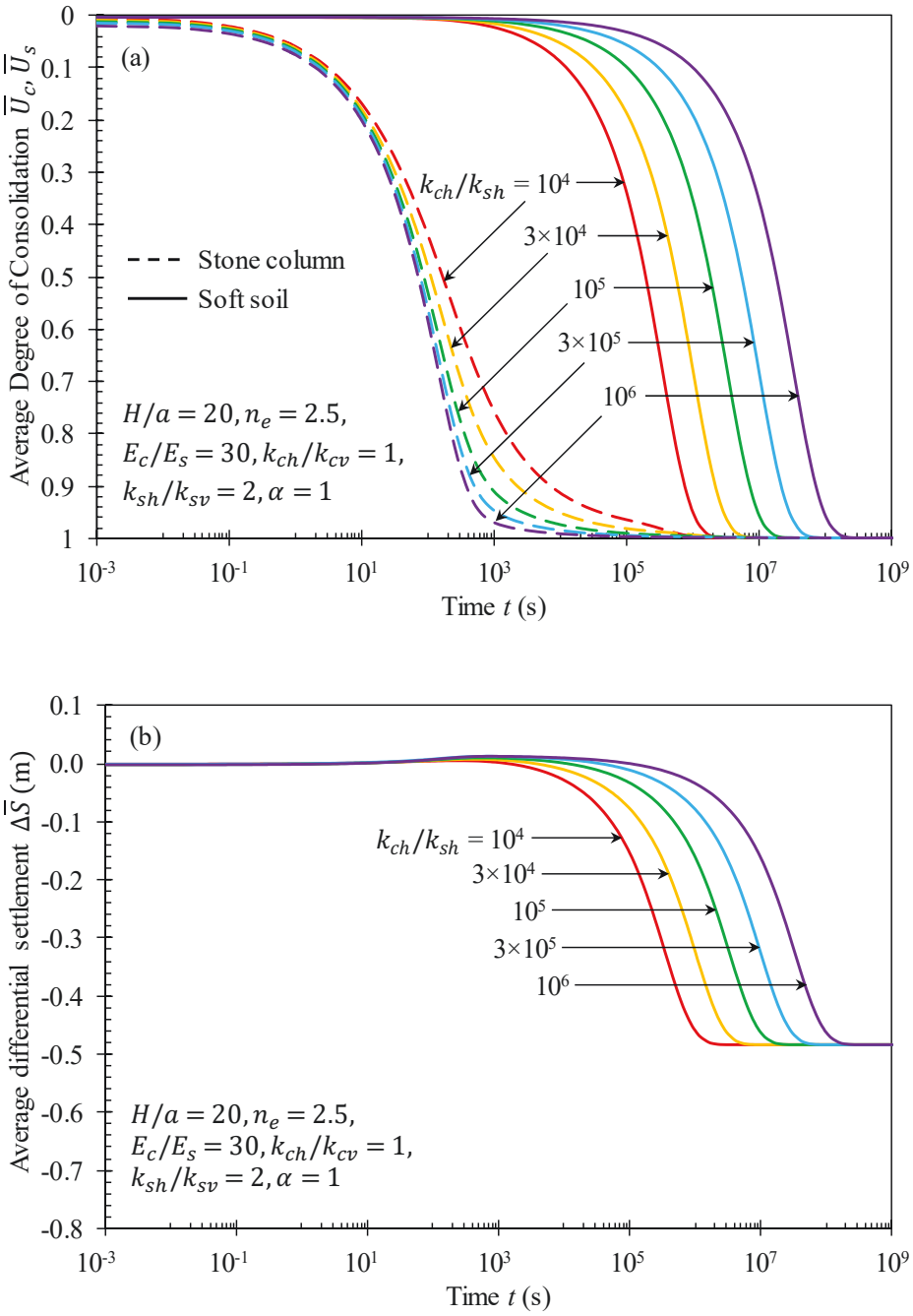

Figure 4.13. Influence of permeability ratio k_{ch}/k_{sh} on (a) average degree of consolidation of stone column and of soft soil, and (b) average differential settlement between stone column and soft soil

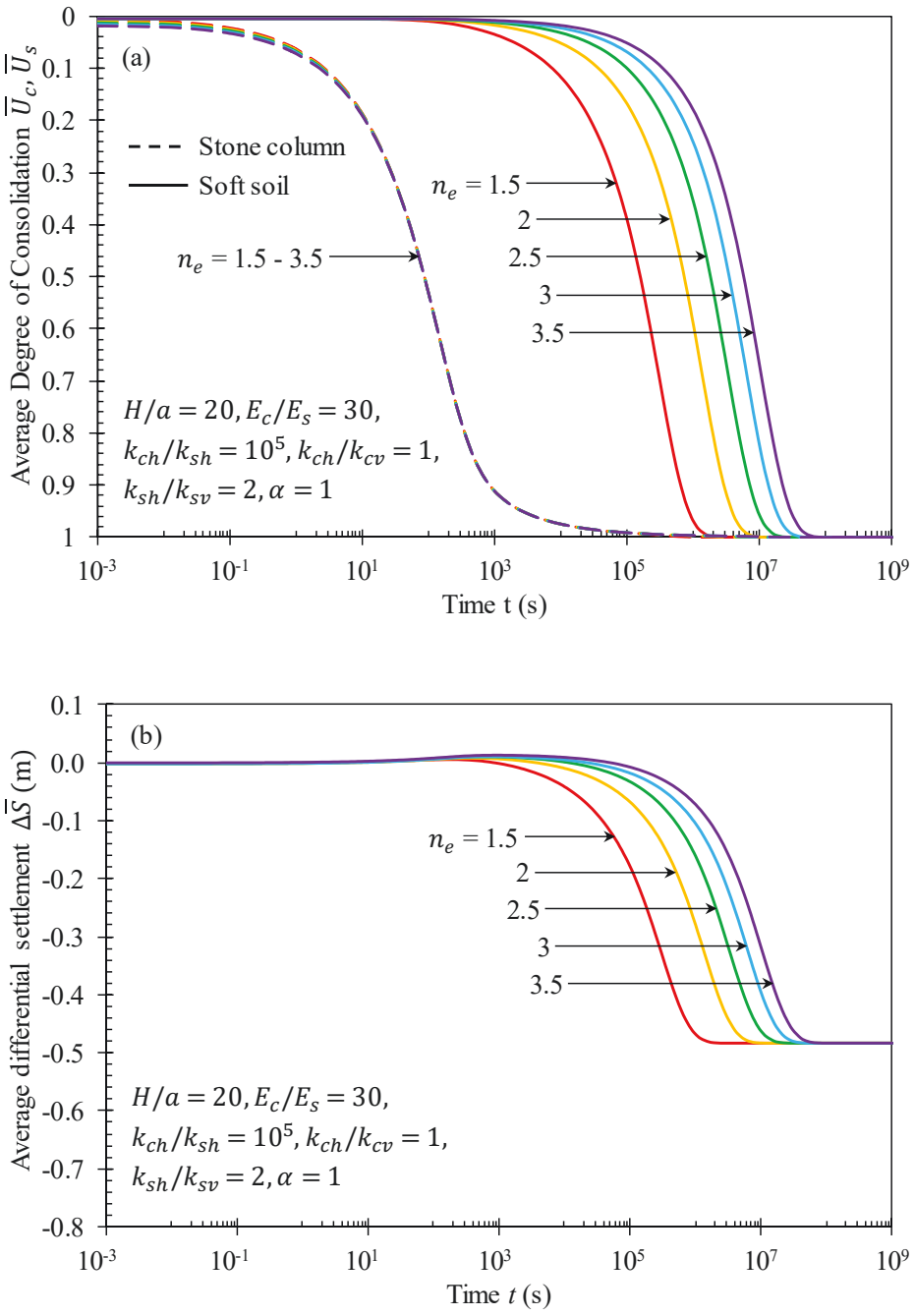

Figure 4.14. Influence of radius ratio n_e on (a) average degree of consolidation of stone column and of soft soil, and (b) average differential settlement between stone column and soft soil

Figure 4.15a demonstrates that a decrease in the modulus ratio E_c / E_s (corresponding to an increase in the modulus of soft soil) accelerated the consolidation of the soil. In fact, during the consolidation process the excess pore water pressure decreases while the effective stress in the soil skeleton increases. The higher the stiffness of the soil, the faster the transfer of excess pore water pressure onto the effective stress in the soil skeleton, resulting in accelerated consolidation. Even though the decrease in E_c / E_s ratio contributed to the acceleration of consolidation process of the composite ground slightly, it reduced the average differential settlement between stone column and surrounding soil considerably (Figure 4.15b). The variations of $\Delta\overline{S}$ with time can be presented as the product of $\overline{U}_s$ and $\overline{S}_s(z_0 = 0, \infty)$; a reduction in the modulus of soft soil diminished $\overline{U}_s$ somewhat but intensified $\overline{S}_s(z_0 = 0, \infty)$. Therefore, the $\Delta\overline{S}$ predictions were amplified as a result of reduced modulus of soft soil, particularly at the later stage of consolidation.

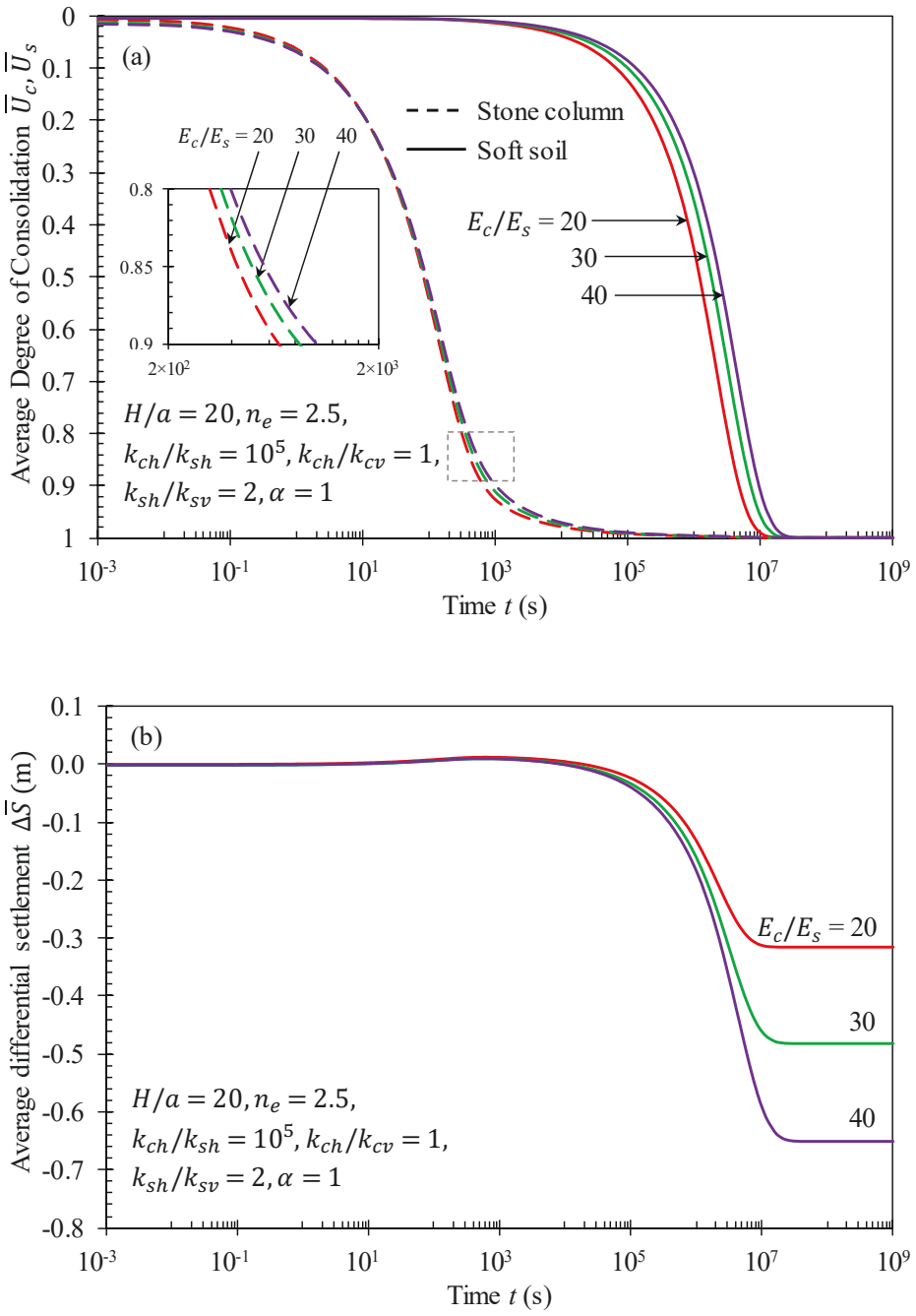

Figure 4.15. Influence of modulus ratio E_c/E_s on (a) average degree of consolidation of stone column and of soft soil, and (b) average differential settlement between stone column and soft soil

Figure 4.16a illustrates that a decline of α value from 1 to 0, corresponding to the alteration of the total stress distribution with depth (i.e. the initial excess pore pressure distribution) from uniform to trapezoidal and then triangular pattern, led to an increase in consolidation rate of stone column as a result of the acceleration of excess pore pressure dissipation. The dissipation rate of excess pore pressure in the entire column region accelerated as α decreased, since more significant portion of the initial excess pore pressure was located closer to the top drainage boundary. Additionally, the faster dissipation rate was also assisted by the greater initial excess pore pressure gradient in positive *z*-direction corresponding to the smaller α value. After undergoing the redistribution process in which the position of maximum excess pore pressure moved towards the column base, the influence of α value on the rate of consolidation decreased gradually with time. The effect of α value on the consolidation rate of soft soil was negligible because of the domination of the radial flow in the soil and the extremely slower dissipation rate of excess pore pressure in the soil in comparison with that in the column. While the reduction of α value had a minor effect on the consolidation rate of the soil, it diminished the average differential settlement in the composite ground substantially (Figure 4.16b). As expected, the average total stress within the soft soil decreased when the smaller α value was adopted, and thus the effective stress acting on the soil skeleton reduced. Then, the consolidation settlement of the soil, as well as the average differential settlement, decreased significantly during the process of consolidation.

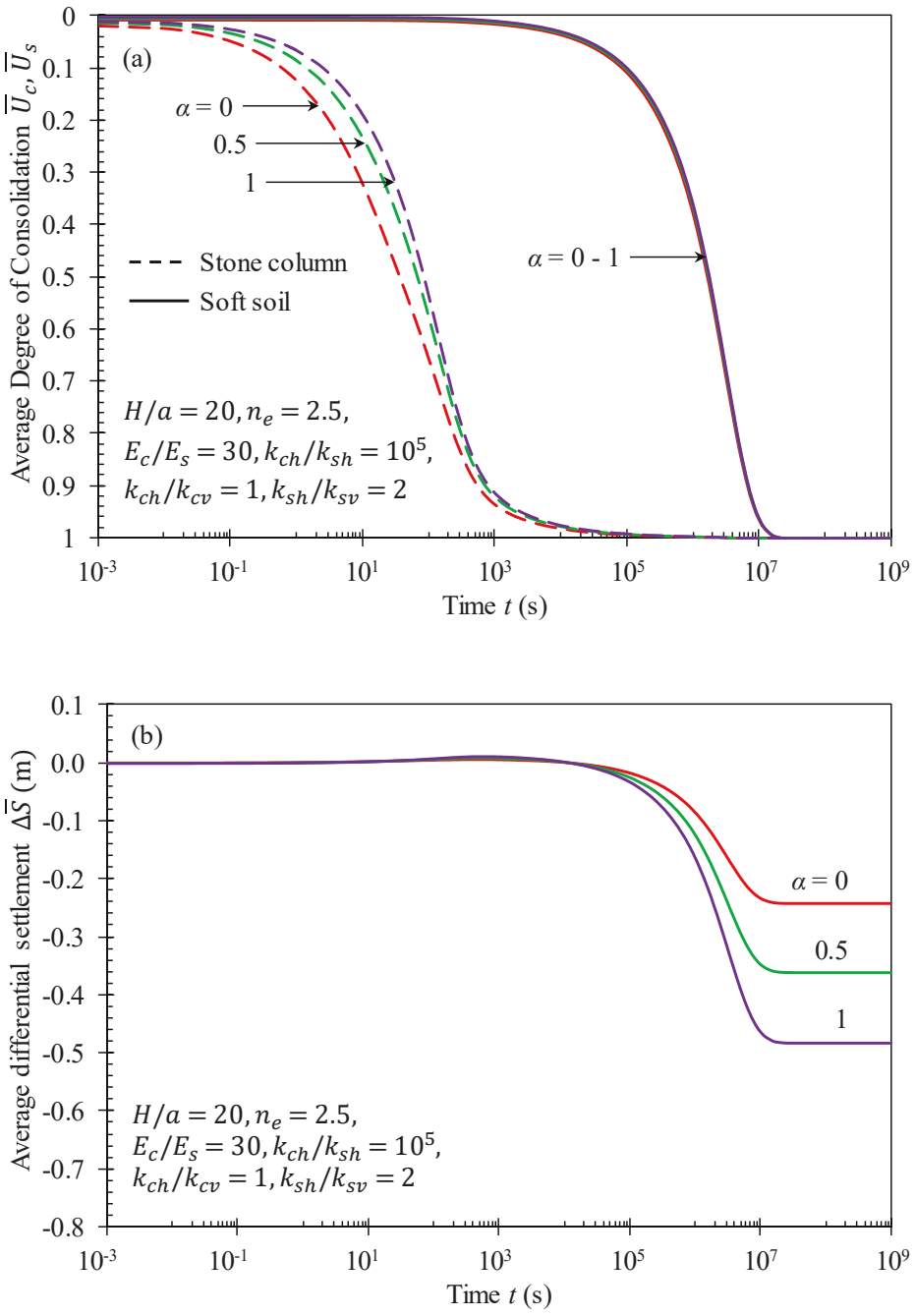

Figure 4.16. Influence of α value on (a) average degree of consolidation of stone column and of soft soil, and (b) average differential settlement between stone column and soft soil

Figure 4.17a presents variations of the average degree of consolidation against time for different values of H/a. The increasing H/a (corresponding to increasing thickness of soft soil) led to a longer vertical drainage path in stone column and thus decelerated the consolidation of the column. In contrast, the effect of H/a ratio on the consolidation of soil was negligible due to the dominance of radial drainage in soft soil towards the column. However, referring to Figure 4.17b, the average differential settlement in the composite ground was observed to be larger for higher H/a ratio (or deeper soft soil) due to the greater increase in the consolidation settlement of the soil than that of the column as a consequence of the extreme difference in stiffness between column and soil.

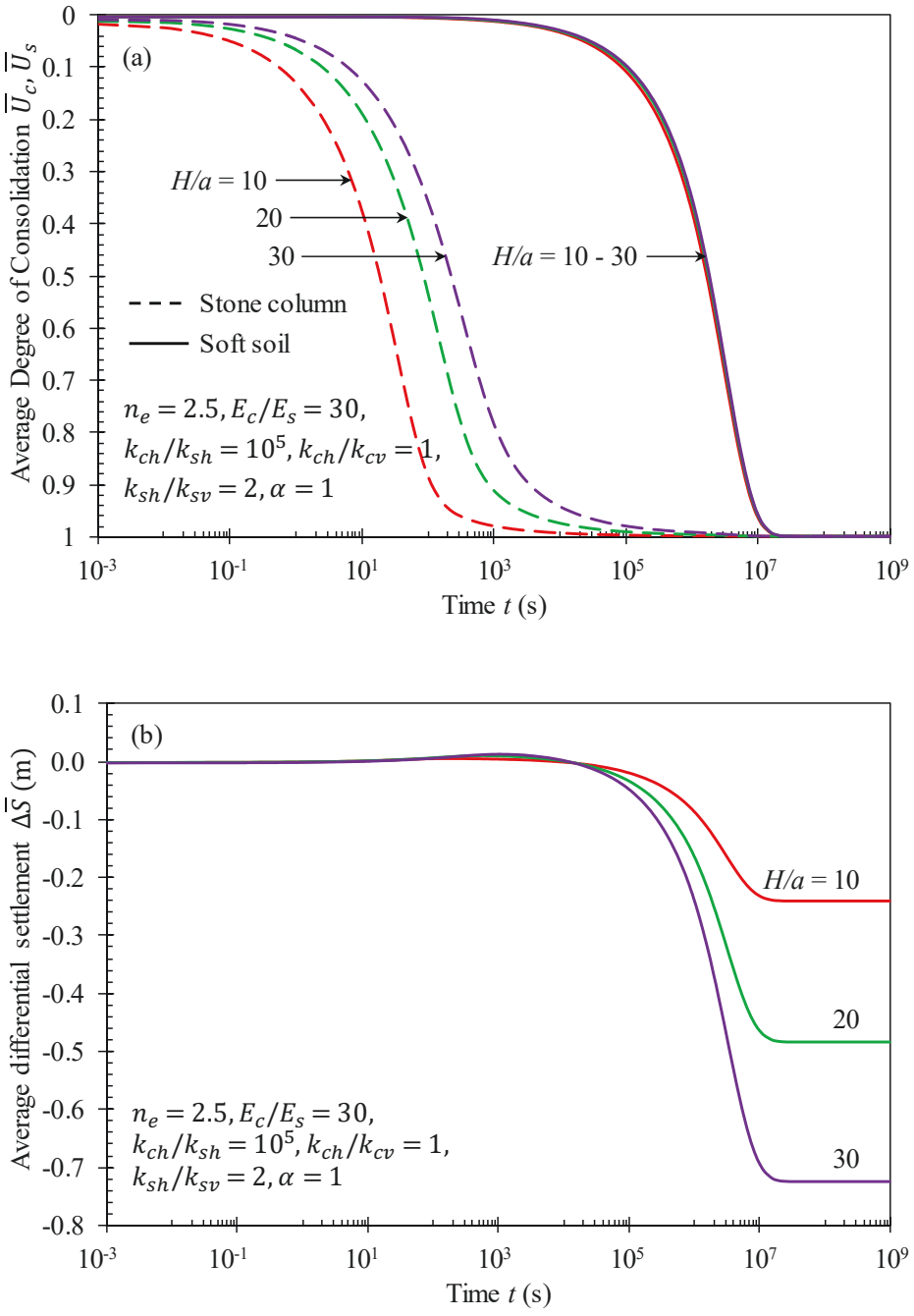

Figure 4.17. Influence of H/a ratio on (a) average degree of consolidation of stone column and of soft soil, and (b) average differential settlement between stone column and soft soil

4.6 Summary

Most available analytical solutions addressing the consolidation of stone column-reinforced soft composite ground adopt the equal strain assumption for the stone column and its surrounding soft soil, which is incapable of predicting the differential settlement of the composite ground under a flexible platform. To fill this knowledge gap, a mathematical model for axisymmetric consolidation of the composite ground adopting free strain condition was established in the present study, in which both radial and vertical flows were considered simultaneously in the stone column and soft soil regions subjected to any instant surface loading. Then, an analytical solution was derived using the separation of variables method in combination with the orthogonal expansion technique to predict the variation of excess pore water pressure and settlement with time for any point in a unit cell model. All possible eigenvalues were taken into account, thus the obtained analytical solution is an exact Fourier-Bessel series solution. Besides, the achieved solution is a generalised solution with respect to the permeability and space-dependent distribution of total stresses caused by the external loading. Indeed, the orthotropic permeability and an arbitrary separable function of total stress for each region of the unit cell were integrated into the mathematical model. A worked example with benchmark values of input data was presented to reveal the capabilities of the proposed analytical solution, in which the complex eigenvalues in the solution contributed to the final solution. The contribution of complex eigenvalues is attributable to the large difference in consolidation coefficients between stone column and soft soil. The verification of the analytical solution employing the finite element simulation was also conducted. The dissipation of excess pore water pressure at investigation points and the average degree of consolidation of each region in the unit cell determined by the proposed

analytical solution agreed well with the results obtained from the finite element simulation. Some disparities were observed between analytical and numerical predictions at the later stages of consolidation due to the presence of shear strain in the soil captured in the finite element model while ignored in the analytical solution. Indeed, the redistribution of total stress in the soft soil induced by shear strain development led to slower excess pore water pressure dissipation and consolidation rates in the finite element simulation compared with the proposed analytical solution. A further verification of the analytical solution derived in the present study with field observations of a real case was also carried out. The excess pore water pressure dissipation and settlement rates in soft clay obtained by the proposed analytical solution adopting the range of stress concentration ratio $n_{scr} = 2 - 6$ for a typical flexible embankment agreed reasonably well with field measurements of the case history in which the loading was nearly instantaneous. Finally, a parametric analysis applying the analytical solution was accomplished to investigate the correlations between performance objectives and influencing factors. The proposed analytical solution is applicable to the consolidation of soft soil with the inclusion of sand drains or prefabricated vertical drains (PVDs) by assigning appropriate consolidation parameters (e.g. constrained modulus and permeability) to sand columns and PVDs. The constrained modulus assigned to PVDs can be assumed equivalent to that of soft soil and the total vertical stress induced by flexible loading distributes uniformly over the top of unit cell. Some factors such as time-dependent loading, smear effect, variation of consolidation parameters are not taken into consideration and further research studies capturing these are recommended. With the aforementioned features, the obtained analytical solution in this study serves as a useful tool for practical designs and cross checking complex numerical simulations.

CHAPTER 5

GREEN'S FUNCTION ANALYTICAL SOLUTION FOR FREE STRAIN CONSOLIDATION OF SOFT SOIL IMPROVED BY STONE COLUMNS SUBJECTED TO TIME-DEPENDENT LOADING

5.1 Introduction

In many real construction projects, the external loads can increase or decrease during construction stages because of distinct construction requirements. Additionally, the repetition of loading and unloading processes can be encountered at the service stage of some construction facilities such as silos, tanks, warehouses and stockpiles [122, 124, 131, 163, 172, 222, 223]. While various analytical consolidation studies for granular column improved soft soil considering time-dependent loadings have been conducted, there is a shortage of analytical development for the same problem adopting the free strain configuration for the composite foundation.

Therefore, the major objective of this chapter is to provide an analytical solution for free strain consolidation of a soft soil stratum strengthened with stone columns and subjected to any time-dependent loading. Besides, the mathematical development in this study incorporated the pore water flows in horizontal and vertical directions simultaneously for both stone column and soft soil regions. The axisymmetric unit cell concept as reported in several available studies was employed to formulate the consolidation problem in the chapter. The final solutions for excess pore water pressures at arbitrary points in stone column and soft soil were derived as Green's function solutions in which the Green's function was developed utilising the method of separation of

variables and Green's formula. Thus, the consolidation settlements of column and soil regions were readily obtained along with the differential settlement between the two regions. The validity of proposed analytical solution was verified via a worked example investigating the influence of loading parameters of different time-dependent loadings on excess pore water pressure dissipations, normalised average surface settlements for stone column and soft soil together with the differential surface settlement between them. Furthermore, a verification exercise against field case history was also conducted to evaluate the variation of excess pore water pressure at an investigation point in soft soil along with the soil settlement against consolidation time.

5.2 Description of the problem

The equivalent axisymmetric unit cell model of the problem is illustrated schematically in Figure 5.1, in which the total diameter of the model is $2b$, while the stone column of diameter $2a$ is fully installed along the soil depth H at the centre of the unit cell. The consolidation problem in this study is mathematically modelled using the fundamental assumptions adopted by Biot [77] and Barron [64]. The column and soil bodies are assumed homogeneous and entirely saturated, which deform vertically under time-dependent loading and free strain conditions. The water and soil particle are assumed incompressible and the dissipation of excess pore water pressure obeys Darcy's law, while the volume change and permeability coefficients of the column and soil remain unchanged for a given surcharge. The adoption of constant values for consolidation parameters (i.e. permeability and volume change coefficients) of the column and encircling soft soil enables the derivation of analytical solutions in this study. It is noteworthy that the consolidation parameters vary in accordance with the changes in void

ratio and effective stress in the composite foundation during the consolidation process. Nonetheless, these parameters could be adopted as constant values for a given increment of loading pressure, similar to several existing studies in the literature. In addition, it is assumed that the total stresses in the stone column and soft soil regions caused by the external load distribute uniformly in each region.

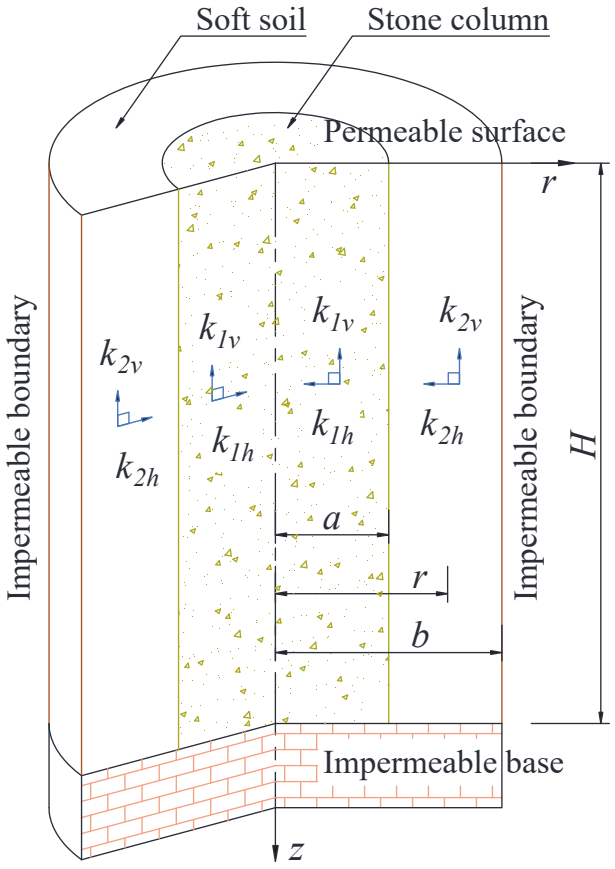

Figure 5.1. The axisymmetric model of the problem

Referring to Zhu and Yin [204] and Lei et al. [46], the equations which govern the consolidation of the composite foundation can be written as the following partial differential equations:

$$\frac{k_{1h}}{\gamma_w}\left(\frac{\partial^2 u_1(r,z,t)}{\partial r^2}+\frac{1}{r}\frac{\partial u_1(r,z,t)}{\partial r}\right)+\frac{k_{1v}}{\gamma_w}\frac{\partial^2 u_1(r,z,t)}{\partial z^2}=-\frac{1}{M_1}\left[\frac{\partial \sigma_1(t)}{\partial t}-\frac{\partial u_1(r,z,t)}{\partial t}\right] \quad (5.1a)$$

$$\frac{k_{2h}}{\gamma_w}\left(\frac{\partial^2 u_2(r,z,t)}{\partial r^2}+\frac{1}{r}\frac{\partial u_2(r,z,t)}{\partial r}\right)+\frac{k_{2v}}{\gamma_w}\frac{\partial^2 u_2(r,z,t)}{\partial z^2}=-\frac{1}{M_2}\left[\frac{\partial \sigma_2(t)}{\partial t}-\frac{\partial u_2(r,z,t)}{\partial t}\right] \quad (5.1b)$$

where σ_1 and σ_2 are the total vertical stresses within the stone column and soft soil, respectively; u_1 and u_2 are the excess pore water pressures in the stone column and soft soil, respectively; r and z are cylindrical spatial coordinates (Figure 5.1); t is the elapsed time; M_1 and k_{1h}, k_{1v} are the constrained modulus and permeability coefficients in horizontal and vertical directions of the stone column, respectively; M_2 and k_{2h}, k_{2v} are the constrained modulus and permeability coefficients in horizontal and vertical directions of the soft soil, respectively; and γ_w is the water unit weight $(10\,kN/m^3)$.

Pertaining to Figure 5.1, the pore water pressure and velocity of radial pore water flow are continuous at the column – soil contact surface and represented by Equations (5.2a) and (5.2b), respectively; whereas the radial flow across the outer boundary surface of the cell is not allowed and can be expressed by Equation (5.2c).

$$u_1(r=a)=u_2(r=a) \quad (5.2a)$$

$$k_{1h}\left.\frac{\partial u_1}{\partial r}\right|_{r=a}=k_{2h}\left.\frac{\partial u_2}{\partial r}\right|_{r=a} \quad (5.2b)$$

$$\left.\frac{\partial u_2}{\partial r}\right|_{r=b}=0 \quad (5.2c)$$

The upper surface of the unit cell is modelled as freely draining, while the cell base is underlain by an impermeable stiff layer (Figure 5.1). Hence, the boundary conditions for the top and bottom of the unit cell model can be described by:

$$u_1(z=0) = u_2(z=0) = 0 \tag{5.3a}$$

$$\left.\frac{\partial u_1}{\partial z}\right|_{z=H} = \left.\frac{\partial u_2}{\partial z}\right|_{z=H} = 0 \tag{5.3b}$$

Considering an external load with a nonzero initial surcharge, the initial total stresses in the composite foundation induced by the load are deemed to be carried completely by the excess pore water pressures. Thus, the initial conditions for excess pore water pressure can be expressed as:

$$u_1(t=0) = \sigma_1(t=0) = \sigma_{01} \tag{5.4a}$$

$$u_2(t=0) = \sigma_2(t=0) = \sigma_{02} \tag{5.4b}$$

where σ_{01} and σ_{02} are the initial total vertical stresses within the stone column and soft soil due to the applied external loading, respectively.

5.3 Analytical solution for excess pore water pressure dissipation and consolidation settlement

The excess pore water pressure solution in this study is presented in terms of Green's function which can be obtained by solving the homogeneous version of the problem [188, 196]. The homogeneous problem consists of the equations which are identical to the set of Equations (5.1)−(5.4) with a modification in the governing equations (i.e. Equations (5.1a) and (5.1b)) by eliminating the terms $\partial\sigma_1/\partial t$ and $\partial\sigma_2/\partial t$.

Referring to the study by Aviles-Ramos et al. [211], the solution for the earlier non-homogeneous problem defined by Equations (5.1)−(5.4) are obtained as:

$$u_i(r,z,t) = u_i^{(i)}(r,z,t) + u_i^{(ii)}(r,z,t) \qquad \left(r_i \le r \le r_{i+1}\right) \quad (i=1,2) \tag{5.5}$$

In which u_i is the excess pore water pressure at any point in the composite foundation; the subscript $i = 1, 2$ denotes the stone column and soft soil regions, respectively; $r_1 = 0$, $r_2 = a$, $r_3 = b$; the components $u_i^{(i)}$ and $u_i^{(ii)}$ can be attained utilising the following Green's formula:

$$\begin{aligned} u_i^{(*)}(r,z,t) = & \sum_{j=1}^{2} \int_{z'=0}^{H} \int_{r'=r_j}^{r_{j+1}} G_{ij}^{(*)}(r,z,t \mid r',z',t')\Big|_{t'=0} \sigma_{0j}\, r'\, dr'\, dz' \\ & + \sum_{j=1}^{2} \int_{t'=0}^{t} \int_{z'=0}^{H} \int_{r'=r_j}^{r_{j+1}} G_{ij}^{(*)}(r,z,t \mid r',z',t') \left[\frac{\partial \sigma_j(t')}{\partial t'} \right] r'\, dr'\, dz'\, dt' \quad (j = 1,2) \end{aligned} \tag{5.6}$$

where the superscripts (i) and (ii) have been replaced by $(*)$ for the sake of succinct presentation due to their similar derivation; $G_{ij}^{(*)}$ is the Green's function to be determined (see Appendix C); the index j and the integration variables r', z' and t' are dummy variables which have been introduced to avoid confusion with the index i and the variables r, z and t, respectively.

By taking average in *r*- and *z*-domains, the average excess pore water pressures for stone column $\overline{u}_1(t)$ and for soft soil $\overline{u}_2(t)$ at any time t are achieved as:

$$\overline{u}_1(t) = \frac{1}{\pi a^2 H} \left[\int_{z=0}^{H} \int_{r=0}^{a} 2\pi\, u_1(r,z,t)\, r\, dr\, dz \right] \tag{5.7a}$$

$$\overline{u}_2(t) = \frac{1}{\pi (b^2 - a^2) H} \left[\int_{z=0}^{H} \int_{r=a}^{b} 2\pi\, u_2(r,z,t)\, r\, dr\, dz \right] \tag{5.7b}$$

Then, the average surface settlements of stone column $\overline{S}_1(t)$ and soft soil $\overline{S}_2(t)$ at time t due to the dissipation of excess pore water pressure are obtainable via the following:

$$\overline{S}_1(t) = \frac{\overline{\sigma}_1(t) - \overline{u}_1(t)}{M_1} H \tag{5.8a}$$

$$\overline{S}_2(t) = \frac{\overline{\sigma}_2(t) - \overline{u}_2(t)}{M_2} H \tag{5.8b}$$

where $\overline{\sigma}_1(t)$ and $\overline{\sigma}_2(t)$ are the average total vertical stresses within stone column and soft soil induced by the external load at time t, respectively. These stresses can be substituted consecutively by $\sigma_1(t)$ and $\sigma_2(t)$ as a consequence of the uniform distribution assumption for the total vertical stresses in this study.

It should be noted that the average degree of consolidation at a particular time is conventionally defined as a ratio of the average surface settlement at that time to the final average surface settlement when consolidation time t approaches infinity. Therefore, the average degree of consolidation is rigorously inapplicable to the foundation subjected to an external loading which fluctuates continuously. Instead of that, the normalised average surface settlements for stone column $\overline{S}_1^*(t)$ and soft soil $\overline{S}_2^*(t)$ would be used in this study for the sake of generalisation as follows:

$$\overline{S}_1^*(t) = \frac{\overline{S}_1(t)}{\overline{S}_{1ref}} \tag{5.9a}$$

$$\overline{S}_2^*(t) = \frac{\overline{S}_2(t)}{\overline{S}_{2ref}} \tag{5.9b}$$

where $\overline{S}_{1ref}$ and $\overline{S}_{2ref}$ are the referenced average surface settlements for stone column and soft soil, respectively.

5.4 Worked examples

To validate the capabilities of the proposed analytical solution, this section provides numerical examples in conjunction with parametric analyses to investigate the effect of

various time-dependent loadings on the consolidation behaviour of the composite ground. Three external loadings which are able to represent the practical simulations including step, ramp and sinusoidal loadings [124, 172, 222] are examined in this study. The variations of loads against time are modelled mathematically as below:

$$\text{Step loading: } q(t)=\begin{cases} q_0 & for \quad t<t_1 \\ q_{\max} & for \quad t\geq t_1 \end{cases} \tag{5.10a}$$

$$\text{Ramp loading: } q(t)=\begin{cases} A\,t+q_0 & for \quad t<t_1 \\ q_{\max} & for \quad t\geq t_1 \end{cases} \quad \text{where} \quad A=\left(q_{\max}-q_0\right)/t_1 \tag{5.10b}$$

$$\text{Sinusoidal loading: } q(t)=q_0\left[B\sin\left(\varphi_B\,t\right)+1\right] \tag{5.10c}$$

where q_0 is the initial surcharge; $q_{\max}$ is the maximum of step and ramp loadings on the composite ground surface; A is the rate of ramp loading; B is the parameter controlling the amplitude and φ_B is the angular frequency of the sinusoidal loading; t_1 is the time duration for the first step loading or the construction time for the ramp loading (see Figure 5.2).

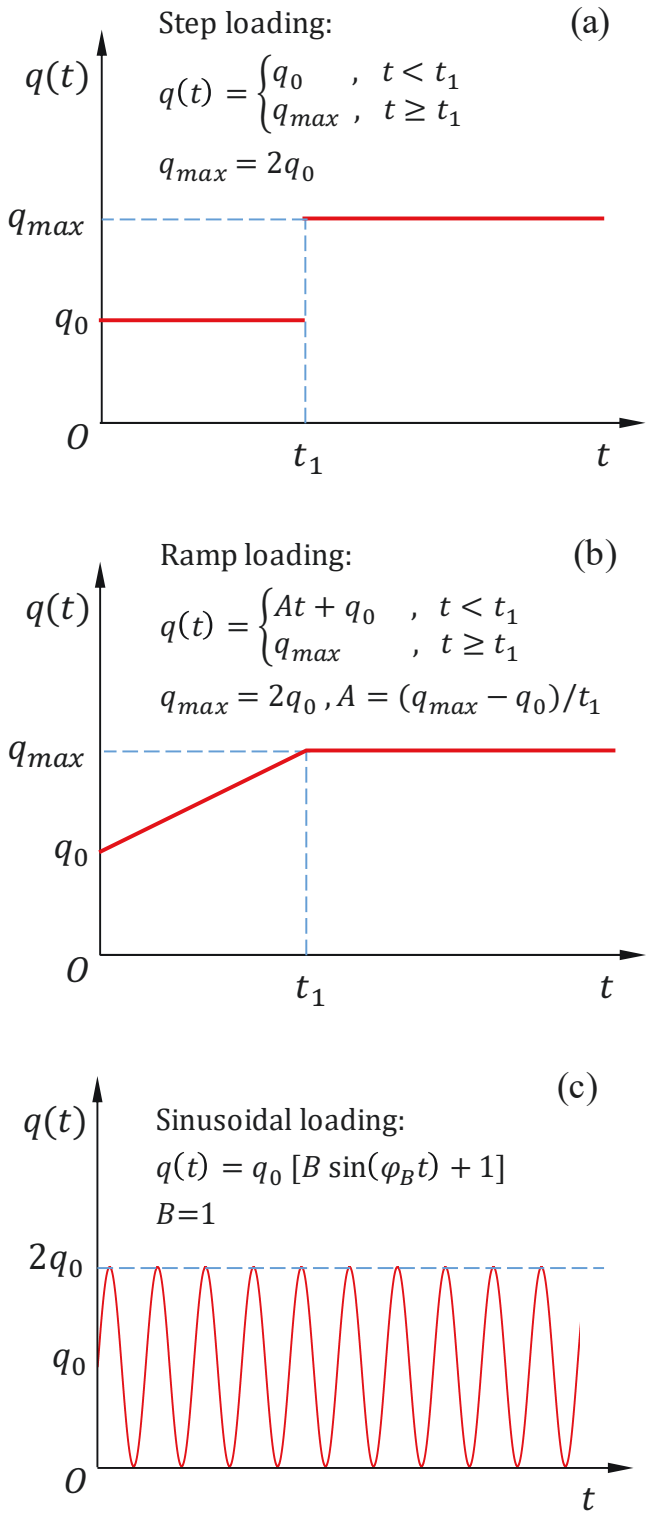

Figure 5.2. Three investigation loading types in the example: (a) Step, (b) Ramp, and (c) Sinusoid

In the examples, the geometric parameters and material properties for the axisymmetric consolidation model, which can reflect the engineering practice were adopted as:

- Geometric parameters:

  $H = 5\,m$, $a = 0.5\,m$, $b = 1.25\,m$;

- Column and soil properties:

  $k_{1h} = 2\times10^{-5}\,m/s$, $k_{1v} = k_{1h}$, $E_1 = 40\times10^3\,kPa$, $\nu_{P1} = 0.3$,

  $k_{2h} = 2\times10^{-9}\,m/s$, $k_{2v} = 0.5\,k_{2h}$, $E_2 = 2\times10^3\,kPa$, $\nu_{P2} = 0.3$;

where E_1 and E_2 denote Young's moduli for stone column and soft soil, respectively; ν_{P1} and ν_{P2} denote Poisson's ratios for stone column and soft soil, respectively. Therefore, the constrained moduli for stone column and soft soil can be calculated using these parameters.

- Constant loading parameters:

  $q_0 = 100\,kPa$, $q_{\max} = 2q_0$, $B = 1$;

while the remaining loading parameters involving loading time t_1 (or loading rate A of the ramp loading), angular frequency φ_B of the sinusoidal loading would be varied in typical ranges in the parametric analyses (see Table 5.1).

Table 5.1. Selected loading parameters for the worked example

Loading types	Parameters	Selected values
Step	$t_1(s)$	5×10^5 10^6 2×10^6
Ramp	$t_1(s)$	2×10^5 $\left(5\times10^{-4}\right)$ 5×10^5 $\left(2\times10^{-4}\right)$ 10^6 $\left(10^{-4}\right)$ 2×10^6 $\left(5\times10^{-5}\right)$
Sinusoid	$\varphi_B\left(rad/s\right)$	$2\pi/5\times10^6$ $2\pi/10^7$ $2\pi/2\times10^7$

Note: The values in parentheses are loading rates $A\left(kPa/s\right)$ obtained from the corresponding selected values $t_1(s)$ of the ramp loading.

The consolidation response of the composite soft ground was evaluated via the dissipation of excess pore water pressure at points with depth $z = 0.5H$ in stone column ($r = 0.5a$) and soft soil ($r = 0.5(a+b)$), the normalised average surface settlements for stone column and soft soil regions and the differential average surface settlement between the two regions. The excess pore water pressure at any point in the foundation is readily calculated utilising Equations (5.5) and (5.6), whereas the differential average surface settlement ($\Delta\overline{S}$) can be computed as the difference between the average surface settlement of stone column $\overline{S}_1(t)$ and that of soft soil $\overline{S}_2(t)$. In order to examine the normalised average surface settlements $\overline{S}_1^*(t)$ and $\overline{S}_2^*(t)$, the following referenced average surface settlements were adopted for the examples:

$$\overline{S}_{1ref} = 2\overline{S}_{\sigma 01} = 2\frac{\sigma_{01}}{M_1}H \tag{5.11a}$$

$$\overline{S}_{2ref} = 2\overline{S}_{\sigma 02} = 2\frac{\sigma_{02}}{M_2}H \tag{5.11b}$$

where $\overline{S}_{\sigma 01}$ and $\overline{S}_{\sigma 02}$ are the average surface settlements of stone column and soft soil due to the total vertical stress values σ_{01} and σ_{02} corresponding to the condition where the excess pore water pressure in the foundation would be fully dissipated (i.e. drained compression condition). For the purpose of cross-reference where the changes of normalised average surface settlements are frequently presented in a range between 0 and 1, the coefficient 2 is introduced into Equations (5.11a) and (5.11b). Hence, $\overline{S}_{1ref}$ and $\overline{S}_{2ref}$ would be equal to the peak values of $\overline{S}_1(t)$ and $\overline{S}_2(t)$, respectively. As a result, $\overline{S}_1^*(t)$ and $\overline{S}_2^*(t)$ calculated by Equations (5.9a) and (5.9b) would vary between 0 and 1.

For the examples in this study, it is assumed that the embankment – platform system is flexible to fulfil the free strain assumption and hence the distributions of external load and accompanying total vertical stresses are uniform on the surface as well as in the stone column and soft soil bodies of the composite ground. Thus, the excess pore water pressure $u_i^{(*)}$ in Equation (5.6) can be derived in more details for the loading conditions considered in this study (refer to Appendix D).

5.4.1 Step loading

For simplification in the case of a quickly rising of load to an expected surcharge on low permeability soils, the load can be modelled as a one-step or multi-step loading (e.g. the two-step loading in Figure 5.2a).

Figures 5.3a and 5.3b illustrate the changes in excess pore water pressure against time for points in the column and soil regions, respectively, considering various durations t_1 of the first surcharge of the step loading. The excess pore water pressure at investigation point in stone column (Figure 5.3a) dissipated almost totally at time $t = 10^5$ s even before applying the second surcharge of step loads, due to the large permeability and discharge capacity of stone column. As expected and similar to the initial excess pore water pressure generated by the first step loading, an immediate application the second step of external loads on the ground surface caused the excess pore water pressure in stone column to rise equal to the loading increment (i.e. 100 kPa). Then, the pore water pressure also dissipated as quickly as the previous loading stage. Figure 5.3b shows that the dissipation rates of excess pore water pressure at examination point in soft soil were much slower than those in stone column because of the low hydraulic conductivity of soft soil. The pore water pressures at the end of the first stage of external loading were approximately 40, 20, and 5 kPa corresponding to durations $t_1 = 5 \times 10^5$, 10^6, and 2×10^6 s, which increased instantaneously by 100 kPa when the composite foundation had been subjected to the second step of the surcharge loading. These indicate that the earlier the application of the second step loading, the less the dissipation portion of excess pore pressure in soft soil over the first surcharge period and thus the more excess pore pressure to be dissipated afterwards. Despite that, the excess pore pressure dissipation in soft soil proceeded faster in accordance with the sooner exerting the second surcharge on the ground. This is due to the larger radial excess pore pressure gradient from soil towards column when the soil was subjected to an earlier application of the second loading increment.

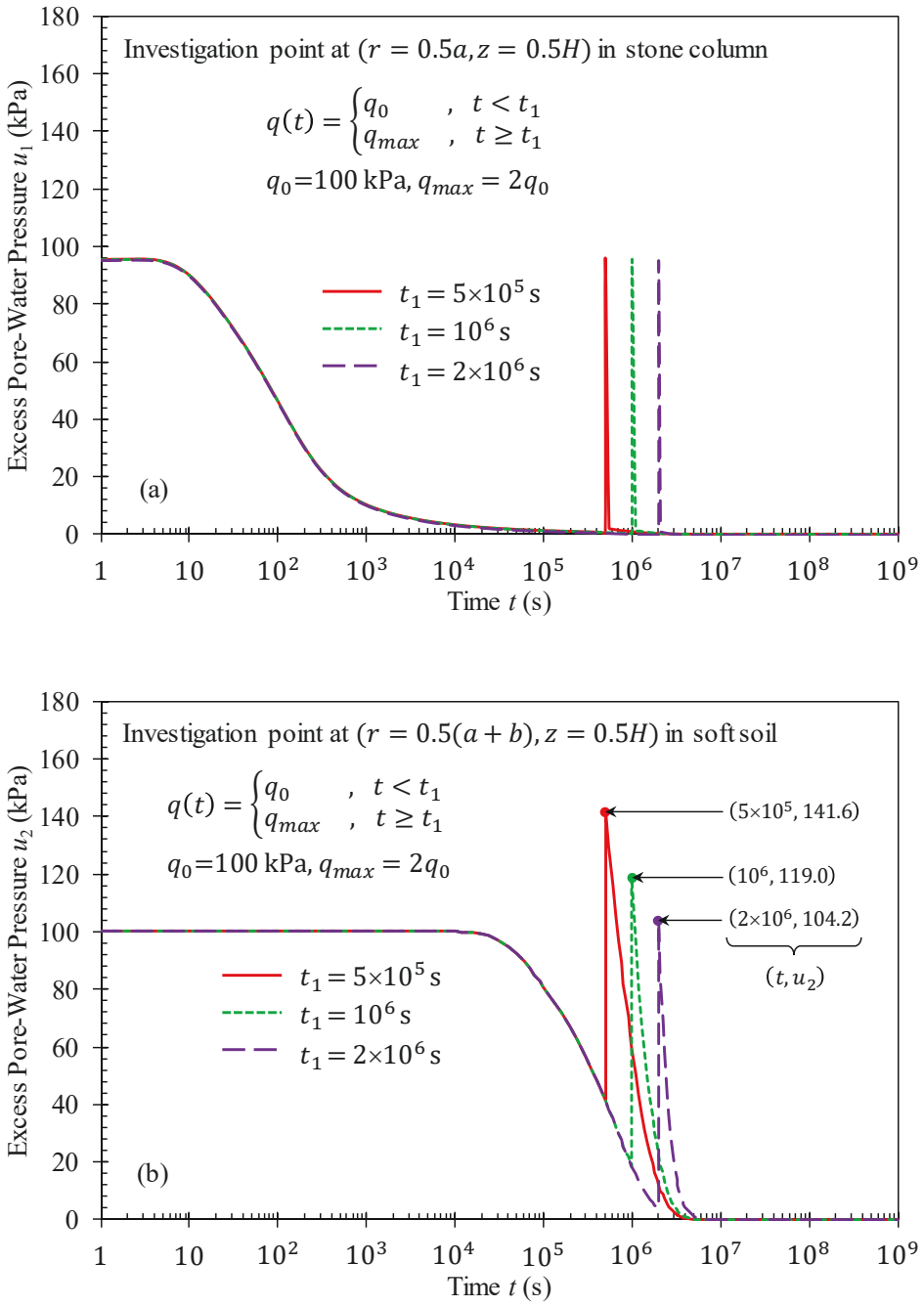

Figure 5.3. Dissipation rates of excess pore water pressure at investigation points in (a) stone column and (b) soft soil varying with time duration t_1 of the step loading

Figures 5.4a and 5.4b present the effect of loading period t_1 of the step loading on normalised average surface settlements of the column and soil regions, respectively. As a result of the fast dissipation of excess pore water pressure in stone column, the settlement rate of the column increased rapidly right after exerting the first surcharge step and then the settlement increased gradually with a slower rate to a value of $\bar{S}_1^* = 0.5$ at the end of the first loading (Figure 5.4a). Similarly, the second increment of external load also resulted in rapid development of settlement to reach the end of consolidation process in which the consolidation was terminated earlier for the case of shorter loading period t_1 . Unlike the stone column, the soft soil endured different normalised settlements for various ending time t_1 (i.e. $\bar{S}_2^* = 0.32, 0.42, \text{and } 0.49$ for $t_1 = 5 \times 10^5,\ 10^6,\ \text{and } 2 \times 10^6$ s, respectively) as demonstrated in Figure 5.4b, owing to the excess pore water pressure not dissipating completely at that time (see Figure 5.3b). The settlement rate of soft soil rose significantly by shortening the first loading period prior to applying the next surcharge.

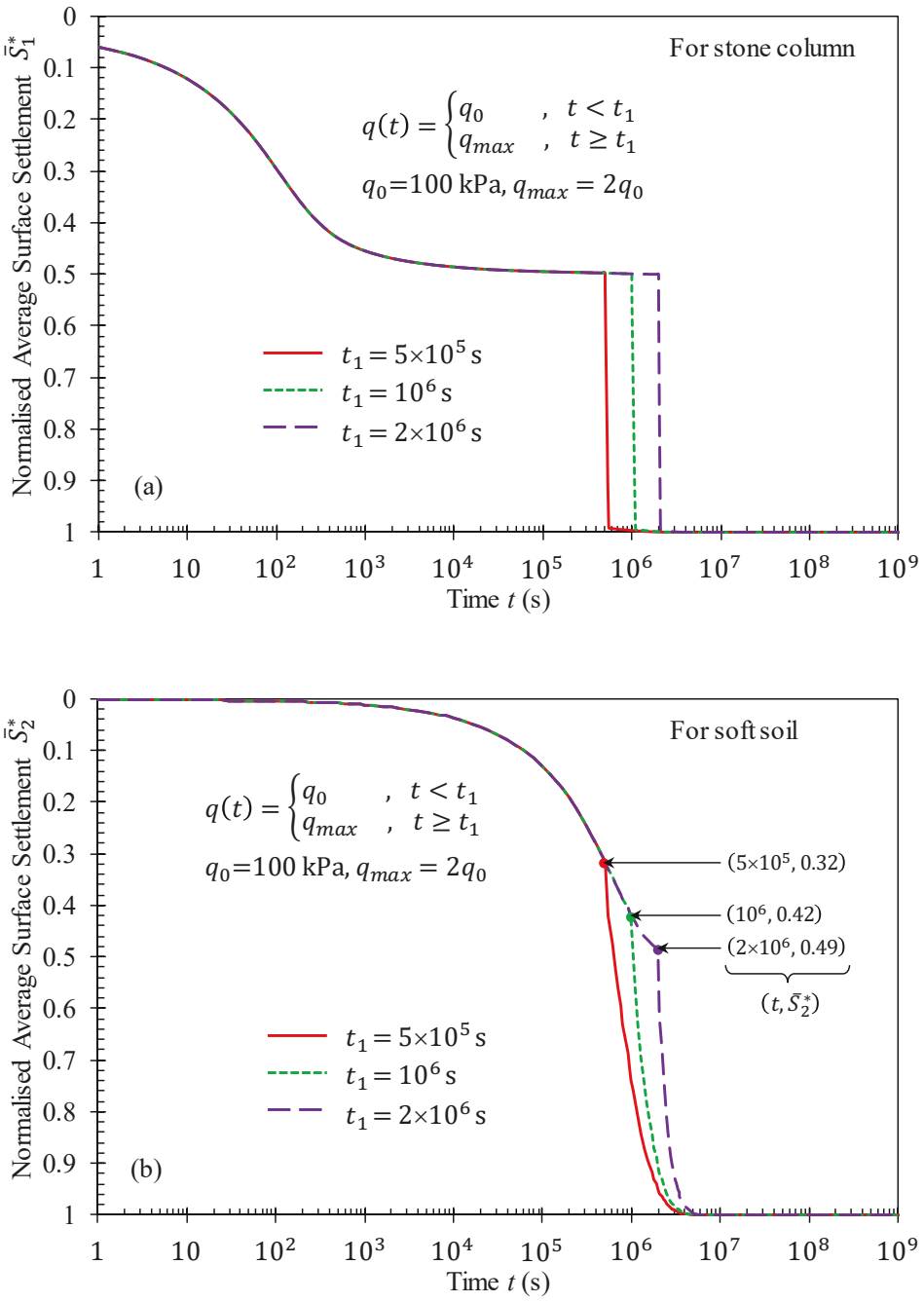

Figure 5.4. Influence of time duration t_1 of the step loading on normalised average surface settlements of (a) stone column and (b) soft soil

Figure 5.5 displays the changes in differential average surface settlement between stone column and soft soil regions with consolidation time, taking the influence of varying loading time t_1 into account. As can be seen, the variation pattern of the differential settlement $\Delta\overline{S}$ almost resembled the shape of the normalised settlement curve $\bar{S}_2^*$ where the differential settlement at the end of the first loading became larger gradually corresponding to an increase of the loading period t_1. The difference in $\Delta\overline{S}$ value at varying time t_1 is visually illustrated in Figures 5.4a and 5.4b, in which the column settlement induced by the first surcharge reached the maximum for all investigating values of t_1 whereas the soil settlement still gradually increased with an extension of loading time t_1. Referring to Equations (5.11a) and (5.11b), the referenced settlement $\overline{S}_{2ref}$ would be much greater than $\overline{S}_{1ref}$ under the uniform external loading (i.e. $\sigma_{01} = \sigma_{02} = q_0$) owing to the considerably lower stiffness of soft soil compared with stone column. For this reason, the $\Delta\overline{S}$ value (i.e. the difference between $\overline{S}_1(t)$ and $\overline{S}_2(t)$) was nearly regulated by the product of $\bar{S}_2^*$ and $\overline{S}_{2ref}$ in connection to Equations (5.9a) and (5.9b) (i.e. neglecting $\overline{S}_1(t)$ or $\bar{S}_1^*$) and thus the $\Delta\overline{S}$ patterns were virtually identical to $\bar{S}_2^*$ curve shapes.

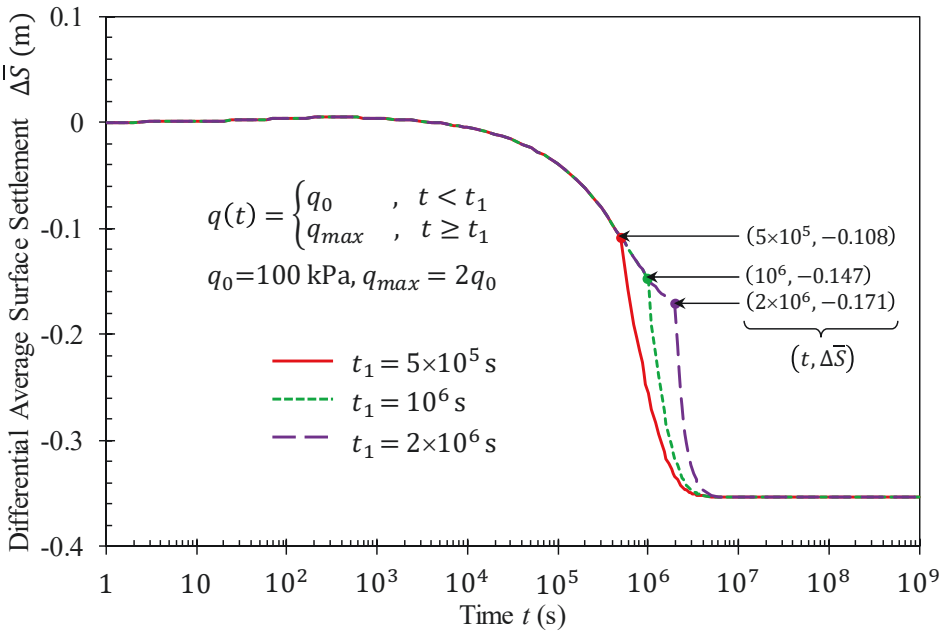

Figure 5.5. Influence of time duration t_1 of the step loading on the differential average surface settlement between stone column and soft soil

5.4.2 Ramp loading

The ramp loading is a generalisation of step loading, which is normally experienced in real construction projects such as the construction of embankments on soft soils. To avoid the potential failure of soft soil foundations under undrained compression exerted by embankment loads, the embankment height is developed progressively to limit the generation of excessive excess pore water pressure that might cause the soil collapse. Such an embankment construction can be simulated as a ramp or multi-stage ramp loading; for instance, the loading in Figure 5.2b is a one-stage ramp case with a nonzero initial surcharge.

Figures 5.6a and 5.6b depict the variation of excess pore pressure dissipation rate with different ramping time t_1 (i.e. construction time period) of the loading case in Figure 5.2b for examination points in the column and soil bodies, correspondingly. The alteration of ramping time t_1, implying a change in loading rate A, affected the dissipation of excess pore water pressure at points of investigation during about the first 10^4 s of consolidation insignificantly. Particularly, the excess pore pressure dissipation in stone column was nearly unchanged when the load ramping time t_1 had been varied (Figure 5.6a). However, the soft soil experienced a significant impact of the ramping time on the dissipation rate during elapsed time when $t > 10^4$ s (Figure 5.6b). It is important to note that the value of excess pore water pressure in the foundation is contingent on the loading and dissipation rates. An acceleration of external loading might induce an increase of excess pore water pressure in the composite stone column – soft soil foundation and the soil in particular when the loading rate is faster than the dissipation rate of excess pore water pressure. For example, Figure 5.6b represents a significant growth in excess pore pressure from initial value (100 kPa) to approximately 150 kPa at the end of ramping time $t_1 = 2 \times 10^5$ s (i.e. equivalent to the loading rate $A = 5 \times 10^{-4}$ kPa/s). After the ramping stage (Figure 5.2b), the external load remained unchanged and hence the amount of excess pore water pressure was entirely dependent upon the dissipation rate. Considering the ending time of the ramping duration $t_1 = 2 \times 10^6$ s (i.e. $A = 5 \times 10^{-5}$ kPa/s) in Figure 5.6b, the excess pore water pressure in the soft soil at that time for faster loading rates was in turn lower and thus dissipated more quickly. This is attributable to the increase in the radial gradient of excess pore water pressure in soft soil towards stone column caused by the acceleration of loading, analogous to the analysis for the above step loading case.

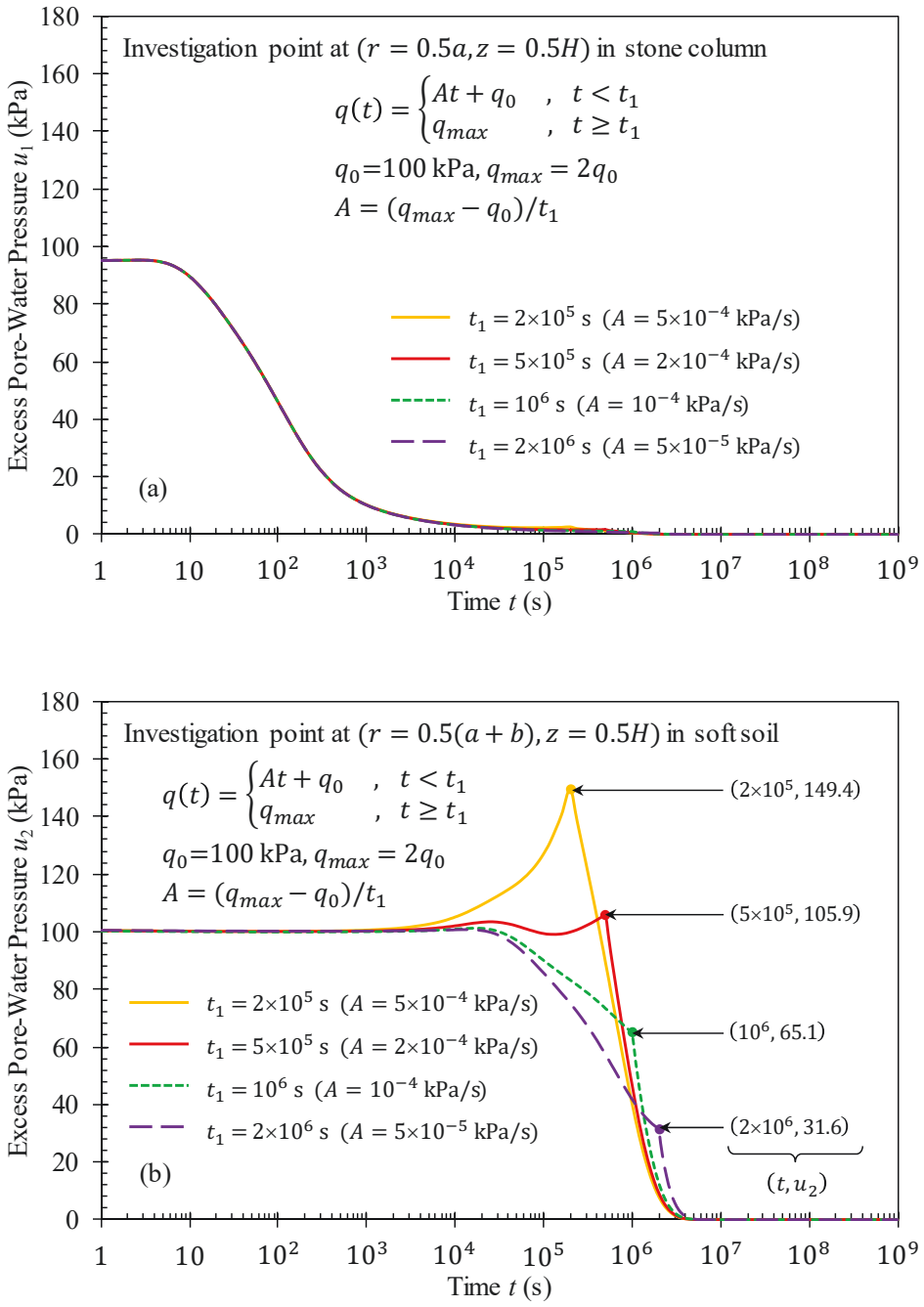

Figure 5.6. Dissipation rates of excess pore water pressure at investigation points in (a) stone column and (b) soft soil varying with construction time t_1 of the ramp loading

Figures 5.7a and 5.7b describe a considerable effect of varying ramping durations on the settlement rates of stone column and soft soil at the later stages of consolidation. The normalised settlements of both regions proceeded faster when the loading process was sped up. Pertaining to Equations (5.8a), (5.9a) and (5.11a) for the determination of the normalised settlement $\bar{S}_1^*$ of stone column, it can be seen that the changes of $\bar{S}_1^*$ would be mostly controlled by the changes of $\overline{\sigma}_1$ because of the insensitivity of the excess pore pressure dissipation in stone column to the variations of loading rate (see Figure 5.6a). Accordingly, a more rapid increase of $\overline{\sigma}_1$ prior to reaching the maximum accelerated the settlement rate of stone column and the column almost consolidated totally at the end of ramping durations (Figure 5.7a). Different from the stone column, the settlement rate of soft soil depends on both rates of external loading and excess pore water pressure dissipation due to the low permeability of soft soil. As observed in Figure 5.7b, the soil settlement still progressed after the maximum load was reached since a large amount of excess pore water pressure still existed in the soil body. It should be noted that such settlements of soft soil were indicated by $\bar{S}_2^* < 1$ at time $t = t_1$. On the other hand, a comparison between the normalised settlement of the soft soil induced by the step loading (Figure 5.4b) and the ramp loading (Figure 5.7b) reveals that the latter resulted in a faster settlement rate than the former when both loadings had the same duration t_1. The reason is attributed to the faster increase of effective vertical stress in soft soil (i.e. the difference between σ_2 and u_2) caused by the latter compared to the former, as can be seen in Figures 5.3b and 5.6b and the increases of total vertical stresses corresponding to the applied loadings.

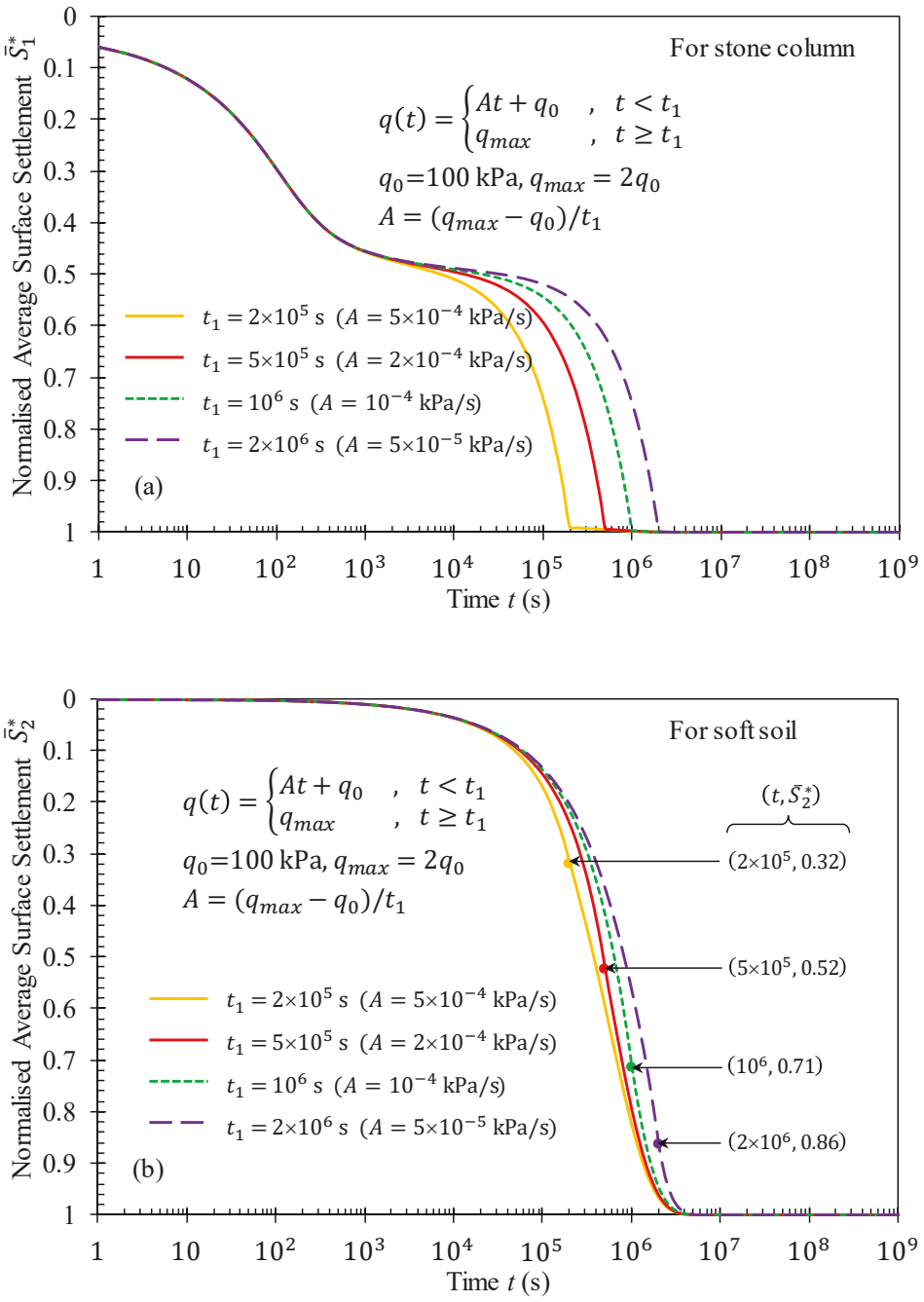

Figure 5.7. Influence of construction time t_1 of the ramp loading on normalised average surface settlements of (a) stone column and (b) soft soil

Similar to the step loading case, the changes of differential settlement $\Delta\bar{S}$ with time considering various ramping durations t_1 (Figure 5.8) had resembling patterns with $\bar{S}_2^*$ curves (Figure 5.7b) due to the much larger settlement of soft soil in comparison with stone column during the consolidation process. The acceleration of the ramp loading expedited the soil settlement along with the differential settlement $\Delta\bar{S}$ considerably. For the ramp and step loadings having the same duration t_1 (see Figures 5.2a and 5.2b), the ramp loading caused a faster rate of soft soil settlement and thus a more rapid increase of differential settlement than the step loading.

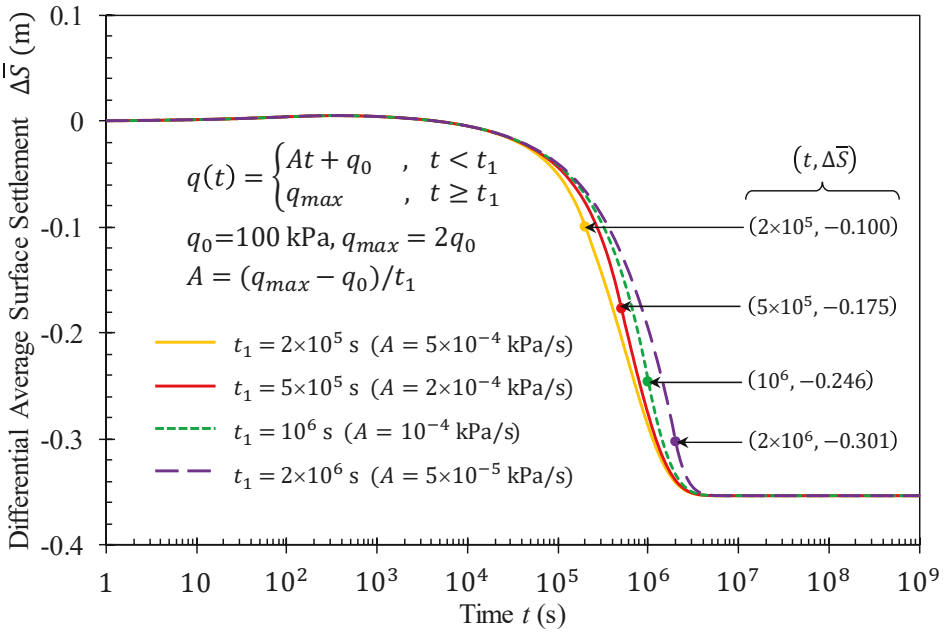

Figure 5.8. Influence of construction time t_1 of the ramp loading on the differential average surface settlement between stone column and soft soil

5.4.3 Sinusoidal loading

The sinusoidal loading is a type of cyclic loading, which can be used to model some repeatedly loading – unloading processes in practice such as the repetition of filling and discharging of storage tanks, silos, stockpiles and warehouses during their service stages. It should be noted that the amplitude, period, loading and unloading rates can be varied for each cycle of loads in real practice. However, the sinusoidal loading in Figure 5.2c as an ideal case of the cyclic load was investigated in this example for simplification while still exhibiting the capabilities of the obtained analytical solution. The loading parameters adopted in this case include the constant $B = 1$ and angular frequency $\varphi_B = 2\pi/5 \times 10^6 - 2\pi/2 \times 10^7$ rad/s (corresponding to the loading period $5 \times 10^6 - 2 \times 10^7$ s).

Figures 5.9a and 5.9b show the changes in excess pore water pressure at points of interest in the composite foundation subjected to the aforementioned sinusoidal loading, considering the effect of varying angular frequency φ_B. The alteration of the applied loading with time virtually had no effect on excess pore water pressure in stone column regardless of the change in angular frequency (Figure 5.9a), analogous to the case of ramp loading or even a constant loading case having the same initial surcharge as the sinusoidal loading. The high permeability of stone column caused the dissipation of initial excess pore water pressure in the column region to be insensitive to the change of applied load during the consolidation. In contrast, the investigation load with varying angular frequencies impacted the excess pore water pressure dissipation in the soft soil dramatically (Figure 5.9b). As observed, the excess pore pressure changed significantly in response to the loading – unloading cycles, which formed oscillating curves with

different amplitudes corresponding to various frequencies. The negative excess pore water pressures indicate the pore water absorption phenomenon of soft soil due to the unloading processes. The increase in angular frequency led to an acceleration of loading process that generated more excess pore pressure to be dissipated in the soft soil and thus decelerated the excess pore pressure dissipation in the soil at the early stages of consolidation (i.e. approximately $t \leq 10^6$ s). Despite that, a higher frequency φ_B resulted in faster rates of pore water dissipation as well as absorption during the later stages of consolidation. Taking consideration of the oscillation curves of excess pore water pressure in soft soil, it is important to note that for each loading stage (i.e. increasing load), the variation of positive excess pore pressure was dependent on the loading rate and dissipation rate. The positive pore pressure increased when the rate of loading was larger than the rate of dissipation and vice versa, then attained the maximum in accordance with the counterbalance between the two rates. On the other side, for an unloading stage (i.e. decreasing load), a quick unloading process while the positive pore pressure had dissipated completely (i.e. equal to zero) might induce an inverting pressure gradient and accompanying vacuum pressure to suck pore water back into soil bodies and cause negative excess pore pressures in the soil. The absorption of pore water counteracted the vacuum pressure generated by the unloading process; thereby, a more rapid unloading rate compared with the pore water absorption rate would reduce the negative excess pore pressures in soft soil more and vice versa. Then, the negative pore pressures reached the minimum when the absorption rate counterbalanced the unloading rate. Figure 5.9b also shows that the number of oscillations together with the amplitudes of excess pore pressure curves reduced substantially with the diminution of frequency φ_B. The decrease in angular frequency slowed down the loading – unloading processes,

which allowed sufficient time for positive excess pore water pressures to dissipate during the loading stages and that for negative excess pore water pressures to absorb during the unloading stages in order to achieve the balance state of excess pore water pressures. As a result, the amplitudes of excess pore pressure oscillations were diminished considerably corresponding to the reduction of φ_B. Referring to Equation (5.6), it is worth mentioning that the value of excess pore water pressure at an arbitrary point in the foundation at a particular time is impacted by the initial excess pore water pressure and the rates of loading – unloading processes. Therefore, once the initial positive excess pore water pressure had fully dissipated, the value of excess pore water pressure at that point is completely governed by the loading – unloading rates. This explains the oscillation patterns of excess pore water pressure in Figure 5.9b during the later stages of consolidation, in which the oscillations for a typical sinusoidal loading reaching the same maximum and minimum values indicated the sole contribution of the loading – unloading rates to the predicted excess pore water pressure.

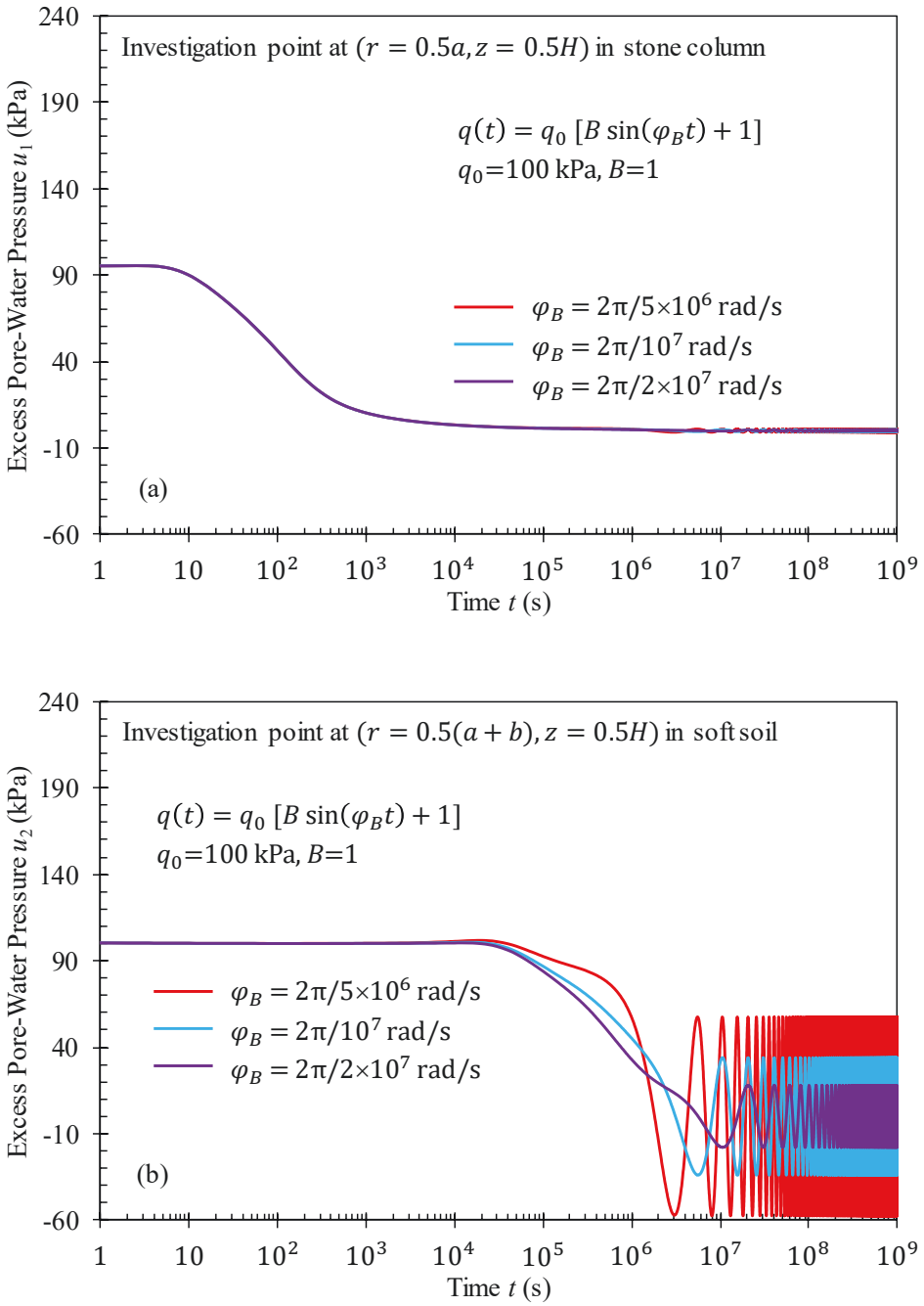

Figure 5.9. Variation of excess pore water pressure at investigation points in (a) stone column and (b) soft soil with time considering different angular frequencies φ_B of the sinusoidal loading

Figures 5.10a and 5.10b display a remarkable impact of the frequency φ_B on the settlement variations of the column and soil bodies with time, respectively. The settlement curves of the stone column and soft soil consisted of indefinite oscillations as a consequence of the continuous loading – unloading processes simulated by periodic sine functions. Particularly, the column and soil settlements proceeded more quickly when a higher frequency was adopted for the applied load. Owing to the negligible changes in dissipation and absorption rates of excess pore water pressure in the stone column subjected to varying sinusoidal loadings (Figure 5.9a), the settlement rate of stone column was almost contingent on the loading – unloading rates. During the first loading stage from the initial surcharge q_0 to the maximum of load $2q_0$, the shapes of column settlement curves under the sinusoidal loading (Figure 5.10a) were analogous to those under the ramp loading (Figure 5.7a). After that, the stone column experienced no settlement ($\bar{S}_1^* = 0$) when the composite ground had been unloaded completely (i.e. $q = 0$); by contrast, the column settlement reached the largest value ($\bar{S}_1^* = 1$) when the composite ground had been loaded to its maximum (i.e. $q = 2q_0$). These reflect the extremely rapid absorption and dissipation of excess pore water pressure thanks to the large permeability of stone column. Noting that the stiffness of the composite ground subjected to a given cyclic load may vary over the time; however, the simplifying assumption of constant stiffnesses for stone column and soft soil was adopted in this study to solve the governing equations. For a typical small amplitude of the cyclic loading, the foundation stiffness might be assumed unchanged for practical applications [124]. Figure 5.10b shows that the deceleration of angular frequency φ_B and accompanying loading – unloading processes led to a considerable increase in amplitude of the soil settlement curve. As predicted, the slower loading – unloading rates enabled more excess pore water dissipation and absorption for

each loading – unloading cycle and thus the soil volume change oscillated more significantly. Moreover, the oscillations of each soil settlement curve had the same maximum and minimum values at the later stages of consolidation, which indicated the sole contribution of loading – unloading rates to the soil settlement variation, while there was no more contribution by the initial conditions.

Figure 5.11 depicts the variation in the differential settlement rate between stone column and soft soil when changing the angular frequency φ_B of the sinusoidal loading. As with the previous loading cases, the change patterns of the differential settlement curves were similar to those of the soil settlement curves because the soft soil region endured much larger settlement than the column region during the loading – unloading processes. The differential settlement progressed faster and the amplitude of differential settlement curve reduced progressively in response to the increase in the angular frequency φ_B.

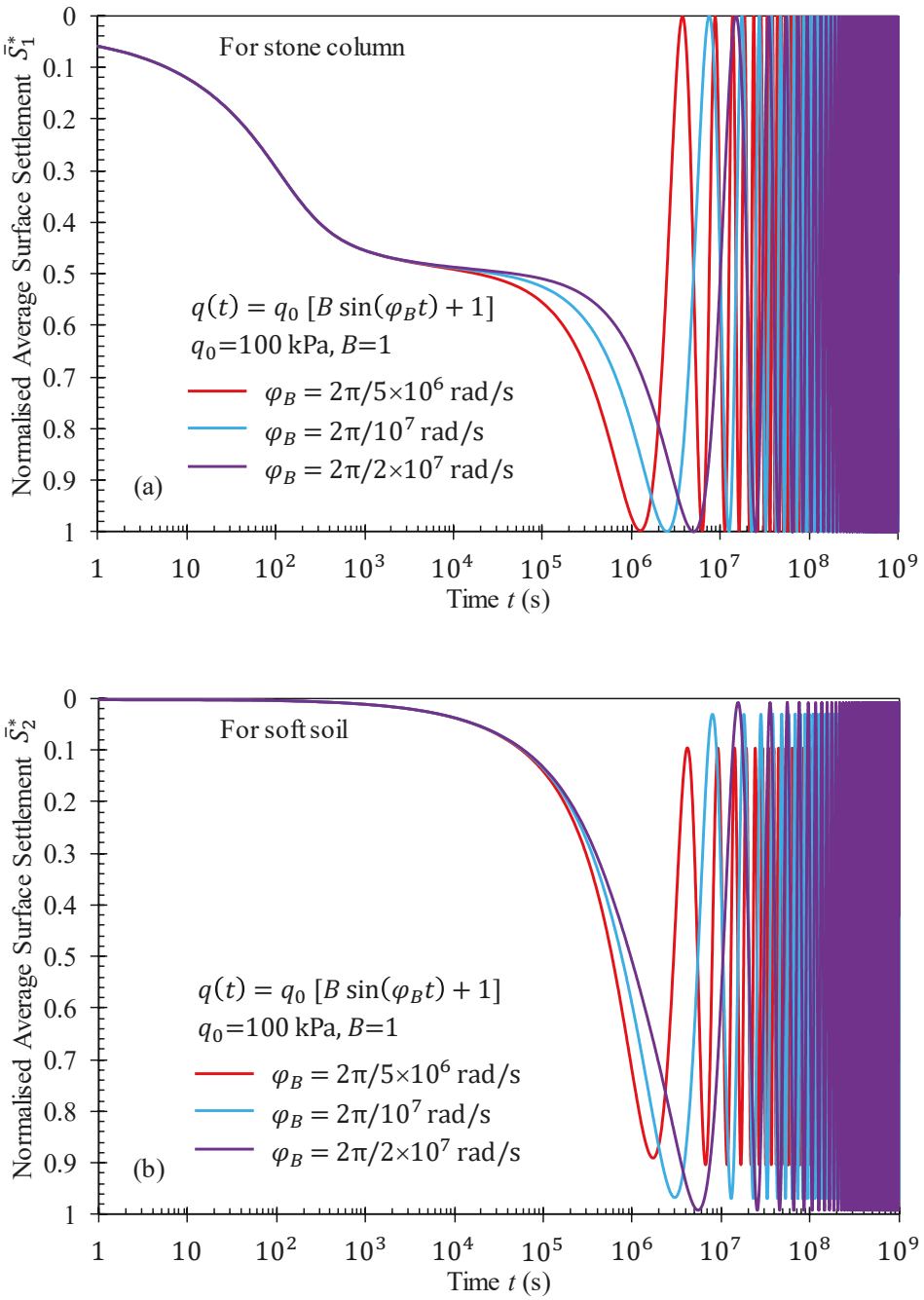

Figure 5.10. Influence of angular frequency φ_B of the sinusoidal loading on normalised average surface settlements of (a) stone column and (b) soft soil

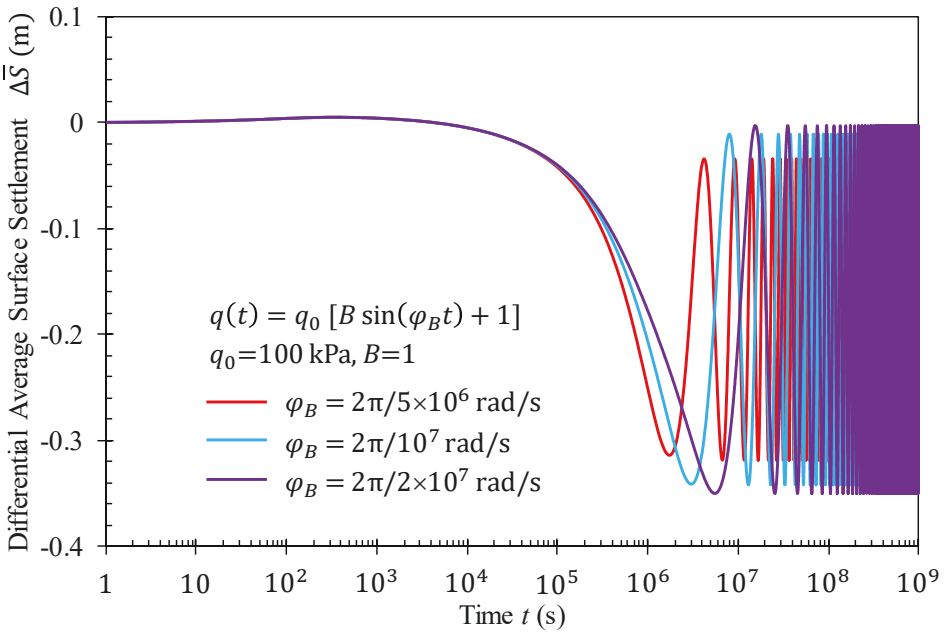

Figure 5.11. Influence of angular frequency φ_B of the sinusoidal loading on the differential average surface settlement between stone column and soft soil

5.5 Verification against field measurements

In this section, the proposed analytical solution is used to calculate the dissipation rate of excess pore water pressure at an investigation point in soft soil and the soil settlement rate of a real case study. The case study for verification is a composite stone column – soft clay foundation of the iron ore storage depot at Nelson Point, Port Hedland, Western Australia. The geotechnical data of this project were presented in the existing studies [218-220], which are summarised in Table 5.2 for reference. The composite foundation was loaded by the iron ore filling in two stages. The first filling to 17 m height had proceeded within approximately 25 h, and then the stockpile height remained unchanged until 900 h. Then, the height of the stockpile was raised very quickly from 17 to 19 m corresponding to the second filling. The average unit weight of the iron ore was evaluated

to be approximately $28\ \mathrm{kN/m^3}$, and thus the first and second fillings caused the external load to be equivalent to $476\ \mathrm{kPa}$ and $532\ \mathrm{kPa}$, respectively.

Table 5.2. Geometric and material parameters for the verification

	H (m)	a (m)	b (m)	$k_{1h}=k_{1v}$ (m/s)	$k_{2h}=k_{2v}$ (m/s)	$c_{2h}=c_{2v}$ (m^2/s)	E_1/E_2	ν_{P1}	ν_{P2}
Field measurement	3	0.55	1.125	-	1.74×10^{-10}	$(0.63-3.17)\times10^{-8}$	$20-40$	-	-
Proposed analytical solution	3	0.55	1.125	5×10^{-5}	1.74×10^{-10}	2.32×10^{-8}	30	0.3	0.3

Before proceeding further with the verification, it is worth mentioning that due to the larger stiffness of stone column compared to the soft soil, dominant portion of the external surcharge is transferred onto the stone column. As a result, the average total vertical stress acting on stone column is much higher than on soft soil. Considering the assumption of uniform distribution of total vertical stresses in each region in this study, the following stress concentration ratio n_{scr} can be defined:

$$n_{scr} = \frac{\bar{\sigma}_1(t)}{\bar{\sigma}_2(t)} \tag{5.12}$$

where $\bar{\sigma}_1(t)$ and $\bar{\sigma}_2(t)$ denote the average total vertical stresses in stone column and soft soil regions induced by the external load at time t, respectively.

Obviously, the stress concentration ratio changes during the consolidation because of the time-varying applied total vertical stresses. While the consideration of time-dependent stress concentration ratio is out of the scope of this study, the verification with the field measurement adopted an assumption for variations of the total stresses against time such that the induced stress concentration ratio remains constant in the consolidation process. Then, $\bar{\sigma}_1(t)$ and $\bar{\sigma}_2(t)$ corresponding to a given n_{scr} value are obtainable by combining Equation (5.12) with the following equilibrium condition of the total vertical stresses:

$$\bar{\sigma}_1(t) + \bar{\sigma}_2(t)\left(n_e^2 - 1\right) = q(t)\, n_e^2 \tag{5.13}$$

where q is the average external loading; $n_e = b/a$ is the radius ratio between unit cell and stone column.

Referring to the field observations reported by Dunbavan and Carter [219], the range of stress concentration ratio $n_{scr} = 2.5 - 5$ was adopted for the verification. Once the

total vertical stresses σ_1 and σ_2 (i.e. $\bar{\sigma}_1$ and $\bar{\sigma}_2$ owing to the uniform distribution assumption of total vertical stresses) have been achieved, the variation of excess pore water pressure at any point in the composite ground with time can be determined applying Equations (5.5) and (5.6).

Figure 5.12 verifies the dissipation rate of excess pore water pressure calculated using the proposed analytical solution against the field observation results at an investigation point in soft soil region of the case history composite ground. As observed, the obtained analytical solution in this study shows a reasonable agreement with the field measurement data, in which the smaller stress concentration ratio n_{scr} should be adopted for the early period of consolidation and vice versa as described by Dunbavan and Carter [219]. The discrepancies between the prediction results and the field observations are attributed to the increase of stress concentration ratio with time in real practice, whereas the proposed analytical solution assumed a constant stress concentration ratio for the adopted range. To address this, the stress concentration ratio could be assumed as a time-varying function capturing lower stress concentration ratios for the early stages of consolidation and higher ones for the later stages. Furthermore, the range of adopting stress concentration ratio should be $n_{scr} = 2 - 6$ for a characteristic flexible surcharge as reported in several existing studies [2, 7, 17] when applying the proposed analytical solution in practice.

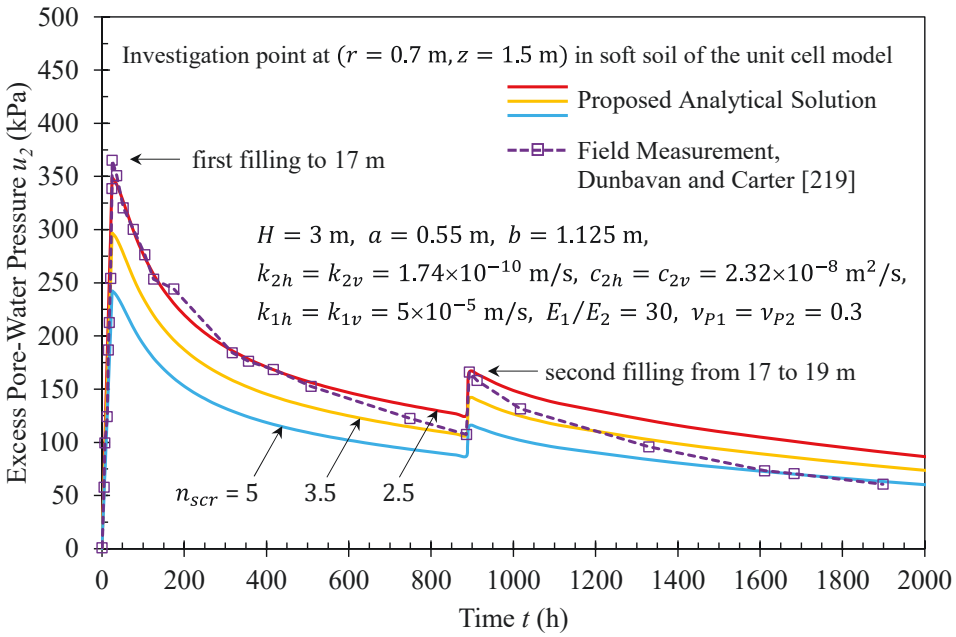

Figure 5.12. Verification of excess pore water pressure dissipation rate obtained from the proposed analytical solution and field measurement at an investigation point in soft soil

Figure 5.13 displays the verification of settlement rate of soft soil resulted from proposed analytical solution against field measurement data. Similar in Chapter 4, an immediate settlement of 230 mm after the first loading of stockpile was adopted and combined with consolidation settlement of soft soil calculated by the proposed analytical solution for time $t \geq 25$ hours, which would result in the settlement variation of soft soil against time as presented in Figure 5.13. As can be seen, there was a reasonable agreement between the predicted values and measured data of soil settlement. The proposed analytical solution adopting larger stress concentration ratio underestimated the soil settlement rate more significantly. This is due to the assumption of constant stress concentration ratio in the proposed analytical solution, whereas this ratio would increase with consolidation time in practice. Despite that, the measured settlement data tended to approach predicted settlements adopting higher stress concentration ratio at the later

stages of consolidation. The inelastic settlement and lateral movement of soft soil are also primary reasons which induce larger measured data compared with the settlements calculated by the proposed analytical solution, as explained in the verification in Chapter 4.

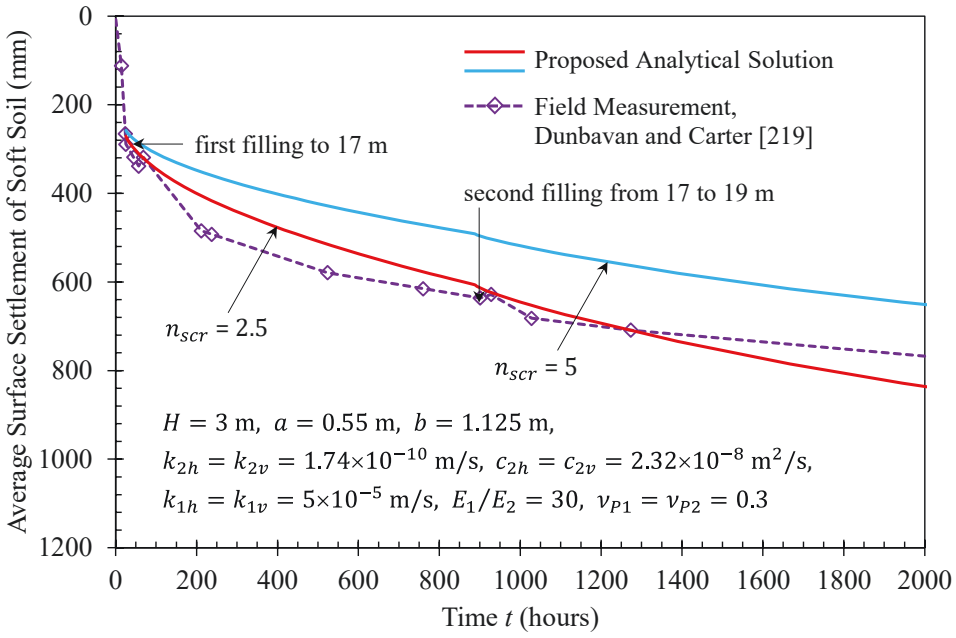

Figure 5.13. Verification of average surface settlement rate of soft soil obtained from the proposed analytical solution and field measurement

Finally, a comparison between analytical solutions proposed in Chapters 4 and 5 shows that the latter provided more reasonable agreement with measured data on excess pore water pressure dissipation and settlement rates in soft soil than the former, considering a continuous increase of stress concentration ratio with time. The inclusion of generalised time-dependent loading functions in the analytical model and solution in Chapter 5 allows to investigate the variation of any surcharge loading with time in practice. Therefore, the

changes of stockpile filling in the case history against time can be captured by the proposed analytical solution in Chapter 5 readily.

5.6 Summary

It has been widely admitted in geotechnical engineering that soft soils can be reinforced effectively using stone column inclusions. A large number of studies have been conducted to examine the performance of stone column improved soft ground, particularly for the consolidation aspect. Nevertheless, most available research studies employed the equal strain hypothesis for the consolidation of composite stone column – soft soil foundation, which cannot capture the differential settlement in the foundation. Therefore, the present study proposed an analytical solution mitigating this shortcoming of most existing analytical studies. The mathematical unit cell model for the consolidation was established as a non-homogeneous problem whose governing equations, boundary and initial conditions were formulated in terms of excess pore water pressure. The analytical development integrated coupled radial – vertical flows of excess pore water pressure concurrently in the composite foundation subjected to any time-dependent loading, adopting a free strain condition for the column and soil settlements. The complete analytical solution for excess pore water pressure at an arbitrary point in the foundation was presented in terms of Green's formula, whereas the Green's function for the solution was derived by solving the homogeneous version of the consolidation problem. Other derivations of the obtained analytical solution can also be developed such as average excess pore water pressures and average surface settlements of the stone column and soft soil. Therefore, the differential settlement between the column and soil regions in the composite ground supporting a typical flexible time-varying surcharge could be captured.

The competence of the achieved analytical solution in this study was validated via a thoroughly worked example investigating three common time-dependent loadings which were simulated as step, ramp and sinusoid loadings. In the example, the effects of various loading parameters on consolidation behaviour of the composite ground were examined in terms of excess pore water pressure dissipation rates at different points in the ground, normalised average surface settlements for stone column and soft soil regions, and the differential average surface settlement between two regions. Lastly, the proposed analytical solution was verified against the field measurements of a real case history where excess pore water pressure dissipation and settlement rates in soft soil improved with stone columns are of interest. The proposed analytical solution predicted the field measurements reasonably well, by adopting appropriate stress concentration ratio n_{scr} increasing with consolidation time. It should be noted that the disparities between analytical predictions and field measurements were primarily due to the assumption of unchanged stress concentration ratio during the consolidation process for the proposed analytical solution, while that increases progressively with time in real practice. Although the consideration of time-varying stress concentration ratio is out of the research scope, it is suggested that the stress concentration ratio might be assumed as a function increasing with time for a typical flexible loading in practical applications.

CHAPTER 6

SIMPLIFIED ANALYTICAL SOLUTION FOR COUPLED ANALYSIS OF CONSOLIDATION AND DEFORMATION OF STONE COLUMN IMPROVED SOFT SOIL

6.1 Introduction

The primary objective of this chapter is to develop an analytical solution to investigate the axisymmetric consolidation and deformation of the composite stone column – soft ground concurrently under free strain configuration and instantaneously applied uniform loading. The mathematical formulation for the consolidation is derived corresponding to the unit cell model in which the governing equations for the stone column and surrounding soft soil regions are non-homogeneous partial differential equations for excess pore water pressure dissipations. The consolidation formulation integrates rigorously the coupled radial – vertical flows of excess pore water pressure in the foundation where the permeabilities of stone column and soft soil are orthotropic. The space- and time-dependent total vertical stresses caused by the external loading, which are the non-homogeneous terms in the governing consolidation equations are formulated in conjunction with the deformation analysis. The settlement model suggested by Alamgir et al. [65] is adopted in the present study for the consideration of deformation pattern with radius. In an attempt to establish analytical solutions, the homogeneous consolidation problem is solved first to obtain the corresponding terminating time of consolidation, using the method of separation of variables. Then, the equations for the induced total vertical stresses are derived satisfying their initial and final conditions in the consolidation process. The total vertical stresses are assumed to be initially distributed uniformly over

the composite ground, whereas their final distributions at the end of consolidation period (i.e. corresponding to the drained compression condition) are derived taking advantage of the study by Alamgir et al. [65]. Once the equations for the total vertical stresses in stone column and soft soil are established, the non-homogeneous consolidation problem is solved to obtain the excess pore water pressure for any points in the foundation by applying the Green's function method. Hence, the average settlement at a given depth owing to the excess pore water pressure dissipation together with the average degree of consolidation (to be derived using the average surface settlement) for each stone column and soft soil region can be readily determined. Thereafter, the average differential settlement between the soft soil and stone column can also be computed for the determination of a settlement parameter which is denoted as a function against depth and time. Thus, the composite ground settlement pattern, shear strains and shear stresses in the soft soil region at any given time during the consolidation process can be obtained. To validate the proposed analytical solution in this study, a worked example accompanied by a verification exercise against finite element modelling results are carried out thoroughly. The results obtained from the proposed analytical solution and finite element simulation are presented graphically in terms of the changes in the total vertical stresses against depth and time, the excess pore water pressure dissipation, the average degree of consolidation, the composite ground settlement pattern and the shear stress distribution in soft soil during the process of consolidation. A further verification of the proposed analytical solution against case study of a full-scale test is also performed investigating surface settlement of a soft soil foundation reinforced by soil-cement deep mixing columns.

6.2 Governing equations, boundary and initial conditions of the consolidation

In this study, the unit cell approach is adopted to develop the analytical solution. Figure 6.1 shows the cylindrical cell model of the problem, which is comprised of a stone column of radius a enclosed by a hollow cylinder of soft soil expanding to the unit cell effective radius b. The composite stone column – soft soil foundation of thickness H is underlain by an undeformable layer and subjected to a flexible uniform loading q_0 on the ground surface. The consolidation of the composite foundation proceeds assuming the orthotropic pore water flows for both stone column and soft soil regions, in which the undeformable layer at the bottom of soft soil stratum is considered as impermeable while the composite ground surface is freely draining. Besides, the mathematical derivation for the consolidation adopts the basic assumptions as reported in several available studies [64, 98, 111, 115]. The column and soil materials are homogeneous and saturated, in which the pore water is incompressible and the flow of pore water complies with Darcy's law. It is assumed that the permeability and compressibility coefficients of the materials remain unchanged under a pressure increment caused by the external loading. It is considered that the composite ground solely deforms along the vertical direction adopting the free strain assumption. In the present study, it is important to note that although the loading is assumed to be applied instantly and maintained constant during the consolidation process, the distribution of the induced total vertical stresses in the foundation vary with spatial coordinates and elapsed time owing to varying excess pore water pressure dissipation rates. Further consideration in the variation in distribution of total vertical stresses is provided in the following sections. It is worth mentioning that the stone column settlement at a given depth stays fairly uniform during the consolidation period because of the rapid dissipation of excess pore water pressure in the column.

Thereby, the induced shear strain along the radius of stone column is minor and the accompanying total vertical stress remains almost unchanged. In other words, the total vertical stress at a particular depth within the stone column is regarded as uniform distribution at any point of time. Then, referring to the existing analytical studies [111, 115], the coupled governing equations for the consolidation of stone column and soft soil regions can be written in terms of non-homogeneous partial differential equations as follows:

$$\frac{k_{1h}}{\gamma_w}\left(\frac{\partial^2 u_1(r,z,t)}{\partial r^2}+\frac{1}{r}\frac{\partial u_1(r,z,t)}{\partial r}\right)+\frac{k_{1v}}{\gamma_w}\frac{\partial^2 u_1(r,z,t)}{\partial z^2}=\frac{1}{M_1}\left[\frac{\partial u_1(r,z,t)}{\partial t}-\frac{\partial \sigma_1(z,t)}{\partial t}\right] \tag{6.1a}$$

$$\frac{k_{2h}}{\gamma_w}\left(\frac{\partial^2 u_2(r,z,t)}{\partial r^2}+\frac{1}{r}\frac{\partial u_2(r,z,t)}{\partial r}\right)+\frac{k_{2v}}{\gamma_w}\frac{\partial^2 u_2(r,z,t)}{\partial z^2}=\frac{1}{M_2}\left[\frac{\partial u_2(r,z,t)}{\partial t}-\frac{\partial \sigma_2(r,z,t)}{\partial t}\right] \tag{6.1b}$$

where σ_1 and σ_2 denote the total vertical stresses induced in the stone column and soft soil, correspondingly; u_1 and u_2 denote the excess pore water pressures in the stone column and soft soil, correspondingly; r and z are the physical coordinates of the unit cell (Figure 6.1); t is the elapsed time; M_1 and M_2 denote the constrained moduli of the stone column and soft soil, respectively; k_{1h} and k_{2h} denote the horizontal permeabilities of the stone column and soft soil, respectively; similarly, k_{1v} and k_{2v} denote the vertical permeabilities of the stone column and soft soil, respectively; and γ_w is the unit weight of water $(10\,kN/m^3)$.

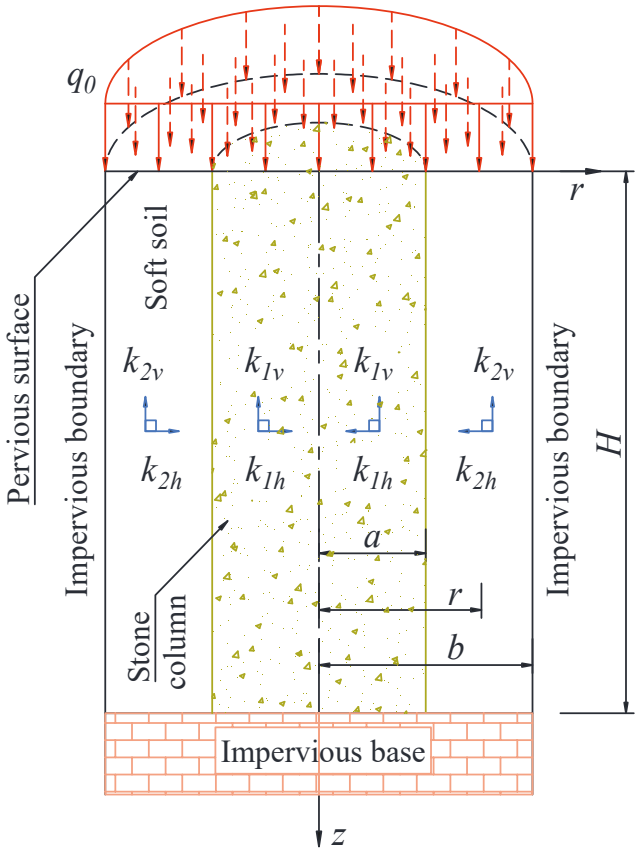

Figure 6.1. The axisymmetric unit cell model for the consolidation analysis

Proceeding from the axisymmetric consolidation model in Figure 6.1, the continuity conditions of excess pore water pressure and radial flow rate at the stone column – soft soil interface can be expressed by Equations (6.2a) and (6.2b), respectively. Additionally, the condition of no radial water flow across the exterior vertical surface of the cell cylinder can be simulated by Equation (6.2c).

$$u_1(a,z,t) = u_2(a,z,t) \tag{6.2a}$$

$$k_{1h}\frac{\partial u_1(a,z,t)}{\partial r} = k_{2h}\frac{\partial u_2(a,z,t)}{\partial r} \tag{6.2b}$$

$$\frac{\partial u_2(b,z,t)}{\partial r} = 0 \tag{6.2c}$$

The free drainage condition of the composite ground surface and the impermeability of the bottom rigid layer, resulting in upward drainage paths for excess pore water pressures in the stone column and soft soil (Figure 6.1), can be expressed by:

$$u_1(r,0,t) = u_2(r,0,t) = 0 \tag{6.3a}$$

$$\frac{\partial u_1(r,H,t)}{\partial z} = \frac{\partial u_2(r,H,t)}{\partial z} = 0 \tag{6.3b}$$

Due to the assumption of the incompressibility of grain particles and pore water, the initial total vertical stresses induced by the surcharge loading are considered to be entirely supported by the initial excess pore water pressures in the stone column and soft soil regions, i.e.

$$u_1(r,z,0) = \sigma_1(z,0) \tag{6.4a}$$

$$u_2(r,z,0) = \sigma_2(r,z,0) \tag{6.4b}$$

where $\sigma_1(z,0)$ and $\sigma_2(r,z,0)$ denote correspondingly the initial total vertical stresses (i.e. the stresses at time $t = 0$) in the column and soil regions of the composite foundation supporting the instantaneously applied loading.

6.3 Deformation of the stone column reinforced ground at the end of consolidation

Before proceeding further with the simultaneous analysis of consolidation and deformation for the composite stone column – soft ground, the deformation of the foundation at the end of consolidation process (i.e. the final deformation corresponding to the drained compression condition) would be taken into account to derive the equations for the distribution of final total vertical stresses in the composite ground induced by external applied loading. In this study, the deformed mode (see Figure 6.2) as suggested

by Alamgir et al. [65] is adopted. At a given depth in the foundation, the final column settlement is assumed remaining uniform over the column area, while the final soil settlement increases from the column – soil contact surface towards the outer radial boundary of the unit cell. Moreover, it is assumed that there is no vertical slip at the column – soil interface, which implies settlement continuity at the column – soil interface. Referring to Alamgir et al. [81], the final settlement pattern can be given by:

$$S_{2f}(r,z) = S_{1f}(z) + \alpha_{1f}(z)\left[\frac{r}{a} - e^{\beta_f\left(\frac{r}{a}-1\right)}\right] \qquad (a \le r \le b) \tag{6.5}$$

where S_{1f} and S_{2f} are the final settlements of the stone column and soft soil, respectively; α_{1f} is the final settlement parameter against *z*-domain and β_f is the settlement parameter against *r*-domain.

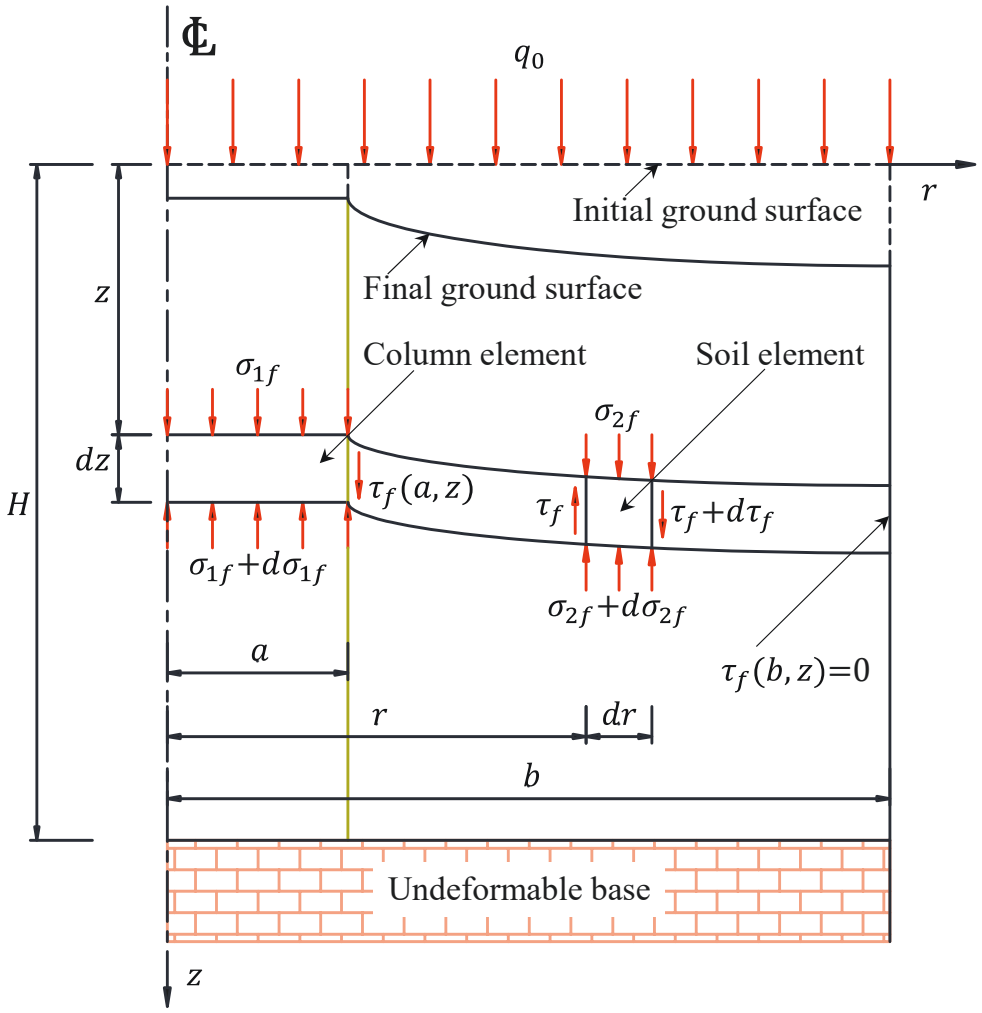

Figure 6.2. Assumed deformation pattern of the composite stone column – soft ground and induced stress components on the column and soil elements at the end of consolidation process

It should be noted that the radial deformation of the composite ground is neglected in the mathematical formulation and the foundation system solely deforms vertically. Therefore, the final shear strain γ_f and final shear stress τ_f in the soft soil can be derived via the following equations:

$$\gamma_f(r,z)=\frac{\partial S_{2f}(r,z)}{\partial r}=\frac{\alpha_{1f}(z)}{a}\left[1-\beta_f e^{\beta_f\left(\frac{r}{a}-1\right)}\right] \tag{6.6}$$

$$\tau_f(r,z)=G_2\,\gamma_f(r,z)=G_2\,\frac{\alpha_{1f}(z)}{a}\left[1-\beta_f e^{\beta_f\left(\frac{r}{a}-1\right)}\right] \tag{6.7}$$

where $G_2=E_2/2(1+\nu_{P2})$ is the shear modulus of soft soil; E_2 and ν_{P2} are Young's modulus and Poisson's ratio of soft soil, respectively.

Noting that the shear stress along the outer vertical surface of the cylindrical cell should be null (i.e. $\tau_f(r=b,z)=0$) due to the axisymmetric conditions of the external loading and geometry. Substituting this condition into Equation (6.7) leads to the following equation for the determination of the settlement parameter β_f:

$$\beta_f e^{\beta_f(n_e-1)}-1=0 \tag{6.8}$$

where $n_e=b/a$ is the radius ratio. Then, referring to Equation (6.5), the final soil settlement S_{2f} can be obtained once the final column settlement S_{1f} and the final settlement parameter α_{1f} have been disclosed. For these purposes, the total vertical stresses in stone column and soft soil at the end of consolidation need to be determined.

It is assumed that the stone column reinforced soft ground is normally consolidated, and thus the settlement of the composite ground is solely due to the external applied loading but not its own weight. Considering the equilibrium of final vertical forces acting on a particular column section dz while excluding the body forces as shown in Figure 6.2, the following ordinary differential equation can be established:

$$\left[\sigma_{1f}(z)+d\sigma_{1f}(z)\right]\pi a^2-\sigma_{1f}(z)\,\pi a^2-\tau_f(a,z)\,2\pi a\,dz=0 \tag{6.9}$$

where $\sigma_{1f}(z)$ denotes the final total vertical stress in stone column at depth z induced by external applied loading.

Simplifying Equation (6.9) and then combining with Equation (6.7) would lead to the following:

$$\frac{d\sigma_{1f}(z)}{dz} = \frac{2G_2\alpha_{1f}(z)}{a^2}\left[1-\beta_f\right] \tag{6.10}$$

Likewise, by writing the equilibrium equations for the vertical forces exerting on a specific soil element at the end of consolidation (Figure 6.2) excluding the body forces, the partial differential equation for the stresses in the soil element can be derived as:

$$\frac{\partial\sigma_{2f}(r,z)}{\partial z} = \frac{\partial\tau_f(r,z)}{\partial r} + \frac{\tau_f(r,z)}{r} \tag{6.11}$$

where $\sigma_{2f}(r,z)$ denotes the final total vertical stress at any point (r,z) in soft soil induced by external applied loading.

Obviously, considering the settlement accumulation closer to the ground surface, the differential settlement between the soft soil and stone column decreases with depth. Thus, an almost equal strain plane at depth z_0 exists in the composite ground below which there is negligible differential settlement between column and soil. Accordingly, the distribution of total vertical stresses in stone column and soft soil regions below this depth can be considered to be uniform in each region. Therefore, the equal strain condition for the composite ground can be employed at depth z_0 as follows:

$$\frac{\sigma_{1f}(z_0)}{M_1} = \frac{\bar{\sigma}_{2f}(z_0)}{M_2} \tag{6.12}$$

where $\bar{\sigma}_{2f}(z_0)$ denotes the average final total vertical stress in soft soil at depth z_0. Moreover, at any depth, both the column and encircling soil carry and share the external applied loading, i.e.

$$\sigma_{1f}(z_0) + \bar{\sigma}_{2f}(z_0)\left(n_e^2 - 1\right) = q_0\, n_e^2 \tag{6.13}$$

where q_0 is the uniform external loading.

Solving Equations (6.12) and (6.13) simultaneously would result in:

$$\sigma_{1f}(z_0) = \frac{M_1\, q_0\, n_e^2}{M_1 + M_2\left(n_e^2 - 1\right)} \tag{6.14a}$$

$$\bar{\sigma}_{2f}(z_0) = \frac{M_2\, q_0\, n_e^2}{M_1 + M_2\left(n_e^2 - 1\right)} \tag{6.14b}$$

It is noticed that the final total vertical stresses $\sigma_{1f}(z)$ and $\sigma_{2f}(r,z)$ in the stone column and soft soil should comply with the boundary conditions on the ground surface as follows:

$$\sigma_{1f}(z=0) = q_0 \tag{6.15a}$$

$$\sigma_{2f}(r, z=0) = q_0 \tag{6.15b}$$

According to Alamgir et al. [65], the final settlement parameter α_{1f} and accompanying stresses σ_{1f}, σ_{2f}, τ_f and shear strain γ_f together with the settlements S_{1f} and S_{2f} can be determined for a finite number of column and soil elements which are discretised from the unit cell geometry. However, to obtain the analytical solution for the combination of consolidation and deformation analyses in this study, the following equation of $\sigma_{1f}(z)$

would be adopted considering the parametric study conducted by Alamgir et al. [65] and incorporating with Equations (6.14a) and (6.15a):

$$\sigma_{1f}(z) = q_0 + \left[\sigma_{1f}(z_0) - q_0\right]\left(1 - e^{-dz}\right) \tag{6.16}$$

where $d = 25/(H\, n_e)$ is the parameter regulating the change of $\sigma_{1f}(z)$ with depth. Thus, the final settlement parameter α_{1f} can be obtained by incorporating Equation (6.16) into Equation (6.10) as follows:

$$\alpha_{1f}(z) = \frac{a^2 d\, \mathrm{e}^{-dz}\left[\sigma_{1f}(z_0) - q_0\right]}{2G_2\left(1-\beta_f\right)} \tag{6.17}$$

As a result, the shear strain γ_f and shear stress τ_f in the soft soil at the end of consolidation can be determined via Equations (6.6) and (6.7), respectively.

Finally, the final total vertical stress in soft soil $\sigma_{2f}(r,z)$ can be derived by substituting Equation (6.7) into Equation (6.11), and then integrating Equation (6.11) with respect to *z*-domain while incorporating the boundary condition provided in Equation (6.15b).

$$\sigma_{2f}(r,z) = \frac{\mathrm{e}^{-dz-\beta_f}}{2r\left(-1+\beta_f\right)}\begin{pmatrix} \mathrm{e}^{\beta_f}\left(2\mathrm{e}^{dz} q_0\, r\left(-1+\beta_f\right) + a\left(-1+\mathrm{e}^{dz}\right)\left[q_0 - \sigma_{1f}(z_0)\right]\right) \\ -\mathrm{e}^{\frac{r\beta_f}{a}}\left(-1+\mathrm{e}^{dz}\right)\beta_f\left(a + r\,\beta_f\right)\left[q_0 - \sigma_{1f}(z_0)\right] \end{pmatrix} \tag{6.18}$$

To this point, the equations for the final total vertical stresses in stone column and soft soil regions induced by the applied loading have been established, which will be used to develop the equations for the total vertical stresses in the composite ground at a point of time during the consolidation process, reported in the following section.

6.4 Coupled analysis for the consolidation and deformation of soft ground reinforced by stone columns

As stated earlier, even though the composite foundation is subjected to a constant loading, the induced total vertical stresses in the foundation change with depth, radius and time when incorporating the consolidation and deformation analyses. Indeed, the increase of the differential settlement between soft soil and stone column with time cause total vertical stress to transfer from the soft soil onto the stone column. Hence, the total vertical stress in stone column increases and that in surrounding soft soil decreases with consolidation time progressively. It is assumed that the initial total vertical stresses caused by the external loading distribute uniformly, i.e.

$$\sigma_1(z,t=0)=q_0 \tag{6.19a}$$

$$\sigma_2(r,z,t=0)=q_0 \tag{6.19b}$$

Moreover, it is supposed that the increase of total vertical stress in stone column and the decrease of that in soft soil have the same rate, which is considered as the load transferring rate of total vertical stress from soft soil to stone column. By accounting for the initial conditions of the total vertical stresses presented in Equations (6.19a) and (6.19b) and the final conditions of those expressed by Equations (6.16) and (6.18), the generalised equations capturing variations of the total vertical stresses in the stone column and the soil with depth, radius and time can be written as follows:

$$\sigma_1(z,t)=q_0+\left[\sigma_{1f}(z)-q_0\right]\left(1-e^{-ct}\right)^{0.5} \tag{6.20a}$$

$$\sigma_2(r,z,t)=q_0+\left[\sigma_{2f}(r,z)-q_0\right]\left(1-e^{-ct}\right)^{0.5} \tag{6.20b}$$

where c $(1/\mathrm{s})$ is the transferring rate of total vertical stress from soft soil to stone column. As discussed in the parametric study in Chapter 4, the consolidation of composite soft ground was mainly governed by column spacing (i.e. length of radial drainage path in soft soil), stiffness and permeability of stone column and surrounding soil. Therefore, by conducting a parametric investigation utilising finite element analysis for similar unit cell model in this chapter, the assuming equation to determine c would be adopted as follows:

$$c = \frac{270}{n_e^{5/2}}\left[0.03\left(\lg N_k\right)^{3/2} + 0.561\right]\left[0.75\left(\lg N_M\right) - 0.107\right]\frac{1}{t_f} \tag{6.21}$$

where $n_e = b/a$ is radius ratio of unit cell to column, $N_k = k_{1h}/k_{2h}$ is horizontal permeability ratio of column to soft soil, $N_M = M_1/M_2$ is constrained modulus ratio of column to soft soil. The parametric analysis to determine c in Equation (6.21) was conducted examining typical ranges $n_e = (1.5 - 5)$, $N_k = (10 - 10^6)$, and $N_M = (10 - 60)$, which can be encountered in practical designs of soft soil foundations reinforced by stone columns, sand columns and soil-cement mixing columns. The notation $t_f(\mathrm{s})$ denotes the ending time of consolidation in soft soil when solving the homogeneous form of the consolidation formulation, which would be determined from the following:

$$\bar{\bar{\Theta}}_2(t_f) = \delta q_0 \tag{6.22}$$

where $\bar{\bar{\Theta}}_2 = \bar{\bar{\Theta}}_2(t)$ is a function against time t and denotes the average excess pore water pressure in the soft soil region corresponding to the homogeneous consolidation formulation. The consolidation of soft soil terminates when $\bar{\bar{\Theta}}_2$ approaches zero. However, due to the nature of $\bar{\bar{\Theta}}_2$ as a positive function, the soil would be considered as reaching the end of consolidation when $\bar{\bar{\Theta}}_2$ achieves a minor positive value denoted by δq_0. The δ is the parameter controlling the required precision, which could be assigned

equal to $0.001 - 0.002$ for a typical value of loading q_0 in practice. For example, the value of $\bar{\bar{\Theta}}_2$ to determine t_f would be $0.1 - 0.2$ kPa corresponding to $q_0 = 100$ kPa. The derivation of $\bar{\bar{\Theta}}_2$ to obtain t_f is presented in Appendix E.

Once the total vertical stresses σ_1 (in the stone column) and σ_2 (in the soft soil) are achieved from Equations (6.20a) and (6.20b), respectively, the solution for the non-homogeneous consolidation formulation given by Equations (6.1) − (6.4) can be derived. Referring to the existing studies [188, 196, 211, 224], the solution of excess pore water pressure at an arbitrary point in the composite ground u_i can be attained as:

$$u_i(r,z,t) = u_i^{(i)}(r,z,t) + u_i^{(ii)}(r,z,t) \qquad \left(r_i \le r \le r_{i+1}\right) \quad (i = 1,2) \tag{6.23}$$

In which the subscript $i = 1,2$ denotes the column and soil regions, correspondingly; $r_1 = 0$, $r_2 = a$, $r_3 = b$; the terms $u_i^{(i)}$ and $u_i^{(ii)}$ can be obtained employing the following Green's formula:

$$\begin{aligned} u_i^{(*)}(r,z,t) = & \sum_{j=1}^{2} \int_{z'=0}^{H} \int_{r'=r_j}^{r_{j+1}} G_{ij}^{(*)}(r,z,t \mid r',z',t')\Big|_{t'=0} \sigma_j(r',z',0)\, r'\, dr'\, dz' \\ & + \sum_{j=1}^{2} \int_{t'=0}^{t} \int_{z'=0}^{H} \int_{r'=r_j}^{r_{j+1}} G_{ij}^{(*)}(r,z,t \mid r',z',t') \left[\frac{\partial \sigma_j(r',z',t')}{\partial t'}\right] r'\, dr'\, dz'\, dt' \qquad (j = 1,2) \end{aligned} \tag{6.24}$$

where the superscript $(*)$ is used to denote (i) or (ii) for concise presentation owing to their similar formulation; $G_{ij}^{(*)}$ denotes Green's function; the index j and integration variables r', z' and t' are dummy variables corresponding to the index i and physical variables r, z and t. The derivation of $u_i^{(*)}$ is provided in details in Appendix F.

Therefore, the consolidation settlement of the composite ground at any depth z and time t resulting from the dissipation of excess pore water pressures can be determined as:

$$S_1(z,t) = \frac{1}{M_1}\int_z^H \left[\sigma_1(z,t) - \overline{u}_1(z,t)\right] dz \tag{6.25a}$$

$$\overline{S}_2(z,t) = \frac{1}{M_2}\int_z^H \left[\overline{\sigma}_2(z,t) - \overline{u}_2(z,t)\right] dz \tag{6.25b}$$

where $S_1(z,t)$ denotes the column settlement and $\overline{S}_2(z,t)$ denotes the average settlement of soft soil along the radius; $\overline{\sigma}_2$ is the average total vertical stress in soft soil against radius, which is obatined by averaging σ_2 along r-domain (i.e. radius).

$$\overline{\sigma}_2(z,t) = q_0 + \left[\overline{\sigma}_{2f}(z) - q_0\right]\left(1 - e^{-ct}\right)^{0.5} \tag{6.26}$$

where $\overline{\sigma}_{2f}$ is the average of the final total vertical stress in soft soil along the radius and can be calculated by:

$$\overline{\sigma}_{2f}(z) = \frac{1}{\pi(b^2 - a^2)}\int_{r=a}^{b} 2\pi\,\sigma_{2f}(r,z)\,r\,dr \tag{6.27}$$

In Equations (6.25a) and (6.25b), $\overline{u}_1$ and $\overline{u}_2$ are the average excess pore water pressures along radii of stone column and soft soil, respectively, which would be determined as follows:

$$\overline{u}_1(z,t) = \frac{1}{\pi a^2}\int_{r=0}^{a} 2\pi\,u_1(r,z,t)\,r\,dr \tag{6.28a}$$

$$\overline{u}_2(z,t) = \frac{1}{\pi(b^2 - a^2)}\int_{r=a}^{b} 2\pi\,u_2(r,z,t)\,r\,dr \tag{6.28b}$$

The average degree of consolidation for stone column $\overline{U}_1$ and for soft soil $\overline{U}_2$ based on the surface settlement of the composite foundation can be written as:

$$\overline{U}_1(t) = \frac{S_1(z=0,t)}{S_1(z=0,\infty)} \tag{6.29a}$$

$$\bar{U}_2(t) = \frac{\bar{S}_2(z=0,t)}{\bar{S}_2(z=0,\infty)} \tag{6.29b}$$

where $S_1(z=0,\infty)$ is the surface settlement of stone column and $\bar{S}_2(z=0,\infty)$ is the average surface settlement of soft soil, corresponding to $t=\infty$ (i.e. the final settlements where the excess pore water pressures in the composite foundation would dissipate completely).

One of the practical requirements in this study is the average differential settlement ($\Delta\bar{S}$) between the soft soil and stone column, which is computed as the difference between the settlement values captured by Equations (6.25a) and (6.25b):

$$\Delta\bar{S}(z,t) = \bar{S}_2(z,t) - S_1(z,t) \tag{6.30}$$

The settlement pattern in soft soil at any time t, satisfying in line with Equation (6.5) adopted in this study would be given by:

$$S_2(r,z,t) = S_1(z,t) + \alpha_1(z,t)\left[\frac{r}{a} - e^{\beta_f\left(\frac{r}{a}-1\right)}\right] \qquad (a \le r \le b) \tag{6.31}$$

where $\alpha_1(z,t)$ denotes the settlement parameter against z-domain at time t.

Taking average of $S_2(r,z,t)$ along radius would lead to:

$$\bar{S}_2(z,t) = S_1(z,t) + \alpha_1(z,t)\,F_{\bar{S}_2} \tag{6.32}$$

where

$$F_{\bar{S}_2} = \frac{2}{b^2-a^2}\int_{r=a}^{b}\left[\frac{r}{a} - e^{\beta_f\left(\frac{r}{a}-1\right)}\right] r\,dr \tag{6.33}$$

Then, $\alpha_1(z,t)$ can be calculated by combining Equations (6.30) and (6.32):

$$\alpha_1(z,t) = \Delta\overline{S}(z,t) \Big/ F_{\overline{S}_2} \tag{6.34}$$

Once the settlement parameter $\alpha_1(z,t)$ is achieved, the soil settlement pattern during the process of consolidation is fully disclosed based on Equation (6.31). In connection to Equations (6.6) and (6.7), the shear strain $\gamma(r,z,t)$ and shear stress $\tau(r,z,t)$ in the soft soil at any time t can also be determined by replacing $\alpha_{1f}(z)$ with $\alpha_1(z,t)$ as:

$$\gamma(r,z,t) = \frac{\partial S_2(r,z,t)}{\partial r} = \frac{\alpha_1(z,t)}{a}\left[1 - \beta_f e^{\beta_f\left(\frac{r}{a}-1\right)}\right] \tag{6.35}$$

$$\tau(r,z,t) = G_2\,\gamma(r,z,t) = G_2\,\frac{\alpha_1(z,t)}{a}\left[1 - \beta_f e^{\beta_f\left(\frac{r}{a}-1\right)}\right] \tag{6.36}$$

Therefore, the consolidation and deformation of the composite ground can be analysed in a coupled fashion. The excess pore water pressure at any point in the composite ground can be computed using Equations (6.23) and (F.2). The settlements of stone column and soft soil at any depth and time can be achieved via Equations (6.25a) and (6.31), respectively; whereas the average differential settlement between soft soil and stone column will be obtained referring to Equations (6.30), (6.25a) and (6.25b). Besides, the average degrees of consolidation of stone column and soft soil can be calculated utilising Equations (6.29a) and (6.29b), respectively. Finally, Equations (6.35) and (6.36) can be employed correspondingly to examine the distribution of shear strains and shear stresses in soft soil during the consolidation process.

6.5 Worked example

This section provides an example for the coupled consolidation – deformation analysis of a stone column improved soft ground subjected to a constant loading $q_0 = 100\,kPa$, employing the simplified analytical solution proposed in this study. The geotechnical input data which can be experienced in real construction projects and adopted in this example is as follows:

- Geometric dimensions:

  $H = 10\,m$, $a = 0.5\,m$, $b = 1.25\,m$;

- Properties of stone column and soft soil:

  $k_{1h} = 4\times10^{-5}\,m/s$, $k_{1v} = k_{1h}$, $E_1 = 60\times10^3\,kPa$, $\nu_{P1} = 0.3$,

  $k_{2h} = 4\times10^{-10}\,m/s$, $k_{2v} = 0.5\,k_{2h}$, $E_2 = 1.5\times10^3\,kPa$, $\nu_{P2} = 0.3$;

where E_1 and ν_{P1} are Young's modulus and Poisson's ratio for stone column, respectively; analogously, E_2 and ν_{P2} are Young's modulus and Poisson's ratio for soft soil, respectively. Thus, the constrained modulus and shear modulus for the column and soil materials can be computed from these parameters.

The numerical results in this example would be demonstrated graphically in terms of the variations of total vertical stresses with depth and time, the dissipation of excess pore water pressures, the consolidation settlements and the distribution of shear stress in soft soil.

6.5.1 Total vertical stresses in stone column and soft soil

Referring to Equations (6.20a) and (6.26), the corresponding variations of the total vertical stresses in the column and soil regions against depth or time can be captured by varying the value of one variable while assigning a constant value to the remaining variable.

Figures 6.3a and 6.3b depict the change of the total vertical stresses in stone column and soft soil with respect to depth at various consolidation time, respectively. As observed, the stress values at depth $z = 0$ for any time during the consolidation were equal to the loading value $q_0 = 100$ kPa, which satisfy the stress boundary conditions on the ground surface. For a particular time, the total vertical stress in stone column increased and the corresponding value in soft soil decreased with the depth. Additionally, the stress in stone column rose and the stress in soft soil declined progressively due to the stress transfer phenomenon from the soil onto the column during the consolidation period. As a result, the ratio of average vertical stresses between stone column and soft soil increased with depth and time. The transfer of total vertical stress almost finished at time $t = 5 \times 10^6$ s where the stresses in stone column and soft soil along depth virtually reached the maximum and minimum, respectively. It can be seen that during the consolidation process, the total vertical stress variations with depth were significant at the upper part of the composite ground. The depth where the total vertical stresses in stone column and soft soil almost approached extreme values moved downwards with elapsed time. For example, the stresses nearly reached the extreme values at depths $z = 0.4H$ and $0.6H$ corresponding to time $t = 4 \times 10^4$ s and 5×10^6 s in which the total vertical stress distributions in stone column and soft soil below these depths were rather uniform (i.e. minor change with depth). This indicates a downward movement of the assuming equal

strain plane (i.e. the plane over the composite ground area where there is negligible differential settlement between soft soil and stone column). Furthermore, considering the stresses in stone column and soft soil regions below the depth $z = 0.6H$ at time $t = \infty$, where the deformation of the composite ground is a fully drained compression (i.e. the final deformation), the stress values in both regions complied with the assuming equal strain condition given by Equation (6.12).

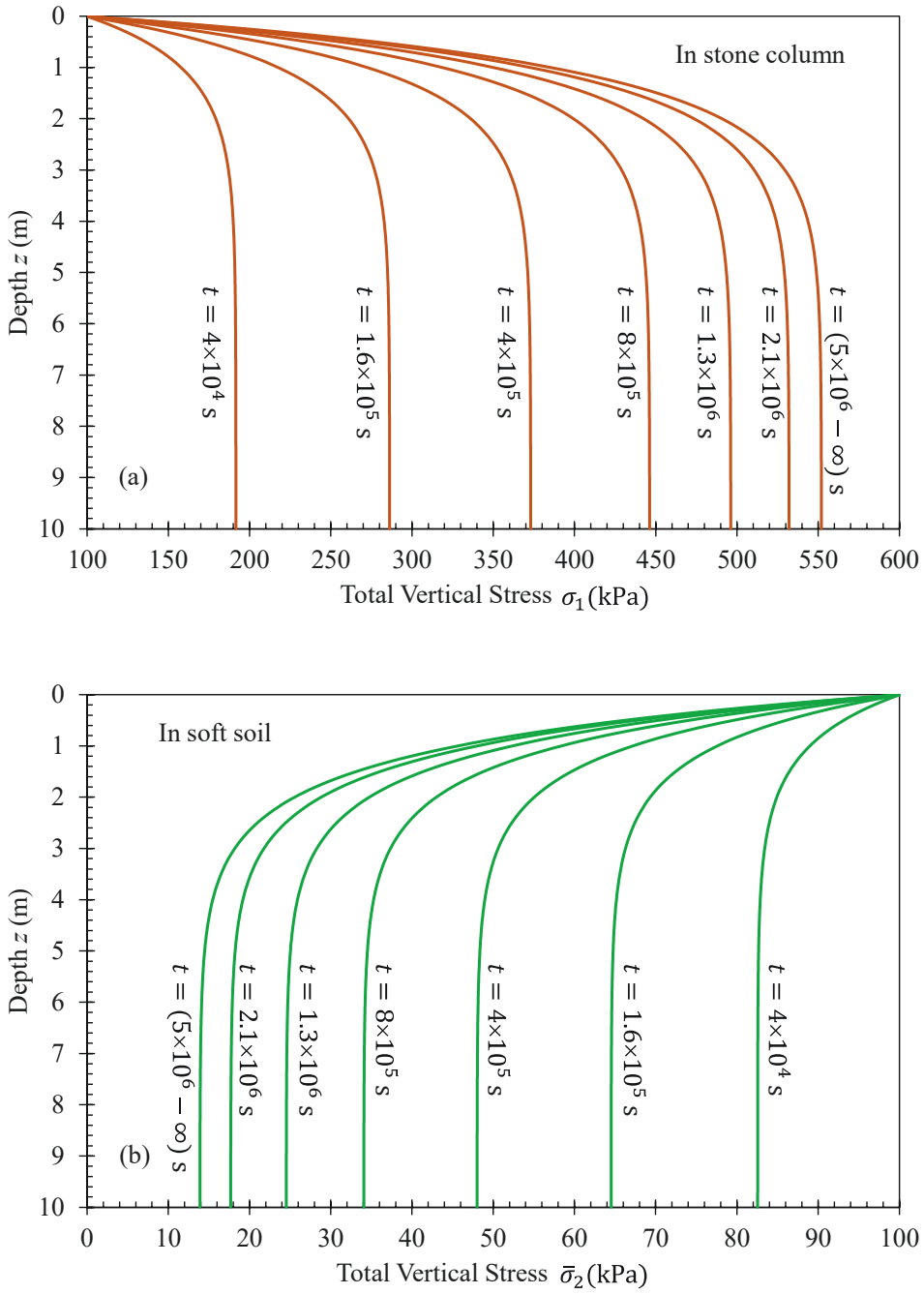

Figure 6.3. Distribution of total vertical stresses in (a) stone column and (b) soft soil against depth varying with time

Figure 6.4 presents the change of the total vertical stresses in the column and soil regions with time for varying depths $z = 0.25H, 0.5H$ and $0.75H$. For a specified depth,

the stress in soft soil reduced as time elapsed and vice versa for that in stone column as a result of the stress transfer between soil and column, corresponding to the development of the differential settlement between soft soil and stone column during the consolidation. The larger the depth of point of interest, the more stress transfer from the soil onto the column. This is due to the accumulation of stress transferred along the column – soil interface (refer to Figures 6.3a and 6.3b). The transfer of total vertical stress from soft soil to stone column progressed quickly during the early stages of consolidation, followed by gradual decrease in the stress transfer rate with time. The stresses in the column and soil areas at the investigation depths were almost unchanged after $t = 5 \times 10^6$ s, which indicates the stress transfer from the soft soil to the stone column via their vertical contact surface was almost complete.

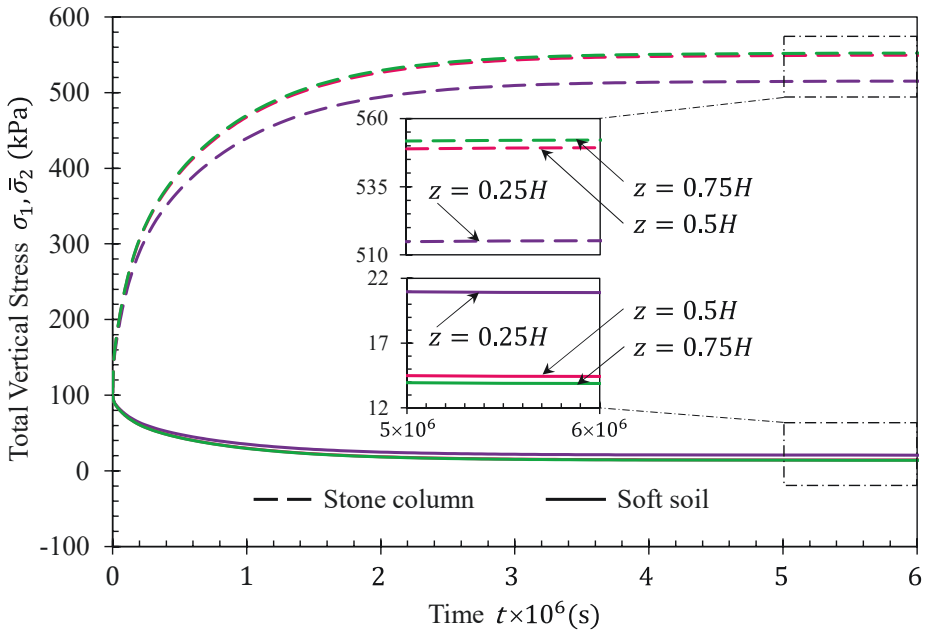

Figure 6.4. Variation of total vertical stresses in stone column and soft soil against time at different depths

6.5.2 Excess pore water pressure dissipations in stone column and soft soil

Employing Equations (6.23) and (F.2), the change of excess pore water pressures against each single variable r, z or t can be obtained by keeping the remaining variables unchanged.

Figures 6.5a and 6.5b illustrate the variation of excess pore water pressures against depth in stone column and soft soil at radii $r = 0.5a$ and $r = 0.5(a + b)$, respectively. The excess pore water pressures generated by the instantaneous loading underwent the dissipation and redistribution process to establish equilibrium state at which the excess pore pressure values at depth $z = 0$ would be reduced to zero immediately after applying the external loading, fulfilling the free drainage boundary condition on the composite ground surface as expressed by Equation (6.3a). However, the excess pore water pressure right below the soft soil surface dissipated slowly due to the low permeability of the soil. It is important to note that the excess pore water pressure values in the foundation are dependent on the variation rates of total vertical stresses during the process of total vertical stress transferring from the soil onto the column and the dissipation rates of excess pore water pressures. Despite the growth of the total vertical stress in the stone column with consolidation time owing to the stress transfer from soft soil to stone column as a result of the larger soil settlement than column settlement, the excess pore pressure along the column depth dissipated rapidly in which the value of excess pore water pressure at the lower part of stone column ($z \geq 0.5H$) was approximate 2 kPa at time $t = 4 \times 10^4$ s (Figure 6.5a). The reason is attributable to the extremely rapid dissipation rate in comparison to the increase rate of total vertical stress in stone column, while the radial flow rate from the surrounding soil into the stone column was much slower than the upward flow out of the column from the top surface. Figure 6.5b shows the

distribution pattern of excess pore water pressure along the soil depth varying with time, impacted by the decline of total vertical stress in soft soil due to the stress transfer from the soil to the column. The excess pore water pressure dissipation in the soft soil progressed much slower than the stone column counterpart even though a large amount of excess pore water pressure in the soil was dissipated due to the total vertical stress reduction (i.e. total stress transfer from soft soil to stone column as the soil settles more than the column) . While the dissipation of excess pore pressure in stone column depends primarily on the discharge flow rate exiting from the column top, that in soft soil is mostly contingent on the radial flow rate in the soil towards the column region. Therefore, the excess pore pressure distribution in Figure 6.5b had similar shapes to the pattern of changes in total vertical stress reported in Figure 6.3b, except for the very top part of the soil region where the soil experienced dominant vertical flow contributing to the dissipation of excess pore water pressure. The combined radial – vertical flows at the top part of soft soil in which the radial permeability is twice of the vertical permeability, as adopted in this example, led to a slight downward shift in the location of the peak excess pore pressure point. As can be seen from Figure 6.5b, there was still a portion of excess pore pressure to be dissipated at the upper part of soft soil at time $t = 5 \times 10^6$ s while the total vertical stress transfer from soft soil to stone column was almost completed (i.e. almost insignificant decrease in the total vertical stress in soft soil as referring to Figures 6.3b and 6.4). Thus, the dissipation of the mentioned excess pore water pressure portion at the upper soil region would result in additional soil settlement and differential settlement.

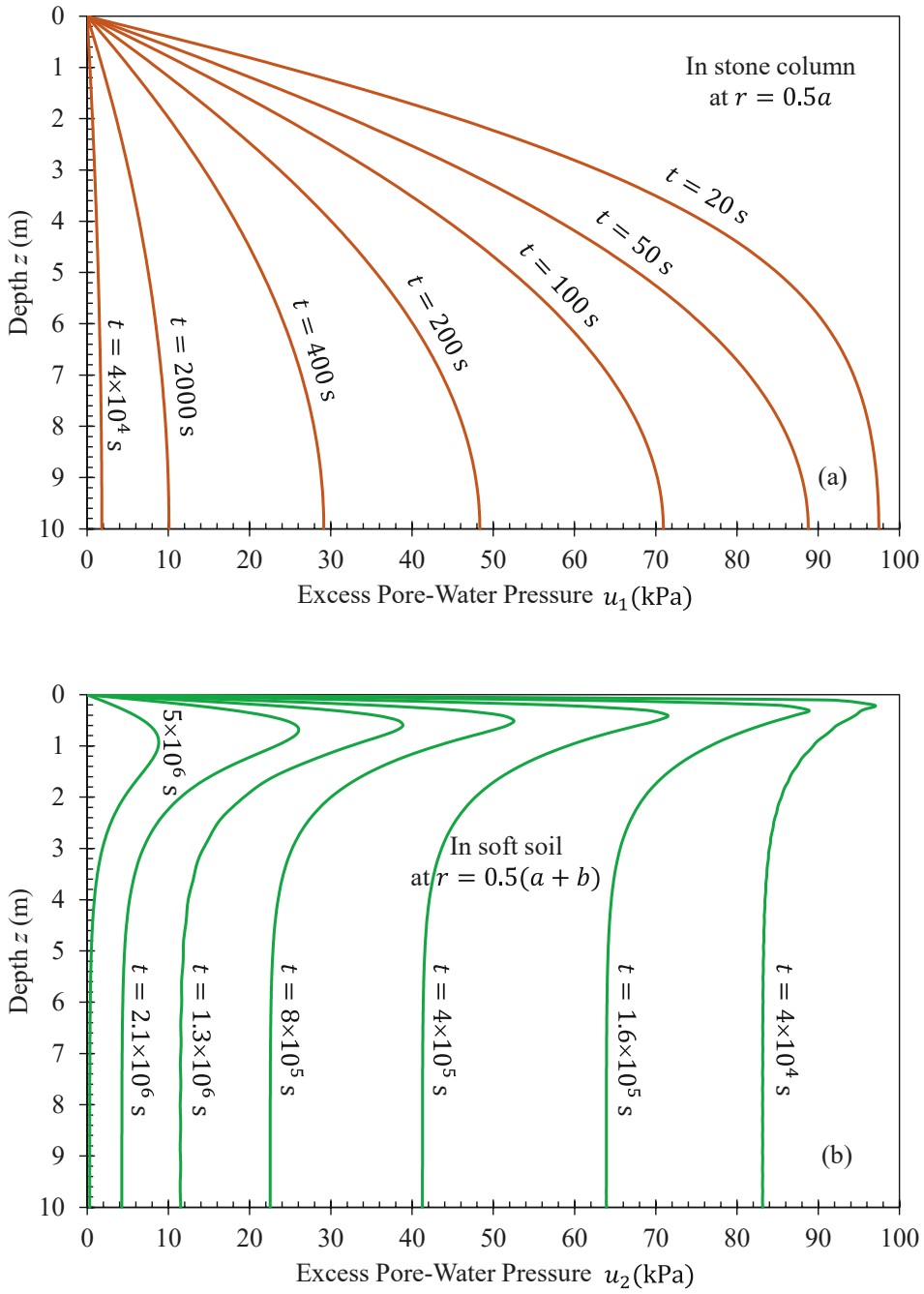

Figure 6.5. Excess pore water pressure isochrones against depth at radii (a) $r = 0.5a$ in stone column and (b) $r = 0.5(a + b)$ in soft soil

Figure 6.6 displays the excess pore water pressure dissipation against time for different investigation points in the column and soil regions. As expected, the deeper the point of

investigation in stone column, the longer drainage path towards the column top boundary, and thus slower the corresponding excess pore water pressure dissipation. However, the dissipation rates at points of interest in soft soil, particularly at depths $z = 0.5H$ and $0.75H$ were almost the same due to the dominant radial flow rate in soft soil. Moreover, the lower part of soft soil experienced more reduction in total vertical stress than the upper soil region during the consolidation (allude to Figure 6.3b); thereby, the excess pore water pressure dissipation for the points of interest at depths $z = 0.5H$ and $0.75H$ progressed faster than that for the point at depth $z = 0.25H$ (see Figure 6.6 in conjunction with Figure 6.5b).

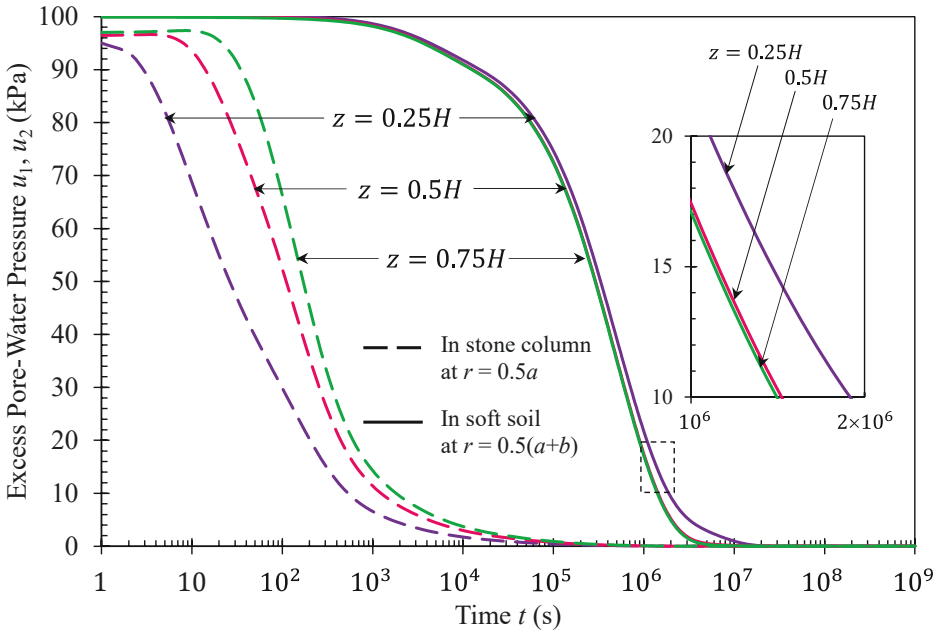

Figure 6.6. Dissipation rates of excess pore water pressure at various investigation points in stone column and soft soil

6.5.3 Consolidation settlements in stone column and soft soil

It is recognised that while excess pore pressure is present in the saturated composite stone column – soft ground, water squeezes out of the column and soil bodies, leading to the volumetric strain of the composite ground and thus the development of the column and soil settlements. Based on Equations (6.25a) and (6.31), the settlements along radius of the composite ground at any depth and time during the consolidation process can be predicted.

Figure 6.7 represents the time-dependent column and soil surface settlements (i.e. corresponding to $z = 0$). The results show that the surface settlements of the column and soil regions along with the predicted differential settlement increased progressively. At a specified time, the column settlement remained uniform over the column area as expected, whereas the soil settlement increased with radius away from the column – soil interface gradually and reached a maximum at the outer radial boundary of the unit cell. Although the excess pore water pressure dissipation in the column progressed extremely rapidly and the predicted excess pore water pressure along the column depth was less than 2 kPa at time $t = 4 \times 10^4$ s (allude to Figure 6.5a), the surface settlement of stone column still developed further and virtually achieved the maximum at time $t = 4 \times 10^6$ s. The reason is attributed to the continuing increase of total vertical stress in the column as a result of the stress transfer from the surrounding soil after time $t = 4 \times 10^4$ s. Unlike the stone column, the surface settlement of soft soil developed until time $t = 2 \times 10^7$ s; and afterwards the soft soil experienced no more settlement which indicates the termination of consolidation process in the composite ground. Although the soil settlement after time $t = 4 \times 10^6$ s still progressed until the end of consolidation, the subsequent differential settlement was not sufficient to induce additional total vertical

stress transfer from soft soil to stone column to induce further settlement in the stone column (i.e. the stress transfer process was almost completed). The soft soil settlement rate after time $t = 4 \times 10^6$ s (i.e. corresponding to the time that stress transfer from soil to column was almost completed) was mainly governed by the dissipation rate of excess pore water pressure in soft soil itself with negligible residual effects from the total vertical stress variations as a result of stress transfer.

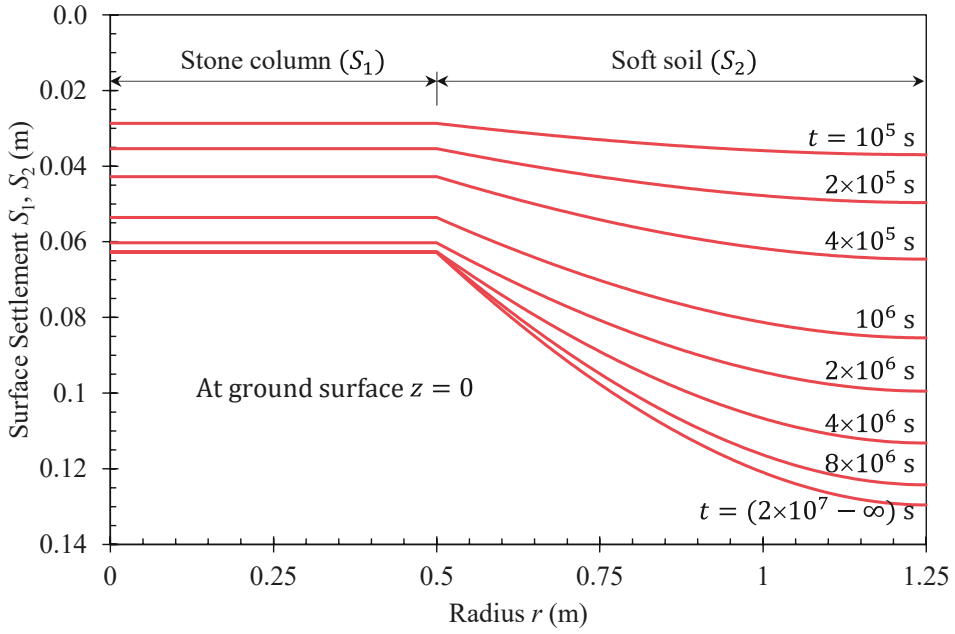

Figure 6.7. Surface settlement isochrones for stone column and soft soil against radius

Figure 6.8 demonstrates the column and soil settlements against radius for various investigation depths at time $t = 10^6$ s. Analogous to the ground surface settlement, the settlements at examination depths between the surface and base of the composite ground stratum included uniform settlements over the column area and unequal settlements over the surrounding soil area. Obviously, settlement at the composite ground bottom ($z = H$) was zero due to consideration of a rigid base in this study (refer to Figure 6.2). The

composite ground settlement, differential settlement between soft soil and stone column as well as in the soft soil itself diminished with depth. Particularly, the differential settlements at the upper part of the composite ground decreased substantially as the investigation depth increased from $z = 0$ to $z = 0.1H$; this observation is a result of the dramatic diminution of the effective vertical stress (i.e. the difference between total vertical stress (Figure 6.3b) and excess pore water pressure (Figure 6.5b)) in soft soil from the soil surface to depth $z = 0.1H$. The effective vertical stresses right close to the soft soil surface were extremely large due to the dominant dissipation of excess pore water pressure along both vertical and radial drainage paths, while those at the lower part of soft soil were much smaller owing to the primary contribution of radial drainage path to the excess pore water pressure dissipation. Below the depth $z = 0.1H$ and towards the rigid base, the effective vertical stress in soft soil declined gradually and hence the differential settlements reduced steadily. On the other hand, the settlements of the composite ground at depths $z \geq 0.4H$ were almost uniform, directing to the points that equal strain plane was located at $z = 0.4H - 0.6H$, which is similar to the observation made in Figures 6.3a and 6.3b.

It is emphasised that the settlements of composite stone column – soft ground in this chapter were obtained on the basis of assuming deformation mode which was demonstrated to reasonably simulate the column and soil settlements in practice as reported by Alamgir et al. [65]. Therefore, the proposed settlement pattern can address the shortcoming of proposed analytical models in Chapters 3 – 5 where the inherent column – soil interaction reflecting practical condition is neglected.

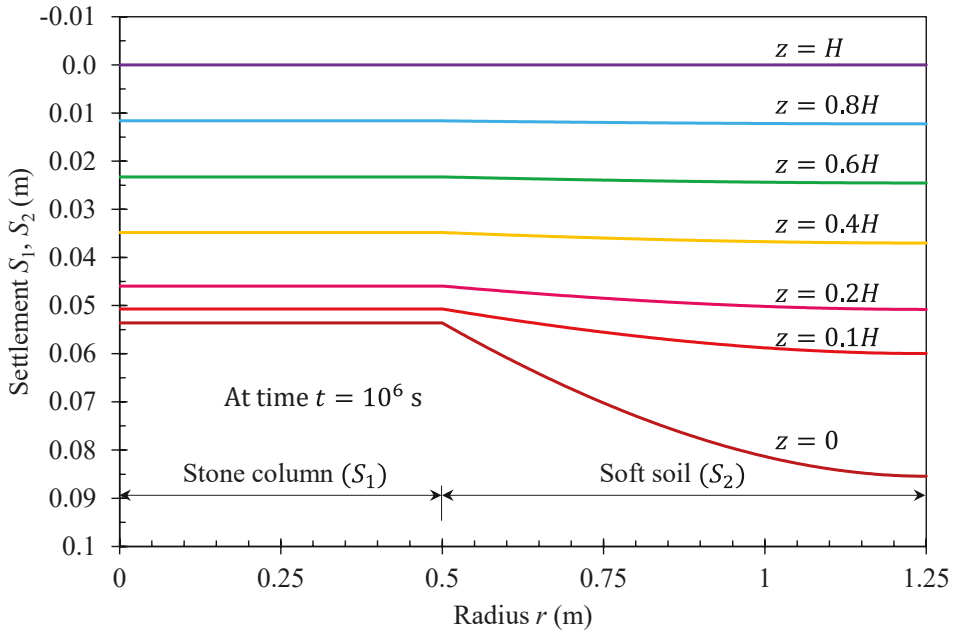

Figure 6.8. Settlements of stone column and soft soil against radius at time $t = 10^6 s$ for different investigation depths

6.5.4 Distribution of shear stresses in soft soil

When considering the consolidation and deformation in a coupled manner under free strain condition in the present study, the shear stresses would be mobilised in soft soil owing to the development of the differential settlements in the composite ground. Referring to Equation (6.36), the variation of the shear stresses in soft soil with radius, depth and time can be obtained readily.

Figure 6.9 shows the shear stress isochrones in soft soil at depth $z = 0.1H$. It is observed that the shear stresses along the radius of soft soil region increased with time as a consequence of the progressive increase in differential settlements. As expected, the induced shear stresses were equal to zero at the outer radial boundary of the unit cell ($r = b$), and then the shear stress increased cumulatively towards the column and achieved the

peak value at the column – soil contact surface. It should be noted that the shear stresses along the soft soil radius varied linearly with the corresponding shear strain (see Equation (6.36)), whereas the shear strains were mathematically derived as the partial derivative of settlement with respect to radius (see Equation (6.35)). Therefore, the development of the shear stresses in soft soil towards the column – soil interface could be explained by the corresponding increases in slope of soft soil settlement curve at the investigation depth $z = 0.1H$.

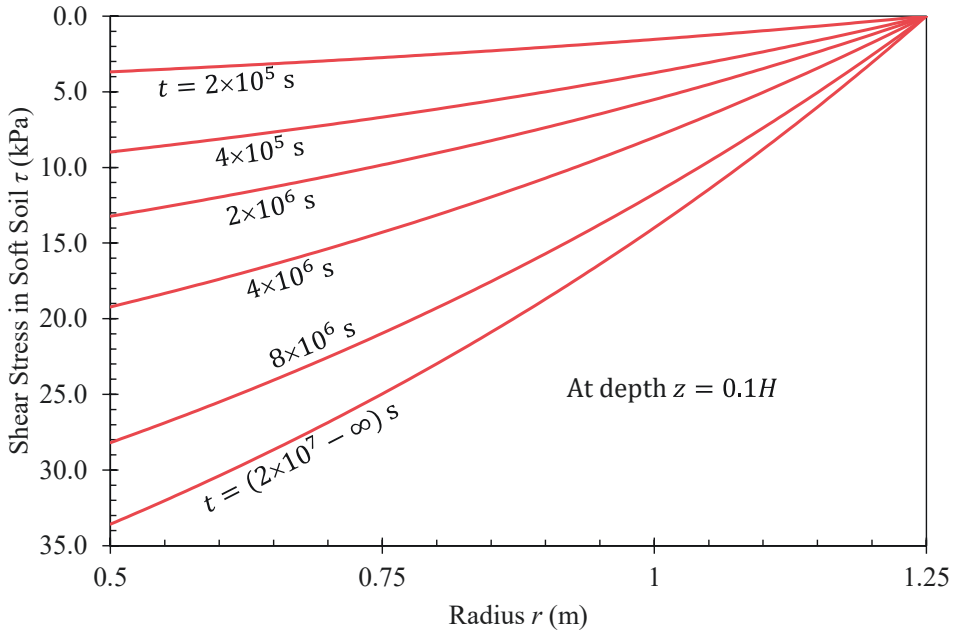

Figure 6.9. Isochrones of the shear stress in soft soil against radius at depth $z = 0.1H$

Figure 6.10 plots the shear stress variation against the soft soil radius at time $t = 10^6$ s for various examination depths. As predicted, the shear stress along soft soil radius reduced with depth due to the corresponding decline of differential settlements towards the composite ground base (pertain to Figure 6.8). The upper composite ground experienced a considerable reduction in shear stresses from the vicinity of ground surface

to about depth $z = 0.1H$ with a substantial diminution in differential settlements. Beneath the depth $z = 0.1H$, the induced shear stresses in soft soil diminished gradually with depth thanks to the corresponding steady decrease in differential settlements. At depth $z = 0.6H$, the maximum shear stress was very minor (i.e. less than 2 kPa) as a result of the insignificant differential settlements. Moreover, similar to the isochrones of shear stresses (Figure 6.9), the shear stresses in soft soil at each examination depth as reported in Figure 6.10 also increased towards the column cumulatively.

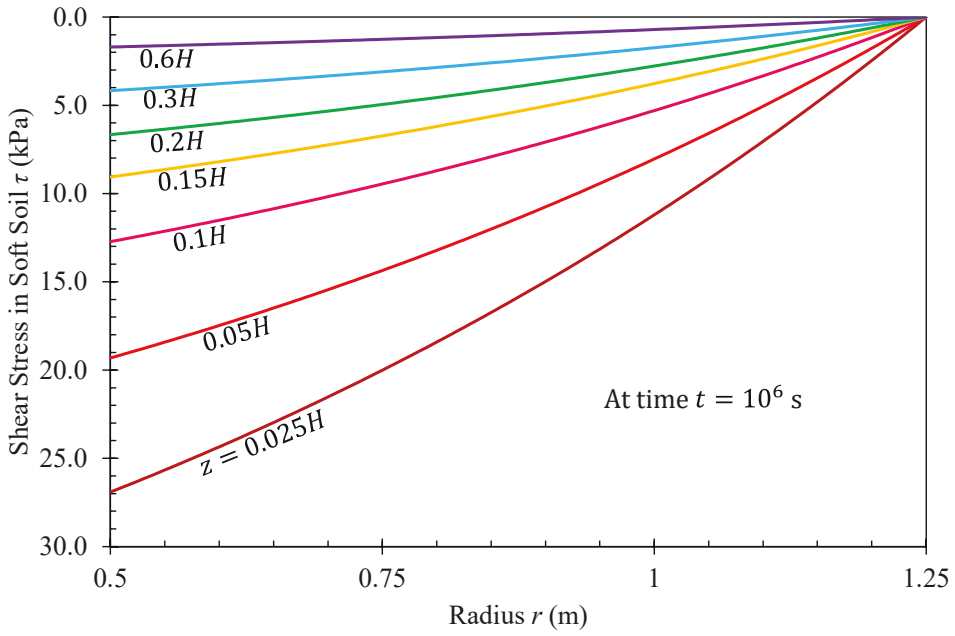

Figure 6.10. Variation of the shear stress in soft soil against radius at time $t = 10^6 s$ for different investigation depths

Figure 6.11 represents the shear stress isochrones at radius $r = 0.5(a + b)$ in soft soil. At any time, the predicted shear stress was maximum at the ground surface corresponding to the point with the largest differential settlement; then the value of shear stresses reduced with depth and reached zero at the rigid ground base. It is observed that the upper

soil region (i.e. $z \leq 0.1H$) underwent a substantial growth of shear stresses with time, which signifies a consecutive development of differential settlements in this region over the consolidation period. However, for the lower soil region (i.e. $z > 0.1H$), the shear stress at the examination radius rose progressively until time $t = 8 \times 10^5$ s; after which the shear stress decreased till time $t = 2 \times 10^6$ s before increasing again significantly during the remaining period of consolidation. During the early stages of consolidation ($t \leq 8 \times 10^5$ s), the shear stresses were present in almost entire soil stratum (i.e. up to depth $z = 0.9H$), which implies the spread of differential settlement from the ground surface towards the base. In contrast, during the later stages of consolidation ($t \geq 2 \times 10^6$ s), the changes in shear stresses were present mainly at the upper half of soil stratum ($z \leq 0.5H$), which indicates the corresponding extent of differential settlement field.

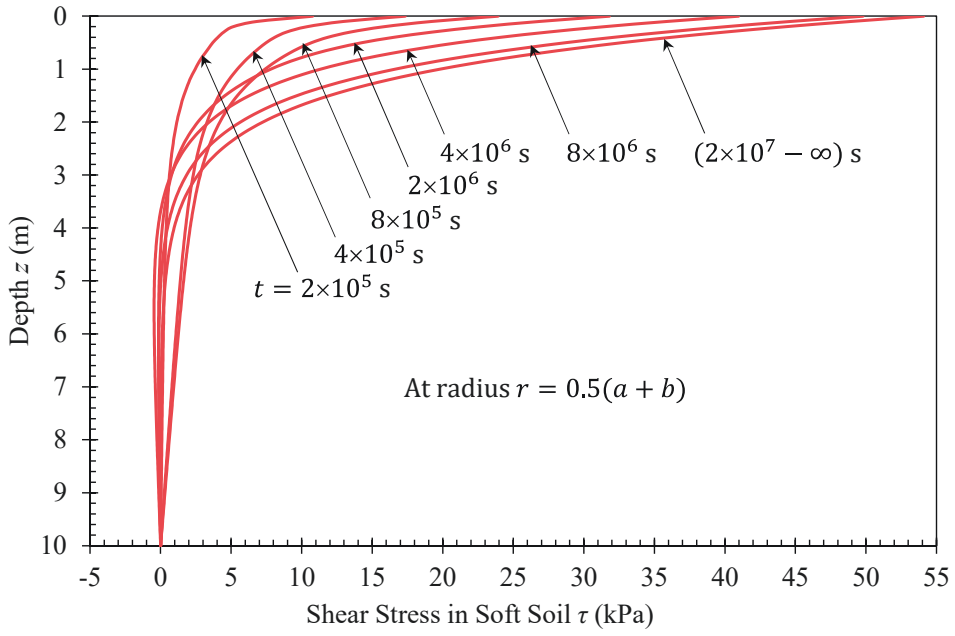

Figure 6.11. Isochrones of the shear stress in soft soil against depth at radius $r = 0.5(a+b)$

Figure 6.12 displays the shear stress variation with depth at time $t = 2 \times 10^6$ s for various examination radii in soft soil. As observed and similar to the shear stresses plotted in Figure 6.11, the shear stress values reported in Figure 6.12 was highest at the top soil surface and reduced with soil depth dramatically. Irrespective of the radius of the investigation point, the shear stress at the lower soil region ($z \geq 0.4H$) almost vanished, which shows that the response of this soil region is virtually identical to the equal strain deformation condition. Indeed, the upper soil region experienced significant changes of shear stresses with radius (particularly for the very top soil layer) in which the column – soil interface (i. e. $r = a$) experienced the largest shear stress values and the shear stress decreased with the increase of investigation radius gradually.

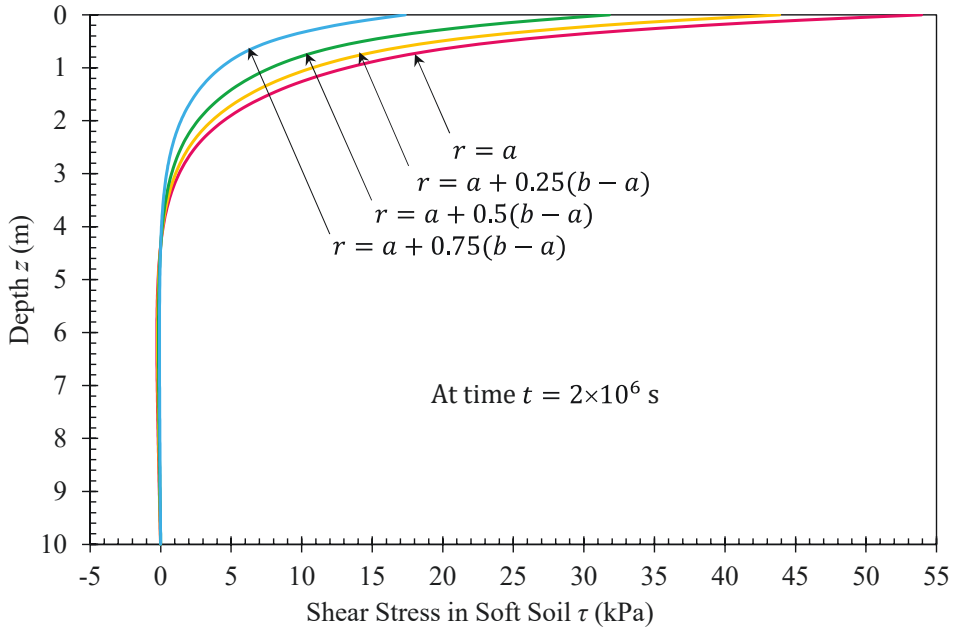

Figure 6.12. Variation of the shear stress in soft soil against depth at time $t = 2 \times 10^6 s$ for different investigation radii

6.6 Verification against finite element modelling

To verify the accuracy of the proposed analytical solution in the present study, a comparison between the predictions obtained from the proposed solution and a finite element simulation was conducted. The column and soil properties and geometries in the finite element model were assigned to be the same as those in the analytical model as adopted in the worked example. Considering the axisymmetry of the applied uniform loading and geometry of the model against the centerline of the unit cell, the numerical model was simulated using the axisymmetry configuration feature and 15-node triangular elements available in PLAXIS 2D [212] shown as in Figure 6.13. The centerline, the exterior vertical surface and the base of the finite element model were set as roller boundaries to ensure no friction along these boundaries and no normal displacements were allowed along those boundaries, whereas the top ground surface was modelled as a free boundary. To reflect the one-dimensional deformation along vertical direction as adopted in the analytical model, solely vertical displacement without slip at the column – soil interface was enabled while the radial displacement was not permitted. Regarding the water flow boundary conditions, the centerline, the outer vertical boundary and the bottom of the numerical model did not allow any pore water flows across the boundaries, meanwhile the top surface of the model held a free drainage condition. Moreover, the column – soil interface was considered as a permeable interface allowing the continuity of excess pore water pressure and radial flow between the column and soil regions as expected. Finally, the loading was applied instantly and kept unchanged during the numerical analysis, which is the same as the analytical formulation in this study.

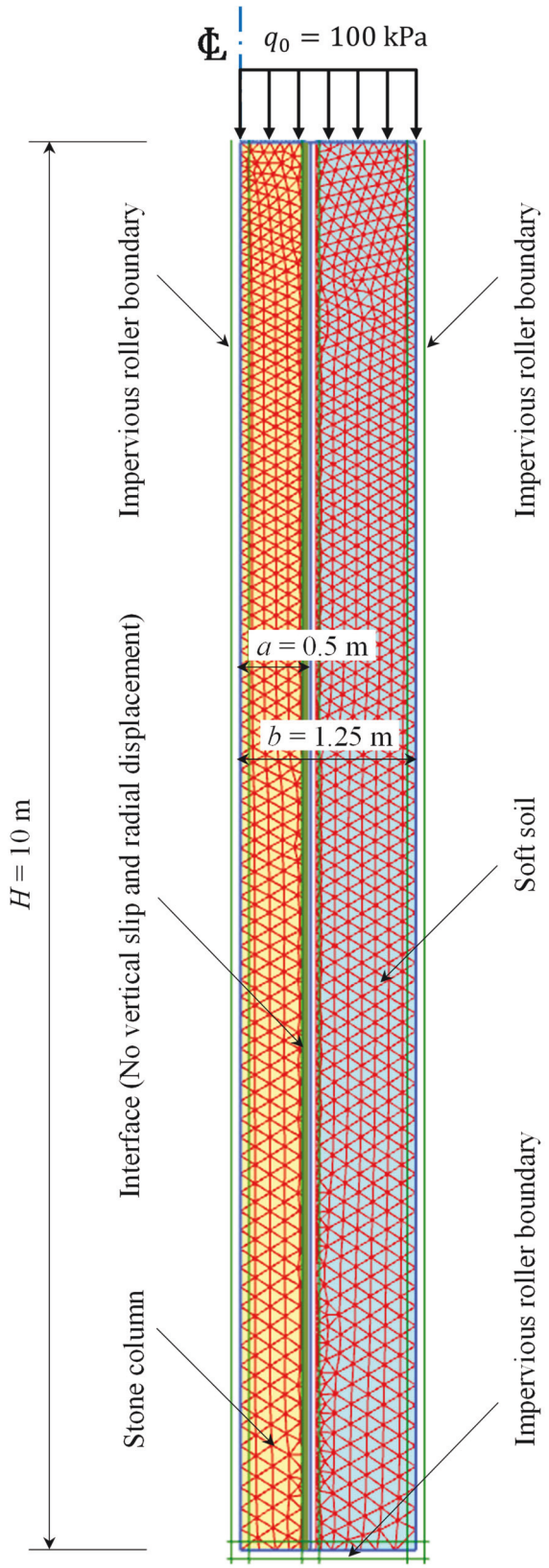

Figure 6.13. Finite element model for the verification exercise

Figure 6.14 plots the final total vertical stress distributions against depth in stone column and soft soil. As observed, the predicted variations of final total vertical stresses (i.e. the total vertical stresses at the end of consolidation) with depth attained from the analytical and numerical simulations agreed well. Due to the stress transfer from soft soil onto stone column through their vertical contact surface, the final total vertical stress in the column increased and that in the soil decreased with depth. Figure 6.15 compares the total vertical stress variations against elapsed time at depth $z = 0.5H$ between the proposed analytical solution and finite element predictions. It is evident that the predictions obtained from the analytical and numerical models are in good agreement. Therefore, the adopted exponential functions for distribution of total vertical stresses in the analytical solution as presented in Equations (6.20a) and (6.20b) are deemed reasonable.

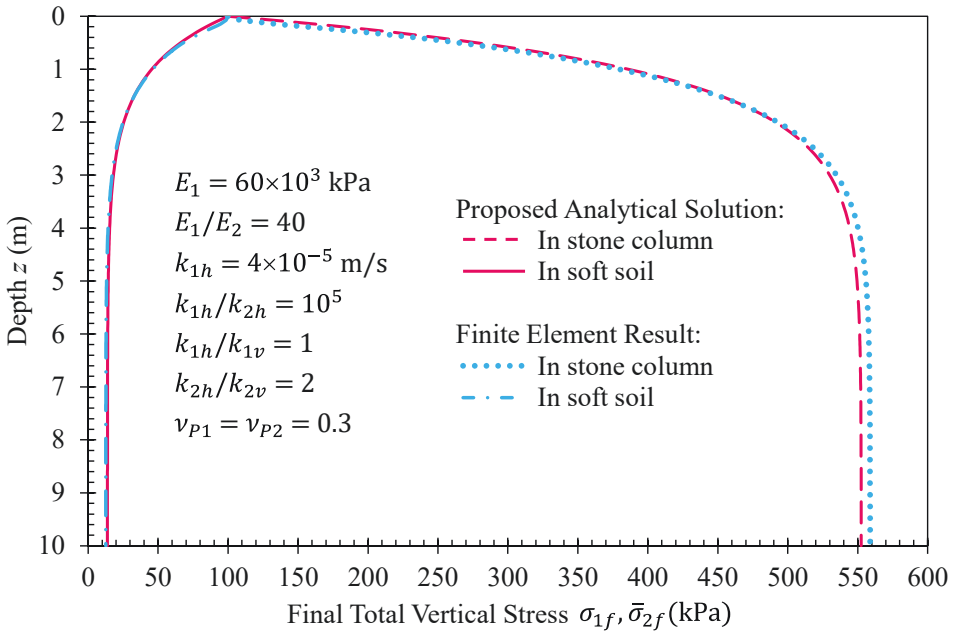

Figure 6.14. Verification on the distribution of final total vertical stresses in stone column and soft soil against depth between proposed analytical solution and finite element result

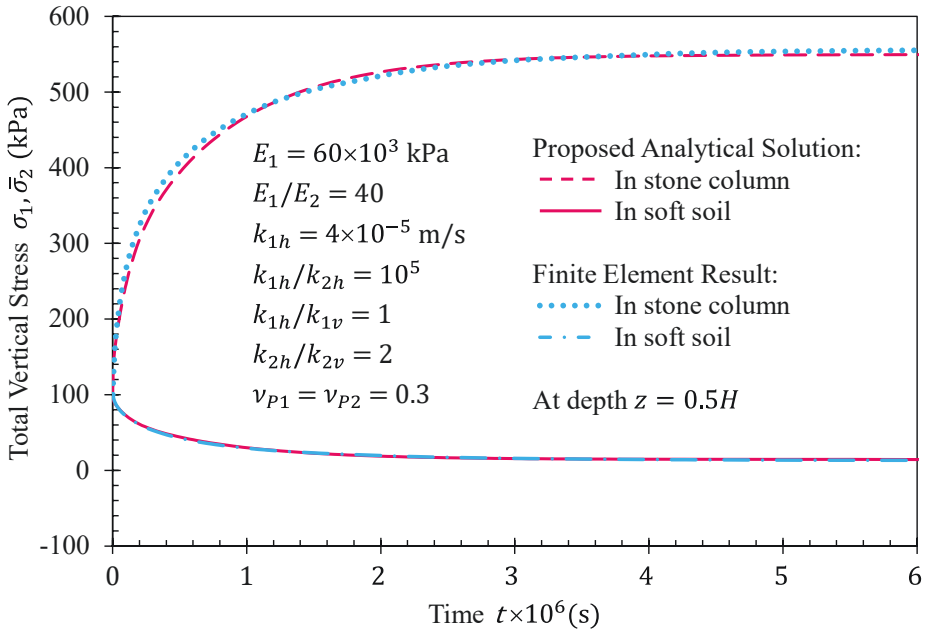

Figure 6.15. Verification on the change of total vertical stresses in stone column and soft soil against time at depth $z = 0.5H$ between proposed analytical solution and finite element result

Figures 6.16a-c present the variations of excess pore water pressure with time at various points in stone column and soft soil. It is evident that the dissipation rates of excess pore water pressure at the examination points obtained from the obtained analytical equations (i.e. Equations (6.23) and (F.2)) were in a reasonable agreement with the finite element predictions. Referring to Fig 16, the excess pore water pressure values at points of interest in stone column ($r = 0.5a; z = 0.25H, 0.5H$ and $0.75H$) right after applying the external loading ($t = 1$ s) captured by the proposed analytical solution were slightly less than corresponding values obtained from the numerical modelling, which led to overestimated dissipation rates afterwards. The observed disparities were due to the selection of a finite number of terms in the obtained double series solution in the analytical

calculation as evident in Equation (F.2). Indeed, the accuracy of the proposed analytical solution in estimating the excess pore water pressure dissipation in stone column can be enhanced by increasing the number of terms from the series solution. Referring to Figures 6.16a-c, there are slight discrepancies between the analytical and numerical predictions of the excess pore water pressure dissipation rates in soft soil. The observed differences can be due to the simplifying assumption of undrained condition immediately after applying the surcharge loading adopted in the analytical solution.

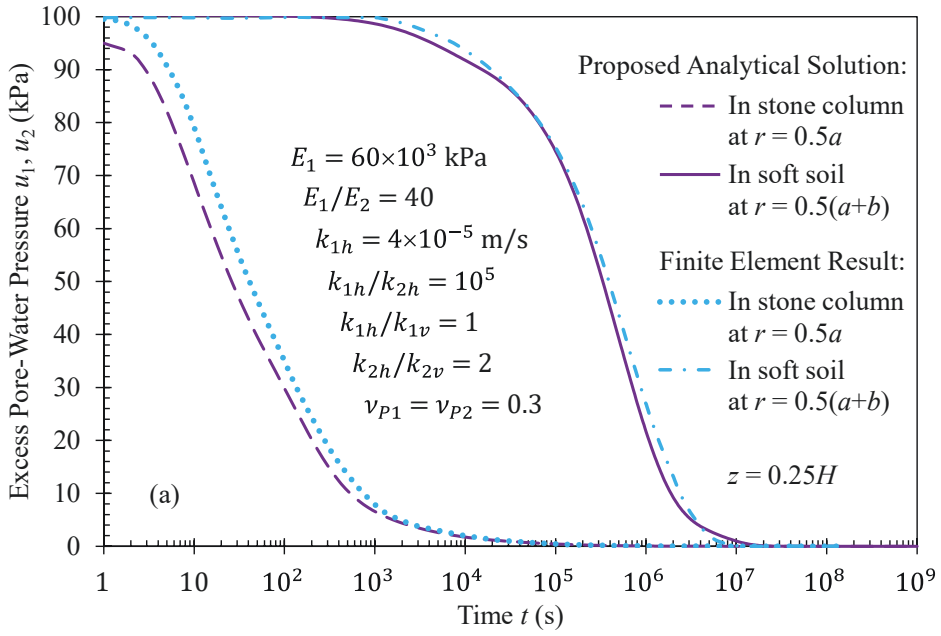

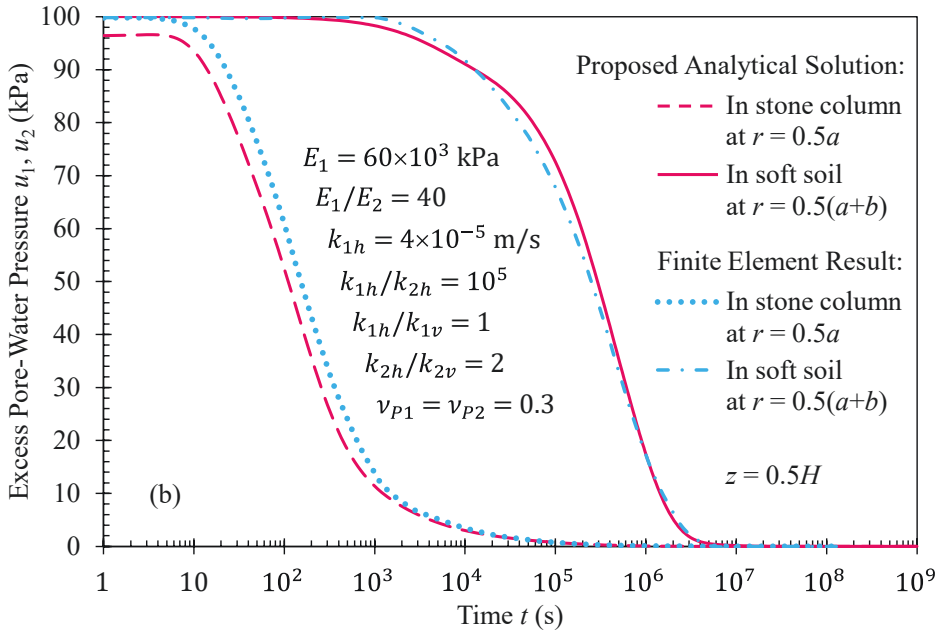

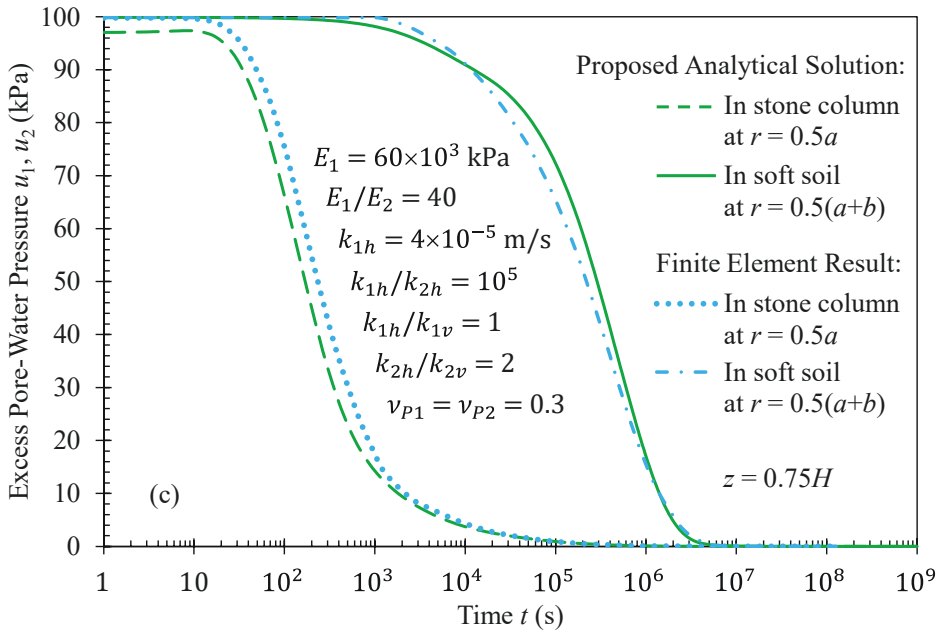

Figure 6.16. Verification on the dissipation rate of excess pore water pressures at various points in stone column and soft soil with depths (a) $z = 0.25H$, (b) $z = 0.5H$, and (c) $z = 0.75H$ between proposed analytical solution and finite element result

Figure 6.17 shows a reasonable agreement between the predicted average degrees of consolidation for stone column and for soft soil via the proposed analytical solution and the finite element modelling. Right after applying loading, the excess pore water pressure dissipation and the consolidation of stone column proceeded very quickly due to the large discharge capacity of stone column, whereas the consolidation of soft soil was negligible and the behaviour of soft soil was almost undrained. After about 100 s of loading, the consolidation of soil region began occurring as the excess pore water pressure in soft soil dissipated towards stone column typically. During the period from about 100 s to approximately 1000 s after applying the load, the radial flow of pore water sped up the consolidation of soft soil and slowed down the consolidation of stone column, which resulted in a concave curve during this consolidation stage of stone column. Thereafter, the consolidation of stone column depends completely on the consolidation of soft soil in which the larger consolidation settlement of soil compared to stone column induced the transfer of total vertical stress from soil region onto column region and accompanying consolidation of stone column. The difference induced between the predictions, particularly at the later stages of consolidation, is attributed to the simplifying approximation of the total vertical stress distribution in soft soil as a uniform distribution against radius (referring to Equations (F.3) and (6.27)) to obtain the explicit analytical solution for the sake of convenience in practical applications. By contrast, the numerical modelling captured the precise integration of the variation of total vertical stresses against radius during the consolidation.

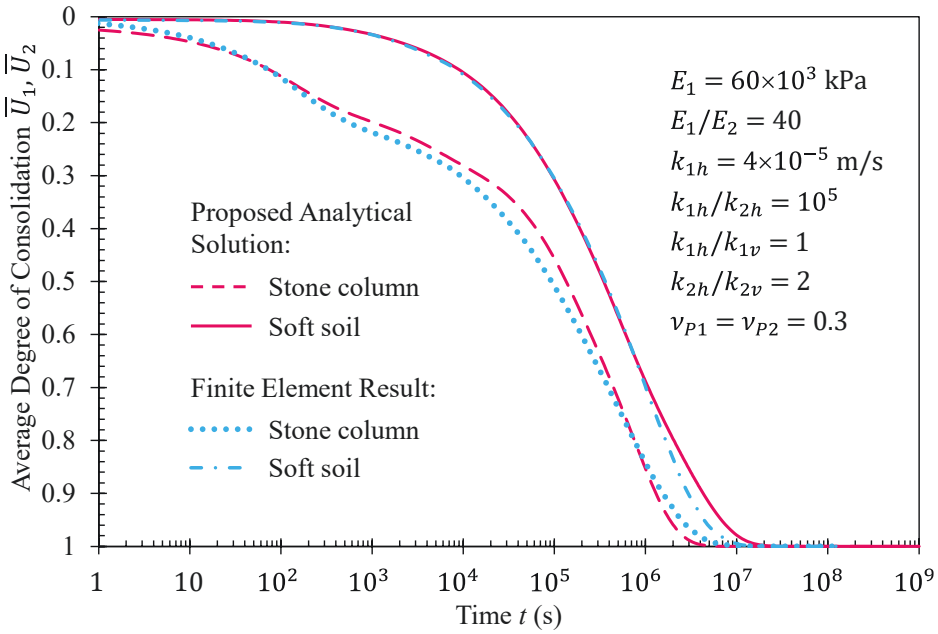

Figure 6.17. Verification on the average degree of consolidation of stone column and of soft soil between proposed analytical solution and finite element result

Figure 6.18 displays the predicted surface settlements of stone column and soft soil varying with consolidation time. It is observed that the proposed analytical solution could estimate the surface settlements pretty well when compared with the finite element results, with some discrepancies observed in the soil region. The observed differences between the two models in predicting the soil surface settlement can be due to the fact that a stringent integration of deformation compatibility was adopted in the finite element model, whereas the analytical model assumed a simplified deformation pattern for soft soil via the function given in Equation (6.31).

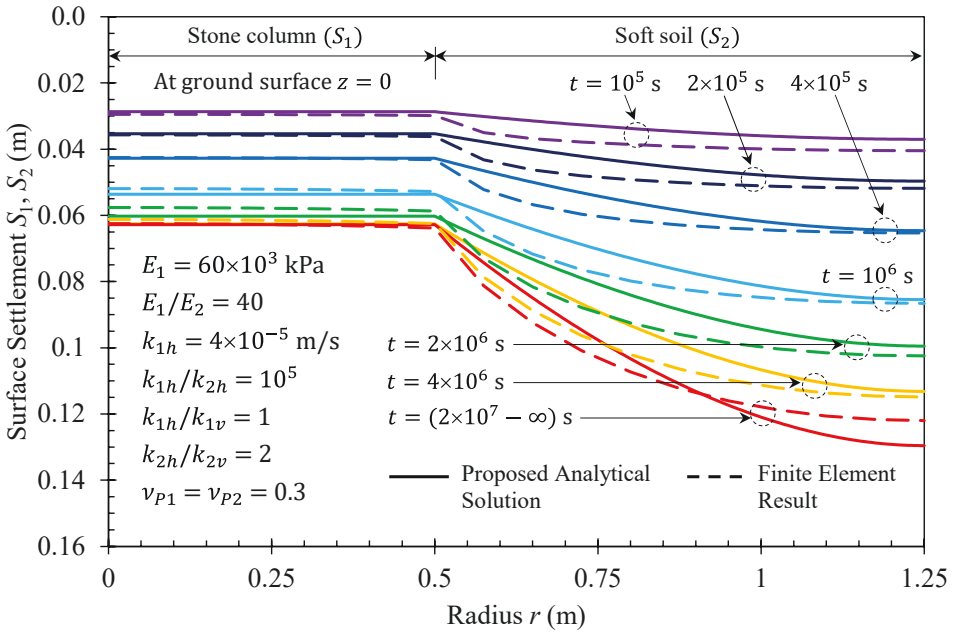

Figure 6.18. Verification on the surface settlement of stone column and soft soil at various time t between proposed analytical solution and finite element result

Finally, Figure 6.19 presents the final distribution of shear stresses against depth at two different radii in soft soil. Indeed, a reasonable comparison could be observed between the proposed analytical and the numerical predictions. Therefore, in summary it is evident that the simplified analytical solution proposed in the present study can predict the coupled consolidation – deformation response of the composite stone column – soft ground subjected to an instantly applied uniform loading reasonably well.

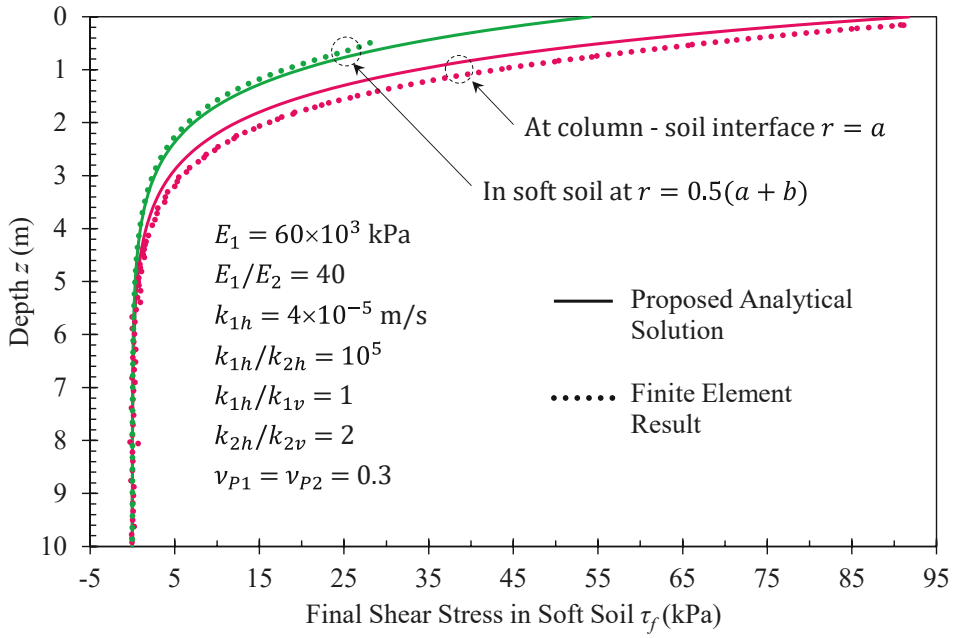

Figure 6.19. Verification on the distribution of final shear stress in soft soil against depth at two different radii between proposed analytical solution and finite element result

6.7 Verification against full-scale test

This section provides an additional verification of the proposed analytical solution against full-scale test of a soil-cement deep mixing column reinforced soft soil. The test was conducted at Wangnoi District, Ayuthaya, Thailand, and details of this field test was summarised in the study by Bergado et al. [225]. The capability of the analytical solution obtained in this chapter is verified against test data in terms of surface settlements of soil-cement column and surrounding soft soil. The field soil layer primarily included soft clay which was reinforced by fully penetrated soil-cement deep mixing columns to depth 9 m below ground level. The composite column – soft clay layer was underlain by medium to stiff clay strata which were almost impermeable. The soil-cement column stabilised soft ground was designed including columns of 0.6 m diameter and 1.5 m center to center

spacing arranged in square pattern to support an embankment up to 6 m height, and the construction of embankment had been completed within 15 days. Table 6.1 summarises measured and back-analysis data reported in the study by Bergado et al. [225] and provides selected parameters in the proposed analytical solution for the verification exercise.

It should be noted that the embankment in the full-scale test might be considered as a typical embankment which induces a rather uniform surcharge loading on the composite ground surface. Thus, the analytical solution for associated consolidation – deformation of composite ground developed in this chapter can be validated using the field test data. In contrast, the analytical solutions derived in Chapters 3 – 5 neglect the column – soil interaction and adopt a stress concentration ratio on composite column – soft ground surface to account for the non-uniform applied vertical stresses between column and surrounding soft soil, as presented in the verifications against field measurements reported by Dunbavan and Carter [219].

According to Bergado et al. [225], the average surface settlements of soil-cement mixing column and encircling soft soil measured right after embankment construction were roughly 122 mm and 162 mm, respectively. Besides, the consolidation settlements at that point of time (i. e. $t = 15$ days) for soil-cement column and surrounding soft soil under instant embankment loading ($q_0 = \gamma h = 18.2 \times 6 = 109.2$ kPa) obtained from the proposed analytical solution were about 45 mm. Therefore, it is supposed that the immediate settlements after completing embankment construction were 77 mm and 117 mm for soil-cement column and soft soil, respectively, as a difference between measured settlements and consolidation settlements. By combining these immediate settlements with consolidation settlements calculated by the proposed analytical solution for time $t \geq$

15 days, the surface settlements of soil-cement deep mixing column and surrounding soil can be plotted in Figure 6.20. As observed, the predictions utilising the proposed analytical solution agreed well with field measurements. The underestimate of analytical predictions compared with field data is attributable to plastic deformations in soil-cement mixing column and encircling soil and lateral displacement of soft soil during consolidation process in real practice, which was ignored in the proposed analytical solution.

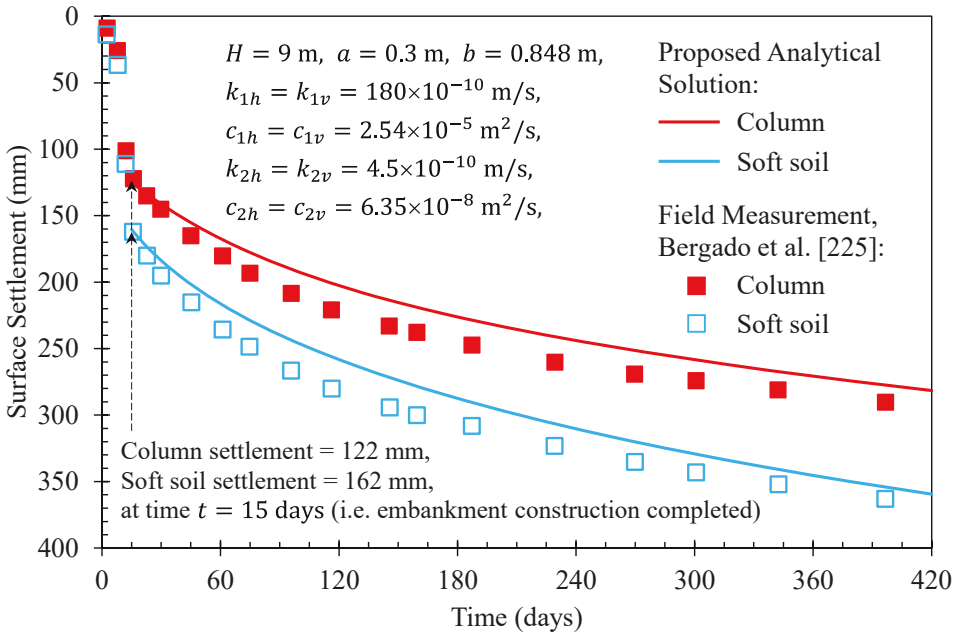

Figure 6.20. Verification on surface settlements of soil-cement deep mixing column and surrounding soft soil between proposed analytical solution and field measurement

Table 6.1. Parameters for the verification against case study

Parameters	Full-scale test reported by Bergado et al. [225]		Proposed analytical solution
	Measured data	Back-analysis	
Embankment height, h (m)	6	6	6
Unit weight of embankment fill, γ (kN/m^3)	18.2	18.2	18.2
Column length, H (m)	9	9	9
Column radius, a (m)	0.3	0.3	0.3
Column spacing (square pattern), s (m)	1.5	-	-
Radius of unit cell, $b = 1.13s/2$ (m)	-	0.848	0.848
Permeability coefficient of column, $k_{1h} = k_{1v}$(m/s)	$(150 - 200)\times10^{-10}$	-	180×10^{-10}
Consolidation coefficient of column, $c_{1h} = c_{1v}$(m^2/s)	$(0.63 - 1.27)\times10^{-5}$	2.54×10^{-5}	2.54×10^{-5}
Permeability coefficient of soft soil, $k_{2h} = k_{2v}$(m/s)	$(3 - 6)\times10^{-10}$	-	4.5×10^{-10}
Consolidation coefficient of soft soil, $c_{2h} = c_{2v}$(m^2/s)	$(3.17 - 9.51)\times10^{-8}$	-	6.35×10^{-8}
Permeability ratio, $N_k = k_{1h}/k_{2h}$	-	40	40
Constrained modulus ratio, $N_M = M_1/M_2$	-	10	10

6.8 Summary

Most available analytical studies on consolidation of soft soil reinforced by stone columns assume the equal strain condition for the column and soil settlements, which cannot capture the differential settlements induced by a typical low embankment via a flexible platform on the composite ground surface. In contrast, several existing theoretical studies investigated the free strain deformation of the mentioned composite foundation under the drained compression condition or incorporated the consolidation effect in an uncoupled fashion. It is worthwhile to mention that the coupled time-dependent consolidation – deformation analysis is stringently required because the deformation of a saturated composite ground is deemed to be time-dependent and direct consequence of the dissipation of excess pore water pressure out of the column and soil bodies during the consolidation process. Thus, this study derived an analytical solution for the coupled consolidation – deformation response of the composite stone column – soft ground to a uniform flexible loading. The axisymmetric unit cell model was adopted for the mathematical derivation in which the external loading was applied instantly to induce a uniform distribution of initial excess pore water pressure over the composite foundation. The orthotropic consolidation formulations for both stone column and soft soil regions were derived applying the vertical drain consolidation theory. The deformation procedure for the composite ground, which is integrated into the consolidation analysis adopted the deformation mode suggested in the literature. For the combined analysis of consolidation and deformation, the formulation of total vertical stresses caused by the applied loading was derived first. Then, the non-homogeneous consolidation problem was solved employing Green's function method to obtain the excess pore water pressure solutions for the column and soil regions. Thereby, the average consolidation settlement against

radius at any depth and the average degree of consolidation for each column and soil regions were attained. The average differential settlement between the soil and column areas could also be determined to verify the settlement parameters used, impacting the soil settlement distribution pattern, shear strain and shear stress in soft soil during the consolidation process.

The validation of the simplified analytical solution derived in this study was exhibited via a worked example examining thoroughly the change of total vertical stresses and excess pore water pressures in stone column and soft soil against depth and time, the column and soil settlements, and the shear stress distribution in soft soil. The accuracy of the proposed analytical solution was verified against the finite element results, which showed a reasonable agreement between the predictions. The observed disparities in the verification could be attributed to the simplifying assumption used in the analytical solution for the stress transfer mechanism at the very beginning stage of consolidation and the distribution of total vertical stress in soft soil along radius. The capability of obtained solution was also validated via verification exercise against a full-scale test, which showed reasonable predictions of the obtained solution. The proposed analytical solutions can be useful to practising engineers for cross-checking complex numerical simulations or conducting extensive parametric studies to optimise the design. Moreover, the obtained analytical solution may be applied for the associated consolidation – deformation analysis of a soft soil reinforced by other permeable columns such as sand columns and soil-cement mixing columns by using corresponding physical and mechanical parameters.

CHAPTER 7

CONCLUSIONS AND RECOMMENDATIONS

7.1 Summary

The soil reinforcement technique using pervious column structures such as sand and stone columns, and soil-cement mixing columns has been studied and applied widely in geotechnical engineering in the last few decades. These column structures could improve the performance of composite pervious column – soft grounds in terms of settlement reduction and bearing capacity enhancement [14, 25, 226-234], stability improvement [29-33, 235-238], liquefaction resistance [43, 239-247], and consolidation acceleration [57, 59, 61, 105, 106, 248-252], as a result of the significant increase in stiffness and shear strength of the composite ground compared to the soft ground itself. Additionally, the columns possess high permeability and large diameter, which behave as vertical drains with great discharge capacity and can provide radial drainage paths for the dissipation of excess pore water pressure in the encircling soft soil during the process of consolidation. Thus, the consolidation of the composite ground is sped up considerably. Due to the complex nature of evaluating the multi effects of pervious columns in improving soft soil, the mentioned performance objectives of the column inclusion in soil foundations are usually investigated separately considering various influencing factors [43, 57, 232, 235]. Among those factors, the consolidation analysis has attracted great interest for geotechnical engineers and researchers studying the time-dependent response of pervious column reinforced soft grounds. The core objective of this thesis is to derive the innovative analytical solutions for the consolidation response of stone column stabilised soft soils under free strain conditions for the column and soil settlements.

Chapter 1 summarised various techniques in soft soil reinforcements and highlighted the improvement of soft soils by stone column inclusions, particularly focusing on the analytical consolidation studies. The research objectives and the structure of thesis were also stated in this chapter. Chapter 2 provided a detailed literature review on the consolidation studies for soft soils. This chapter firstly introduced the conventional theory introduced by Terzaghi [75] for one-dimensional consolidation of saturated soils, followed by the more complex theories developed by Biot [77] and Barron [64] for multi-dimensional consolidation of the soils. On the other hand, this chapter also discussed comprehensively the existing theoretical studies on consolidation of soft soils assisted by vertical drains and high modulus pervious columns. Several influencing factors on the consolidation behaviour of drain and permeable column supported soft grounds were highlighted, which are related to the effects of the construction processes and construction methods and the nature of soft soils. The deformation mechanism in the composite stone column – soft ground during the free strain consolidation process was also emphasised in the literature review. Finally, this chapter summarised the potential analytical methods which could be employed to solve the consolidation problems.

Chapters 3 and 4 presented the analytical solutions for two-dimensional plane strain and axisymmetric consolidations of the stone column improved soft soils subjected to instant loadings under free strain conditions. The governing equations of consolidation were incorporated with the horizontal and vertical flows of excess pore water pressure in which the permeabilities of stone column and soft soil are orthotropic. The plane strain model adopted a uniform distribution of total vertical stresses in the composite ground induced by the external loading, whereas the axisymmetric model captured an arbitrary distribution of those against radius and depth. The obtained analytical solutions in both

chapters were validated via worked examples investigating the excess pore water pressure dissipations in the column and soil regions against width (or radius), depth and elapsed time, specifically the example in Chapter 4 plotted the ground surface settlement varying with time and the ground settlement at a given time varying with depth as a result of excess pore water pressure dissipations. Furthermore, the accuracy of the achieved analytical solutions in these two chapters was verified against finite element simulations by comparing the dissipation rates of excess pore water pressures at various points (Chapter 4) and average degrees of consolidation in the column and soil areas (Chapters 3 and 4) obtained from the analytical and numerical predictions. A further verification of the attained analytical solution in Chapter 4 against field measurements was also conducted regarding the rate of excess pore water pressure dissipation at an investigation point in soft soil in the adopted field case history. Lastly, parametric analyses utilising the proposed analytical solutions were performed to examine the effects of the stiffness and permeability of soft soils (Chapters 3 and 4) and the column spacing, the distribution pattern of total vertical stresses against depth and the thickness of soft soil stratum (Chapter 4) on the average degrees of consolidation in stone column and soft soil regions and the average differential settlement between these two regions.

Chapter 5 developed an analytical solution for the axisymmetric consolidation of stone column supported soft soil under any time-dependent loading and free strain conditions. Similar to the previous chapters, the mathematical model included the associated radial – vertical excess pore water pressure flows simultaneously with orthotropic permeabilities of stone column and soft soil regions, while the induced total vertical stresses in the composite ground were assumed to distribute uniformly. Worked examples were executed to confirm the proposed analytical solution, inspecting the effects of different

time-varying loadings (including step, ramp and sinusoidal loadings) on the consolidation behaviour of the composite stone column – soft ground. The calculation results were plotted in terms of the variations of the excess pore water pressures at various points, the normalised average surface settlements in stone column and soft soil areas and the differential average surface settlement between the two areas against consolidation time. On the other hand, the reliability of the attained analytical solution in this chapter was also examined by comparing the dissipation rate of excess pore water pressure at the examination point in soft soil for the case history in Chapter 4 obtained from the field observations and the analytical estimation (considering time-dependent loading).

Eventually, Chapter 6 proposed a simplified analytical solution for the associated free strain consolidation – deformation analysis of stone column reinforced soft ground under constant loading and axisymmetric conditions. The governing consolidation equations, which are non-homogeneous due to the presence of time-varying total vertical stresses as a result of the incorporation of the composite ground deformation analysis during the consolidation process, also captured the orthotropic permeabilities and excess pore water pressure flows in the column and soil domains. The validations of the proposed analytical solution were exhibited through a comprehensive example together with a verification exercise against finite element simulations. The results achieved from the analytical and numerical estimations were illustrated graphically, which include the variations of the total vertical stresses, the excess pore water pressures and the settlements in stone column and soft soil against depth and time. Moreover, the average degrees of consolidation in the column and soil regions and the shear stress distribution in the soft soil were also reported in this chapter.

7.2 Key concluding remarks

7.2.1 General

Thanks to the outstanding development of computer technology along with the advancement of experimental techniques and equipment, several numerical and experimental studies were conducted to investigate thoroughly the consolidation response of soft soil stabilised by pervious columns [35, 54, 133, 207, 221, 253-265]. Analytical studies on the same problem have also been carried out vigorously. Although most analytical examinations usually adopt some assumptions to simplify the problem under consideration and derive the final solution, they can serve as helpful tools for cross-checking complicated numerical modellings. The analytical approaches can also provide an understanding of the problem by implementing parametric analyses, which could be more incommodious using numerical simulations. Particularly, analytical methods can be useful for preliminary designs used by practising engineers due to the convenience in utilising the established analytical solutions. As a result, several analytical studies were accomplished examining influencing factors such as drain resistance and smear effects, combined horizontal – vertical consolidations, time- and depth-varying loadings [109, 129, 130, 132, 146], partially drained boundaries [46, 47], clogging in pervious columns [52, 53], layered soils and partially penetrated columns [149, 151, 153, 155, 158, 266-268], nonlinear properties of soils [60, 112, 164], yielding and lateral deformation of columns [55, 269, 270], and unsaturated soils [123, 124, 177-182]. However, most available analytical studies on the consolidation of soft soils reinforced by stone columns adopt the equal strain assumption that cannot capture the more realistic behaviour of the composite ground (i.e. unequal column and soil settlements). Thus, the existing analytical

studies ignore the interaction between stone column and encircling soft soil areas due to the differential settlements during the process of consolidation. Consequently, the analytical solutions in the literature may provide limited applications in predicting the consolidation response of the composite stone column – soft soil foundations.

In an effort to develop novel analytical solutions which can capture the free strain consolidation and associated deformation (i.e. unequal settlements) of stone column improved soft soils, the method of separation of variables in combination with the orthogonal expansion technique, the Green's function method and Green's formula have been utilised for the analytical derivations. The application of the method of separation of variables and the eigenfunction expansion (orthogonal expansion) technique would allow deriving the generalised analytical solutions in terms of series against spatial domains of the homogeneous consolidation formulations. On the other side, the utilisation of the Green's function approach and Green's formula would allow further developing the previous analytical solutions for the generalised non-homogeneous consolidation formulations, in which the non-homogeneous terms in the governing equations are arbitrary functions with respect to space and time variables. Therefore, the mathematical models for the consolidation can be solved directly to achieve the final solutions without the requirement of intermediate transformation steps which could be encountered in several existing analytical studies, such as those using the Laplace transform and Integral transform techniques. The obtained analytical solutions in this study can provide insight into the time-dependent response of the composite stone column – soft ground by carrying out worked examples, verification exercises and parametric examinations.

7.2.2 Analytical investigation of the two-dimensional plane strain and axisymmetric consolidations under constant loadings

The mathematical model was derived corresponding to the unit cell configuration, where the governing consolidation equations are homogeneous linear partial differential equations of excess pore water pressures in stone column and soft soil areas. The composite ground surface was modelled as a freely drained surface by a homogeneous boundary condition of the first type (i.e. homogeneous Dirichlet boundary condition), whereas the zero flow conditions across the impermeable cell base and the outer vertical surface of the unit cell were simulated by homogeneous boundary conditions of the second type (i.e. homogeneous Neumann boundary conditions). The column – soil interface was assumed as a perfect hydraulic contact surface, which is characterised by the continuities of excess pore water pressures and pore water fluxes (i.e. flow rates) between the column and soil areas. Under the symmetry conditions of applied loadings and geometries of unit cell, half of unit cell was modelled. Thus, the centerline of the plane strain model was assigned a perfectly insulated condition of excess pore water pressure to reflect no horizontal flow at this boundary. On the other hand, a finiteness condition as a pseudoboundary condition of excess pore water pressure was assigned to the centerline of the axisymmetric model to avoid the infinity nature of functions containing zero argument, which occurs in the analytical solution of excess pore water pressure in cylindrical coordinates. The application of the finiteness condition would also reduce some computational manipulations in the mathematical derivations. While the plane strain model adopted a uniform distribution of total vertical stresses in the composite foundation, the axisymmetric model captured generalised total vertical stress distributions against radius and depth. The analytical solutions were derived employing

the method of separation of variables and eigenfunction expansion technique. The obtained analytical solutions were used to investigate the changes in excess pore water pressure and consolidation settlement at any point in the composite ground. Therefore, the differential settlement in the foundation and the average degrees of consolidation of stone column and surrounding soft soil regions can also be obtained easily. Moreover, the drain resistance effect in stone column can be captured owing to the incorporation of finite orthotropic permeability and size of stone column in the mathematical formulations. The anisotropic nature of soft soil permeability usually encountered in real practice was modelled as orthotropic, which induces unequal flow rates in horizontal and vertical directions are also available in the obtained analytical solutions. The consolidation analyses using the attained analytical solutions in Chapters 3 and 4 are presented below.

The variation of permeability and stiffness of soft soils had a significant impact on the consolidation behaviour of composite grounds. An increase in the permeability of soft soil accelerated the excess pore water pressure flows in soft soil, and thus the soil consolidated more quickly, particularly owing to the accelerated radial flow of excess pore water pressure. The differential settlement between soft soil and stone column areas tends to take place and achieve the maximum earlier when the higher permeability of soft soil is adopted. Moreover, the change patterns of differential settlement against time were similar to those of average degree of consolidation of soft soil due to the dramatic larger settlement of soft soil compared to stone column. The increase in the modulus of soft soil not only sped up the consolidation but also reduced the differential settlement substantially. The stiffer the soil, the faster the transfer of the excess pore water pressure from void spaces onto the effective stress in soil skeleton, leading to the accelerated consolidation. Besides, the higher adopted modulus of soft soil would result in lesser soil

settlement and a reduction in the differential settlement. Chapter 4 shows that the stone column spacing had a major effect on soil consolidation and the differential settlement. The rates of consolidation and differential settlement decreased substantially with an increase in the column spacing. A larger column spacing would lead to a longer radial drainage path for the dissipation of excess pore water pressure in soft soil, which causes the dissipation and accompanying consolidation processes to prolong. However, the changes in the soil consolidation and differential settlement are prone to be less conspicuous in accordance with a larger column spacing, particularly when the radius ratio of stone column to unit cell $n_e > 3$. The variation patterns in the soft soil consolidation and the differential settlement were almost identical mainly due to the significantly larger soil settlement compared to column settlement. Chapter 4 also exhibits that even though the distribution pattern of total vertical stresses against depth and the thickness of soft soil stratum had minor effects on the soil consolidation (thanks to the dominance of the radial flow rate of excess pore water pressure in soft soil), they affected the differential settlement between soft soil and stone column dramatically. The more reduction of total vertical stresses with depth, the less effective vertical stresses acting on the composite ground, resulting in less settlement of the composite ground and the soil in particular. Thus, the differential settlement was diminished during the consolidation process considerably. On the other side, the differential settlement increased corresponding to the deeper soil stratum, owing to the greater increase of soil settlement than column settlement as a result of the extreme lower stiffness of the soft soil compared to the stone column.

7.2.3 Analytical examination of the axisymmetric consolidation under time-dependent loadings

In Chapter 5, the axisymmetric unit cell model was considered, where the consolidation equations governing the dissipation of excess pore water pressure are non-homogeneous linear partial differential equations (non-homogeneous linear PDEs). The non-homogeneous terms in the PDEs are first partial derivatives of total vertical stresses in the composite ground induced by time-varying loadings with respect to time variable. The boundary conditions for the excess pore water pressure dissipation in the composite foundation were adopted similar to those of the axisymmetric consolidation problem in Chapter 4. The induced total vertical stresses in the foundation were assumed to distribute uniformly in each region of the unit cell (i.e. stone column and soft soil) that is the total vertical stresses are time-dependent but space-independent. The associated radial – vertical excess pore water pressure flows were also integrated into the model with orthotropic hydraulic conductivity (permeability) for stone column and soft soil. To derive the analytical solutions for the excess pore water pressure dissipation, the separation of variables was taken to separate the PDEs into ordinary differential equations (ODEs) with respect to radius, depth and time. The ODEs and accompanying boundary conditions in radial and vertical directions produce corresponding boundary value problems to develop eigenfunctions and eigenvalues against spatial domains for the final analytical solutions. The ODE of time-dependent function is a first-order differential equation which can be solved readily to obtain the function against time domain. The application of superposition principle for product of the space-dependent eigenfunctions and the time-dependent function would lead to a double series solution for the homogeneous linear PDEs (i.e. the PDEs without the derivatives of total vertical stresses

against time) in which the Fourier-Bessel coefficients are determined utilising eigenfunction expansion technique. The obtained solution of the homogeneous PDEs would be rearranged in form of Green's formula to achieve the Green's function, which formulates the final generalised solution of excess pore water pressure at any point in the foundation capturing the time-varying total vertical stresses in the original non-homogeneous PDEs. As a result, the column and soil settlements and their differential settlement during the consolidation process can be captured. The consolidation examination of the composite stone column – soft ground subjected to various investigation time-dependent loadings utilising the achieved analytical solutions in Chapter 5 are summarised below.

The change in loading and unloading rates almost had no effect on the excess pore water pressure in stone column thanks to the extremely large permeability and drainage efficiency (discharge capacity) of stone column. As a result, the settlement rate of stone column was virtually contingent on the rates of loading and unloading processes. In contrast, the loading and unloading rates had major impacts on the variation of excess pore water pressure in soft soil against time because of the low permeability of soft soil. During a loading stage, the excess pore water pressure in soft soil may increase if the loading rate is higher than the dissipation rate; whereas, during an unloading stage, the soft soil may undergo a decline of excess pore water pressure to negative values if the unloading rate is faster than the pore water absorption rate. For a composite ground subjected to a non-zero initial surcharge which causes positive initial excess pore water pressures, the acceleration of loading and unloading processes might result in the increase of excess pore water pressure in soft soil during the early stages of consolidation as the above explanation, yet accelerates the dissipation and absorption processes afterwards

considerably. The reason is ascribed to the rise in the radial gradient of pore water pressure from soft soil towards stone column during the loading accelerations and the inverting radial gradient of those from the column to soil areas during the accelerated unloading processes. Due to the low permeability, the change of soft soil settlement against time depends upon the rates of loading and unloading and the rates of dissipation and absorption of pore water. The rate of soil volume change increased corresponding to the acceleration of loading and unloading processes. The variation patterns of the differential settlement between soft soil and stone column and the soil settlement against time were virtually identical due to the significant larger soil settlement than column settlement. Lastly, the verifications of the proposed analytical solution against field observations show that the stress concentration ratio between stone column and surrounding soft soil $n_{scr} = 2 - 6$ should be adopted for a composite stone column – soft soil foundation supporting a typical flexible embankment – platform system. Furthermore, the stress concentration ratio included in the proposed analytical solutions should be assumed varying with time as captured in real practice, adopting a lower bound value $(\text{i. e. } n_{scr} = 2)$ for the early stages of consolidation and an upper bound value $(\text{i. e. } n_{scr} = 6)$ for the later stages.

7.2.4 Analytical evaluation of the associated consolidation – deformation response under constant loading condition

The last analytical model established in this study is for the associated analysis of consolidation and deformation of the composite stone column – soft ground subjected to constant loading. The mathematical formulation was derived considering the combined radial – vertical flows of excess pore water pressure in stone column and soft soil areas

(orthotropic permeability for each area), and adopting the settlement pattern for the composite ground suggested by an existing study in the literature. The mathematical model captured the variation of total vertical stresses in the foundation against radius, depth and time as a result of the total vertical stress transferring from soft soil to stone column due to differential settlement during the consolidation process. Therefore, the consolidation governing equations are non-homogeneous linear partial differential equations owing to the presence of time-varying total vertical stresses. The homogeneous consolidation formulations were solved first to develop Green's function for final excess pore water pressure solutions, employing the method of separation of variables and eigenfunction expansion technique. Then, the final solutions for excess pore water pressure corresponding to the non-homogeneous consolidation formulations were derived in terms of Green's formula, which can be expanded readily into a double series solution. The obtained analytical solutions can be used to examine the variation of excess pore water pressure against time at any point in the composite foundation. Thus, the consolidation settlements of stone column and soft soil areas and the differential settlement between them can be captured. The average differential settlement between the soil and column areas was used to compute the shear strains and shear stresses in the composite ground during the consolidation process. The investigation of associated excess pore water pressure dissipation and deformation behaviour of the stone column reinforced soft ground under constant loading condition employing the proposed analytical solution in Chapter 6 are provided below.

During the consolidation process, the dissipation of excess pore water pressure and the transfer of total vertical stress from soft soil onto stone column progress concurrently. When pore water in the soft soil squeezes out, the soil settles and induces the differential

settlement between the soil and column (i.e. the soil settlement is larger than the column settlement). The differential settlement causes total vertical stress to transfer from soft soil to stone column, which leads to the increase of the column settlement to counteract the differential settlement. As a result, both stone column and soft soil settlements increase during the dissipation process of excess pore water pressure until the differential settlement reaches the maximum at the end of consolidation (i.e. excess pore water pressure would dissipate entirely). The verification against finite element results shows that the adopted analytical model using the assumed settlement pattern and the established total vertical stress distribution in the stone column reinforced soft soil in terms of exponential functions are deemed reasonable. Furthermore, the proposed analytical solution may be used to analyse the coupled consolidation – deformation response of soft soils stabilised by other pervious columns, for example, compacted sand columns and soil-cement mixing columns by considering corresponding mechanical and physical factors.

7.3 Recommendations for further studies

Although the analytical studies presented in this thesis can capture the consolidation and associated deformation of saturated soft soils reinforced by stone columns under free strain condition, the present study can be expanded further to consider the following points:

- The analytical models developed in this study included the combined horizontal – vertical flows of excess pore water pressure with finite orthotropic permeability for both stone column and soft soil regions (i.e. included drain resistance effect in

stone column). However, the smear and clogging effects should be incorporated into the proposed models to reflect these unavoidable effects in real practice.

- To obtain the analytical solutions in the current study, the column and soil areas were assumed to deform vertically, adopting the elastic column and soil materials. The analysis would be more realistic when the lateral deformation and non-elastic materials (e.g. elasto-plastic response) are integrated into the column and soil areas.
- For the sake of simplification and inspired by many previous studies, the compressibility and permeability of stone column and soft soil were constant in the proposed analytical models. These simplifications may be acceptable for a given pressure increment due to surcharge loadings. Obviously, these consolidation parameters would change corresponding to the variation of void ratio and effective pressure during the consolidation process. To capture these influencing factors, nonlinear consolidation parameters could be combined with the proposed analytical models. The more complex effect regarding the rheological property of soft soil might be incorporated to account for the secondary consolidation of the soil.
- The analytical solutions in this study were derived corresponding to the homogeneous single-layered soil stratum. Multi-layered soils are usually encountered in real construction projects and thus the analytical models should be expanded to consider this factor. The partial penetration of stone columns in single-layered soils, which has a similar nature to fully penetrated stone columns in multi-layered soils could also be taken into consideration for future studies.

- The current study ignored the effect of soil arching developing in the embankment fill as a result of the mobilisation of shear stresses in the fill under the differential settlement between soft soil and stone column. This is a major effect in combined consolidation – deformation analyses of the stone column stabilised soft ground under flexible embankment loadings. Derivation of analytical solutions capturing progressive soil arching is very challenging yet might be potential for further studies using the same assumptions as adopted in the present study for the sake of simplicity.
- The analytical solutions derived in this study are for saturated soils. There have been very limited numerical examinations and almost no analytical studies for consolidation of unsaturated soils supported by stone columns under the free strain condition or even the equal strain condition. Therefore, this point is highly recommended for future research studies.

REFERENCES

[1] Leroueil S. Notes de cours: Comportement des massifs de sols. *Université Laval, Québec, Canada*. 1997.

[2] Barksdale R, Bachus R. Design and construction of stone columns - volume I. Federal Highway Administration, Washington, DC, USA1983.

[3] Taube MG, Herridge J. Stone columns for industrial fills. 33rd Ohio River Valley Soil Seminar (ORVSS)2002.

[4] Balaam N, Booker J. Analysis of rigid rafts supported by granular piles. *International Journal for Numerical and Analytical Methods in Geomechanics*. 1981;5:379-403.

[5] Hugher J, Withers N. Reinforcing of soft cohesive soils with stone columns. *Ground engineering*. 1974;7.

[6] McKenna J, Eyre W, Wolstenholme D. Performance of an embankment supported by stone columns in soft ground. *Geotechnique*. 1975;25:51-9.

[7] Mitchell JK, Huber TR. Performance of a stone column foundation. *Journal of Geotechnical Engineering*. 1985;111:205-23.

[8] Bergado DT, Lam FL. Full scale load test of granular piles with different densities and different proportions of gravel and sand on soft Bangkok clay. *Soils and foundations*. 1987;27:86-93.

[9] Greenwood DA. Load tests on stone columns. Deep foundation improvements: Design, construction, and testing: ASTM International, 1991.

[10] Priebe HJ. The design of vibro replacement. *Ground engineering*. 1995;28:31.

[11] Muir Wood D, Hu W, Nash D. Group effects in stone column foundations: model tests. *Geotechnique*. 2000;50:689-98.

[12] Black J, Sivakumar V, McKinley J. Performance of clay samples reinforced with vertical granular columns. *Canadian geotechnical journal*. 2007;44:89-95.

[13] Oh E, Balasubramaniam A, Surarak C, Bolton M, Chai G, Huang M, et al. Behaviour of a highway embankment on stone columns improved estuarine clay. Proc, 16th Southeast Asian Geotechnical Conf2007. p. 567-72.

[14] Black J, Sivakumar V, Bell A. The settlement performance of stone column foundations. *Géotechnique*. 2011;61:909-22.

[15] Indraratna B, Ngo NT, Rujikiatkamjorn C, Sloan SW. Coupled discrete element–finite difference method for analysing the load-deformation behaviour of a single stone column in soft soil. *Computers and Geotechnics*. 2015;63:267-78.

[16] Basack S, Indraratna B, Rujikiatkamjorn C, Siahaan F. Modeling the Stone Column Behavior in Soft Ground with Special Emphasis on Lateral Deformation. *Journal of Geotechnical and Geoenvironmental Engineering*. 2017:04017016.

[17] Kumar Das A, Deb K. Response of stone column-improved ground under c-ϕ soil embankment. *Soils and Foundations*. 2019.

[18] Barksdale R, Bachus R. Design and construction of stone columns - volume II, appendixes. Federal Highway Administration, Washington, DC, USA1983.

[19] Fatahi B, Basack S, Premananda S, Khabbaz H. Settlement prediction and back analysis of Young's modulus and dilation angle of stone columns. *Australian Journal of Civil Engineering*. 2012;10:67-79.

[20] Miranda M, Da Costa A, Castro J, Sagaseta C. Influence of gravel density in the behaviour of soft soils improved with stone columns. *Canadian Geotechnical Journal*. 2015;52:1968-80.

[21] Ambily A, Gandhi SR. Behavior of stone columns based on experimental and FEM analysis. *Journal of geotechnical and geoenvironmental engineering*. 2007;133:405-15.

[22] Zhao L-S, Zhou W-H, Yuen K-V. A simplified axisymmetric model for column supported embankment systems. *Computers and Geotechnics*. 2017;92:96-107.

[23] Zhao L-S, Zhou W-H, Geng X, Yuen K-V, Fatahi B. A closed-form solution for column-supported embankments with geosynthetic reinforcement. *Geotextiles and Geomembranes*. 2019;47:389-401.

[24] Malarvizhi S, Ilamparuthi K. Load versus settlement of clay bed stabilized with stone and reinforced stone columns. 3rd Asian Regional Conference on Geosynthetics2004. p. 322-9.

[25] Ghazavi M, Afshar JN. Bearing capacity of geosynthetic encased stone columns. *Geotextiles and Geomembranes*. 2013;38:26-36.

[26] Malarvizhi S. Comparative study on the behavior of encased stone column and conventional stone column. *Soils and Foundations*. 2007;47:873-85.

[27] Murugesan S, Rajagopal K. Geosynthetic-encased stone columns: numerical evaluation. *Geotextiles and Geomembranes*. 2006;24:349-58.

[28] Murugesan S, Rajagopal K. Studies on the behavior of single and group of geosynthetic encased stone columns. *Journal of Geotechnical and Geoenvironmental Engineering*. 2010;136:129-39.

[29] Giannaros C, Tsiambaos G. Stabilization of embankment foundations by using stone columns. *Geotechnical & Geological Engineering*. 1997;15:247-58.

[30] Sabhahit N, Basudhar P, MADHAV M. Generalized stability analysis of embankments on granular piles. *Soils and foundations*. 1997;37:13-22.

[31] Deb K, Dhar A, Bhagat P. Evolutionary approach for optimal stability analysis of geosynthetic-reinforced stone column-supported embankments on clay. *KSCE Journal of Civil Engineering*. 2012;16:1185-92.

[32] Zhang Z, Han J, Ye G. Numerical investigation on factors for deep-seated slope stability of stone column-supported embankments over soft clay. *Engineering Geology*. 2014;168:104-13.

[33] Gueguin M, Hassen G, De Buhan P. Stability analysis of homogenized stone column reinforced foundations using a numerical yield design approach. *Computers and Geotechnics*. 2015;64:10-9.

[34] Murugesan S, Rajagopal K. Shear load tests on stone columns with and without geosynthetic encasement. *Geotechnical Testing Journal*. 2009;32:76-85.

[35] Yoo C. Performance of geosynthetic-encased stone columns in embankment construction: numerical investigation. *Journal of Geotechnical and Geoenvironmental Engineering*. 2010;136:1148-60.

[36] Hanna A, Etezad M, Ayadat T. Mode of failure of a group of stone columns in soft soil. *International journal of geomechanics*. 2013;13:87-96.

[37] Hassen G, Gueguin M, De Buhan P. A homogenization approach for assessing the yield strength properties of stone column reinforced soils. *European Journal of Mechanics-A/Solids*. 2013;37:266-80.

[38] Chen J-F, Li L-Y, Xue J-F, Feng S-Z. Failure mechanism of geosynthetic-encased stone columns in soft soils under embankment. *Geotextiles and Geomembranes*. 2015;43:424-31.

[39] Baez J, Martin G. Quantitative evaluation of stone column techniques for earthquake liquefaction mitigation. Proceedings of the 10th World Conference on Earthquake Engineering, Madrid, Spain1992. p. 1477-83.

[40] Adalier K, Elgamal A, Meneses J, Baez J. Stone columns as liquefaction countermeasure in non-plastic silty soils. *Soil Dynamics and Earthquake Engineering*. 2003;23:571-84.

[41] Shenthan T, Nashed R, Thevanayagam S, Martin GR. Liquefaction mitigation in silty soils using composite stone columns and dynamic compaction. *Earthquake Engineering and Engineering Vibration*. 2004;3:39-50.

[42] Tang L, Cong S, Ling X, Lu J, Elgamal A. Numerical study on ground improvement for liquefaction mitigation using stone columns encased with geosynthetics. *Geotextiles and Geomembranes*. 2015;43:190-5.

[43] Lu J, Kamatchi P, Elgamal A. Using stone columns to mitigate lateral deformation in uniform and stratified liquefiable soil strata. *International Journal of Geomechanics*. 2019;19:04019026.

[44] Xie K-H, Lu M-M, Hu A-F, Chen G-H. A general theoretical solution for the consolidation of a composite foundation. *Computers and Geotechnics*. 2009;36:24-30.

[45] Lu M-m, Xie K-h, Li C-x, Wang K. Consolidation solution for composite foundation considering a time-and depth-dependent stress increment along with three distribution patterns of soil permeability. *Journal of Zhejiang University-SCIENCE A*. 2011;12:268-77.

[46] Lei G, Fu C, Ng CW. Vertical-drain consolidation using stone columns: An analytical solution with an impeded drainage boundary under multi-ramp loading. *Geotextiles and Geomembranes*. 2016;44:122-31.

[47] Zhou Y, Zhou G-q, Lu M-m, Shi X-y. Analytical Solution for the Consolidation Process of a Stone-Column Reinforced Foundation under Partially Drained Boundaries. *International Journal of Geomechanics*. 2018;18:06017023.

[48] Walker RT, Indraratna B. Application of spectral Galerkin method for multilayer consolidation of soft soils stabilised by vertical drains or stone columns. *Computers and Geotechnics*. 2015;69:529-39.

[49] Chai J, Pongsivasathit S. A method for predicting consolidation settlements of floating column improved clayey subsoil. *Frontiers of Architecture and Civil engineering in China*. 2010;4:241-51.

[50] Ng K, Tan S. Design and analyses of floating stone columns. *Soils and Foundations*. 2014;54:478-87.

[51] Nissa Mat Said K, Safuan A Rashid A, Osouli A, Latifi N, Zurairahetty Mohd Yunus N, Adekunle Ganiyu A. Settlement evaluation of soft soil improved by floating soil cement column. *International Journal of Geomechanics*. 2019;19:04018183.

[52] Deb K, Shiyamalaa S. Effect of Clogging on Rate of Consolidation of Stone Column–Improved Ground by Considering Particle Migration. *International Journal of Geomechanics*. 2016;16:04015017.

[53] Tai P, Indraratna B, Rujikiatkamjorn C. Experimental simulation and mathematical modelling of clogging in stone column. *Canadian Geotechnical Journal*. 2017;55:427-36.

[54] Basack S, Siahaan F, Indraratna B, Rujikiatkamjorn C. Stone Column–Stabilized Soft-Soil Performance Influenced by Clogging and Lateral Deformation: Laboratory and Numerical Evaluation. *International Journal of Geomechanics*. 2018;18:04018058.

[55] Castro J, Sagaseta C. Consolidation around stone columns. Influence of column deformation. *International Journal for Numerical and Analytical Methods in Geomechanics*. 2009;33:851-77.

[56] Castro J, Sagaseta C. Consolidation and deformation around stone columns: Numerical evaluation of analytical solutions. *Computers and Geotechnics*. 2011;38:354-62.

[57] Cimentada A, Da Costa A, Cañizal J, Sagaseta C. Laboratory study on radial consolidation and deformation in clay reinforced with stone columns. *Canadian Geotechnical Journal*. 2011;48:36-52.

[58] Castro J, Cimentada A, da Costa A, Cañizal J, Sagaseta C. Consolidation and deformation around stone columns: Comparison of theoretical and laboratory results. *Computers and Geotechnics*. 2013;49:326-37.

[59] Jiang Y, Han J, Zheng G. Influence of column yielding on degree of consolidation of soft foundations improved by deep mixed columns. *Geomech Eng*. 2014;6:173-94.

[60] Wang C, Xu Y. Semi-analytical solution of consolidation for composite ground. *Mechanics Research Communications*. 2013;48:24-31.

[61] Dai Z-H, Chen B-L, Qin Z-Z. Three-dimensional nonlinear numerical analysis of consolidation of soft ground improved by sand columns under a freeway embankment in shallow sea: case study. *International Journal of Geomechanics*. 2017;17:05017001.

[62] Sexton B, McCabe B. Numerical modelling of the improvements to primary and creep settlements offered by granular columns. *Acta Geotechnica*. 2013;8:447-64.

[63] Sexton BG, McCabe BA, Karstunen M, Sivasithamparam N. Stone column settlement performance in structured anisotropic clays: the influence of creep. *Journal of Rock Mechanics and Geotechnical Engineering*. 2016;8:672-88.

[64] Barron RA. Consolidation of fine-grained soils by drain wells. *Transactions of the American Society of Civil Engineers*. 1948;113:718-42.

[65] Alamgir M, Miura N, Poorooshasb H, Madhav M. Deformation analysis of soft ground reinforced by columnar inclusions. *Computers and Geotechnics*. 1996;18:267-90.

[66] KR A. Soil Mechanics and Foundation Engineering. Delhi: Nai Sarak, 2004.

[67] Das BM, Sobhan K. Principles of Geotechnical Engineering. 9 ed: Cl-Engineering, 2018.

[68] Terzaghi K. Theoretical soil mechanics. New York: John Wiley & Sons, 1943.

[69] Mesri G, Choi Y. Settlement analysis of embankments on soft clays. *Journal of Geotechnical Engineering*. 1985;111:441-64.

[70] Mesri G, Godlewski PM. Time and stress-compressibility interrelationship. *ASCE J Geotech Eng Div*. 1977;103:417-30.

[71] Mesri G, Choi Y. The uniqueness of the end-of-primary (EOP): void ratio-effective stress relationship. *Unknown Journal*. 1985:587-90.

[72] Kabbaj M, Tavenas F, Leroueil S. In situ and laboratory stress–strain relationships. *Geotechnique*. 1988;38:83-100.

[73] Nash D, Ryde S. Modelling consolidation accelerated by vertical drains in soils subject to creep. *Géotechnique*. 2001;51:257-73.

[74] Degago S, Grimstad G, Jostad H, Nordal S, Olsson M. Use and misuse of the isotache concept with respect to creep hypotheses A and B. *Géotechnique*. 2011;61:897-908.

[75] Terzaghi K. Erdbaumechanik auf bodenphysikalischer Grundlage. 1925.

[76] Biot MA. Le problem de la consolidation des matieres argileuses sous une charge. *Annaies de la Societe Scientifique de Bruxelles*. 1935:110-3.

[77] Biot MA. General theory of three-dimensional consolidation. *Journal of applied physics*. 1941;12:155-64.

[78] Selvadurai A. The analytical method in geomechanics. *Applied Mechanics Reviews*. 2007;60:87-106.

[79] Biot MA. Consolidation settlement under a rectangular load distribution. *Journal of Applied Physics*. 1941;12:426-30.

[80] Biot MA, Clingan F. Consolidation settlement of a soil with an impervious top surface. *Journal of Applied Physics*. 1941;12:578-81.

[81] Biot MA, Clingan F. Bending settlement of a slab resting on a consolidating foundation. *Journal of Applied Physics*. 1942;13:35-40.

[82] De Jong GDJ. Consolidation around pore pressure meters. *Journal of Applied Physics*. 1953;24:922-8.

[83] Biot MA. General solutions of the equations of elasticity and consolidation for a porous material. *J appl Mech*. 1956;23:91-6.

[84] De Jong GDJ. Application of stress functions to consolidation problems. Soil Mechanics and Transport in Porous Media: Springer, 2006. p. 98-101.

[85] Gibson R, McNamee J. The consolidation settlement of a load uniformly distributed over a rectangular area. *Proc 4th ht Cont Soil Mech*. 1957;1:297-9.

[86] Mandel J. Consolidation des sols (étude mathématique). *Geotechnique*. 1953;3:287-99.

[87] Cryer C. A comparison of the three-dimensional consolidation theories of Biot and Terzaghi. *The Quarterly Journal of Mechanics and Applied Mathematics*. 1963;16:401-12.

[88] Gibson R. A critical experiments to examine theories of three-dimensional consolidation. Proc Europ Conf Soil Mech, 19631963.

[89] Booker J. The consolidation of a finite layer subject to surface loading. *International Journal of Solids and structures*. 1974;10:1053-65.

[90] Booker JR, Small J. Finite layer analysis of consolidation. II. *International Journal for Numerical and Analytical Methods in Geomechanics*. 1982;6:173-94.

[91] Booker JR, Small J. Finite layer analysis of consolidation. I. *International Journal for Numerical and Analytical Methods in Geomechanics*. 1982;6:151-71.

[92] Smith DW, Booker JR. Green's functions for a fully coupled thermoporoelastic material. *International Journal for Numerical and Analytical Methods in Geomechanics*. 1993;17:139-63.

[93] Jiang Q, Rajapakse R. ON COUPLED HEAT—MOISTURE TRANSFER IN DEFORMABLE POROUS MEDIA. *The Quarterly Journal of Mechanics and Applied Mathematics*. 1994;47:53-68.

[94] Ai ZY, Wu QL. The behavior of a multilayered porous thermo-elastic medium with anisotropic thermal diffusivity and permeability. *Computers and Geotechnics*. 2016;76:129-39.

[95] Ai ZY, Li Y, Mu JJ, Li HT. Transient dynamic response of multilayered saturated media subjected to impulsive loadings. *International Journal for Numerical and Analytical Methods in Geomechanics*. 2018;42:1154-71.

[96] Ai ZY, Zhao YZ, Song X, Mu JJ. Multi-dimensional consolidation analysis of transversely isotropic viscoelastic saturated soils. *Engineering Geology*. 2019;253:1-13.

[97] Ai ZY, Yang JJ, Li HT. General solutions of transversely isotropic multilayered media subjected to rectangular time-harmonic or moving loads. *Applied Mathematical Modelling*. 2019;75:865-91.

[98] Yoshikuni H, Nakanodo H. Consolidation of soils by vertical drain wells with finite permeability. *Soils and Foundations*. 1974;14:35-46.

[99] Kjellman W. Accelerating consolidation of fine-grained soils by means of cardboard wicks. Rotterdam, 1948.

[100] Rendulic L. Der hydrodynamische spannungsausgleich in zentral entwässerten Tonzylindern. *Wasserwirtschaft und technik*. 1935;2:250-3.

[101] Rendulic L. Porenziffer und porenwasserdruck in Tonen. *Der Bauingenieur*. 1936;17:559-64.

[102] Hird C, Pyrah I, Russel D. Finite element modelling of vertical drains beneath embankments on soft ground. *Geotechnique*. 1992;42:499-511.

[103] Indraratna B, Redana I. Plane-strain modeling of smear effects associated with vertical drains. *Journal of Geotechnical and Geoenvironmental Engineering*. 1997;123:474-8.

[104] Tan SA, Tjahyono S, Oo K. Simplified plane-strain modeling of stone-column reinforced ground. *Journal of Geotechnical and Geoenvironmental Engineering*. 2008;134:185-94.

[105] Parsa-Pajouh A, Fatahi B, Khabbaz H. Experimental and numerical investigations to evaluate two-dimensional modeling of vertical drain–assisted preloading. *International Journal of Geomechanics*. 2015;16:B4015003.

[106] Indraratna B, Redana I. Numerical modeling of vertical drains with smear and well resistance installed in soft clay. *Canadian Geotechnical Journal*. 2000;37:132-45.

[107] Hansbo S. Consolidation of fine-grained soils by prefabricated drains. *Proc 10th ICSMFE, 1981*. 1981;3:677-82.

[108] Lekha K, Krishnaswamy N, Basak P. Consolidation of clay by sand drain under time-dependent loading. *Journal of Geotechnical and Geoenvironmental Engineering*. 1998;124:91-4.

[109] Tang XW, Onitsuka K. Consolidation by vertical drains under time-dependent loading. *International Journal for Numerical and Analytical Methods in Geomechanics*. 2000;24:739-51.

[110] Leo CJ. Equal Strain Consolidation by Vertical Drains. *Journal of Geotechnical and Geoenvironmental Engineering*. 2004;3:316-27.

[111] Zhu G, Yin J-H. Consolidation analysis of soil with vertical and horizontal drainage under ramp loading considering smear effects. *Geotextiles and Geomembranes*. 2004;22:63-74.

[112] Indraratna B, Rujikiatkamjorn C, Sathananthan I. Radial consolidation of clay using compressibility indices and varying horizontal permeability. *Canadian Geotechnical Journal*. 2005;42:1330-41.

[113] Conte E, Troncone A. Radial consolidation with vertical drains and general time-dependent loading. *Canadian Geotechnical Journal*. 2009;46:25-36.

[114] Lu M, Xie K, Wang S. Consolidation of vertical drain with depth-varying stress induced by multi-stage loading. *Computers and Geotechnics*. 2011;38:1096-101.

[115] Lei G, Zheng Q, Ng CWW, Chiu ACF, Xu B. An analytical solution for consolidation with vertical drains under multi-ramp loading. *Géotechnique*. 2015;65:531-47.

[116] Wang L, Sun Da, Li P, Xie Y. Semi-analytical solution for one-dimensional consolidation of fractional derivative viscoelastic saturated soils. *Computers and Geotechnics*. 2017;83:30-9.

[117] Liu Q, Deng Y-B, Wang T-Y. One-dimensional nonlinear consolidation theory for soft ground considering secondary consolidation and the thermal effect. *Computers and Geotechnics*. 2018;104:22-8.

[118] Qin A, Sun Da, Tan Y. Analytical solution to one-dimensional consolidation in unsaturated soils under loading varying exponentially with time. *Computers and Geotechnics*. 2010;37:233-8.

[119] Qin A, Sun Da, Zhang J. Semi-analytical solution to one-dimensional consolidation for viscoelastic unsaturated soils. *Computers and Geotechnics*. 2014;62:110-7.

[120] Zhou WH, Zhao LS, Li XB. A simple analytical solution to one-dimensional consolidation for unsaturated soils. *International Journal for Numerical and Analytical Methods in Geomechanics*. 2014;38:794-810.

[121] Zhou W-H, Zhao L-S, Garg A, Yuen K-V. Generalized analytical solution for the consolidation of unsaturated soil under partially permeable boundary conditions. *International Journal of Geomechanics*. 2017;17:04017048.

[122] Ho L, Fatahi B. One-dimensional consolidation analysis of unsaturated soils subjected to time-dependent loading. *International Journal of Geomechanics*. 2015;16:04015052.

[123] Ho L, Fatahi B, Khabbaz H. Analytical solution to axisymmetric consolidation in unsaturated soils with linearly depth-dependent initial conditions. *Computers and Geotechnics*. 2016;74:102-21.

[124] Ho L, Fatahi B. Axisymmetric Consolidation in Unsaturated Soil Deposit Subjected to Time-Dependent Loadings. *International Journal of Geomechanics*. 2016:04016046.

[125] Huang M, Li J. Generalized analytical solution for 2D plane strain consolidation of unsaturated soil with time-dependent drainage boundaries. *Computers and Geotechnics*. 2018;103:218-28.

[126] Wang L, Xu Y, Xia X, He Y, Li T. Semi-analytical solutions to two-dimensional plane strain consolidation for unsaturated soils under time-dependent loading. *Computers and Geotechnics*. 2019;109:144-65.

[127] Han J, Ye S-L. Simplified method for consolidation rate of stone column reinforced foundations. *Journal of Geotechnical and Geoenvironmental Engineering*. 2001;127:597-603.

[128] Balaam N, Booker J. Effect of stone column yield on settlement of rigid foundations in stabilized clay. *International journal for numerical and analytical methods in geomechanics*. 1985;9:331-51.

[129] Han J, Ye S-L. A theoretical solution for consolidation rates of stone column-reinforced foundations accounting for smear and well resistance effects. *The International Journal Geomechanics*. 2002;2:135-51.

[130] Zhang Y, Xie K, Wang Z. Consolidation analysis of composite ground improved by granular columns considering variation of permeability coefficient of soil. Ground Modification and Seismic Mitigation2006. p. 135-42.

[131] Wang G. Consolidation of soft clay foundations reinforced by stone columns under time-dependent loadings. *Journal of geotechnical and geoenvironmental engineering*. 2009;135:1922-31.

[132] Lu M-M, Xie K-H, Guo B. Consolidation theory for a composite foundation considering radial and vertical flows within the column and the variation of soil permeability within the disturbed soil zone. *Canadian Geotechnical Journal*. 2010;47:207-17.

[133] Indraratna B, Basack S, Rujikiatkamjorn C. Numerical solution of stone column–improved soft soil considering arching, clogging, and smear effects. *Journal of Geotechnical and Geoenvironmental Engineering*. 2013;139:377-94.

[134] Basack S, Indraratna B, Rujikiatkamjorn C. Modeling the performance of stone column–reinforced soft ground under static and cyclic loads. *Journal of Geotechnical and Geoenvironmental Engineering*. 2016;142:04015067.

[135] Deng Y-B, Xie K-H, Lu M-M. Consolidation by vertical drains when the discharge capacity varies with depth and time. *Computers and Geotechnics*. 2013;48:1-8.

[136] Deng Y-B, Xie K-H, Lu M-M, Tao H-B, Liu G-B. Consolidation by prefabricated vertical drains considering the time dependent well resistance. *Geotextiles and Geomembranes*. 2013;36:20-6.

[137] Chai J-C, Miura N. Investigation of factors affecting vertical drain behavior. *Journal of Geotechnical and Geoenvironmental Engineering*. 1999;125:216-26.

[138] Sharma J, Xiao D. Characterization of a smear zone around vertical drains by large-scale laboratory tests. *Canadian Geotechnical Journal*. 2000;37:1265-71.

[139] Hawlader BC, Imai G, Muhunthan B. Numerical study of the factors affecting the consolidation of clay with vertical drains. *Geotextiles and Geomembranes*. 2002;20:213-39.

[140] Indraratna B, Redana I. Laboratory determination of smear zone due to vertical drain installation. *Journal of geotechnical and geoenvironmental engineering*. 1998;124:180-4.

[141] Gray H. Simultaneous consolidation of contiguous layers of unlike compressible soils. *Trans, ASCE*. 1945;110:1327-44.

[142] Mesri G. One-dimensional consolidation of a clay layer with impeded drainage boundaries. *Water Resources Research*. 1973;9:1090-3.

[143] Schiffmann R, Stein JR. One-dimensional consolidation of layered systems. *Journal of Soil Mechanics & Foundations Div*. 1970.

[144] Xie K-H, Xie X-Y, Gao X. Theory of one dimensional consolidation of two-layered soil with partially drained boundaries. *Computers and Geotechnics*. 1999;24:265-78.

[145] Walker R, Indraratna B. Vertical drain consolidation with overlapping smear zones. *Geotechnique*. 2007;57:463-8.

[146] Deb K, Behera A. Rate of Consolidation of Stone Column–Improved Ground Considering Variable Permeability and Compressibility in Smear Zone. *International Journal of Geomechanics*. 2017;17:04016128.

[147] Xie K-H, Xie X-Y, Jiang W. A study on one-dimensional nonlinear consolidation of double-layered soil. *Computers and Geotechnics*. 2002;29:151-68.

[148] Lee P, Xie K, Cheung Y. A study on one-dimensional consolidation of layered systems. *International Journal for Numerical and Analytical Methods in Geomechanics*. 1992;16:815-31.

[149] Liu J-C, Lei G-H, Zheng M-X. General solutions for consolidation of multilayered soil with a vertical drain system. *Geotextiles and Geomembranes*. 2014;42:267-76.

[150] Zhou W-H, Lok TM-H, Zhao L-S, Mei G-x, Li X-B. Analytical solutions to the axisymmetric consolidation of a multi-layer soil system under surcharge combined with vacuum preloading. *Geotextiles and Geomembranes*. 2017;45:487-98.

[151] Tang X, Niu B, Cheng G, Shen H. Closed-form solution for consolidation of three-layer soil with a vertical drain system. *Geotextiles and Geomembranes*. 2013;36:81-91.

[152] Boyd J. Chebyshev and Fourier Spectral Methods. Dover Publications Inc. *New York*. 2000.

[153] Walker R, Indraratna B, Sivakugan N. Vertical and radial consolidation analysis of multilayered soil using the spectral method. *Journal of geotechnical and geoenvironmental engineering*. 2009;135:657-63.

[154] Cole KD. Analysis of Photothermal Characterization of Layered Materials–Design of Optimal Experiments. *International journal of thermophysics*. 2004;25:1567-84.

[155] Miao L, Wang X, Kavazanjian Jr E. Consolidation of a double-layered compressible foundation partially penetrated by deep mixed columns. *Journal of geotechnical and geoenvironmental engineering*. 2008;134:1210-4.

[156] Yang T, Yang JZ, Ni J. Analytical solution for the consolidation of a composite ground reinforced by partially penetrated impervious columns. *Computers and Geotechnics*. 2014;57:30-6.

[157] Gong X-n, Tian X-j, Hu W-t. Simplified method for predicating consolidation settlement of soft ground improved by floating soil-cement column. *Journal of Central South University*. 2015;22:2699-706.

[158] Yu C, Zhang A, Wang Y, Ren W. Analytical solution for consolidation of combined composite foundation reinforced with penetrated impermeable columns and partially penetrated permeable stone columns. *Computers and Geotechnics*. 2020;124:103606.

[159] Davis E, Raymond G. A non-linear theory of consolidation. *Geotechnique*. 1965;15:161-73.

[160] Gibson R, England G, Hussey M. The Theory of one-dimensional consolidation of saturated clays: 1. finite non-Linear consildation of thin homogeneous layers. *Geotechnique*. 1967;17:261-73.

[161] Gibson RE, Schiffman RL, Cargill KW. The theory of one-dimensional consolidation of saturated clays. II. Finite nonlinear consolidation of thick homogeneous layers. *Canadian geotechnical journal*. 1981;18:280-93.

[162] Xie K, Li B, Li Q. A nonlinear theory of consolidation under time-dependent loading. Proceedings of 2nd International Conference on Soft Soil Engineering Nanjing: Hohai University Press1996. p. 193-8.

[163] Lu M, Wang S, Sloan SW, Indraratna B, Xie K. Nonlinear radial consolidation of vertical drains under a general time-variable loading. *International Journal for Numerical and Analytical Methods in Geomechanics*. 2015;39:51-62.

[164] Lu M, Wang S, Sloan SW, Sheng D, Xie K. Nonlinear consolidation of vertical drains with coupled radial–vertical flow considering well resistance. *Geotextiles and Geomembranes*. 2015;43:182-9.

[165] LU M-m, XIE K-h, WANG Y-l, Cai X. Analytical solution for nonlinear consolidation of stone column reinforced composite ground. *Rock and Soil Mechanics*. 2010;31:1833-40.

[166] Taylor DW, Merchant W. A theory of clay consolidation accounting for secondary compression. *Journal of Mathematics and Physics*. 1940;19:167-85.

[167] Gibson R. A theory consolidation for soils exhibiting secondary compression. *Report*. 1961;41.

[168] Lo KY. Secondary compression of clays. *Journal of the Soil Mechanics and Foundations Division*. 1961;87:61-88.

[169] Xie KH, Xie XY, Li XB. Analytical theory for one-dimensional consolidation of clayey soils exhibiting rheological characteristics under time-dependent loading. *International journal for numerical and analytical methods in geomechanics*. 2008;32:1833-55.

[170] Yin J-H, Feng W-Q. A new simplified method and its verification for calculation of consolidation settlement of a clayey soil with creep. *Canadian Geotechnical Journal*. 2016;54:333-47.

[171] Feng WQ, Yin JH. A new simplified Hypothesis B method for calculating consolidation settlements of double soil layers exhibiting creep. *International Journal for Numerical and Analytical Methods in Geomechanics*. 2017;41:899-917.

[172] Huang Mh, Li Jc. Consolidation of viscoelastic soil by vertical drains incorporating fractional-derivative model and time-dependent loading. *International Journal for Numerical and Analytical Methods in Geomechanics*. 2019;43:239-56.

[173] Blight GE. Strength and consolidation characteristics of compacted soils: Imperial College London, 1961.

[174] Scott R. Principle of Soil Mechanics, Addison. Wesley Publishing Comp. Inc, New York, 1963.

[175] Barden L. Consolidation of compacted and unsaturated clays. *Geotechnique*. 1965;15:267-86.

[176] Fredlund DG, Hasan JU. One-dimensional consolidation theory: unsaturated soils. *Canadian Geotechnical Journal*. 1979;16:521-31.

[177] Wang L, Zhou A, Xu Y, Xia X. Consolidation of unsaturated composite ground reinforced by permeable columns. *Computers and Geotechnics*. 2020;125:103706.

[178] Ho L, Fatahi B. Analytical solution to axisymmetric consolidation of unsaturated soil stratum under equal strain condition incorporating smear effects. *International Journal for Numerical and Analytical Methods in Geomechanics*. 2018;42:1890-913.

[179] Zhou W-H. Axisymmetric consolidation of unsaturated soils by differential quadrature method. *Mathematical Problems in Engineering*. 2013;2013.

[180] Zhou W-H, Zhao L-S, Lok TM-H, Mei G-x, Li X-B. Analytical solutions to the axisymmetrical consolidation of unsaturated soils. *Journal of Engineering Mechanics*. 2017;144:04017152.

[181] Wang L, Xu Y, Xia X, Sun Da. Semi-analytical solutions to two-dimensional plane strain consolidation for unsaturated soil. *Computers and Geotechnics*. 2018;101:100-13.

[182] Qin A, Sun Da, Yang L, Weng Y. A semi-analytical solution to consolidation of unsaturated soils with the free drainage well. *Computers and Geotechnics*. 2010;37:867-75.

[183] Chan K, Poon B. New Analytical Approach for Predicting Horizontal Displacement of Stone Columns. *Ground Improvement Case Histories: Embankments with Special Reference to Consolidation and Other Physical Methods*. 2015:479.

[184] Deb K. A mathematical model to study the soil arching effect in stone column-supported embankment resting on soft foundation soil. *Applied Mathematical Modelling*. 2010;34:3871-83.

[185] Basack S, Indraratna B, Rujikiatkamjorn C, Siahaan F. Theoretical and numerical perspectives on performance of stone-column-improved soft ground with reference to transport infrastructure. 2015.

[186] Polyanin AD, Nazaikinskii VE. Handbook of linear partial differential equations for engineers and scientists: CRC press, 2015.

[187] Polyanin AD, Zaitsev VF. Handbook of nonlinear partial differential equations: CRC press, 2004.

[188] Hahn DW, Özişik MN. Heat conduction. 3rd ed. Hoboken, New Jersey: John Wiley & Sons, 2012.

[189] Leung AW. Nonlinear systems of partial differential equations. *Application to life and physical sciences: World Scientific Publishing*. 2009;38.

[190] Cherniha R, Serov M, Pliukhin O. Nonlinear Reaction-Diffusion-Convection Equations: Lie and Conditional Symmetry, Exact Solutions, and Their Applications: Chapman and Hall/CRC, 2017.

[191] Pao C, Wang Y-M. Numerical solutions of a three-competition Lotka–Volterra system. *Applied Mathematics and computation*. 2008;204:423-40.

[192] Pao C. Numerical analysis of coupled systems of nonlinear parabolic equations. *SIAM journal on numerical analysis*. 1999;36:393-416.

[193] Pao C. Numerical methods for coupled systems of nonlinear parabolic boundary value problems. *Journal of mathematical analysis and applications*. 1990;151:581-608.

[194] Pao C. Finite difference reaction–diffusion systems with coupled boundary conditions and time delays. *Journal of mathematical analysis and applications*. 2002;272:407-34.

[195] Bear J. Dynamics of fluids in porous media: Courier Corporation, 2013.

[196] Cole KD, Beck JV, Haji-Sheikh A, Litkouhi B. Heat conduction using Green's functions. 2 ed: CRC Press, 2011.

[197] Duffy DG. Green's functions with applications. 2nd ed. Boca Raton: CRC Press, 2015.

[198] Churchill RV. Fourier series and boundary value problems. 1941.

[199] Deb K, Mohapatra SR. Analysis of stone column-supported geosynthetic-reinforced embankments. *Applied Mathematical Modelling*. 2013;37:2943-60.

[200] Deb K, Basudhar P, Chandra S. Generalized model for geosynthetic-reinforced granular fill-soft soil with stone columns. *International Journal of Geomechanics*. 2007;7:266-76.

[201] Deb K. Modeling of granular bed-stone column-improved soft soil. *International journal for numerical and analytical methods in geomechanics*. 2008;32:1267-88.

[202] Deb K, Chandra S, Basudhar P. Response of multilayer geosynthetic-reinforced bed resting on soft soil with stone columns. *Computers and Geotechnics*. 2008;35:323-30.

[203] Carrillo N. Simple two and three dimensional case in the theory of consolidation of soils. *Journal of Mathematics and Physics*. 1942;21:1-5.

[204] Zhu G, Yin J. Consolidation of soil with vertical and horizontal drainage under ramp load. *Geotechnique*. 2001;51:361-7.

[205] Helm D. Three-dimensional consolidation theory in terms of the velocity of solids. *Geotechnique*. 1987;37:369-92.

[206] McKinley JD. Coupled consolidation of a solid, infinite cylinder using a Terzaghi formulation. *Computers and Geotechnics*. 1998;23:193-204.

[207] Chai J-C, Shrestha S, Hino T, Ding W-Q, Kamo Y, Carter J. 2D and 3D analyses of an embankment on clay improved by soil–cement columns. *Computers and Geotechnics*. 2015;68:28-37.

[208] Jamsawang P, Phongphinittana E, Voottipruex P, Bergado DT, Jongpradist P. Comparative performances of two-and three-dimensional analyses of soil-cement mixing columns under an embankment load. *Marine Georesources & Geotechnology*. 2018:1-18.

[209] Das AK, Deb K. Response of Cylindrical Storage Tank Foundation Resting on Tensionless Stone Column-Improved Soil. *International Journal of Geomechanics*. 2017;17:04016035.

[210] Sexton BG, Sivakumar V, McCabe BA. Creep improvement factors for vibro-replacement design. *Proceedings of the Institution of Civil Engineers-Ground Improvement*. 2017;170:35-56.

[211] Aviles-Ramos C, Haji-Sheikh A, Beck J. Exact solution of heat conduction in composite materials and application to inverse problems. *Journal of heat transfer*. 1998;120:592-9.

[212] PLAXIS BV. PLAXIS 2D, version 2017 - two-dimensional finite element program. The Netherlands2017.

[213] Mitchell JK. Soil Improvement — State-of-the-Art Report. Proc, 11th Int Conf on SMFE1981. p. 509-65.

[214] Le TM, Fatahi B, Khabbaz H, Sun W. Numerical optimization applying trust-region reflective least squares algorithm with constraints to optimize the non-linear creep parameters of soft soil. *Applied Mathematical Modelling*. 2017;41:236-56.

[215] Aviles-Ramos C, Rudy C. Exact solution of heat conduction in a two-domain composite cylinder with an orthotropic outer layer. Los Alamos National Lab., NM (US), 2000.

[216] Zill DG, Wright WS, Cullen MR. Differential Equations with Boundary-Value Problems. 8 ed: Boston, MA : Brooks/Cole, Cengage Learning, 2013.

[217] Zhu G, Yin J-H. Consolidation of soil under depth-dependent ramp load. *Canadian Geotechnical Journal*. 1998;35:344-50.

[218] Stewart D, Fahey M. Centrifuge modelling of a stone column foundation system. Ground improvement techniques: proceedings of the Seminar on Ground Improvement Techniques featuring the Nelson Point ore handling facility at Port Hedland, Perth/19 May 1994: Curtin Printing Services, 1994. p. 101-11.

[219] Dunbavan M, Carter JP. Response of a composite stone column-clay foundation system. Ground improvement techniques: proceedings of the Seminar on Ground Improvement Techniques featuring the Nelson Point ore handling facility at Port Hedland, Perth/19 May 1994: Curtin Printing Services, 1994. p. 113-26.

[220] Doig S, Boxshall B, Mazur A. Monitoring of 19m High Iron Ore Stockpiles during Commissioning. Ground improvement techniques: proceedings of the Seminar on Ground Improvement Techniques featuring the Nelson Point ore handling facility at Port Hedland, Perth/19 May 1994: Curtin Printing Services, 1994. p. 139-49.

[221] Das AK, Deb K. Experimental and 3D numerical study on time-dependent behavior of stone column–supported embankments. *International Journal of Geomechanics*. 2018;18:04018011.

[222] Lu M, Jing H, Zhou Y, Xie K. General Analytical Model for Consolidation of Stone Column–Reinforced Ground and Combined Composite Ground. *International Journal of Geomechanics*. 2017;17:04016131.

[223] Ho L, Fatahi B. Analytical solution for the two-dimensional plane strain consolidation of an unsaturated soil stratum subjected to time-dependent loading. *Computers and Geotechnics*. 2015;67:1-16.

[224] Haji-Sheikh A, Beck J. Temperature solution in multi-dimensional multi-layer bodies. *International Journal of Heat and Mass Transfer*. 2002;45:1865-77.

[225] Bergado D, Jamsawang P, Tanchaisawat T, Lai Y, Lorenzo G. Performance of reinforced load transfer platforms for embankments supported by deep cement mixing piles. GeoCongress 2008: Geosustainability and Geohazard Mitigation2008. p. 628-37.

[226] Baumann V, Bauer GEA. The Performance of Foundations on Various Soils Stabilized by the Vibro-compaction Method. *Canadian Geotechnical Journal*. 1974;11:509-30.

[227] Hughes J, Withers N, Greenwood D. A field trial of the reinforcing effect of a stone column in soil. *Geotechnique*. 1975;25:31-44.

[228] Juran I, Guermazi A. Settlement response of soft soils reinforced by compacted sand columns. *Journal of Geotechnical Engineering*. 1988;114:930-43.

[229] Poorooshasb H, Meyerhof G. Analysis of behavior of stone columns and lime columns. *Computers and Geotechnics*. 1997;20:47-70.

[230] Bergado DT, Ruenkrairergsa T, Taesiri Y, Balasubramaniam AS. Deep soil mixing used to reduce embankment settlement. *Proceedings of the Institution of Civil Engineers - Ground Improvement*. 1999;3:145-62.

[231] Lin KQ, Wong IH. Use of deep cement mixing to reduce settlements at bridge approaches. *Journal of geotechnical and geoenvironmental engineering*. 1999;125:309-20.

[232] Zhou C, Yin J-H, Ming J-P. Bearing capacity and settlement of weak fly ash ground improved using lime fly ash or stone columns. *Canadian Geotechnical Journal*. 2002;39:585-96.

[233] Etezad M, Hanna A, Ayadat T. Bearing capacity of a group of stone columns in soft soil. *International Journal of Geomechanics*. 2015;15:04014043.

[234] Mohanty P, Samanta M. Experimental and numerical studies on response of the stone column in layered soil. *International Journal of Geosynthetics and Ground Engineering*. 2015;1:27.

[235] Abusharar SW, Han J. Two-dimensional deep-seated slope stability analysis of embankments over stone column-improved soft clay. *Engineering Geology*. 2011;120:103-10.

[236] Jamsawang P, Voottipruex P, Boathong P, Mairaing W, Horpibulsuk S. Three-dimensional numerical investigation on lateral movement and factor of safety of slopes stabilized with deep cement mixing column rows. *Engineering geology*. 2015;188:159-67.

[237] Kitazume M, Maruyama K. External stability of group column type deep mixing improved ground under embankment loading. *Soils and foundations*. 2006;46:323-40.

[238] Kitazume M, Maruyama K. Internal stability of group column type deep mixing improved ground under embankment loading. *Soils and Foundations*. 2007;47:437-55.

[239] Scott RF. Solidification and consolidation of a liquefied sand column. *Soils and Foundations*. 1986;26:23-31.

[240] Badanagki M, Dashti S, Paramasivam B, Tiznado JC. How do granular columns affect the seismic performance of non-uniform liquefiable sites and their overlying structures? *Soil Dynamics and Earthquake Engineering*. 2019;125:105715.

[241] Brennan A, Madabhushi S. Effectiveness of vertical drains in mitigation of liquefaction. *Soil Dynamics and Earthquake Engineering*. 2002;22:1059-65.

[242] Pal S, Deb K. Effect of stiffness of stone column on drainage capacity during soil liquefaction. *International Journal of Geomechanics*. 2018;18:04018003.

[243] Rayamajhi D, Ashford SA, Boulanger RW, Elgamal A. Dense granular columns in liquefiable ground. I: shear reinforcement and cyclic stress ratio reduction. *Journal of Geotechnical and Geoenvironmental Engineering*. 2016;142:04016023.

[244] Rayamajhi D, Boulanger RW, Ashford SA, Elgamal A. Dense granular columns in liquefiable ground. II: effects on deformations. *Journal of Geotechnical and Geoenvironmental Engineering*. 2016;142:04016024.

[245] Asgari A, Oliaei M, Bagheri M. Numerical simulation of improvement of a liquefiable soil layer using stone column and pile-pinning techniques. *Soil Dynamics and Earthquake Engineering*. 2013;51:77-96.

[246] Badanagki M, Dashti S, Kirkwood P. Influence of dense granular columns on the performance of level and gently sloping liquefiable sites. *Journal of Geotechnical and Geoenvironmental Engineering*. 2018;144:04018065.

[247] Zou Y-X, Zhang J-M, Wang R. Seismic analysis of stone column improved liquefiable ground using a plasticity model for coarse-grained soil. *Computers and Geotechnics*. 2020;125:103690.

[248] Horpibulsuk S, Chinkulkijniwat A, Cholphatsorn A, Suebsuk J, Liu MD. Consolidation behavior of soil–cement column improved ground. *Computers and Geotechnics*. 2012;43:37-50.

[249] Jiang Y, Zheng G, Han J. Numerical Evaluation of Consolidation of Soft Foundations Improved by Sand–Deep-Mixed Composite Columns. *International Journal of Geomechanics*. 2017;17:04017034.

[250] Yin J-H, Fang Z. Physical modelling of consolidation behaviour of a composite foundation consisting of a cement-mixed soil column and untreated soft marine clay. *Geotechnique*. 2006;56:63-8.

[251] Pongsivasathit S, Chai J, Ding W. Consolidation settlement of floating-column-improved soft clayey deposit. *Proceedings of the Institution of Civil Engineers-Ground Improvement*. 2013;166:44-58.

[252] Zhu G, Yin JH. Finite element consolidation analysis of soils with vertical drain. *International Journal for Numerical and Analytical Methods in Geomechanics*. 2000;24:337-66.

[253] Voottipruex P, Bergado D, Suksawat T, Jamsawang P, Cheang W. Behavior and simulation of deep cement mixing (DCM) and stiffened deep cement mixing (SDCM) piles under full scale loading. *Soils and Foundations*. 2011;51:307-20.

[254] Zhang Z, Ye G, Cai Y, Zhang Z. Centrifugal and numerical modeling of stiffened deep mixed column-supported embankment with a slab over soft clay. *Canadian Geotechnical Journal*. 2018.

[255] Hosseinpour I, Almeida M, Riccio M. Full-scale load test and finite-element analysis of soft ground improved by geotextile-encased granular columns. *Geosynthetics International*. 2015;22:428-38.

[256] Dang LC, Dang CC, Khabbaz H, Fatahi B. Numerical assessment of fibre inclusion in a load transfer platform for pile-supported embankments over soft soil. Geo-China 20162016. p. 148-55.

[257] Dang L, Dang C, Khabbaz M. Behaviour of columns and fibre reinforced load transfer platform supported embankments built on soft soil. the 15th International Conference of the International Association for Computer Methods and Advances in Geomechanics2017.

[258] Dang LC, Dang CC, Khabbaz H. Numerical analysis on the performance of fibre reinforced load transfer platform and deep mixing columns supported embankments. International Congress and Exhibition" Sustainable Civil Infrastructures: Innovative Infrastructure Geotechnology": Springer, 2017. p. 157-69.

[259] Dang LC, Dang CC, Khabbaz H. A parametric study of deep mixing columns and fibre reinforced load transfer platform supported embankments. Civil Infrastructures Confronting Severe Weathers and Climate Changes Conference: Springer, 2018. p. 179-94.

[260] Dang CC, Dang LC. Numerical investigation on the stability of soil-cement columns reinforced riverbank. International Conference on Information Technology in Geo-Engineering: Springer, 2019. p. 879-88.

[261] Dang CC, Dang LC. Influence of Fibre-Reinforced Load Transfer Platform Supported Embankment on Floating Columns Improved Soft Soils. *Advances in Environmental Vibration and Transportation Geodynamics: Proceedings of ISEV 2018*. 2020;66:215.

[262] Dang CC, Dang LC. Evaluation of the at-rest lateral earth pressure coefficient of fibre reinforced load transfer platform and columns supported embankments. CIGOS 2019, Innovation for Sustainable Infrastructure: Springer, 2020. p. 647-52.

[263] Dang LC, Dang CC, Khabbaz H. Modelling of columns and fibre-reinforced load-transfer platform-supported embankments. *Proceedings of the Institution of Civil Engineers-Ground Improvement*. 2020;173:197-215.

[264] Dang CC, Dang LC, Khabbaz H. Predicting the stability of riverbank slope reinforced with columns under various river water conditions. 4th International Conference on Transportation Geotechnics (ICTG). Chicago, USA: Springer, 2021.

[265] Dang CC, Dang LC, Khabbaz H, Sheng D. Numerical study on deformation characteristics of fibre-reinforced load-transfer platform and columns-supported embankments. *Canadian Geotechnical Journal*. 2021;58:328-50.

[266] Tang XW, Onitsuka K. Consolidation of double-layered ground with vertical drains. *International Journal for Numerical and Analytical Methods in Geomechanics*. 2001;25:1449-65.

[267] Tang X, Onitsuka K. Consolidation of ground with partially penetrated vertical drains. *Geotechnical Engineering*. 1998;29.

[268] Geng X, Indraratna B, Rujikiatkamjorn C. Effectiveness of partially penetrating vertical drains under a combined surcharge and vacuum preloading. *Canadian Geotechnical Journal*. 2011;48:970-83.

[269] Pulko B, Logar J. Fully coupled solution for the consolidation of poroelastic soil around elastoplastic stone column. *Acta Geotechnica*. 2017;12:869-82.

[270] Pulko B, Logar J. Fully coupled solution for the consolidation of poroelastic soil around geosynthetic encased stone columns. *Geotextiles and Geomembranes*. 2017;45:616-26.

APPENDICES

Appendix A. Derivation of the solutions for excess pore water pressure $(u_c^{(i)}, u_s^{(i)})$ and $(u_c^{(ii)}, u_s^{(ii)})$ corresponding to the eigenfunctions $(R_{cmn}^{(i)}, R_{smn}^{(i)})$ and $(R_{cmn}^{(ii)}, R_{smn}^{(ii)})$

Considering the real value pair $(\nu_{cmn}^r, \nu_{smn}^r)$ (i.e. $(\nu_{cmn}^{(i)}, \nu_{smn}^{(i)})$), the accompanying Equations (4.12a) and (4.12b) are standard parametric Bessel equations of order zero in which the general solutions can be presented in the following forms:

$$R_{cmn}^{(i)}(r) = A_{cmn}^{(i)} J_0\left(\nu_{cmn}^{(i)} r\right) + B_{cmn}^{(i)} Y_0\left(\nu_{cmn}^{(i)} r\right) \tag{A.1a}$$

$$R_{smn}^{(i)}(r) = A_{smn}^{(i)} J_0\left(\nu_{smn}^{(i)} r\right) + B_{smn}^{(i)} Y_0\left(\nu_{smn}^{(i)} r\right) \tag{A.1b}$$

where $A_{cmn}^{(i)}$, $B_{cmn}^{(i)}$, $A_{smn}^{(i)}$ and $B_{smn}^{(i)}$ are the constants to be determined; J_0 and Y_0 are the Bessel functions of the first and second kind of order zero, respectively.

The time-dependent functions of the eigenvalues $\beta_{mn}^{(i)}$ corresponding to $(\nu_{cmn}^{(i)}, \nu_{smn}^{(i)})$ are shown as:

$$T_{cmn}^{(i)}(t) = T_{smn}^{(i)}(t) = T_{mn}^{(i)}(t) = e^{-\beta_{mn}^{(i)\,2} t} \tag{A.2}$$

Then, the general solution for the excess pore water pressure at any point in the unit cell due to the contribution of the eigenvalues pair $(\nu_{cmn}^{(i)}, \nu_{smn}^{(i)})$, is constructed by substituting the solutions in Equations (4.15), (A.2), (A.1a), and (A.1b) into Equations (4.8a) and (4.8b), introducing a new constant $C_{mn}^{(i)}$, and applying the superposition principle as:

$$u_c^{(i)}(r,z,t) = \sum_{m=1}^{\infty}\sum_{n=1}^{\infty} C_{mn}^{(i)}\, Z_m(z)\; R_{cmn}^{(i)}(r)\; e^{-\frac{c_{ch}\,\mu_{cmn}^{(i)\,2}}{b^2}t} \qquad \left(0 \le r \le a\right) \tag{A.3a}$$

$$u_s^{(i)}(r,z,t) = \sum_{m=1}^{\infty}\sum_{n=1}^{\infty} C_{mn}^{(i)}\, Z_m(z)\; R_{smn}^{(i)}(r)\; e^{-\frac{c_{sh}\,\mu_{smn}^{(i)\,2}}{b^2}t} \qquad \left(a \le r \le b\right) \tag{A.3b}$$

where the eigenvalues $\beta_{mn}^{(i)}$ have been expressed in terms of their constant multiples (i.e. $\mu_{cmn}^{(i)}$ and $\mu_{smn}^{(i)}$) (see Appendix B).

To finalize the solutions in Equations (A.3), the initial conditions in Equations (4.7) are applied that yield:

$$\sigma_c(r,z) = \sum_{m=1}^{\infty}\sum_{n=1}^{\infty} C_{mn}^{(i)}\, Z_m(z)\; R_{cmn}^{(i)}(r) \qquad \left(0 \le r \le a\right) \tag{A.4a}$$

$$\sigma_s(r,z) = \sum_{m=1}^{\infty}\sum_{n=1}^{\infty} C_{mn}^{(i)}\, Z_m(z)\; R_{smn}^{(i)}(r) \qquad \left(a \le r \le b\right) \tag{A.4b}$$

The series in Equations (A.4) with the coefficients $C_{mn}^{(i)}$ are known as Fourier-Bessel series. Thus, the corresponding Fourier-Bessel coefficients can be determined using the orthogonal expansion technique over the 2-region cylinder as follows:

$$C_{mn}^{(i)} = \frac{1}{N_{mn}^{(i)}}\left[\begin{array}{l} \dfrac{k_{ch}}{c_{ch}}\displaystyle\int_{z=0}^{H}\int_{r=0}^{a} Z_m(z)\; R_{cmn}^{(i)}(r)\; \sigma_c(r,z)\; r\, dr\, dz \\ +\dfrac{k_{sh}}{c_{sh}}\displaystyle\int_{z=0}^{H}\int_{r=a}^{b} Z_m(z)\; R_{smn}^{(i)}(r)\; \sigma_s(r,z)\; r\, dr\, dz \end{array}\right] \tag{A.5}$$

where $N_{mn}^{(i)}$ are the norms corresponding to the eigenfunctions for both *r*- and *z*-directions and defined as:

$$N_{mn}^{(i)} = \frac{k_{ch}}{c_{ch}}\int_{z=0}^{H}\int_{r=0}^{a}\left[Z_m(z)\; R_{cmn}^{(i)}(r)\right]^2 r\, dr\, dz + \frac{k_{sh}}{c_{sh}}\int_{z=0}^{H}\int_{r=a}^{b}\left[Z_m(z)\; R_{smn}^{(i)}(r)\right]^2 r\, dr\, dz \tag{A.6}$$

Finally, the solutions in Equations (A.3) are fully achieved once the coefficients $C_{mn}^{(i)}$ are determined.

Considering the pair $(\nu_{cmn}^{c}, \nu_{smn}^{r})$ (i.e. corresponding to the real value pair $(\nu_{cmn}^{(ii)}, \nu_{smn}^{(ii)})$), the accompanying Equations (4.12a) and (4.12b) are in the modified form and standard form of parametric Bessel equation of order zero, respectively. Thus, general solutions can be obtained as follows:

$$R_{cmn}^{(ii)}(r) = A_{cmn}^{(ii)}\, I_0\left(\nu_{cmn}^{(ii)} r\right) + B_{cmn}^{(ii)}\, K_0\left(\nu_{cmn}^{(ii)} r\right) \tag{A.7a}$$

$$R_{smn}^{(ii)}(r) = A_{smn}^{(ii)}\, J_0\left(\nu_{smn}^{(ii)} r\right) + B_{smn}^{(ii)}\, Y_0\left(\nu_{smn}^{(ii)} r\right) \tag{A.7b}$$

where I_0 and K_0 are the modified Bessel functions of the first and second kind of order zero, respectively.

The time-dependent functions of the eigenvalues $\beta_{mn}^{(ii)}$ corresponding to $(\nu_{cmn}^{(ii)}, \nu_{smn}^{(ii)})$ are:

$$T_{cmn}^{(ii)}(t) = T_{smn}^{(ii)}(t) = T_{mn}^{(ii)}(t) = e^{-\beta_{mn}^{(ii)\,2} t} \tag{A.8}$$

Following the procedure to derive the solutions in Equations (A.3), the general solution for the excess pore water pressure at any point in the unit cell due to the contribution of the eigenvalues pair $(\nu_{cmn}^{(ii)}, \nu_{smn}^{(ii)})$ is obtained by substituting the solutions in Equations (4.15), (A.8), (A.7a), and (A.7b) into Equations (4.8a) and (4.8b), introducing a new constant $C_{mn}^{(ii)}$, then applying the superposition principle as:

$$u_c^{(ii)}(r,z,t) = \sum_{m=1}^{\infty} \sum_{n=1}^{F(m)} C_{mn}^{(ii)}\, Z_m(z)\, R_{cmn}^{(ii)}(r)\, e^{-\frac{c_{ch}\, \mu_{cmn}^{(ii)\,2}}{b^2} t} \qquad \left(0 \le r \le a\right) \tag{A.9a}$$

$$u_s^{(ii)}(r,z,t) = \sum_{m=1}^{\infty} \sum_{n=1}^{F(m)} C_{mn}^{(ii)}\, Z_m(z)\, R_{smn}^{(ii)}(r)\, e^{-\frac{c_{sh}\,\mu_{smn}^{(ii)\,2}}{b^2} t} \qquad \left(a \le r \le b\right) \tag{A.9b}$$

where the upper limit $F(m)$ of the second summation is exactly equal to the number of eigenvalues $\beta_{mn}^{(ii)}$ that can be obtained in the interval $\kappa_s\,\lambda_m\sqrt{c_{sh}} \le \beta_{mn}^{(ii)} < \kappa_c\,\lambda_m\sqrt{c_{ch}}$ for each specified value of m. Therefore, the index n accepts a finite value of the upper limit $F(m)$ in this case. The eigenvalues $\beta_{mn}^{(ii)}$ have been expressed in terms of their constant multiples (i.e. $\mu_{cmn}^{(ii)}$ and $\mu_{smn}^{(ii)}$) (see Appendix B).

Similar to the determination of $C_{mn}^{(i)}$, the Fourier-Bessel coefficients $C_{mn}^{(ii)}$ are produced by applying the initial conditions in Equations (4.7) to the solutions in Equations (A.9) and utilising the orthogonal expansion technique.

$$C_{mn}^{(ii)} = \frac{1}{N_{mn}^{(ii)}} \left[\begin{array}{l} \dfrac{k_{ch}}{c_{ch}} \displaystyle\int_{z=0}^{H} \int_{r=0}^{a} Z_m(z)\, R_{cmn}^{(ii)}(r)\, \sigma_c(r,z)\, r\, dr\, dz \\ + \dfrac{k_{sh}}{c_{sh}} \displaystyle\int_{z=0}^{H} \int_{r=a}^{b} Z_m(z)\, R_{smn}^{(ii)}(r)\, \sigma_s(r,z)\, r\, dr\, dz \end{array} \right] \tag{A.10}$$

where $N_{mn}^{(ii)}$ are the norms corresponding to the eigenfunctions for both *r*- and *z*-directions and given by:

$$N_{mn}^{(ii)} = \frac{k_{ch}}{c_{ch}} \int_{z=0}^{H} \int_{r=0}^{a} \left[Z_m(z)\, R_{cmn}^{(ii)}(r) \right]^2 r\, dr\, dz + \frac{k_{sh}}{c_{sh}} \int_{z=0}^{H} \int_{r=a}^{b} \left[Z_m(z)\, R_{smn}^{(ii)}(r) \right]^2 r\, dr\, dz \tag{A.11}$$

The solutions in Equations (A.9) are finalized when the coefficients $C_{mn}^{(ii)}$ are obtained.

Appendix B. Derivation of the eigenvalues pairs $(\nu_{cmn}^{(i)}, \nu_{smn}^{(i)})$ and $(\nu_{cmn}^{(ii)}, \nu_{smn}^{(ii)})$ and their corresponding eigenfunctions $(R_{cmn}^{(i)}, R_{smn}^{(i)})$ and $(R_{cmn}^{(ii)}, R_{smn}^{(ii)})$

The combination $(\nu_{cmn}^{r}, \nu_{smn}^{r})$ (i.e. $(\nu_{cmn}^{(i)}, \nu_{smn}^{(i)})$) is solely attained if the expressions under the square roots in Equations (4.19a) and (4.19b) are both non-negative; i.e.

$$\frac{\beta_{mn}^2}{c_{ch}} - \kappa_c^2 \lambda_m^2 \geq 0 \qquad \text{and} \qquad \frac{\beta_{mn}^2}{c_{sh}} - \kappa_s^2 \lambda_m^2 \geq 0 \tag{B.1}$$

Thus, the equations for $\nu_{cmn}^{(i)}$ and $\nu_{smn}^{(i)}$ are given by:

$$\nu_{cmn}^{(i)} = \sqrt{\frac{\beta_{mn}^{(i)\,2}}{c_{ch}} - \kappa_c^2 \lambda_m^2} \qquad \text{where} \quad \frac{\beta_{mn}^{(i)\,2}}{c_{ch}} - \kappa_c^2 \lambda_m^2 \geq 0 \tag{B.2a}$$

$$\nu_{smn}^{(i)} = \sqrt{\frac{\beta_{mn}^{(i)\,2}}{c_{sh}} - \kappa_s^2 \lambda_m^2} \qquad \text{where} \quad \frac{\beta_{mn}^{(i)\,2}}{c_{sh}} - \kappa_s^2 \lambda_m^2 \geq 0 \tag{B.2b}$$

where the new notation $\beta_{mn}^{(i)}$ is used along with the real eigenvalues pair $(\nu_{cmn}^{(i)}, \nu_{smn}^{(i)})$.

Applying the finiteness condition for excess pore water pressure at the centerline of stone column to Equation (A.1a) yields, $B_{cmn}^{(i)} = 0$. It should also be noted that the boundary conditions presented in Equations (4.5a), (4.5b) and (4.5c) produce a system of 3 linear, homogeneous equations in which the coefficients (i.e. the constants $A_{cmn}^{(i)}$, $A_{smn}^{(i)}$ and $B_{smn}^{(i)}$) can be resolved in terms of any non-vanishing coefficient [188]. Therefore, by setting $A_{cmn}^{(i)} = 1$ for simplicity, the solutions for the two regions of the unit cell in Equations (A.1a), and (A.1b) are recast as follows:

$$R_{cmn}^{(i)}(r) = J_0\left(\nu_{cmn}^{(i)} r\right) \tag{B.3a}$$

$$R_{smn}^{(i)}(r) = A_{smn}^{(i)} J_0\left(\nu_{smn}^{(i)} r\right) + B_{smn}^{(i)} Y_0\left(\nu_{smn}^{(i)} r\right) \tag{B.3b}$$

To satisfy the two inequalities captured in Equations (B.2a) and (B.2b) simultaneously, $\beta_{mn}^{(i)}$ values must satisfy the following condition:

$$\beta_{mn}^{(i)} \geq \max\left\{\kappa_c\, \lambda_m \sqrt{c_{ch}},\, \kappa_s\, \lambda_m \sqrt{c_{sh}}\right\} \tag{B.4}$$

Although the present problem can be solved directly in terms of the eigenvalues $\beta_{mn}^{(i)}$ in mathematical sense, it is inconsistent in physical meaning (i.e. in dimensions) when the eigenvalues $\nu_{cmn}^{(i)}$ and $\nu_{smn}^{(i)}$ expressed in terms of $\beta_{mn}^{(i)}$ as shown in Equations (B.2a) and (B.2b) are introduced to their corresponding eigenfunctions $R_{cmn}^{(i)}$ and $R_{smn}^{(i)}$. To resolve this, the following change of variable is applied where $\mu_{cmn}^{(i)}$ and $\mu_{smn}^{(i)}$ are constant multiples of $\beta_{mn}^{(i)}$ and vice versa because of the constant values of $\sqrt{c_{ch}}$, $\sqrt{c_{sh}}$ and b.

$$\frac{\beta_{mn}^{(i)}}{\sqrt{c_{ch}}} = \frac{\mu_{cmn}^{(i)}}{b} \qquad \text{and} \qquad \frac{\beta_{mn}^{(i)}}{\sqrt{c_{sh}}} = \frac{\mu_{smn}^{(i)}}{b} \tag{B.5a}$$

As a result, the arguments of Bessel functions in $R_{cmn}^{(i)}$ and $R_{smn}^{(i)}$ are dimensionless with an actual physical meaning. Additionally, the condition reported in Equation (4.10) followed by Equation (A.2) leads to the following equations:

$$\beta_{mn}^{(i)} = \frac{\sqrt{c_{ch}}\, \mu_{cmn}^{(i)}}{b} = \frac{\sqrt{c_{sh}}\, \mu_{smn}^{(i)}}{b} \tag{B.5b}$$

$$\mu_{cmn}^{(i)} = \mu_{smn}^{(i)} \sqrt{\frac{c_{sh}}{c_{ch}}} \tag{B.5c}$$

where $\mu_{cmn}^{(i)}$ and $\mu_{smn}^{(i)}$ are the alternative forms of the eigenvalues $\beta_{mn}^{(i)}$ for the stone column and surrounding soil regions, respectively.

Substituting $\beta_{mn}^{(i)} = \sqrt{c_{sh}}\,\mu_{smn}^{(i)} / b$ into Equation (B.4) and taking advantage of Equations (4.14) and (4.16) along with the fact that $c_{cv} > c_{sv}$, the eigenvalues $\mu_{smn}^{(i)}$ should satisfy the following:

$$\mu_{smn}^{(i)} \geq \frac{\sqrt{c_{cv}}}{\sqrt{c_{sh}}}\frac{b}{H}\omega_m = \sqrt{\frac{c_{cv}}{c_{sh}}}\frac{b}{H}\omega_m \tag{B.6}$$

Combining Equations (4.16) and (B.5a) with Equations (B.2a) and (B.2b), the following equations can be derived for $\nu_{cmn}^{(i)}$ and $\nu_{smn}^{(i)}$:

$$\nu_{cmn}^{(i)} = \sqrt{\frac{\mu_{cmn}^{(i)\,2}}{b^2} - \kappa_c^2\frac{\omega_m^2}{H^2}} = \sqrt{\left(\frac{\mu_{cmn}^{(i)}}{b}\right)^2 - \left(\kappa_c\frac{\omega_m}{H}\right)^2} \tag{B.7a}$$

$$\nu_{smn}^{(i)} = \sqrt{\frac{\mu_{smn}^{(i)\,2}}{b^2} - \kappa_s^2\frac{\omega_m^2}{H^2}} = \sqrt{\left(\frac{\mu_{smn}^{(i)}}{b}\right)^2 - \left(\kappa_s\frac{\omega_m}{H}\right)^2} \tag{B.7b}$$

Incorporating boundary conditions reported in Equations (4.5a), (4.5b) and (4.5c) into solutions presented in Equations (B.3a) and (B.3b), the transcendental equation for determining the eigenvalues $\mu_{cmn}^{(i)}$ and $\mu_{smn}^{(i)}$ and the subsequent equations of the constants $A_{smn}^{(i)}$ and $B_{smn}^{(i)}$ are achieved.

Indeed, the transcendental equation can be presented in the following form:

$$\nu_{smn}^{(i)}\begin{bmatrix} N_k\,\nu_{cmn}^{(i)}J_1\left(\nu_{cmn}^{(i)}a\right)\left[J_1\left(\nu_{smn}^{(i)}b\right)Y_0\left(\nu_{smn}^{(i)}a\right) - J_0\left(\nu_{smn}^{(i)}a\right)Y_1\left(\nu_{smn}^{(i)}b\right)\right] \\ +\nu_{smn}^{(i)}J_0\left(\nu_{cmn}^{(i)}a\right)\left[-J_1\left(\nu_{smn}^{(i)}b\right)Y_1\left(\nu_{smn}^{(i)}a\right) + J_1\left(\nu_{smn}^{(i)}a\right)Y_1\left(\nu_{smn}^{(i)}b\right)\right] \end{bmatrix} = 0 \tag{B.8}$$

where the eigenvalues $\mu_{cmn}^{(i)}$ and $\mu_{smn}^{(i)}$ are determined by substituting Equations (B.7a), (B.7b) and (B.5c) into Equation (B.8), J_1 and Y_1 are the Bessel functions of the first and second kind of order one, respectively, $N_k = k_{ch} / k_{sh}$ is the horizontal permeability ratio

of the column to the surrounding soil. When $\mu_{cmn}^{(i)}$ and $\mu_{smn}^{(i)}$ have been achieved, $\nu_{cmn}^{(i)}$ and $\nu_{smn}^{(i)}$ can also be determined via Equations (B.7a) and (B.7b).

The corresponding equations for $A_{smn}^{(i)}$ and $B_{smn}^{(i)}$ with respect to $\nu_{cmn}^{(i)}$ and $\nu_{smn}^{(i)}$ are:

$$A_{smn}^{(i)} = \frac{1}{\Delta_{mn}^{(i)}}\left[N_k \, \nu_{cmn}^{(i)} J_1\left(\nu_{cmn}^{(i)} a\right) Y_0\left(\nu_{smn}^{(i)} a\right) - \nu_{smn}^{(i)} J_0\left(\nu_{cmn}^{(i)} a\right) Y_1\left(\nu_{smn}^{(i)} a\right)\right] \tag{B.9a}$$

$$B_{smn}^{(i)} = -\frac{1}{\Delta_{mn}^{(i)}}\left[N_k \, \nu_{cmn}^{(i)} J_1\left(\nu_{cmn}^{(i)} a\right) J_0\left(\nu_{smn}^{(i)} a\right) - \nu_{smn}^{(i)} J_0\left(\nu_{cmn}^{(i)} a\right) J_1\left(\nu_{smn}^{(i)} a\right)\right] \tag{B.9b}$$

where

$$\Delta_{mn}^{(i)} = \nu_{smn}^{(i)}\left[J_1\left(\nu_{smn}^{(i)} a\right) Y_0\left(\nu_{smn}^{(i)} a\right) - J_0\left(\nu_{smn}^{(i)} a\right) Y_1\left(\nu_{smn}^{(i)} a\right)\right] \tag{B.10}$$

Once the eigenvalues $\nu_{cmn}^{(i)}$ and $\nu_{smn}^{(i)}$ and the constants $A_{smn}^{(i)}$ and $B_{smn}^{(i)}$ have been obtained, the eigenfunctions $R_{cmn}^{(i)}$ and $R_{smn}^{(i)}$ are determined according to Equations (B.3a) and (B.3b).

Considering the combination $(\nu_{cmn}^{c}, \nu_{smn}^{r})$ (i.e. corresponding to the real value pair $(\nu_{cmn}^{(ii)}, \nu_{smn}^{(ii)})$), this pair is attained if the following condition is satisfied:

$$\frac{\beta_{mn}^2}{c_{ch}} - \kappa_c^2 \, \lambda_m^2 < 0 \qquad \text{and} \qquad \frac{\beta_{mn}^2}{c_{sh}} - \kappa_s^2 \, \lambda_m^2 \geq 0 \tag{B.11}$$

It is clear that the inequalities captured in Equation (B.11) are in agreement with Equation (4.20). Hence, the combination $(\nu_{cmn}^{c}, \nu_{smn}^{r})$ will also lead to a transcendental equation by following the above-mentioned procedure. Before developing further on the transcendental equation, the following transformation of the complex number ν_{cmn}^{c} in $(\nu_{cmn}^{c}, \nu_{smn}^{r})$ should be highlighted for performing the analysis.

$$\nu_{cmn}^{c} = i\,\nu_{cmn}^{r} \tag{B.12}$$

where the notation i here denotes the imaginary unit and ν_{cmn}^{r} is a real number.

$$i = \sqrt{-1} \tag{B.13a}$$

$$\nu_{cmn}^{r} = \sqrt{\kappa_c^2\,\lambda_m^2 - \frac{\beta_{mn}^2}{c_{ch}}} \qquad \text{where} \quad \kappa_c^2\,\lambda_m^2 - \frac{\beta_{mn}^2}{c_{ch}} > 0 \tag{B.13b}$$

As a result, the original pair (complex, real) was transformed into a new pair (real, real). To distinguish from the previous real pair $(\nu_{cmn}^{(i)}, \nu_{smn}^{(i)})$ as defined by Equations (B.7a) and (B.7b), the new one is denoted by $(\nu_{cmn}^{(ii)}, \nu_{smn}^{(ii)})$ and given as:

$$\nu_{cmn}^{(ii)} = \sqrt{\kappa_c^2\,\lambda_m^2 - \frac{\beta_{mn}^{(ii)\,2}}{c_{ch}}} \qquad \text{where} \quad \kappa_c^2\,\lambda_m^2 - \frac{\beta_{mn}^{(ii)\,2}}{c_{ch}} > 0 \tag{B.14a}$$

$$\nu_{smn}^{(ii)} = \sqrt{\frac{\beta_{mn}^{(ii)\,2}}{c_{sh}} - \kappa_s^2\,\lambda_m^2} \qquad \text{where} \quad \frac{\beta_{mn}^{(ii)\,2}}{c_{sh}} - \kappa_s^2\,\lambda_m^2 \geq 0 \tag{B.14b}$$

where the new notation $\beta_{mn}^{(ii)}$ is used along with the pair $(\nu_{cmn}^{(ii)}, \nu_{smn}^{(ii)})$.

Similar to the above process with $(\nu_{cmn}^{(i)}, \nu_{smn}^{(i)})$, the finiteness condition for excess pore water pressure at the centerline of stone column leads to $B_{cmn}^{(ii)} = 0$ in Equation (A.7a). By setting $A_{cmn}^{(ii)} = 1$ without loss of generality as explained above, the solutions for the two regions of the unit cell in Equations (A.7a) and (A.7b) are written as:

$$R_{cmn}^{(ii)}(r) = I_0\left(\nu_{cmn}^{(ii)} r\right) \tag{B.15a}$$

$$R_{smn}^{(ii)}(r) = A_{smn}^{(ii)}\,J_0\left(\nu_{smn}^{(ii)} r\right) + B_{smn}^{(ii)}\,Y_0\left(\nu_{smn}^{(ii)} r\right) \tag{B.15b}$$

To satisfy the two inequalities presented in Equations (B.14a) and (B.14b) concurrently, the $\beta_{mn}^{(ii)}$ values must satisfy the following:

$$\kappa_s \lambda_m \sqrt{c_{sh}} \le \beta_{mn}^{(ii)} < \kappa_c \lambda_m \sqrt{c_{ch}} \tag{B.16}$$

The following equations can also be derived analogous to Equations (B.5a), (B.5b) and (B.5c):

$$\frac{\beta_{mn}^{(ii)}}{\sqrt{c_{ch}}} = \frac{\mu_{cmn}^{(ii)}}{b} \qquad \text{and} \qquad \frac{\beta_{mn}^{(ii)}}{\sqrt{c_{sh}}} = \frac{\mu_{smn}^{(ii)}}{b} \tag{B.17a}$$

$$\beta_{mn}^{(ii)} = \frac{\sqrt{c_{ch}}\,\mu_{cmn}^{(ii)}}{b} = \frac{\sqrt{c_{sh}}\,\mu_{smn}^{(ii)}}{b} \tag{B.17b}$$

$$\mu_{cmn}^{(ii)} = \mu_{smn}^{(ii)} \sqrt{\frac{c_{sh}}{c_{ch}}} \tag{B.17c}$$

where $\mu_{cmn}^{(ii)}$ and $\mu_{smn}^{(ii)}$ are the alternative forms of the eigenvalues $\beta_{mn}^{(ii)}$ for the stone column and surrounding soil regions, respectively.

Substituting $\beta_{mn}^{(ii)} = \sqrt{c_{sh}}\,\mu_{smn}^{(ii)} / b$ into Equation (B.16) and taking advantage of Equations (4.14) and (4.16), the condition for the eigenvalues $\mu_{smn}^{(ii)}$ is given by:

$$\sqrt{\frac{c_{sv}}{c_{sh}}} \frac{b}{H} \omega_m \le \mu_{smn}^{(ii)} < \sqrt{\frac{c_{cv}}{c_{sh}}} \frac{b}{H} \omega_m \tag{B.18}$$

Integrating Equations (4.16) and (B.17a) with Equations (B.14a) and (B.14b), the equations for $\nu_{cmn}^{(ii)}$ and $\nu_{smn}^{(ii)}$ are written as:

$$\nu_{cmn}^{(ii)} = \sqrt{\kappa_c^2 \frac{\omega_m^2}{H^2} - \frac{\mu_{cmn}^{(ii)\,2}}{b^2}} = \sqrt{\left(\kappa_c \frac{\omega_m}{H}\right)^2 - \left(\frac{\mu_{cmn}^{(ii)}}{b}\right)^2} \tag{B.19a}$$

$$\nu_{smn}^{(ii)} = \sqrt{\frac{\mu_{smn}^{(ii)\,2}}{b^2} - \kappa_s^2 \frac{\omega_m^2}{H^2}} = \sqrt{\left(\frac{\mu_{smn}^{(ii)}}{b}\right)^2 - \left(\kappa_s \frac{\omega_m}{H}\right)^2} \tag{B.19b}$$

Carrying out the procedure similar to the case of eigenvalues pair $(\nu_{cmn}^{(i)}, \nu_{smn}^{(i)})$, a new transcendental equation is obtained:

$$\nu_{smn}^{(ii)} \begin{bmatrix} N_k \nu_{cmn}^{(ii)} I_1\left(\nu_{cmn}^{(ii)} a\right)\left[-J_1\left(\nu_{smn}^{(ii)} b\right) Y_0\left(\nu_{smn}^{(ii)} a\right) + J_0\left(\nu_{smn}^{(ii)} a\right) Y_1\left(\nu_{smn}^{(ii)} b\right)\right] \\ +\nu_{smn}^{(ii)} I_0\left(\nu_{cmn}^{(ii)} a\right)\left[-J_1\left(\nu_{smn}^{(ii)} b\right) Y_1\left(\nu_{smn}^{(ii)} a\right) + J_1\left(\nu_{smn}^{(ii)} a\right) Y_1\left(\nu_{smn}^{(ii)} b\right)\right] \end{bmatrix} = 0 \tag{B.20}$$

where the eigenvalues $\mu_{cmn}^{(ii)}$ and $\mu_{smn}^{(ii)}$ are determined by substituting Equations (B.19a), (B.19b), and (B.17c) into Equation (B.20); I_1 is the modified Bessel function of the first kind of order one. The values of $\nu_{cmn}^{(ii)}$ and $\nu_{smn}^{(ii)}$ can also be determined via Equations (B.19a) and (B.19b) once $\mu_{cmn}^{(ii)}$ and $\mu_{smn}^{(ii)}$ have been resolved.

The corresponding equations for $A_{smn}^{(ii)}$ and $B_{smn}^{(ii)}$ with respect to $\nu_{cmn}^{(ii)}$ and $\nu_{smn}^{(ii)}$ are:

$$A_{smn}^{(ii)} = -\frac{1}{\Delta_{mn}^{(ii)}}\left[N_k \nu_{cmn}^{(ii)} I_1\left(\nu_{cmn}^{(ii)} a\right) Y_0\left(\nu_{smn}^{(ii)} a\right) + \nu_{smn}^{(ii)} I_0\left(\nu_{cmn}^{(ii)} a\right) Y_1\left(\nu_{smn}^{(ii)} a\right)\right] \tag{B.21a}$$

$$B_{smn}^{(ii)} = \frac{1}{\Delta_{mn}^{(ii)}}\left[N_k \nu_{cmn}^{(ii)} I_1\left(\nu_{cmn}^{(ii)} a\right) J_0\left(\nu_{smn}^{(ii)} a\right) + \nu_{smn}^{(ii)} I_0\left(\nu_{cmn}^{(ii)} a\right) J_1\left(\nu_{smn}^{(ii)} a\right)\right] \tag{B.21b}$$

where

$$\Delta_{mn}^{(ii)} = \nu_{smn}^{(ii)}\left[J_1\left(\nu_{smn}^{(ii)} a\right) Y_0\left(\nu_{smn}^{(ii)} a\right) - J_0\left(\nu_{smn}^{(ii)} a\right) Y_1\left(\nu_{smn}^{(ii)} a\right)\right] \tag{B.22}$$

Consequently, the eigenfunctions $R_{cmn}^{(ii)}$ and $R_{smn}^{(ii)}$ are completely disclosed according to Equations (B.15a) and (B.15b).

Appendix C. Derivation of Green's function for the non-homogeneous consolidation problem

Before proceeding the derivation to attain the Green's function for the non-homogeneous consolidation problem defined by Equations (5.1) − (5.4), the notation Θ would be used to denote the excess pore water pressure solution for the homogeneous problem. Then, applying the method of separation of variables, the solution of the homogeneous problem for the excess pore water pressure at any point in the foundation can be defined as:

$$\Theta_i(r,z,t) = \Theta_i^{(i)}(r,z,t) + \Theta_i^{(ii)}(r,z,t) \quad \left(r_i \le r \le r_{i+1}\right) \quad (i=1,2) \tag{C.1}$$

where the components $\Theta_i^{(i)}$ and $\Theta_i^{(ii)}$ are determined as follows:

$$\Theta_i^{(i)}(r,z,t) = \sum_{m=1}^{\infty}\sum_{n=1}^{\infty} C_{mn}^{(i)}\,\Psi_{imn}^{(i)}(r,z)\,e^{-\beta_{mn}^{(i)\,2}t} \qquad \left(r_i \le r \le r_{i+1}\right) \tag{C.2a}$$

$$\Theta_i^{(ii)}(r,z,t) = \sum_{m=1}^{\infty}\sum_{n=1}^{F(m)} C_{mn}^{(ii)}\,\Psi_{imn}^{(ii)}(r,z)\,e^{-\beta_{mn}^{(ii)\,2}t} \qquad \left(r_i \le r \le r_{i+1}\right) \tag{C.2b}$$

where m and n are integer; $C_{mn}^{(i)}$ and $C_{mn}^{(ii)}$ are the Fourier-Bessel coefficients to be determined; $\Psi_{imn}^{(i)}$ and $\Psi_{imn}^{(ii)}$ for the subscript $i=1,2$ are the eigenfunctions defined by:

$$\Psi_{1mn}^{(i)}(r,z) = J_0\left(\nu_{1mn}^{(i)} r\right)\sin\left(\lambda_m z\right) \tag{C.3a}$$

$$\Psi_{2mn}^{(i)}(r,z) = \left[A_{2mn}^{(i)}\,J_0\left(\nu_{2mn}^{(i)} r\right) + B_{2mn}^{(i)}\,Y_0\left(\nu_{2mn}^{(i)} r\right)\right]\sin\left(\lambda_m z\right) \tag{C.3b}$$

$$\Psi_{1mn}^{(ii)}(r,z) = I_0\left(\nu_{1mn}^{(ii)} r\right)\sin\left(\lambda_m z\right) \tag{C.3c}$$

$$\Psi_{2mn}^{(ii)}(r,z) = \left[A_{2mn}^{(ii)}\,J_0\left(\nu_{2mn}^{(ii)} r\right) + B_{2mn}^{(ii)}\,Y_0\left(\nu_{2mn}^{(ii)} r\right)\right]\sin\left(\lambda_m z\right) \tag{C.3d}$$

where J_0 and Y_0 are the Bessel functions of the first and second kind of order zero, respectively; I_0 is the modified Bessel function of the first kind of order zero; $\lambda_m = (2m-1)\pi/2H$ are the eigenvalues in z-domain; $A_{2mn}^{(i)}$, $B_{2mn}^{(i)}$, $A_{2mn}^{(ii)}$ and $B_{2mn}^{(ii)}$ are the constants; $\nu_{1mn}^{(i)}$, $\nu_{2mn}^{(i)}$, $\nu_{1mn}^{(ii)}$ and $\nu_{2mn}^{(ii)}$ are the eigenvalues for $\Psi_{1mn}^{(i)}$, $\Psi_{2mn}^{(i)}$, $\Psi_{1mn}^{(ii)}$ and $\Psi_{2mn}^{(ii)}$, respectively, which can be determined via λ_m, $\beta_{mn}^{(i)}$ and $\beta_{mn}^{(ii)}$ as:

$$\nu_{1mn}^{(i)} = \sqrt{\left(\beta_{mn}^{(i)\,2} - c_{1v}\,\lambda_m^2\right)/c_{1h}} \quad \text{and} \quad \nu_{2mn}^{(i)} = \sqrt{\left(\beta_{mn}^{(i)\,2} - c_{2v}\,\lambda_m^2\right)/c_{2h}} \tag{C.4a}$$

$$\nu_{1mn}^{(ii)} = \sqrt{\left(c_{1v}\,\lambda_m^2 - \beta_{mn}^{(ii)\,2}\right)/c_{1h}} \quad \text{and} \quad \nu_{2mn}^{(ii)} = \sqrt{\left(\beta_{mn}^{(ii)\,2} - c_{2v}\,\lambda_m^2\right)/c_{2h}} \tag{C.4b}$$

in which $c_{1v} = k_{1v}M_1/\gamma_w$ and $c_{1h} = k_{1h}M_1/\gamma_w$ are the consolidation coefficients for vertical and horizontal directions for the column, respectively; $c_{2v} = k_{2v}M_2/\gamma_w$ and $c_{2h} = k_{2h}M_2/\gamma_w$ are the consolidation coefficients for vertical and horizontal directions for the soil, respectively. It is important to note that due to the much higher modulus and permeability of stone column than those of soft soil, the conditions $c_{1v} > c_{2v}$ and $c_{1h} > c_{2h}$ are valid. Consequently, the eigenvalues $\nu_{1mn}^{(i)}$, $\nu_{2mn}^{(i)}$, $\nu_{1mn}^{(ii)}$ and $\nu_{2mn}^{(ii)}$ calculated by Equations (C.4a) and (C.4b) are real when $\beta_{mn}^{(i)}$ and $\beta_{mn}^{(ii)}$ satisfy the following:

$$\beta_{mn}^{(i)} \geq \lambda_m\sqrt{c_{1v}} \quad \text{and} \quad \lambda_m\sqrt{c_{2v}} \leq \beta_{mn}^{(ii)} < \lambda_m\sqrt{c_{1v}} \tag{C.5}$$

It is observed that the number of eigenvalues $\beta_{mn}^{(ii)}$ is finite for a given value of m, which is denoted by the upper limit $F(m)$ of the double series in Equation (C.2b).

Replacing the subscript $i = 1, 2$ in Equations (C.1) and (C.2) and incorporating with the boundary conditions in Equations (5.2a), (5.2b) and (5.2c), the following matrix

equations to calculate the constants $A_{2mn}^{(i)}$, $B_{2mn}^{(i)}$, $A_{2mn}^{(ii)}$, $B_{2mn}^{(ii)}$ and the eigenvalues $\nu_{1mn}^{(i)}$, $\nu_{2mn}^{(i)}$, $\nu_{1mn}^{(ii)}$, $\nu_{2mn}^{(ii)}$ can be achieved as:

$$\begin{bmatrix} J_0\left(\nu_{1mn}^{(i)}a\right) & -J_0\left(\nu_{2mn}^{(i)}a\right) & -Y_0\left(\nu_{2mn}^{(i)}a\right) \\ N_k\,\nu_{1mn}^{(i)}\,J_1\left(\nu_{1mn}^{(i)}a\right) & -\nu_{2mn}^{(i)}\,J_1\left(\nu_{2mn}^{(i)}a\right) & -\nu_{2mn}^{(i)}\,Y_1\left(\nu_{2mn}^{(i)}a\right) \\ 0 & -\nu_{2mn}^{(i)}\,J_1\left(\nu_{2mn}^{(i)}b\right) & -\nu_{2mn}^{(i)}\,Y_1\left(\nu_{2mn}^{(i)}b\right) \end{bmatrix} \begin{Bmatrix} 1 \\ A_{2mn}^{(i)} \\ B_{2mn}^{(i)} \end{Bmatrix} = \begin{Bmatrix} 0 \\ 0 \\ 0 \end{Bmatrix} \tag{C.6a}$$

$$\begin{bmatrix} I_0\left(\nu_{1mn}^{(ii)}a\right) & -J_0\left(\nu_{2mn}^{(ii)}a\right) & -Y_0\left(\nu_{2mn}^{(ii)}a\right) \\ -N_k\,\nu_{1mn}^{(ii)}\,I_1\left(\nu_{1mn}^{(ii)}a\right) & -\nu_{2mn}^{(ii)}\,J_1\left(\nu_{2mn}^{(ii)}a\right) & -\nu_{2mn}^{(ii)}\,Y_1\left(\nu_{2mn}^{(ii)}a\right) \\ 0 & -\nu_{2mn}^{(ii)}\,J_1\left(\nu_{2mn}^{(ii)}b\right) & -\nu_{2mn}^{(ii)}\,Y_1\left(\nu_{2mn}^{(ii)}b\right) \end{bmatrix} \begin{Bmatrix} 1 \\ A_{2mn}^{(ii)} \\ B_{2mn}^{(ii)} \end{Bmatrix} = \begin{Bmatrix} 0 \\ 0 \\ 0 \end{Bmatrix} \tag{C.6b}$$

where $N_k = k_{1h}/k_{2h}$ is the column to soil horizontal permeability ratio; J_1 and Y_1 are the Bessel functions of the first and second kind of order one, respectively; I_1 is the modified Bessel function of the first kind of order one. Referring to Chapter 4, $\beta_{mn}^{(i)}$ and $\beta_{mn}^{(ii)}$ along with $\nu_{1mn}^{(i)}$, $\nu_{2mn}^{(i)}$, $\nu_{1mn}^{(ii)}$ and $\nu_{2mn}^{(ii)}$ are attainable by enforcing the determinants of coefficient matrices in Equations (C.6a) and (C.6b) to be zero in combination with Equations (C.4a) and (C.4b).

To finalise the solutions in Equations (C.2a) and (C.2b), the initial conditions in Equations (5.4a) and (5.4b) are applied for which the coefficients $C_{mn}^{(i)}$ and $C_{mn}^{(ii)}$ are obtainable by taking the orthogonal expansion over the stone column and soft soil regions as follows:

$$C_{mn}^{(*)} = \frac{1}{N_{mn}^{(*)}} \sum_{j=1}^{2} \frac{k_{jh}}{c_{jh}} \int_{z'=0}^{H} \int_{r'=r_j}^{r_{j+1}} \Psi_{jmn}^{(*)}(r', z')\, \sigma_{0j}\, r'\, dr'\, dz' \quad (j = 1, 2) \tag{C.7}$$

and

$$N_{mn}^{(*)} = \sum_{j=1}^{2} \frac{k_{jh}}{c_{jh}} \int_{z'=0}^{H} \int_{r'=r_j}^{r_{j+1}} \left[\Psi_{jmn}^{(*)}(r', z') \right]^2 r' \, dr' \, dz' \tag{C.8}$$

where the superscript $(*)$ has been recalled to denote the superscript (i) or (ii) in order to avoid repeating expressions which have the same formulation in Equations (C.7) and (C.8) as well as the following derivation.

Substituting Equation (C.7) into Equations (C.2a) and (C.2b) and rearranging the resulting expressions, the solutions $\Theta_i^{(i)}$ and $\Theta_i^{(ii)}$ can be rewritten applying Green's formula [188, 196] as:

$$\Theta_i^{(*)}(r, z, t) = \sum_{j=1}^{2} \int_{z'=0}^{H} \int_{r'=r_j}^{r_{j+1}} G_{ij}^{(*)}(r, z, t \mid r', z', t') \Big|_{t'=0} \sigma_{0j} \, r' \, dr' \, dz' \tag{C.9}$$

where

$$G_{ij}^{(*)}(r, z, t \mid r', z', t') \Big|_{t'=0} = \sum_{m=1}^{\infty} \sum_{n=1}^{\infty / F(m)} \Psi_{imn}^{(*)}(r, z) \, e^{-\beta_{mn}^{(*)\,2} t} \frac{1}{N_{mn}^{(*)}} \frac{k_{jh}}{c_{jh}} \Psi_{jmn}^{(*)}(r', z') \tag{C.10}$$

Noting that the index n of the second summation in Equation (C.10) accepts the upper limit as infinity or $F(m)$ when the superscript $(*)$ stands for (i) or (ii), respectively. Then, the Green's function $G_{ij}^{(*)}(r, z, t \mid r', z', t')$ for $t' > 0$, can be obtained by replacing t in Equation (C.10) with $\left(t - t'\right)$ as follows:

$$G_{ij}^{(*)}(r, z, t \mid r', z', t') = \sum_{m=1}^{\infty} \sum_{n=1}^{\infty / F(m)} \Psi_{imn}^{(*)}(r, z) \, e^{-\beta_{mn}^{(*)\,2} (t - t')} \frac{1}{N_{mn}^{(*)}} \frac{k_{jh}}{c_{jh}} \Psi_{jmn}^{(*)}(r', z') \tag{C.11}$$

Therefore, the solutions in Equations (5.6) and (5.5) are completely disclosed when the Green's function $G_{ij}^{(*)}$ has been achieved.

Appendix D. Derivation of the excess pore water pressure $u_i^{(*)}$ in Equation (5.6) corresponding to the investigation loadings in the example

Taking consideration of Equation (5.6), the expression of excess pore water pressure dissipation $u_i^{(*)}$ is formulated corresponding to a time-dependent loading which is applied instantaneously on the composite ground at time $t = 0$. Referring to [188, 196] regarding the characteristics of Green's function, the Green's formula of excess pore water pressure dissipation for a particular duration of load should include all previous instantaneous (step) changes of the load. Therefore, the detailed expressions of $u_i^{(*)}$ for the three investigation loadings can be derived as follows:

Step loading

In connection to Equation (5.10a) and Figure 5.2a, the applied loading includes the step increments q_0 at time $t = 0$ and $\Delta q_{t_1} = q_{\max} - q_0$ at time $t = t_1$, in which the load remains unchanged during each loading duration. Hence, the second term on the right-hand side of Equation (5.6) should be removed due to the zero loading rates for any time $t \neq \{0, t_1\}$; then, the expression of $u_i^{(*)}$ has the following form:

$$u_i^{(*)}(r,z,t) = \begin{cases} \sum_{j=1}^{2} \int_{z'=0}^{H} \int_{r'=r_j}^{r_{j+1}} G_{ij}^{(*)}(r,z,t \mid r',z',t')\Big|_{t'=0} \sigma_{0j}\, r'\, dr'\, dz' & (t < t_1) \\ \sum_{j=1}^{2} \int_{z'=0}^{H} \int_{r'=r_j}^{r_{j+1}} G_{ij}^{(*)}(r,z,t \mid r',z',t')\Big|_{t'=0} \sigma_{0j}\, r'\, dr'\, dz' & \\ + \sum_{j=1}^{2} \int_{z'=0}^{H} \int_{r'=r_j}^{r_{j+1}} G_{ij}^{(*)}(r,z,t \mid r',z',t')\Big|_{t'=t_1} \Delta\sigma_{t_1,j}\, r'\, dr'\, dz' & (t \geq t_1) \end{cases} \tag{D.1}$$

where $\Delta\sigma_{t_1,1}$ and $\Delta\sigma_{t_1,2}$ in accordance with $j=1,2$ are the total vertical stress increments within the stone column and soft soil caused by the instantaneous increase Δq_{t_1} of load at time $t=t_1$.

It should be noted that $\sigma_{01}=\sigma_{02}=q_0$ and $\Delta\sigma_{t_1,1}=\Delta\sigma_{t_1,2}=\Delta q_{t_1}$ owing to the assumption of the uniform distribution of total vertical stresses in the composite ground adopted in the example. Then, substituting Equation (C.11) into Equation (D.1) and combining with Equation (C.7), the equation of $u_i^{(*)}$ for the step loading can be achieved as:

$$u_i^{(*)}(r,z,t)=\begin{cases}\displaystyle\sum_{m=1}^{\infty}\sum_{n=1}^{\infty/F(m)}\Psi_{imn}^{(*)}(r,z)\;C_{mn}^{(*)}\,e^{-\beta_{mn}^{(*)\,2}t} & \left(t<t_1\right)\\ \displaystyle\sum_{m=1}^{\infty}\sum_{n=1}^{\infty/F(m)}\Psi_{imn}^{(*)}(r,z)\;C_{mn}^{(*)}\left[e^{-\beta_{mn}^{(*)\,2}t}+\frac{q_{\max}-q_0}{q_0}e^{-\beta_{mn}^{(*)\,2}(t-t_1)}\right] & \left(t\geq t_1\right)\end{cases} \tag{D.2}$$

Ramp loading and sinusoidal loading

Considering Equations (5.10b) and (5.10c), and Figures 5.2b and 5.2c, both the ramp and sinusoidal loadings are applied instantly at time $t=0$ with an initial surcharge q_0 and then varied with time. Thus, the following equation of $u_i^{(*)}$ for both the loading cases can be obtained by substituting Equation (C.11) into Equation (5.6) and combining with Equation (C.7):

$$u_i^{(*)}(r,z,t)=\sum_{m=1}^{\infty}\sum_{n=1}^{\infty/F(m)}\Psi_{imn}^{(*)}(r,z)\;C_{mn}^{(*)}\left[e^{-\beta_{mn}^{(*)\,2}t}+T_{mn}^{G(*)}\right] \tag{D.3}$$

where

$$T_{mn}^{G(*)} = \frac{1}{q_0}\int_{t'=0}^{t} e^{-\beta_{mn}^{(*)\,2}(t-t')}\,\frac{dq(t')}{dt'}\,dt' \tag{D.4}$$

In which $\sigma_1 = \sigma_2 = q$ has been used for the derivation due to the uniform distribution of the total vertical stresses in the composite stone column – soft ground. The detailed expression of $T_{mn}^{G(*)}$ for the ramp and sinusoidal loadings can be derived by substituting Equations (5.10b) and (5.10c) into Equation (D.4), respectively, as follows:

$$\text{Ramp loading: } T_{mn}^{G(*)} = \begin{cases} \dfrac{A}{q_0\,\beta_{mn}^{(*)\,2}}\left[1 - e^{-\beta_{mn}^{(*)\,2}t}\right] & \left(t < t_1\right) \\ \dfrac{A}{q_0\,\beta_{mn}^{(*)\,2}}\left[e^{-\beta_{mn}^{(*)\,2}(t-t_1)} - e^{-\beta_{mn}^{(*)\,2}t}\right] & \left(t \geq t_1\right) \end{cases} \tag{D.5}$$

$$\text{Sinusoidal loading: } T_{mn}^{G(*)} = \frac{B\,\varphi_B\left[-\beta_{mn}^{(*)\,2}\,e^{-\beta_{mn}^{(*)\,2}t} + \beta_{mn}^{(*)\,2}\cos\left(\varphi_B\,t\right) + \varphi_B\sin\left(\varphi_B\,t\right)\right]}{\beta_{mn}^{(*)\,4} + \varphi_B^2} \tag{D.6}$$

Appendix E. Derivation of the average excess pore water pressure in soft soil $\bar{\bar{\Theta}}_2$ corresponding to the homogeneous consolidation formulation

The homogeneous consolidation formulation is the same as the consolidation problem defined by Equations (6.1) − (6.4), in which the non-homogeneous terms $\partial\sigma_1/\partial t$ and $\partial\sigma_2/\partial t$ would be eliminated from the governing equations described by Equations (6.1a) and (6.1b). To distinguish from the excess pore water pressure solutions for the non-homogeneous consolidation problem, the solutions for the homogeneous formulation would be denoted as Θ, similar to that presented in Appendix C of Chapter 5. Then, referring to Appendix C, the excess pore water pressure solution at an arbitrary point in the composite ground corresponding to the homogeneous problem would be determined as:

$$\Theta_i(r,z,t) = \Theta_i^{(i)}(r,z,t) + \Theta_i^{(ii)}(r,z,t) \quad \left(r_i \le r \le r_{i+1}\right) \quad (i=1,2) \tag{E.1}$$

where the components $\Theta_i^{(i)}$ and $\Theta_i^{(ii)}$ are determined as in Appendix C; the coefficient $C_{mn}^{(*)}$ corresponding to the initial total vertical stresses derived in Chapter 6 would be expressed as:

$$C_{mn}^{(*)} = \frac{1}{N_{mn}^{(*)}} \sum_{j=1}^{2} \frac{k_{jh}}{c_{jh}} \int_{z'=0}^{H} \int_{r'=r_j}^{r_{j+1}} \Psi_{jmn}^{(*)}(r',z')\, \sigma_j(r',z',0)\, r'\, dr'\, dz' \quad (j=1,2) \tag{E.2}$$

The average excess pore water pressure for soft soil $\bar{\bar{\Theta}}_2(t)$ at any time t of the homogeneous consolidation problem can be obtained by averaging $\Theta_2(r,z,t)$ captured by Equation (C.1) against radius and depth as follows:

$$\bar{\bar{\Theta}}_2(t) = \frac{1}{\pi(b^2-a^2)H}\left[\int_{z=0}^{H}\int_{r=a}^{b} 2\pi\,\Theta_2(r,z,t)\, r\, dr\, dz\right] \tag{E.3}$$

Therefore, the ending time of the consolidation in soft soil corresponding to the homogeneous consolidation formulation (t_f) can be obtained by combining Equation (E.3) with the condition in Equation (6.22).

Appendix F. Derivation of the excess pore water pressure solutions for the non-homogeneous consolidation formulation

To finalise the solution of excess pore water pressure $u_i^{(*)}$ in Equation (6.24) corresponding to the non-homogeneous consolidation problem, the following Green's function $G_{ij}^{(*)}$ derived in Appendix C of Chapter 5 would be utilised:

$$G_{ij}^{(*)}(r,z,t\,|\,r',z',t') = \sum_{m=1}^{\infty}\sum_{n=1}^{\infty/F(m)} \Psi_{imn}^{(*)}(r,z)\; e^{-\beta_{mn}^{(*)\,2}(t-t')}\,\frac{1}{N_{mn}^{(*)}}\frac{k_{jh}}{c_{jh}}\Psi_{jmn}^{(*)}(r',z') \tag{F.1}$$

By substituting Equation (F.1) into Equation (6.24) and incorporating Equation (C.7), the following equation for $u_i^{(*)}$ would be attained:

$$u_i^{(*)}(r,z,t) = \sum_{m=1}^{\infty}\sum_{n=1}^{\infty/F(m)} \Psi_{imn}^{(*)}(r,z)\left[C_{mn}^{(*)}\,e^{-\beta_{mn}^{(*)\,2}t} + C_{mn}^{T(*)}\,T_{mn}^{G(*)}\right] \tag{F.2}$$

where

$$C_{mn}^{T(*)} = \frac{1}{N_{mn}^{(*)}}\sum_{j=1}^{2}\frac{k_{jh}}{c_{jh}}\int_{z'=0}^{H}\int_{r'=r_j}^{r_{j+1}} \Psi_{jmn}^{(*)}(r',z')\left[\sigma_{jf}(r',z') - q_0\right]r'\,dr'\,dz' \tag{F.3}$$

$$T_{mn}^{G(*)} = \int_{t'=0}^{t} e^{-\beta_{mn}^{(*)\,2}(t-t')}\,\frac{df(t')}{dt'}\,dt' \qquad \text{where} \qquad f(t') = \left(1-e^{-ct'}\right)^{0.5} \tag{F.4}$$

It should be noted that although the Fourier-Bessel coefficient $C_{mn}^{T(*)}$ in Equation (F.3) can be calculated using numerical integrations, an explicit form of $C_{mn}^{T(*)}$ can also be obtained for the convenient computational purposes for practical application by replacing the total vertical stresses σ_{jf} in Equation (F.3) with their corresponding average expressions against radius.

Consequently, the excess pore water pressures $u_i^{(*)}$ in Equation (F.2) and then u_i in Equation (6.23) are entirely revealed when $C_{mn}^{T(*)}$ and $T_{mn}^{G(*)}$ have been attained via Equations (F.3) and (F.4), respectively.